

I. DEVELOPMENT OF THE DI-*tert*-BUTYLPHOSPHINYL DIRECTED METALATION
GROUP. APPLICATION TO THE SYNTHESIS OF AROMATIC PHOSPHINES,
SUBSTITUTED FERROCENES, AND 7-SUBSTITUTED INDOLES. II. STUDIES
DIRECTED TOWARDS THE TOTAL SYNTHESIS OF BIRULOQUINONE.

by

Brian John Chapell

A thesis
presented to the University of Waterloo
in fulfilment of the
thesis requirement for the degree of
Doctor of Philosophy
in
Chemistry

Waterloo, Ontario, Canada, 2001

©Brian J. Chapell, 2001



National Library
of Canada

Acquisitions and
Bibliographic Services

395 Wellington Street
Ottawa ON K1A 0N4
Canada

Bibliothèque nationale
du Canada

Acquisitions et
services bibliographiques

395, rue Wellington
Ottawa ON K1A 0N4
Canada

Your file Votre référence

Our file Notre référence

The author has granted a non-exclusive licence allowing the National Library of Canada to reproduce, loan, distribute or sell copies of this thesis in microform, paper or electronic formats.

The author retains ownership of the copyright in this thesis. Neither the thesis nor substantial extracts from it may be printed or otherwise reproduced without the author's permission.

L'auteur a accordé une licence non exclusive permettant à la Bibliothèque nationale du Canada de reproduire, prêter, distribuer ou vendre des copies de cette thèse sous la forme de microfiche/film, de reproduction sur papier ou sur format électronique.

L'auteur conserve la propriété du droit d'auteur qui protège cette thèse. Ni la thèse ni des extraits substantiels de celle-ci ne doivent être imprimés ou autrement reproduits sans son autorisation.

0-612-60527-2

Canada

The University of Waterloo requires the signatures of all persons using or photocopying this thesis. Please sign below, and give address and date.

Abstract

A new directed metalation group (DMG) has been investigated and developed. The di-*tert*-butylphosphinyl substituent has been shown to be effective in directing aromatic metalation reactions to the *ortho* position providing direct access to 1,2-disubstituted aromatic phosphine oxides in high yield. A preliminary determination of the relative position in the DMG hierarchy has been established. In addition, access to aromatic phosphines has been demonstrated through reduction of the phosphine oxide, and access to hindered biaryls has been demonstrated through homocoupling. Similar reactivity was demonstrated for ferrocenyl substrates, in which deprotonation occurs adjacent to the di-*tert*-butylphosphinyl substituent.

A new and efficient route for the synthesis of 7-substituted indoles has been established. *N*-Di-*tert*-butylphosphinylindole was smoothly metalated in the presence of *n*-butyllithium to provide 7-lithio-*N*-di-*tert*-butylphosphinylindole, which reacted with electrophiles to furnish 7-substituted indoles in high yield. Using the new methodology, a preliminary investigation of the total synthesis of a sterriquinone CT4 was performed.

Progress has been made towards the total synthesis of the naturally occurring 9,10-phenanthraquinone biruloquinone. The synthetic strategy involved the combined use of directed *ortho* metalation and transition metal catalyzed cross coupling protocols in the synthesis of key intermediates.

Acknowledgements

I would like to take this opportunity to express my sincere thanks to all those who have made it possible for me to achieve my goals. Firstly, none of this work could have been completed without the guidance, leadership, support, and patience of my supervisor, Professor Victor Snieckus. The outstanding research achievements that have emanated from the Snieckus group over the last 30 years speak volumes about the individual whose knowledge and dedication has provided leadership to countless researchers. Thank you also to the members of my advisory committee - Professors Morris Tchir, Gary Dmitrienko, and Adrian Schwan - for their continued support and advice. A special thank you to Professor Michael Chong for graciously accepting the role of co-supervisor upon the departure of Professor Snieckus from Waterloo. In addition I would like to thank Professor Scott Denmark of the University of Illinois at Urbana-Champaign Chemistry Department and Professor Bruce Greenberg of the University of Waterloo Biology Department for kindly agreeing to act as external examiners.

Throughout my time at the University of Waterloo I had the distinct pleasure of working and sharing laboratory space with a world-class group of researchers. In addition to providing a pleasant working atmosphere, the Snieckus group provided me with an inspirational, multicultural, and highly educational environment in which to pursue my studies. My sincere thanks go to each member of the group that I had the pleasure of working with. Although it would be impractical to name everybody in the group, I feel that it is important to make a special mention of certain individuals whose presence in the laboratory on a daily basis made my experience one that will not be forgotten. For these reasons, I would like to give special thanks, to Dr. Marcos Brandão, Dr. Ed Griffen, Dr. Markus Wicki, Dr. Clint James, Dr. Claude Quesnelle, Dr. Neville Emslie, Dr. Masao Tsukazaki, Steve MacNeil, Aaron Kinsman, Brian Chauder, Dr. Matthew Gray, Dr. Paul Bury, Dr. David Roe, Dr. Alexei Kalinine, Dr. Stephen Houldsworth, Chris Kendall, Rob Milburn, Claire Milburn, and Andrew Larkin.

In addition to those mentioned above, I would like to express my thanks to Dr. Nick Taylor whose heroic efforts have maintained the chemistry department's top-notch crystallography service for many years, and who provided me a unique opportunity and atmosphere for hands-on learning. I would also like to thank Jan Venne for her diligence in maintaining the chemistry department's NMR facilities, and Cathy Van Esch for all of her assistance in administrative matters with the department.

Finally, I would like to thank all of the members of my family for their support and encouragement over the last several years. My special thanks to my wife, Sandy Chapell, for continuing unconditional love, support, and patience through good and bad. Thank you, I love you very much.

To Sandy, I love you now and always.

Table of Contents

1.0	The Di- <i>tert</i> -butylphosphinyl Directed <i>ortho</i> Metalation Group	1
1.1	Introduction	1
1.2	Directed Metalation	1
1.2.1	The Directed <i>ortho</i> Metalation (DoM) Reaction	1
1.2.2	Directed Metalation Groups (DMGs)	2
1.2.3	Phosphorus-based DMGs	5
1.2.3.1	Triarylphosphine Oxides	5
1.2.3.2	Phosphine Imides	12
1.2.3.3	Phosphorus Amides and Thioamides	13
1.2.3.4	Miscellaneous DMGs	15
1.2.4	Mechanism of the DoM Reaction	17
1.2.4.1	Bases	17
1.2.4.2	Solvents and Additives	18
1.2.4.3	Mechanistic Studies - Complexation	20
1.2.4.4	Mechanistic Studies - Induction	22
1.2.5	Directed Remote Metalation (DreM)	26
1.2.5.1	Fluorenones, Phenanthrols, and 9-Aminophenanthrenes	28
1.2.5.2	Dibenzo-[<i>b,d</i>]-pyranones	29
1.2.5.3	Acridones, Xanthenones, Phosphininones, and Thioxanthenones	30
1.3	Ferrocene Metalation	31
1.3.1	Directed <i>ortho</i> Metalation of Ferrocenes	33
1.3.2	Planar Chiral Ferrocenes	35
1.3.2.1	Planar Chiral Ferrocenes <i>via</i> Resolution	38
1.3.2.2	Planar Chiral Ferrocenes <i>via</i> Diastereoselective Metalation	40

1.3.2.3	Planar Chiral Ferrocenes <i>via</i> Enantioselective Metalation	45
1.4	Phosphine Ligands	48
1.4.1	Di- <i>tert</i> -butylphosphines	48
1.5	Results and Discussion	51
1.5.1	(-)-Sparteine-mediated Enantioselective DoM of <i>N,N</i> -Diisopropyl Ferrocenecarboxamide	51
1.5.2	DoM of Ferrocenes bearing other DMGs	57
1.5.3	DoM of Di- <i>tert</i> -butylphenylphosphine Oxide	63
1.5.4	Synthesis of Hindered Biaryl Bisphosphine Oxides	70
1.5.5	Aryl Phosphine Oxide Reduction	73
1.5.6	Relative DMG Hierarchy of the P(O) <i>t</i> Bu ₂ DMG	74
1.5.7	Cooperative Metalation of the P(O) <i>t</i> Bu ₂ DMG	78
1.6	Future Work	79
2.0	Regioselective C-7 Metalation of Indoles	82
2.1	Introduction	82
2.2	Functionalization Indoles	82
2.2.1	2- and 3-Substituted Indoles	82
2.2.2	Benzenoid Substitution	87
2.3	Indole Natural Products	96
2.3.1	Prenyl Substituted Indoles	96
2.3.2	Previous Syntheses of Asterriquinones	97
2.3.3	Biosynthesis	99
2.3.4	Biological Acitivity	102
2.4	Results and Discussion	104
2.4.1	Metalation of <i>N</i> -(Di- <i>tert</i> -butylphosphinyl)indole	104
2.4.2	DMG Cleavage	108
2.4.3	Application to Natural Products	113

2.5	Future Work	119
2.5.1	DMG Cleavage	119
2.5.2	Total Synthesis of Asterriquinone CT4	120
2.5.3	Total Synthesis of Leiocarpol	122
3.0	Studies Directed Toward the Total Synthesis of Biruloquinone	124
3.1	Introduction	124
3.2	Aryl-Aryl Cross Coupling	124
3.3	Biruloquinone and Related Natural Products	129
3.3.1	Biological Activity	132
3.3.2	Previous Syntheses of 9,10-Phenanthraquinones	133
3.3.3	Previous Syntheses of Dibenzo-[<i>b,d</i>]pyranones	139
3.4	Synthetic Strategy	140
3.5	Results and Discussion	144
3.6	Future Work	151
4.0	Experimental Section	154
5.0	Appendices	215
5.1	Appendix 1 - X-ray analysis of 1.158d	216
5.2	Appendix 2 - X-ray analysis of 1.160	225
5.3	Appendix 3 - ¹ H-NMR spectrum of 1.169a	235
5.4	Appendix 4 - X-ray analysis of 1.170	237
5.5	Appendix 5 - X-ray analysis of 1.171n	246
5.6	Appendix 6 - X-ray analysis of 1.176	255
5.7	Appendix 7 - X-ray analysis of 2.78c	264
5.8	Appendix 8 - ¹ H-NMR spectra of 2.101a	273
6.0	References and Notes	277

List of Abbreviations

Ac	Acetyl
Am	<i>N,N</i> -Diethylcarbanyl
BINAP	2,2'-Bis(diphenylphosphino)-1,1'-binaphthyl
Boc	<i>tert</i> -Butoxycarbonyl
BPPFA	(<i>R</i>)- <i>N,N</i> -Dimethyl-1-[(<i>S</i>)-1',2-bis(diphenylphosphino)ferrocenyl]ethylamine
BuLi	Butyllithium
CIPE	Complexed Induced Proximity Effect
Cp	Cyclopentadienyl
Cy	Cyclohexyl
DME	1,2-Dimethoxyethane
DMF	<i>N,N</i> -Dimethyl formamide
DMG	Directed Metalation Group
DoM	Directed <i>ortho</i> Metalation
dppf	1,1'-Bis(diphenylphosphino)ferrocene
DreM	Directed remote Metalation
E ⁺	Electrophile
LAH	Lithium aluminum hydride
LDA	Lithium diisopropylamide
LiHMDS	Lithium hexamethyldisilazide
LiTMP	Lithium tetramethylpiperidide
MOM	Methoxymethyl
Ms	Methanesulfonyl
P-DMG	Phosphorus-based DMG
PAH	Polycyclic aromatic hydrocarbon
PMDPTA	<i>N,N,N',N',N''</i> -Pentamethyldipropylenetriamine

PMDTA	<i>N,N,N',N',N''</i> -Pentamethyldiethylenetriamine
PPFA	(<i>R</i>)- <i>N,N</i> -Dimethyl-1-[(<i>S</i>)-2-(diphenylphosphino)ferrocenyl]ethylamine
py	Pyridine
SAR	Structure activity relationship
SEM	Trimethylsilylethoxymethyl
TBAF	Tetrabutylammonium fluoride
TBS	<i>tert</i> -Butyldimethylsilyl
TES	Triethylsilyl
TFA	Trifluoroacetic acid
THP	Tetrahydropyranyl
TIPS	Triisopropylsilyl
TMEDA	<i>N,N,N',N'</i> -Tetramethylethylenediamine
TMS	Trimethylsilyl; tetramethylsilane
Tf	Trifluoromethanesulfonyl
Ts	<i>p</i> -Toluenesulfonyl

1.0 The Di-*tert*-butylphosphinyl Directed *ortho* Metalation Group

1.1 Introduction

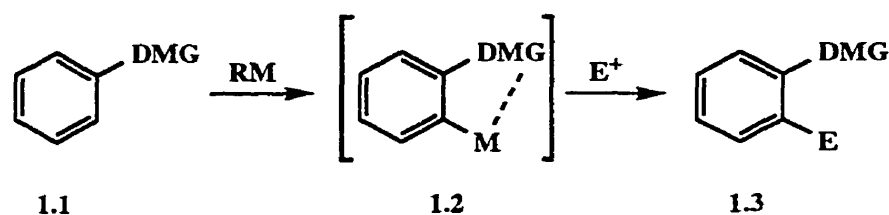
Since the inception of synthetic organic chemistry, chemists have sought new ways of putting molecules together. Whether searching for a new headache remedy, generalizing a new reaction, or simply studying a reaction for purely academic interest, the lure of constructing complex molecules has challenged the synthetic chemist continually. With the sophistication of modern synthetic techniques steadily evolving, the chemist is driven to increasingly more difficult targets and tasks in the development of new methodology.

Electrophilic aromatic substitution has been a staple of organic synthesis for generations. When Gilman and Bebb,¹ and Wittig and Fuhrman² independently discovered that anisole could be deprotonated in an *ortho* position by treatment with butyllithium, a new synthetic weapon, complementing the electrophilic substitution reaction, was added to the synthetic chemists' arsenal that would have impact on the field for years to come. The subsequent evolution of what is now known as the Directed *ortho* Metalation (DoM) reaction has progressed to the point where it is now the subject of several reviews³⁻⁹ and has seen numerous commercial applications.^{10,11} The long term impact of the discovery by Gilman and Wittig is evidenced by the efficient and regioselective synthesis of complex aromatic systems today. Despite the expanse of available DoM methods, new protocols and substrates continue to appear in the literature.

1.2 Directed Metalation

1.2.1 The Directed *ortho* Metalation (DoM) Reaction

Directed *ortho* Metalation (DoM) refers to the process whereby an aromatic system containing a Directed Metalation Group (DMG) (**1.1**) is treated with a strong base (usually an alkyllithium reagent) resulting in the abstraction of a weakly-acidic proton from a position *ortho* to the DMG. The intermediate organometallic species **1.2** is quenched with an electrophile to produce a 1,2-disubstituted aromatic system **1.3** (Scheme 1.1).



Scheme 1.1

Structure **1.2** and "RM" are oversimplifications of the species involved in the DoM process. In reality, the alkyllithium base and the intermediate organometallic species are present as aggregates. The degree of aggregation is dependent on choice of base, solvent, and other additives such as *N,N,N',N'*-tetramethylethylenediamine (TMEDA), believed to be responsible for breaking down the degree of aggregation thus creating a more reactive base^{12,13} (see, however, ref. ¹⁴). This concept will be discussed in greater detail in Section 1.2.4.1. The range of DMGs available to the synthetic chemist is enormous and will be discussed in Section 1.2.2.

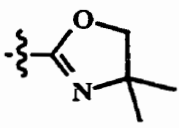
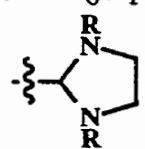
Scheme 1.1 constitutes a simple representation of the DoM process for which much more complex examples involving highly substituted and fused ring systems, heteroaromatics, or metallocenes are available. The following sections will cite several interesting examples of DoM reactions as a means of illustrating the concepts.

1.2.2 Directed Metalation Groups (DMGs)

In the 1990s, a glance through a modern synthetic journal will find numerous examples of directed metalation reactions. What does one look for when designing a synthetic step based on a metalation reaction, and in particular, how does one choose a suitable DMG for the task at hand? An important factor, common to all DMGs, is the presence of a heteroatom which serves to coordinate the incipient *ortho*-lithium atom in intermediate **1.2** ($M = Li$). One of the earliest concepts taught in organic chemistry is the importance of basicity and nucleophilicity. Thus, a particularly important quality of a DMG is that it must be resistant to nucleophilic attack by the base. Also important in selecting a DMG is the ability to manipulate the DMG after *ortho*-functionalization.

Frequently, DMGs are broadly classed into two categories: those which are bound to the aromatic system through a carbon atom, and those which are bound through a heteroatom. This distinction is not only convenient but proves to have some significance in mechanistic studies as described by Slocum and co-workers (*cf.* Section 1.2.4). Table 1.1 provides a sampling of some common and lesser known DMGs yet is only a partial list as the inventory of available DMGs continues to grow.

Table 1.1 - Common DMGs

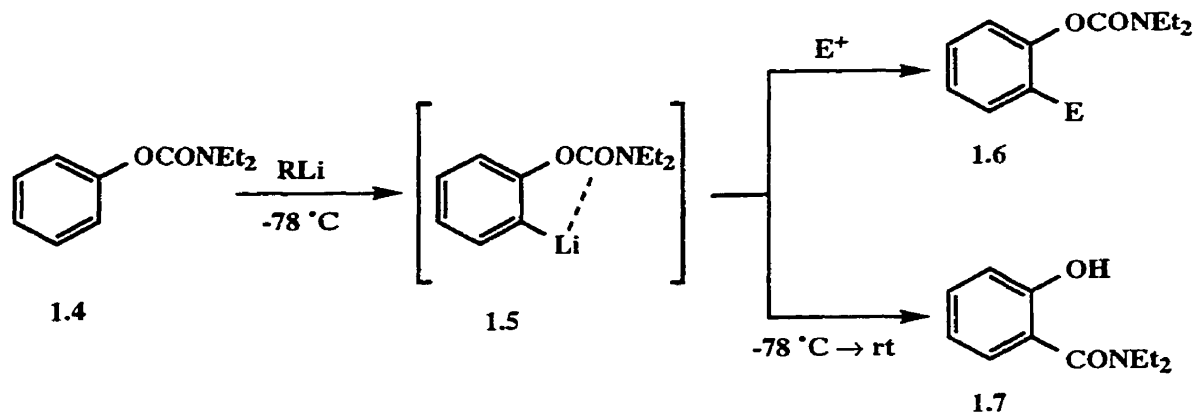
Carbon Based DMGs	ref.	Heteroatom Based DMGs	ref.
CONR ₂	5-7	N-CO ₂ 'Bu	7,15
	16,17	N-CO'Bu	18,19
CON-R	4,20	OMe	3,4
CSN-R	25	OMOM	21-24
CO ₂ R	26,27	OCONR ₂	7
CO ₂ ⁻	29	OCSNR ₂	28
CF ₃	4,32,33	OP(O)R ₂	30,31
CN	26	S ⁻	34-36
CH(NR ₂)O ⁻	46	S(O) _x R, x = 0,1	26,37-45
C=NC ₆ H ₁₁	50,51	SO ₂ N-R	47-49
	53	SO ₂ NR ₂	49,52
CH(OR) ₂	58	SO ₃ R	54,55
		P(O)Ph ₂	56,57
		P(NR')R ₂	59
		P(X)(NR ₂) ₂ , X = O,S	60,61
		P(S)PhNR ₂	62
		Br	63
		F	32,33,64-66

Since the original experiments by Gilman and Wittig on the *DoM* of anisole, numerous publications have appeared regarding metalation using the OMe DMG, including several mechanistic studies which will be discussed in a Section 1.2.4. There are several other DMGs in Table 1.1 that warrant some discussion based on their synthetic utility.

One of the most widely explored DMGs is the tertiary amide.⁶⁷ Usually diethyl or diisopropyl amides are used, though other amides have also been applied.⁶⁸ The power of the tertiary amide DMG is evidenced by the numerous natural product syntheses which involve an amide metalation as a key step. Classes of natural products which have been prepared include fluorenones,⁶⁹ quinones,⁷⁰ xanthenones,⁷¹ dibenzopyranones,⁷² and anthraquinones.⁷³ The tertiary amide DMG has now evolved to the extent that several reviews have been written about this DMG alone.⁵⁻⁷

Closely related to the tertiary amide DMG is the tertiary *O*-aryl carbamate, the most powerful known DMG.^{7,41} Contributing to the utility of this DMG is its ability to undergo the anionic *ortho* Fries rearrangement as outlined in Scheme 1.2.⁷⁴ After metalation of the substrate, the intermediate anion **1.5** is usually stable at low temperature (examples are known in which the metalated species undergoes migration even at low temperature)⁷⁵ and may react with electrophiles to give disubstituted products **1.6**. Alternatively, upon warming the solution the carbamoyl moiety may undergo a 1,3-O→C migration to produce a salicylamide (**1.7**). Similar migrations have been observed with other oxygen based DMGs such as phosphates^{30,31,76} and oxytetrazoles.⁷⁷ The utility of the tertiary carbamate in metalation chemistry is further realized when the resulting tertiary amide is subsequently used as a DMG. The tertiary carbamate DMG has also been reviewed.⁷

Other carbon based DMGs which have garnered significant attention include the oxazolines¹⁷ masked aldehydes,^{46,78} while in heteroatom based DMGs, the OMOM,^{21,23} NHBoc, and sulfones⁴¹ are well explored. On the other hand, phosphorus-based DMGs have not received equal attention.



1.2.3 Phosphorus-Based DMGs (P-DMGs)

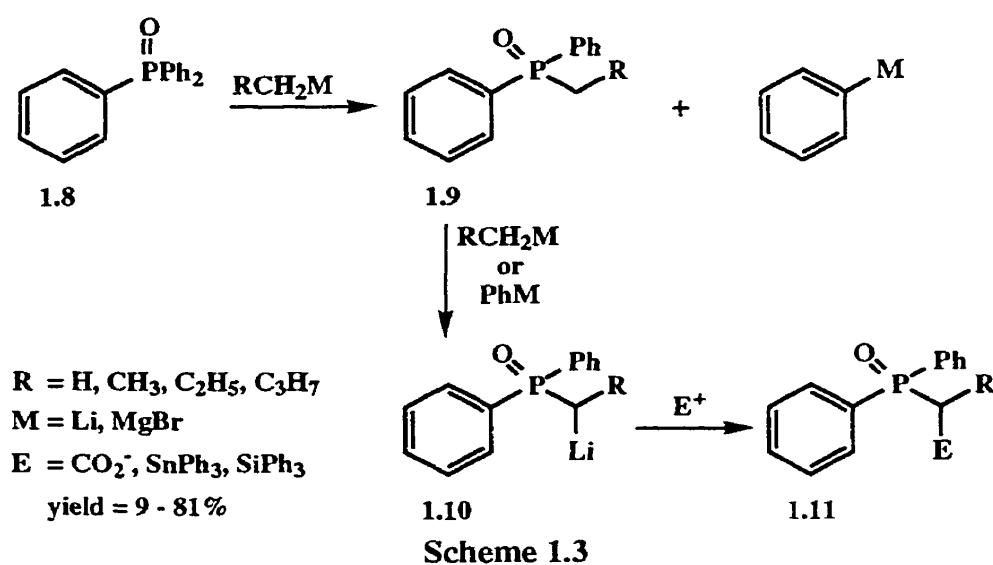
Today's push for more environmentally friendly and cost effective manufacturing processes has fueled efforts for the design and synthesis of numerous phosphine-based ligands. Metal catalyzed processes involving phosphine ligands continue to become more prevalent providing the impetus for the development of new synthetic methods in organophosphorus chemistry.⁷⁹⁻⁸²

Of particular interest are aryl phosphines and methods of their synthesis, an area which seems ideally suited for metalation chemistry involving P-DMGs. When compared with the carbon, oxygen, and sulfur based DMGs, P-DMGs have received significantly less attention. Known P-DMGs also have various associated problems such as poor synthetic utility, hygroscopicity, susceptibility to nucleophilic attack, and harsh metalation conditions. The following sections provide a comprehensive survey of existing P-DMGs and the scope of their applicability to the synthesis of functionalized aromatic systems. The various limitations associated with each P-DMG are also discussed.

1.2.3.1 Triarylphosphine Oxides

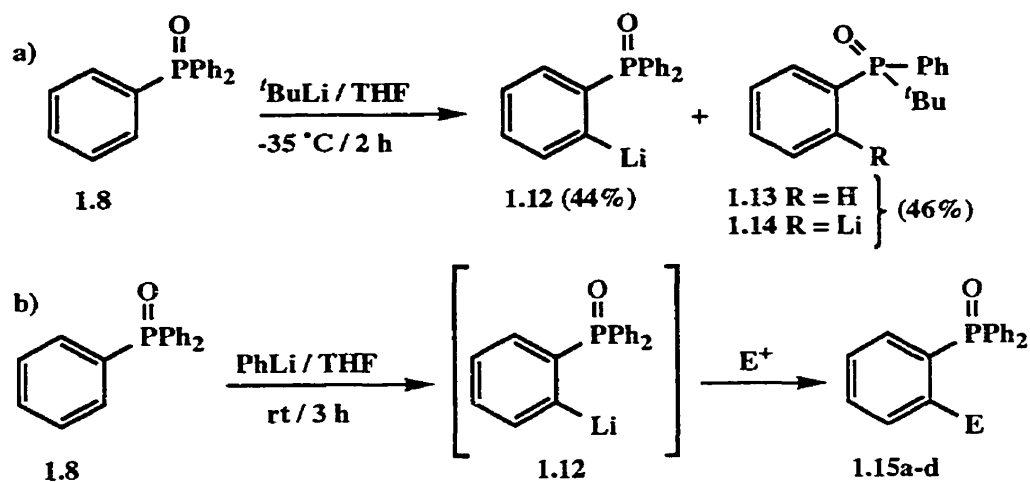
In 1963, Seyferth and co-workers^{83,84} found that treatment of triphenylphosphine oxide (1.8) with alkyllithium or Grignard reagents resulted primarily in direct nucleophilic addition of the organometallic reagent to phosphorus with the concomitant expulsion of

phenyllithium or phenyl Grignard, respectively (Scheme 1.3). The resulting alkyldiphenylphosphine oxide **1.9** underwent an α -deprotonation by reaction with either the newly formed PhM or with excess RCH₂M. Quenching of the α -metalated product **1.10** with electrophiles provided α -substituted products **1.11a-g** in varying yields. Similar results were found when triphenylphosphine sulfide was used as the substrate,⁸⁵ although a later report by Yoshifuji⁶² and co-workers claims the isolation of diphenyl(*ortho*-tolyl)phosphine sulfide (26% yield) upon treatment of triphenylphosphine sulfide with *s*-BuLi and quench with methyl iodide.



Two decades later, Schlosser⁵⁷ and co-workers used this information to their advantage in the *ortho* metalation of triphenylphosphine oxide. They noted that even the use of the sterically demanding *t*-BuLi resulted in only 44% of **1.12** while the remainder was **1.13** and the corresponding *ortho* lithiated intermediate **1.14**,⁸⁶ both resulting from addition of *t*-BuLi to phosphorus with loss of PhLi (Scheme 1.4a). In order to avoid side products resulting from addition of the base to phosphorus, PhLi was chosen as the metalating agent. Despite conflicting earlier reports by Gilman and Brown⁸⁷ that PhLi and PhMgBr are unreactive towards **1.8**, and by Wittig and Cristau⁸⁸ that *meta* metalation of **1.8** occurs, Schlosser and co-workers found that **1.12** could be cleanly prepared upon treatment of **1.8** with PhLi for 3 h

at room temperature. Thus derivatives **1.15a-d** were prepared in moderate yields according to Scheme 1.4b.

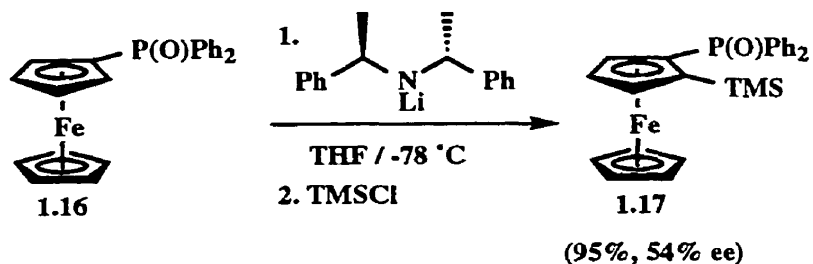


entry	E ⁺	E	product 1.15	yld (%)
1	MeI	Me	a	72
2	MeCHO	C(OH)Me	b	68
3	CO ₂	CO ₂ H	c	53
4	I ₂	I	d	*

* yield not reported

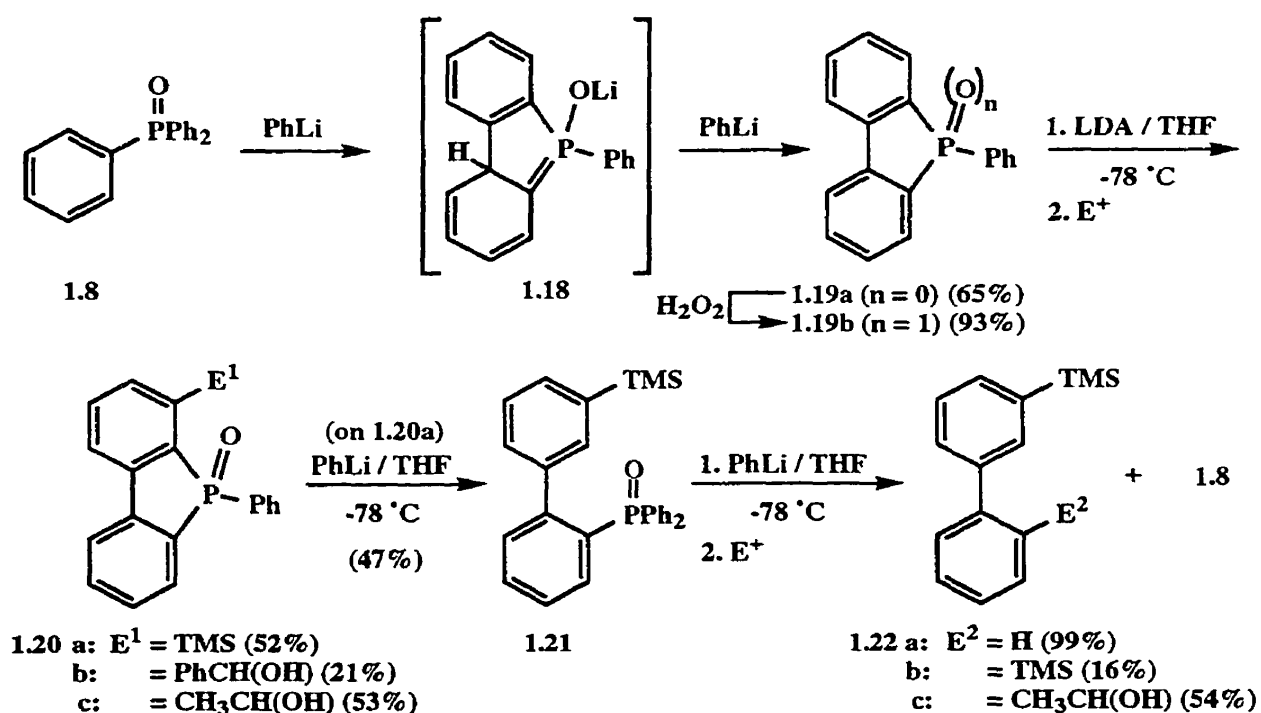
Scheme 1.4

Desponds and Schlosser⁵⁶ recently used the same procedure to prepare iodide **1.15d** for use in homocoupling. Price and Simpkins⁸⁹ have used the P(O)Ph₂ DMG in conjunction with a chiral lithium amide base to prepare the planar chiral ferrocene derivative **1.17** in high yield but low %ee (Scheme 1.5). The significance of this result will be discussed further in Section 1.3.2.3.



Scheme 1.5

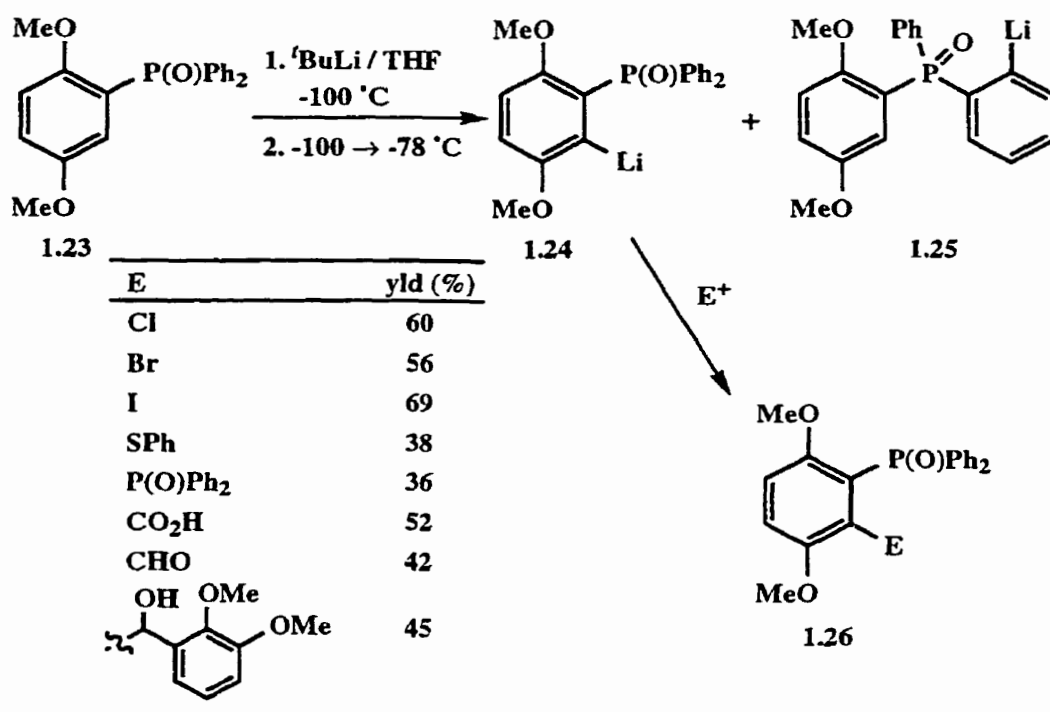
Phenyllithium-mediated metalation of triphenylphosphine oxide was proposed as a mechanistic step by Ogawa and co-workers in the preparation of substituted biphenyls.⁹⁰ Thus, when **1.8** was treated with PhLi in THF at reflux, (2,2'-biphenylene)phenylphosphine (**1.19a**, Scheme 1.6) was obtained in 65% yield, presumably through an intramolecular nucleophilic attack to give intermediate **1.18**, which, upon oxidation, gave phosphine oxide **1.19b**. Similar intramolecular cyclizations have been reported by Zbiral,⁹¹ Seyferth,⁹² and Schlosser.^{56,93} Interestingly, phosphine oxide **1.19b** was treated with LDA followed by an electrophile to give derivatives **1.20a-c** in modest yield. Repeat treatment of **1.20a** with PhLi in a two-step process furnished first **1.21** and finally **1.22a-c** in moderate yields, along with recovered **1.8** which could be reused in further reactions (Scheme 1.6). This sequence of reactions further demonstrates the susceptibility of phosphorus to nucleophilic attack by organolithiums.



Scheme 1.6

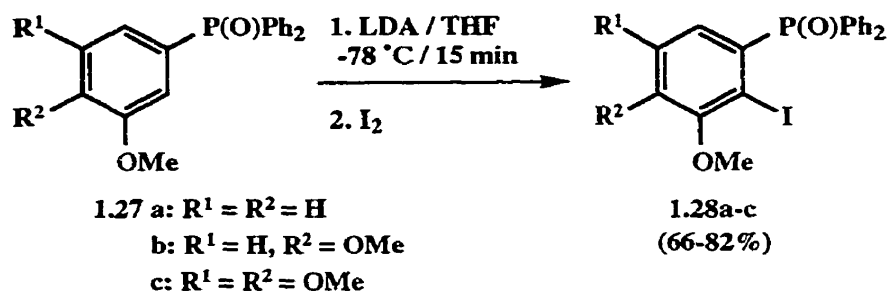
Yields for metalations involving triarylphosphine oxides have been somewhat improved by using a cooperative DMG effect. This was best exemplified by Brown and Woodward⁹⁴

and by Schmid⁹⁵ who successfully employed a *meta*-methoxy group to aid in the metalation process. Thus, in Brown's approach,⁹⁴ (2,5-dimethoxyphenyl)diphenylphosphine oxide (**1.23**, Scheme 1.7) was treated with *t*-BuLi at -100 °C and then warmed to -78 °C and maintained for varying lengths of time. It was observed that longer reaction times favoured equilibration to the "in between" position as determined by quenching of the anion mixture with D₂O and analyzing the product mixture by NMR. These results suggest that **1.24** is thermodynamically favoured over **1.25**. Using a metalation period of 4 h to maximize the ratio of **1.24** : **1.25**, a variety of derivatives **1.26** were prepared in 36-69% yield.



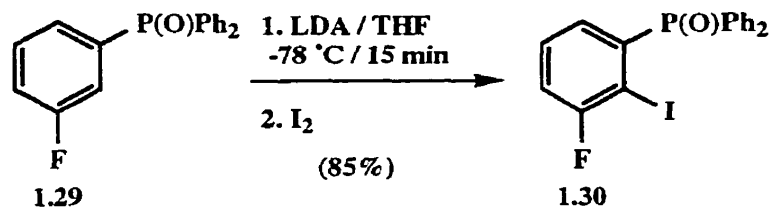
Scheme 1.7

Schmid used LDA as the metalating agent on related substrates **1.27a-c** to prepare iodides **1.28a-c** in good yields and with complete regioselectivity using a metalation period of only 15 minutes (Scheme 1.8).⁹⁵ In accordance with Brown's results, Schmid also found that use of alkylolithium (or phenyllithium) reagents gave lower regioselectivity and yield.



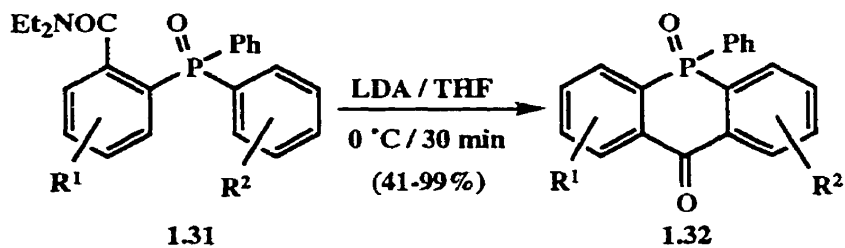
Scheme 1.8

The use of a *meta*-F DMG to assist in metalation of a phosphine oxide was also demonstrated by Jendralla⁹⁶ and co-workers (Scheme 1.9). Thus phosphine oxide **1.29** underwent smooth metalation with LDA and quench with iodine to provide **1.30** regioselectively and in good yield.



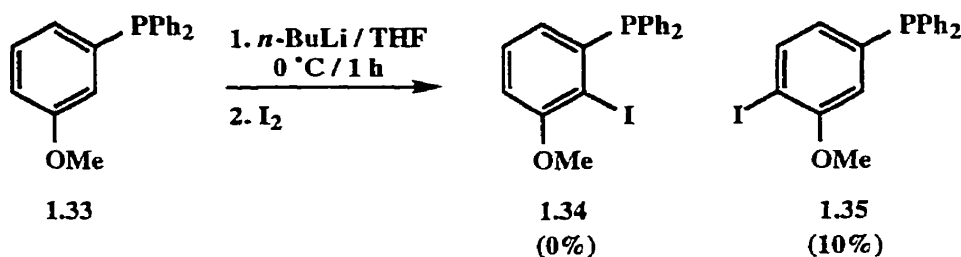
Scheme 1.9

Finally, Gray⁹⁷ and co-workers have utilized metalation of triarylphosphine oxides **1.31** as a general route to dibenzo[*b,e*]phosphininones **1.32** (Scheme 1.10). Here the metalation is probably assisted by the DMG in the 2' position and the regioselectivity is driven by the irreversible cyclization (*cf.* Section 1.2.5.3).

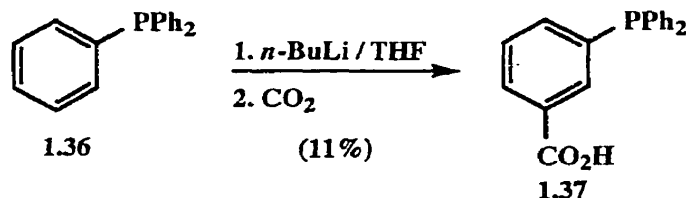


Scheme 1.10

In the realm of triarylphosphorus metalations, three unsuccessful examples are noteworthy. In the course of studies⁹⁵ mentioned above (Scheme 1.8), metalation of the corresponding triarylphosphine **1.33** was attempted. Thus, treatment of **1.33** with *n*-BuLi produced none of the desired cooperative metalation product **1.34**, but rather a 10% yield of **1.35** suggesting that the phosphine functionality has negligible directing ability (Scheme 1.11). This is supported by the early findings of Gilman⁸⁷ who reported that metalation of triphenylphosphine (**1.36**) with *n*-BuLi resulted in metalation in the *meta* position and production in low yield of acid **1.37** after quench with carbon dioxide (Scheme 1.12). Kellner and Tzschach have disclosed⁹⁸ that Ph₂PCH₂NMe₂ is metalated in the α position with *n*-BuLi and undergoes rearrangement to the thermodynamically favoured *ortho* metalated product. However, the dimethylamino functionality seems to be the main contributor to the regioselectivity in this case.

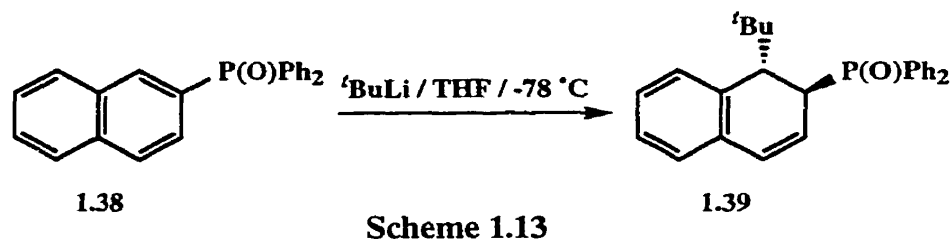


Scheme 1.11



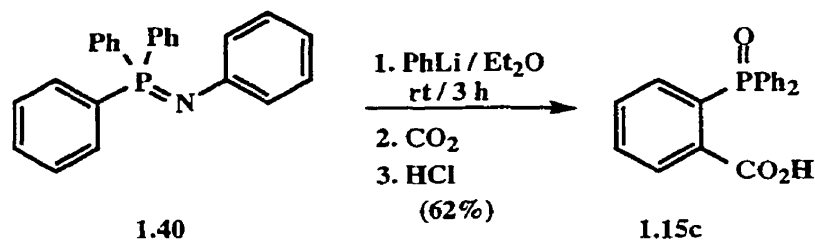
Scheme 1.12

In the final example, Alcock⁹⁹ and co-workers have demonstrated that (2-naphthyl)diphenylphosphine oxide (**1.38**) acts as a Michael acceptor when treated with *t*-BuLi in THF furnishing the addition product **1.39** (Scheme 1.13).



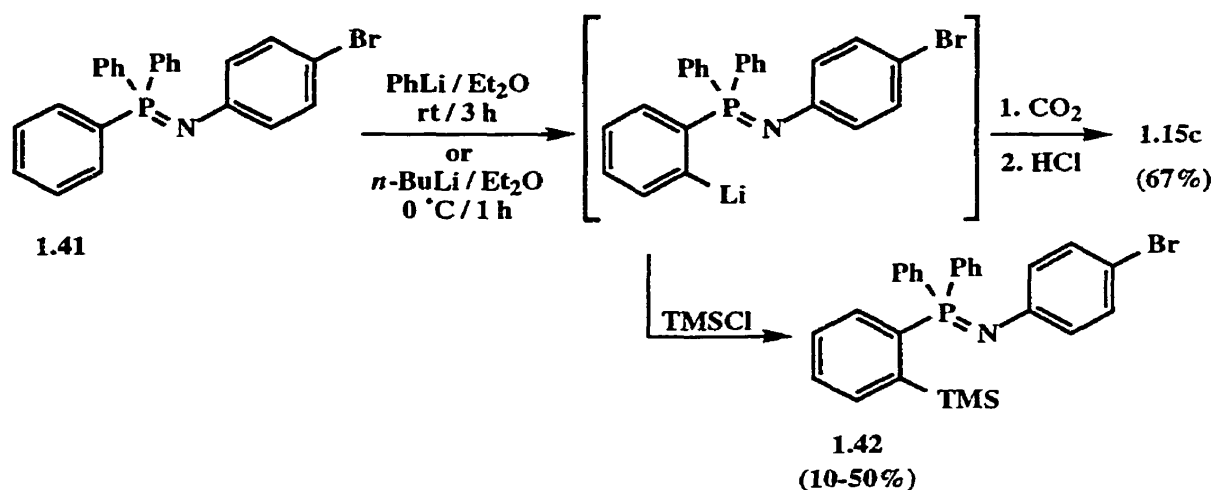
1.2.3.2 Phosphine Imides

In an effort to find a more effective P-DMG than the diphenylphosphinyl (P(O)Ph₂) group, Stuckwisch investigated the use of the synthetically equivalent phosphine imides.⁵⁹ As with triphenylphosphine oxide metalation, PhLi proved to be the most effective base for *ortho* metalation (Scheme 1.14) with alkyllithium bases undergoing predominantly P-nucleophilic attack analogous to the phosphine oxides in Scheme 1.3. Treatment of the parent triphenylphosphine *N*-phenylimide (1.40) with phenyllithium and subsequent exposure to CO₂ furnished, after hydrolytic workup, 2-diphenylphosphinyl benzoic acid (1.15c) in acceptable yield.



Scheme 1.14

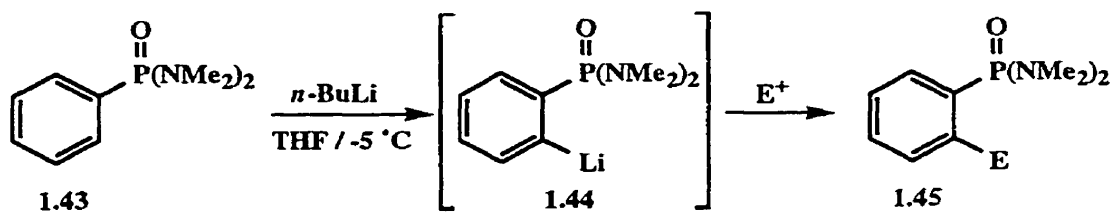
The scope of phosphine imide metalation has not been fully explored as only a limited number of other examples can be found in the literature. Interestingly, using triphenylphosphine *N*-(4-bromophenyl)imide (1.41) as the substrate,⁵⁹ *ortho* metalation was the principle reaction pathway upon treatment with either phenyllithium or *n*-BuLi as indicated by the isolation of TMS derivative 1.42 or acid 1.15c (Scheme 1.15). There was no evidence of metal halogen exchange as demonstrated by the quantitative recovery of *p*-bromoaniline after hydrolysis of the products.



Scheme 1.15

1.2.3.3 Phosphorus Amides and Thioamides

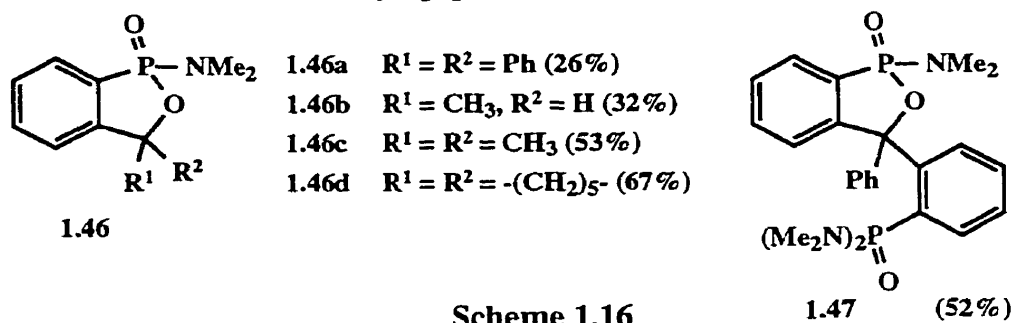
In the first report of phosphorus amide *DoM*, Dashan and Trippett observed that treatment of *N,N,N',N'*-tetramethyl phenylphosphonic diamide (**1.43**) with *n*-BuLi followed by a variety of electrophiles gave products **1.45a-e** in mostly good yields (Scheme 1.16).⁶⁰ When the intermediate aryllithium species **1.44** was treated with methyl iodide, *o*-ethyl and *o*-isopropyl products were obtained in a mixture along with the expected methyl derivative. The undesired side products presumably are formed from tolyl metalation of the initially formed methyl derivative. The use of various ketones as electrophiles provided predominantly the cyclized adducts **1.46a-d**, although benzophenone gave a 1:1 mixture of cyclized and uncyclized products. Quenching anion **1.44** with diethyl benzoylphosphonate furnished a 52% yield of **1.47**, which is proposed to arise from addition of two equivalents of **1.44** with the electrophile followed by cyclization. In contrast, a reaction involving a 2:1 electrophile:**1.44** ratio is proposed to account for the formation of **1.48** in 83% yield when benzonitrile was used to quench the anion. The proposed mechanism for formation of this interesting heterocycle (Scheme 1.17) represents a unique transformation.



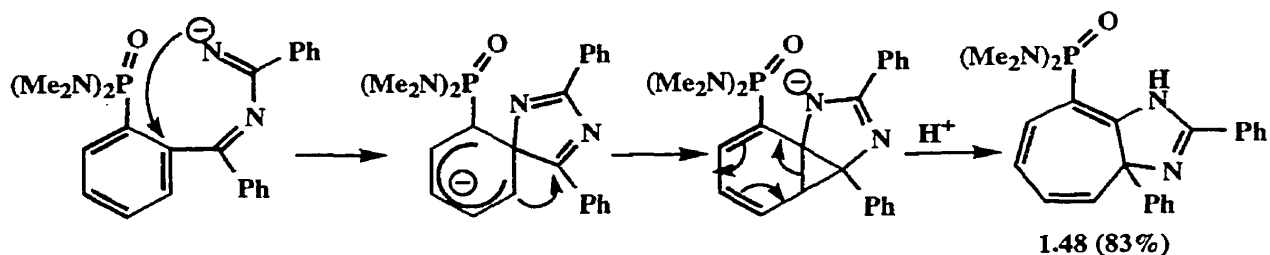
entry	E ⁺	E	product	yield (%)
1	PhCHO	CH(OH)Ph	a	72
2	Ph ₂ CO	C(OH)Ph ₂	b	25*
3	TMSCl	TMS	c	74
4	CO ₂	CO ₂ H	d	87
5	ClPPh ₂	P(O)Ph ₂ **	e	81

* accompanied by 26% of 1.46a

** after oxidation by H₂O₂



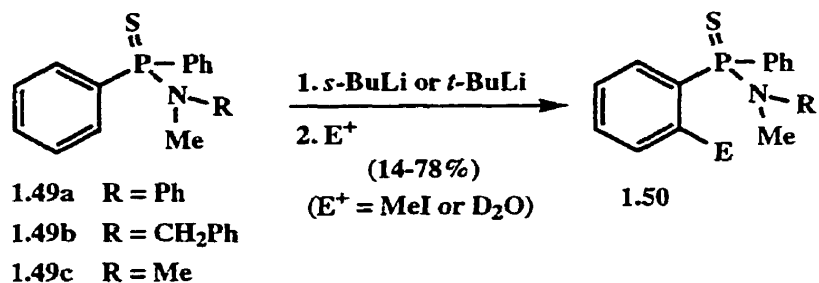
Scheme 1.16



Scheme 1.17

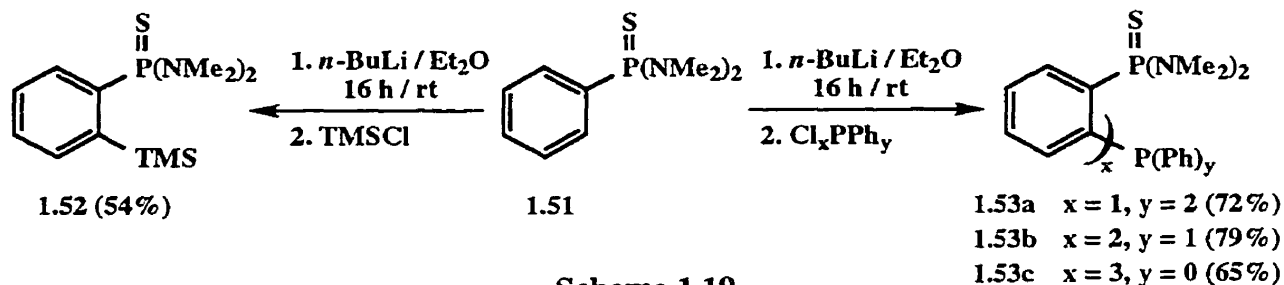
Yoshifuji and co-workers⁶² reported on the metalation of diphenylphosphinothioamides **1.49a-c** (Scheme 1.18). In attempting to α -lithiate the *N*-alkyl groups, it was found that DoM was the preferred reaction pathway leading to amides **1.50**. Although the scope of the reaction was poorly defined, it is clear that either *s*-BuLi or *t*-BuLi may be used in conjunction

with TMEDA as the metalating agent while the use of *n*-BuLi results in amine displacement at phosphorus producing alkyldiarylphosphine sulfides.



Scheme 1.18

Noting that compounds of the type 1.43 were hygroscopic, and thus not ideal for metalation chemistry, Craig⁶¹ and co-workers investigated the potential of the sulfur analogue 1.51. Although lengthy metalation times were required (16 h), they successfully reacted 1.51 with *n*-BuLi in ether, followed by electrophile quench providing 1.52 and 1.53a-c in good yields (Scheme 1.19).

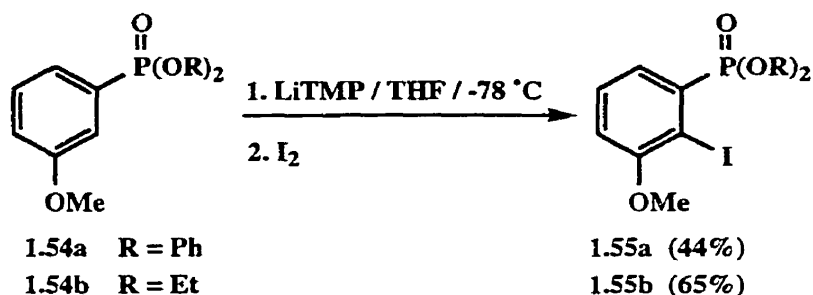


Scheme 1.19

1.2.3.4 Miscellaneous

Few additional and limited reports of P-DMG metalation are scattered throughout the literature. Expanding on the methoxy-assisted phosphine oxide metalation (Scheme 1.8), Schmid has recently reported the metalation of arylphosphonates.⁸⁰ Replacing LDA with the more bulky LiTMP, arylphosphonates 1.54 were smoothly metalated and quenched with I₂ to give aryl iodides 1.55 in 44% and 65% yield respectively (Scheme 1.20). Although modest yielding, this method finds its utility in the ability to modify the substituents on phosphorus at a later time through alkylation / arylation with Grignard reagents in one step, or in two steps *via*

the phosphinyl chlorides. Schmid has effectively used this protocol to provide numerous 2,2'-bis(phosphino)biphenyls.



Scheme 1.20

Schlosser^{57,93} and co-workers have shown that *ortho* metalation of triphenylphosphonio-methylid (1.56) is a facile process (Scheme 1.21). Thus treatment of 1.56 with an alkyllithium, resulted in the formation of anions 1.57 and 1.58 in varying amounts depending on base and were accompanied by products resulting from nucleophilic attack at phosphorus. Accordingly, the use of methyllithium resulted mainly in addition to phosphorus. The relative proportion of addition product was lowered as the base became more sterically demanding such that the use of *t*-BuLi resulted in negligible nucleophilic attack, and near quantitative formation of 1.58. Subsequent treatment of 1.58 with methyl iodide, *n*-BuLi, and finally benzaldehyde, allowed isolation of diphenyl(*ortho*-tolyl)phosphine oxide 1.15a in 58% yield. Unfortunately, study of this reaction is limited to one example, and the process has limited synthetic utility since it ultimately produces a low yield of a phosphine oxide which is accessible by other methods.

evidence.¹⁰⁴ While aggregation of the alkyllithiums may be crucial for the outcome of a reaction, selection of the most suitable base is often just as important and frequently must be determined experimentally.

The superbases mixtures (alkyllithium / potassium *t*-butoxide - "LICKOR"; or LDA / potassium *t*-butoxide - "LIDAKOR"), discovered by Lochmann and developed by Schlosser and co-workers,^{105,106} have not been widely used for DoM chemistry. However, recent reports of deprotonation in the three isomers of fluorotoluene³² and methoxytoluene¹⁰⁷ indicate that superbasic mixtures may have profound effects on the regioselectivity of metalation reactions. Similar base mixtures have been shown by Gros and co-workers to have a dramatic effect on the regioselectivity in certain pyridine metalations.¹⁰⁸

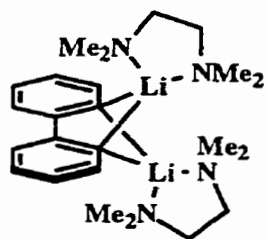
1.2.4.2 Solvents and Additives

Aggregation of alkyllithium bases in solution has a strong dependence on the solvent and the presence of any additives in solution. Solutions of *n*-BuLi in hydrocarbon solvents such as benzene or cyclohexane have been shown to exist as the hexameric aggregate.^{109,110} By contrast, *s*-BuLi in cyclopentane exists as an equilibrium between hexamer and tetramer aggregates,¹¹¹ while *t*-BuLi in hexane, cyclohexane, or benzene exists solely as the tetrameric species.^{110,112} With such solutions in hydrocarbon solvents, it seems likely that the steric demand of the alkyl group is the predominating factor in determining level of aggregation. On the other hand, the presence of coordinating atoms (i.e. in solvents or additives) clearly has some effect in breaking down aggregates as *n*-BuLi has been shown to exist as a tetramer in either THF or Et₂O solution.¹¹³⁻¹¹⁶ Similarly, the equilibrium hexamer / tetramer mixture of *s*-BuLi that was evident in hydrocarbon solvents disappears in favour of the tetramer in THF or Et₂O,¹¹⁷ and *t*-BuLi is reduced to a dimer in THF solution.¹¹⁷

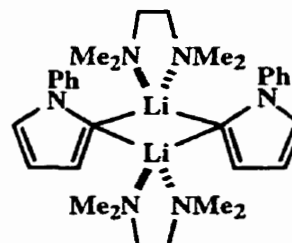
Without a doubt, the most commonly used additive in DoM reactions is *N,N,N',N'*-tetramethylethylenediamine (TMEDA), which was first observed to accelerate the rate of *ortho* metalation reactions by Slocum and co-workers over 30 years ago.¹¹⁸ The use of such additives has been vigorously investigated in the context of mechanistic understanding of

reactivity between substrates and bases. While it is clear that the presence of chelating additives often provides increased yields and reaction rates, the mechanism by which this takes place is unclear,¹⁴ and has been the subject of considerable debate.¹¹⁹ In principle, the additive serves to deaggregate alkyllithiums rendering them more reactive towards deprotonation of a substrate.^{7,13} However, Collum demonstrated that with lithium amide bases such as lithium hexamethyldisilazide (LiHMDS), THF is a far superior ligand for lithium than TMEDA.¹⁴ Thus, a solution of LiHMDS in THF / pentane affords solvated LiHMDS exclusively as the dimer [(LiHMDS)(THF)]₂, while in a TMEDA / pentane mixture the monomeric chelate (LiHMDS)(TMEDA) is the only observable form of the base. This observation might lead one to the conclusion that TMEDA is a superior ligand since the LiHMDS aggregates have been broken down further; however, LiHMDS in a THF / TMEDA / pentane solution affords only the dimeric THF complex with no evidence of the monomeric form. The implication is that deaggregation of LiHMDS in a pentane / TMEDA mixture is not necessarily due to a strong metal-ligand interaction. Concentration effects may also play a role as demonstrated with solutions of *n*-BuLi. Thus, addition of TMEDA to a low concentration of *n*-BuLi results in monomeric base, a species which dimerizes when higher concentrations are reached.¹²⁰

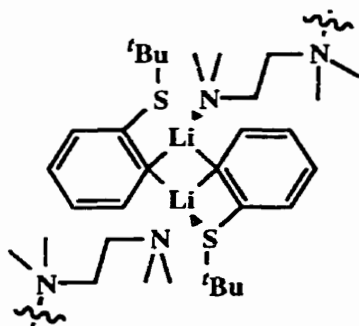
As evidenced by the numerous reported X-ray structures,^{121,122} and spectroscopic data,^{123,124} TMEDA is believed to act primarily as bidentate ligand (*eg.* **1.60** and **1.61**) on lithium; however, monodentate and mixed structures have also been reported (*eg.* **1.62** and **1.63** respectively).^{125,126} Despite the suggestion that TMEDA *may not* be a good ligand for lithium,¹⁴ TMEDA-assisted lithiations continue to pervade the literature.¹²⁷⁻¹³⁰ It has also been demonstrated that aggregates of LDA break up in neat TMEDA, but that the presence of THF will displace the TMEDA ligands.¹³¹ In addition, the presence of TMEDA has also been shown to provide rate accelerations in certain metalation reactions.¹³¹⁻¹³³ Though the mode of action of TMEDA is still a matter of some debate, its ability to enhance certain reaction rates cannot be argued (*cf.* Section 1.2.4.2).



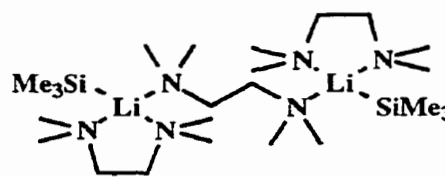
1.60



1.61



1.62



1.63

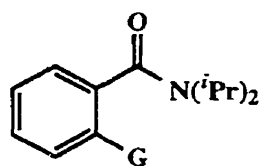
Other similar chelating amines have also been used. *N,N,N',N',N''*-Pentamethyldiethylenetriamine (PMDTA), a tridentate analogue of TMEDA, has been used successfully as an additive in metalation reactions,^{33,66} though it has been noted that the cost of the reagent may be responsible for preventing its widespread application in synthesis.¹³⁴ Thurner and co-workers have recently offered *N,N,N',N',N''*-pentamethyldipropyl-enetriamine (PMDPTA) as a more cost effective alternative¹³⁴ since it is manufactured on industrial scale and available in large quantities.¹³⁵ The scope of this additive has not yet been fully explored.

1.2.4.3 Mechanistic Studies - Complexation

Although interest in the mechanism of the DoM reaction began shortly after its discovery, there is still incomplete knowledge. The *ortho* metalation of anisole has received the greatest amount of attention though several other DMGs have been studied.

In 1946, Roberts and Curtin first proposed that a complexation between anisole and *n*-BuLi occurs initially which facilitates *ortho* metalation.¹³⁶ This reaction pathway, now known as the *Complex Induced Proximity Effect* or "*CIPE*", has been used in describing several *ortho*

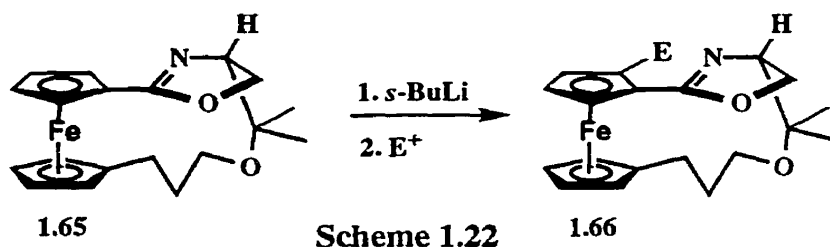
lithiations⁷⁻⁹ and has also been implicated in metal-halogen exchange reactions.¹³⁷ The enhanced acidity of the *ortho* protons is said to derive from the precomplexation between a heteroatom(s) in the DMG and the alkyllithium reagent. The newly formed complex places the base in a favourable location near the *ortho* proton resulting in deprotonation. Examples of proposals for precomplexation affecting regiochemistry in metalation reactions are replete in the literature.^{12,138-141} In the context of DoM chemistry, Beak¹⁴² demonstrated the contribution of CIPE by measuring relative metalation efficiency of DMGs which are electronically similar but are restricted in orientation. Thus, for a series of tertiary amides, secondary amides, and benzylic alcohols, orientation of the heteroatoms may have a significant effect on the relative rates of reaction. For example, competitive measurement of the metalating ability of amides **1.64a-d** gave relative efficiencies of 1800, 57, 1.2, and 1 respectively, correlating nicely with the calculated dihedral angles about the Ar-C(O) bond. Similar results were found in the secondary amide and benzylic alcohol series.



1.64

- a: G = H
- b: G = CH(Me)₂
- c: G = C(Me)₃
- d: G = TMS

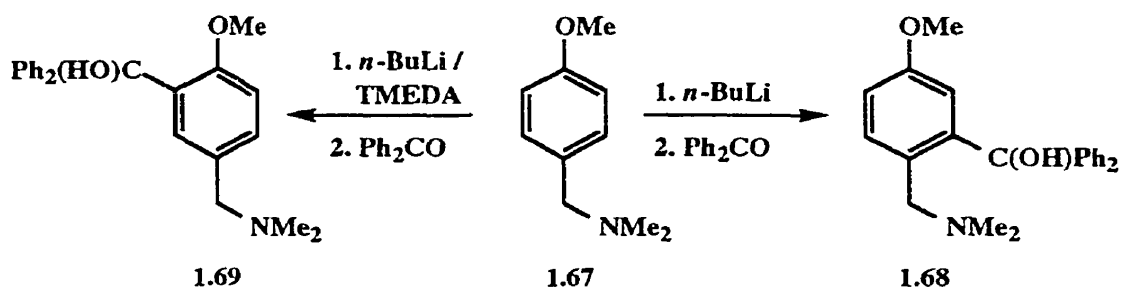
An interesting example of CIPE was recently provided by Sammakia and Latham.¹⁴³ Stemming from their earlier work on metalation of chiral oxazolinoferrrocenes¹⁴⁴ (*cf.* Section 1.3.2.2), an effort was undertaken to determine whether it was nitrogen or oxygen which was responsible for directing metalation. A chiral ferrocene derivative with an oxazoline DMG (**1.65**) in a fixed orientation was prepared. Metalation and quench with electrophiles demonstrated that the nitrogen dominated the directing since only a single product **1.66** (E = Me, TMS) was obtained (Scheme 1.22).



1.2.4.4 Mechanistic Studies - Induction

In a contradicting hypothesis, Schleyer suggested that precomplexation may not be a requirement for metalation and that the inductive effect of the DMG is the principal effect governing the regioselectivity. The term "kinetically enhanced metalation" has been coined to describe the overall process.¹⁴⁵⁻¹⁴⁸ The *n*-BuLi-mediated metalation of a series of substituted anisoles¹⁴⁹⁻¹⁵² examined by Slocum and co-workers suggested that this pathway is much more significant for DMGs with a heteroatom *directly bound to the aromatic ring*. Slocum proposed¹⁴⁹ that the complexation step between the alkyllithium and the unshared OMe electrons is a relatively slow step due to the ground state resonance delocalization of the electrons into the ring, a pathway which is not accessible to DMGs in which the heteroatom is one or more atoms removed from the ring. Subsequent to complexation, the deprotonation was proposed to be a fast step, generating the lithiated intermediate. This mechanism is supported by the slow observed rate (approx. 55% completion after 24 h at rt) of metalation of anisole by 1.0 equiv. of *n*-BuLi, a rate which was only marginally increased when 2.0 equiv. of *n*-BuLi were used. However, inclusion of a stoichiometric amount of TMEDA drastically increased the rate such that the reaction had reached > 95% completion after only a few minutes. Interestingly, it was found that even a catalytic amount of TMEDA dramatically increased the reaction rate. The observed rate increase in the presence of TMEDA was taken to indicate that the rate limiting coordination step is unnecessary, that the added TMEDA serves to increase basicity, and that the regioselectivity is governed by the inductive effect provided by the methoxy group. Further evidence of this proposal was found when *N,N*-dimethyl *p*-methoxybenzylamine (1.67) was metalated with or without TMEDA (Scheme 1.23).^{118,153}

In the absence of TMEDA, metalation occurred exclusively *ortho* to the dimethylaminomethyl group affording **1.68**, while the inclusion of TMEDA (1 equiv.) furnished **1.69**, derived from metalation exclusively *ortho* to the methoxy group. This remarkable regioselectivity was rationalized by the coordinative vs. inductive mechanisms. When no TMEDA is present, the coordinative mechanism dominates since the nitrogen lone pair is one atom removed from the aromatic ring and is thus not delocalized. Alternatively, when TMEDA is added, the inductive metalation pathway of the methoxy group overrides the coordinative metalation pathway of the benzylic amine DMG.

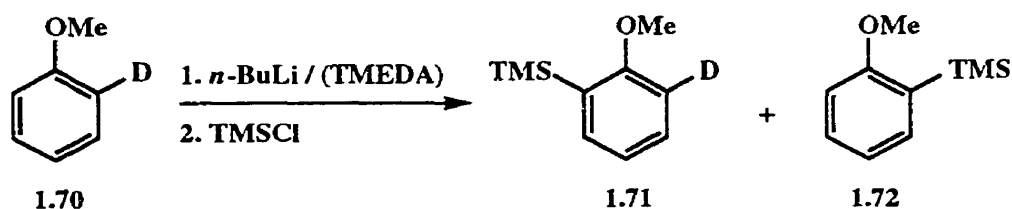


Scheme 1.23

Additional supportive evidence was found in the metalation of *p*-fluoroanisole.¹⁵⁰ The faster rate of metalation of this substrate compared to anisole was rationalized on the basis that the resonance effect of the fluoro substituent decreases the resonance contribution of the methoxy substituent making it a better *coordinative* director. In addition, the inductive effects of the two electron withdrawing substituents combine to render the ring protons more acidic. Consistent with these results is the observation that *p*-dimethoxybenzene undergoes metalation at a considerably faster rate than anisole.¹⁵²

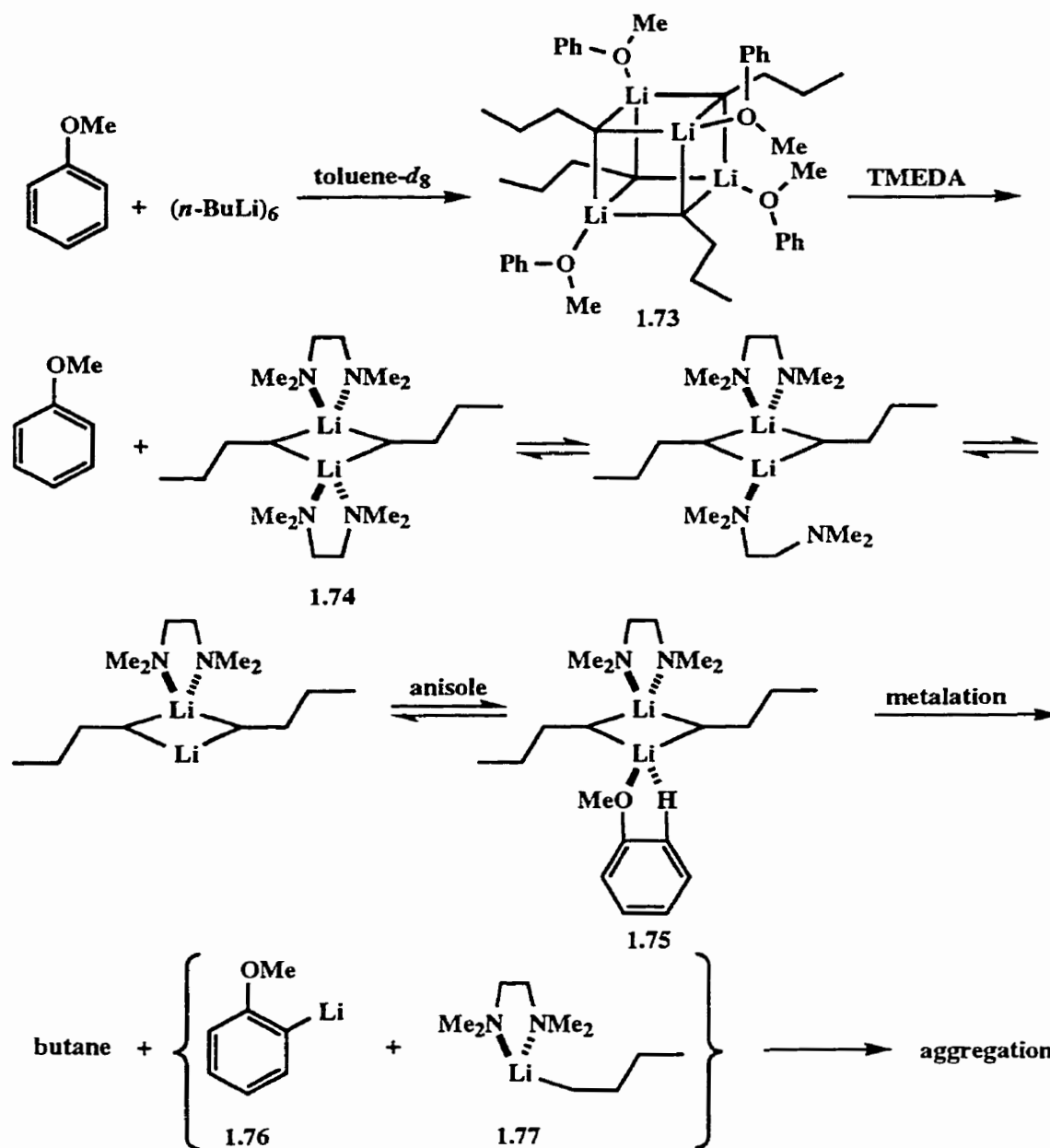
Contradictory to Slocum's study is the recent kinetic isotope effects (KIE) study by Stratakis.¹²⁸ Metalation of 2-deuterioanisole (**1.70**) with *n*-BuLi (with *or* without TMEDA) proceeded to give, after quench with TMSCl, a mixture of substituted anisoles **1.71** and **1.72** (Scheme 1.24). Based on product mixture analysis $k_{\text{H}} / k_{\text{D}} = 2.3 \pm 0.1$ in the absence of TMEDA and $k_{\text{H}} / k_{\text{D}} = 3.1 \pm 0.1$ in the presence of TMEDA were measured. Similarly,

competitive intermolecular experiments between anisole and anisole- d_5 gave values for k_H / k_D of 2.5 ± 0.2 and 3.2 ± 0.2 for reactions with and without TMEDA respectively. These results indicate that the deprotonation step is the rate determining step in the reaction. However, Stratakis emphasized that these results neither require nor eliminate the formation of a preequilibrium n -BuLi-anisole complex. From previous spectroscopic studies,^{148,154,155} and trapping of lithiated intermediates with TMSCl, Collum established that the lithiation of anisole in toluene proceeds via $(n\text{-BuLi})_2(\text{TMEDA})_2(\text{anisole})$.¹²⁹ In agreement with Stratakis, kinetic isotope evidence showed that deprotonation is the rate limiting step, however, $k_H / k_D = 20 \pm 3$ for metalation of anisole vs. metalation of anisole- d_8 was established in contrast to Stratakis' value of approximately 3. Although the methods used for determination of k_H / k_D are different, it is unclear why such a large discrepancy exists.



Scheme 1.24

Based on ^6Li - ^1H HOESY NMR experiments and supporting MNDO calculations, Bauer and Schleyer¹⁴⁸ demonstrated that a complex is formed between n -BuLi and anisole, but that no metalation of anisole takes place until TMEDA is added. Thus, addition of n -BuLi to a solution of anisole in toluene- d_8 results in destruction of the hexameric n -BuLi aggregate and formation of a tetrameric anisole- n -BuLi complex **1.73** (Scheme 1.25). Despite the proximity of the *ortho* protons to the alkyllithium reagent, no *ortho* metalation takes place after one hour. Notably, addition of a stoichiometric amount of TMEDA to the mixture releases the complex (as evidenced by NMR) and results in the formation of a n -BuLi / TMEDA dimeric complex **1.74** which readily metalates anisole. Though the stepwise mechanism by which **1.74**



Scheme 1.25

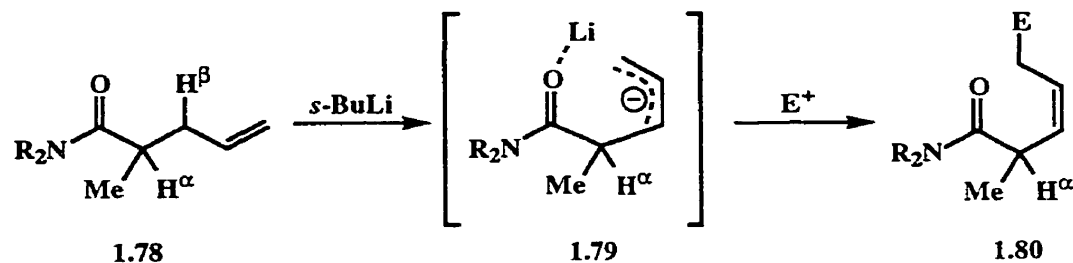
metalates anisole was not discerned, Schleyer proposed that one of the TMEDA ligands undergoes dissociation from **1.74** in a stepwise fashion leaving two coordination sites available at one of the lithium atoms. The free coordination sites are then occupied by the OMe lone pair in an agostic Li-H interaction (**1.75**) and an irreversible deprotonation takes place

liberating butane, a *n*-BuLi / TMEDA monomer (**1.77**) that can reaggregate, and lithiated anisole (**1.76**) which may also aggregate. Saá has also concluded from MNDO calculations that agostic interactions are important in the metalation of 1,3-bis-DMG systems,¹²⁷ phenols,^{156,157} and naphthols.¹⁵⁸

Collum and co-workers have provided evidence that, in addition to anisole,¹²⁹ other PhDMG systems (DMG = H; 1,3-di-OMe; OMOM; OCH₂CH₂NMe₂) are metalated by *n*-BuLi / TMEDA by a common mechanism involving *n*-BuLi dimers.¹¹⁹ While the rate studies support an inductive model^{159,160} and do not necessarily support a CIPE argument, the authors are quick to point out that their results do not conflict with earlier work of Beak and co-workers¹² providing evidence of a CIPE mechanism in amide metalations.

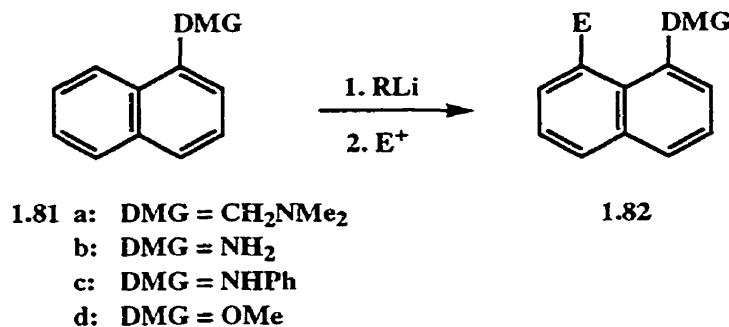
1.2.5 Directed Remote Metalation (DreM)

The CIPE concept has also been used in describing Directed remote Metalation (DreM), that is, deprotonation in a position which is distant (not *ortho*) from the activating functional group.^{8,161} In the context of aliphatic chemistry, this usually means that deprotonation occurs in a position which would not be expected based on thermodynamic acidity. An instructive illustration of this process was provided by Beak in the metalation and substitution in the δ -position of tertiary amides (Scheme 1.26).¹⁶² When amides **1.78** were treated with *s*-BuLi, and quenched with electrophiles, the δ -substituted products **1.80** were obtained, presumably through initial coordination of the base to a heteroatom and β -deprotonation to produce a stabilized intermediate such as **1.79**. That there is no deprotonation in the α position, despite the considerably higher thermodynamic acidity, was shown through isotopic substitution experiments. An estimated pK_a difference between the α and β protons of 9 ± 2 drives this point home.



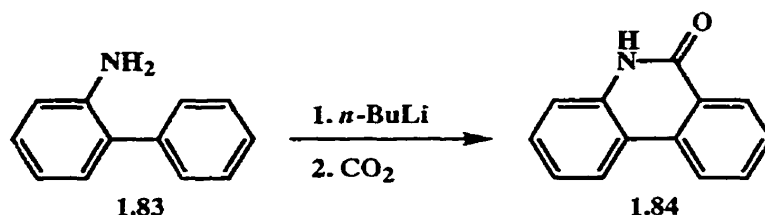
Scheme 1.26

In an early example of DreM in aromatics, Hauser¹⁶³ and co-workers reported that 1-dimethylaminomethylnaphthalene (**1.81a**) underwent deprotonation in the 8-position, while Eaborn¹⁶⁴ and co-workers and Narasimhan and Ranade¹⁶⁵ reported analogous reactivity for 1-aminonaphthalene (**1.81b**) and *N*-phenyl-1-aminonaphthalene (**1.81c**), respectively. Similarly, Shirley and Cheng¹⁶⁶ noted that 1-methoxynaphthalene (**1.81d**) underwent selective metalation in the 8-position when *t*-BuLi in pentane / cyclohexane (1:1) was employed as the metalating agent (Scheme 1.27). In contrast, metalation was selective for the 2-position when either *n*-BuLi or *t*-BuLi was used in conjunction with a diamine (TMEDA or TEEDA).



Scheme 1.27

The first case of DreM in a biaryl system was reported by Narasimhan and Alurkar¹⁶⁷ in 1969 who showed that treatment of 2-aminobiphenyl (**1.83**) with *n*-BuLi followed by quench with CO₂ resulted in 34% yield of phenanthridone (**1.84**, Scheme 1.28). The reaction was later adapted to produce phenanthridines upon quench with DMF instead of CO₂.¹⁶⁸

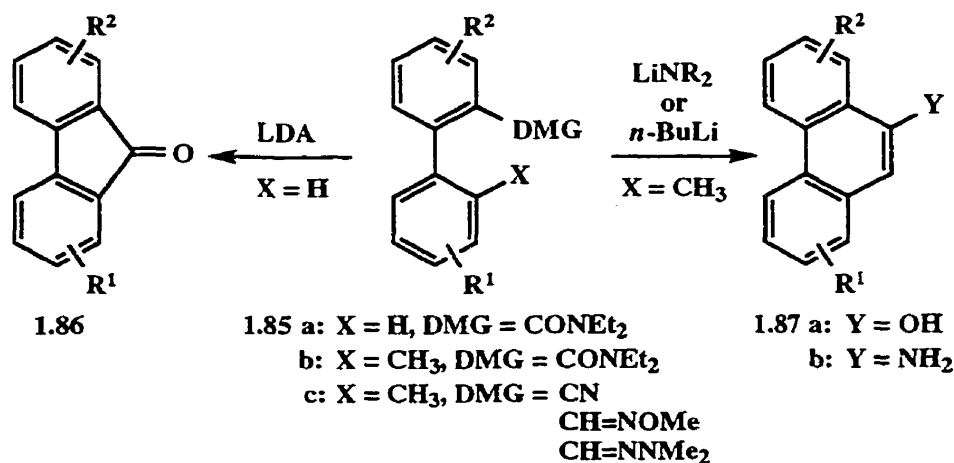


Scheme 1.28

While many of these early experiments were low yielding, they were regioselective and thus laid the groundwork for development of modern DreM reactions. As discussed below, several ring systems are now available through remote metalation pathways.

1.2.5.1 Fluorenones, Phenanthrols and 9-Aminophenanthrenes

The utility of the tertiary amide DMG in DreM reactions has been established in 2-amidobiaryls which undergo DreM with RLi or LiNR₂ bases to provide fluorenones and phenanthrols (Scheme 1.29). Thus, treatment of amides **1.85a** with LDA effects a remote deprotonation in the 2'-position, which is followed by an intramolecular cyclization reaction to afford, after workup, fluorenones **1.86**.¹⁶⁹ This procedure has found application as a key step in the synthesis of several natural products.^{69,169-171} Alternatively, the presence of a methyl group



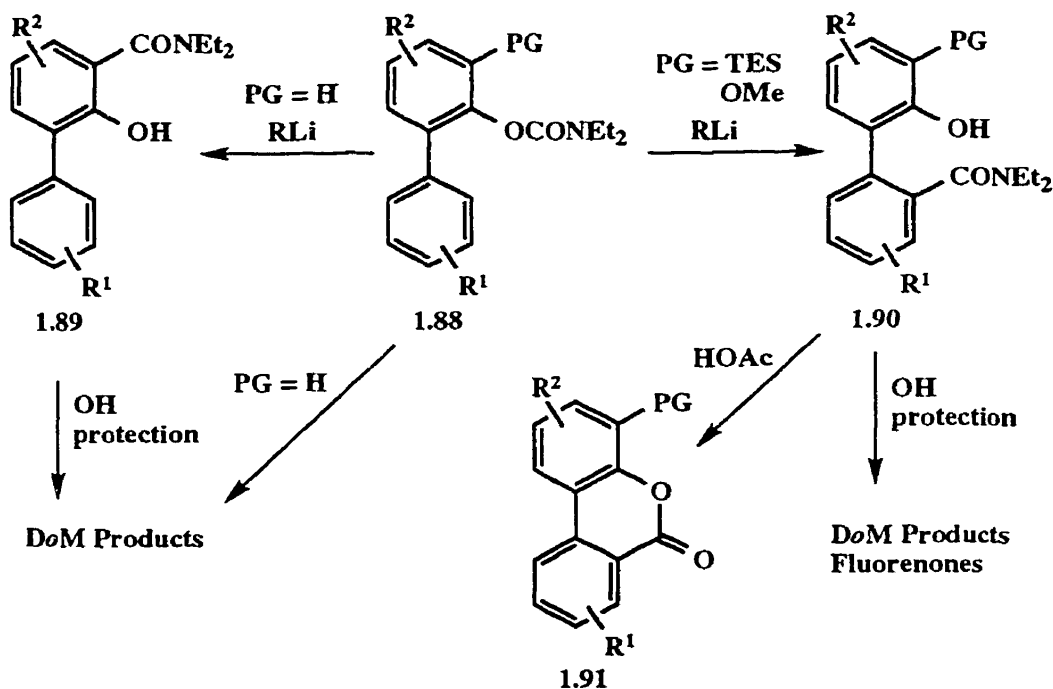
Scheme 1.29

in the 2'-position radically changes the outcome of the reaction. Treatment of amides **1.85b** with LDA or *n*-BuLi results in a remote tolyl deprotonation and intramolecular cyclization. The presumed loss of diethylamine on workup results in formation of 9-phenanthrols **1.87a**.¹⁷²

The phenanthrol products have proven to be valuable intermediates in the synthesis of natural products^{70,173} and polycyclic aromatic hydrocarbons (PAHs).¹⁷⁴ Analogous treatment of nitriles, oximes, or hydrazones **1.85c** with lithium diethylamide proceeds to give 9-aminophenanthrenes **1.87b** and this reaction has been applied to the synthesis of the alkaloid piperolactam C.¹⁷⁵

1.2.5.2 Dibenzo-[*b,d*]-pyranones

Analogous study of biaryl 2-*O*-carbamates led to the development of a DreM version of the anionic Fries rearrangement.⁷⁴ Careful selection of protection groups and reaction conditions allows for selective synthesis of a variety of products from common starting materials (Scheme 1.30). Thus, the versatile carbamate DMG in **1.88** may be used in straightforward DoM chemistry (PG = H) producing *ortho*-substituted or anionic *ortho* Fries



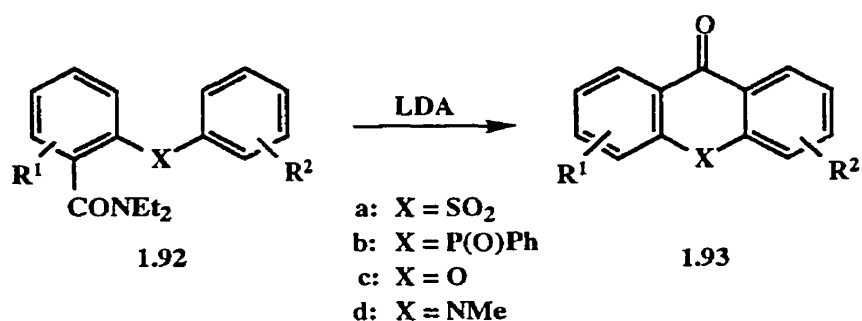
Scheme 1.30

rearrangement products (**1.89**). After *OH* protection, further DoM chemistry on this Fries product may then be accomplished utilizing the amide DMG. Alternatively, an appropriate

protecting group in the 3-position (PG = TES, OMe) allows metalation in a remote position resulting in a ring-to-ring carbamoyl migration to give biaryl amides **1.90**.¹⁷⁶ The resulting hydroxyamide may be protected and subjected to *DoM* chemistry or fluorenone formation (Scheme 1.29), or treated with acid to form dibenzo-*[b,d]*-pyranones **1.91**, a method which has also been applied to the synthesis of several natural products.^{72,176}

1.2.5.3 Acridones, Xanthenones, Phosphininones, Thioxanthenones

Recently, the DreM concept has been expanded to encompass biaryl systems with a heteroatom spacer between the two rings providing access to a wide variety of fused heterocycles (Scheme 1.31).



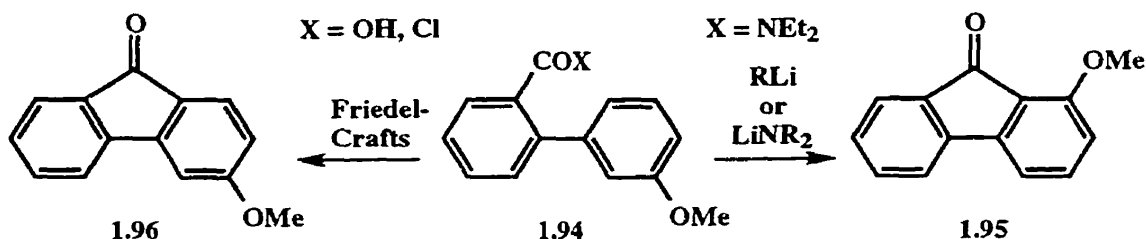
Scheme 1.31

The first example, reported by Beaulieu and Snieckus,⁴³ involves the treatment of diarylsulfone-2-amides **1.92a** with LDA effecting a remote metalation-cyclization sequence to form thioxanthen-9-one 10,10-dioxides **1.93a**. Again the tertiary amide DMG, which may be derived from an *ortho* or remote anionic Fries rearrangement of a carbamate, is utilized in an anionic cyclization to form the central ring.

Extension of this methodology for the synthesis of other heterocycles soon followed. Accordingly, triarylphosphine oxides **1.92b**, diaryl ethers **1.92c**, and *N*-methyldiarylamines **1.92d**, upon similar treatment with LDA, resulted in the formation of dibenzo-*[b,e]*-phosphininones **1.93b**,⁹⁷ xanthen-9-ones **1.93c**,⁷¹ and *N*-methylacridones **1.93d**¹⁷⁷ respectively. This new methodology has provided a mild, general means of synthesizing

complex fused heterocycles that would be difficult or impossible to prepare by classical, usually Friedel-Crafts, methods.

A significant aspect of DreM concerns systems where more than one mode of cyclization is possible. For each of the cyclizations described above, DMGs in the 2- and 3'-positions cooperate to direct metalation, and thus cyclization in the common "in between" site. For example, remote metalation - cyclization of biaryl amide **1.94** proceeds to give **1.95** exclusively (Scheme 1.32), a product which would be disfavoured by the classical Friedel-Crafts approach. The current procedure, while providing a mild, selective, and general route to several condensed aromatic systems and heterocycles, therefore constitutes a complementary methodology to classical electrophilic substitution methods.¹⁷⁸



Scheme 1.32

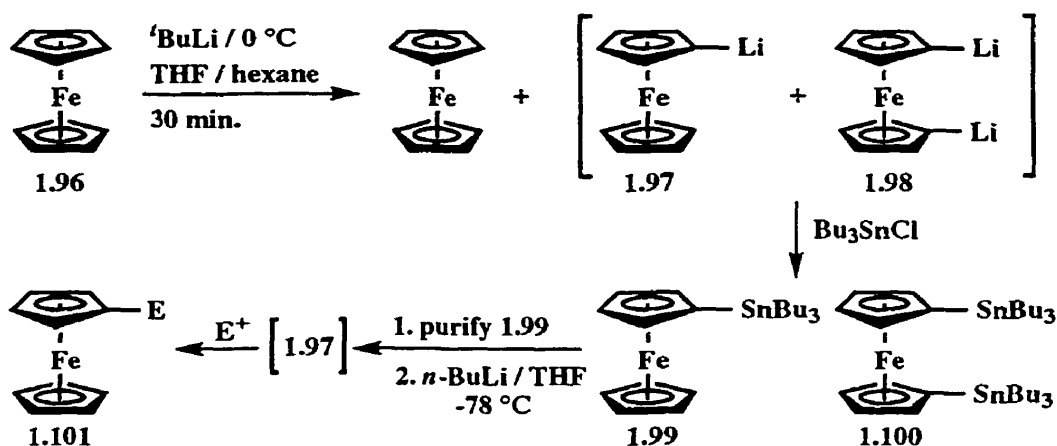
1.3 Ferrocene Metalation

Since the independent discovery of ferrocene by Kealy and Pauson,¹⁷⁹ and by Miller, Tebboth and Tremaine¹⁸⁰ in 1951, its reactivity has been vigorously explored. Although it was a serendipitous synthesis by both groups, the impact of this discovery on organometallic chemistry could not possibly have been predicted. Incorrect structural assignments were shortlived and soon Wilkinson and co-workers recognized the now familiar sandwich structure of ferrocene.¹⁸¹ Not long after the discovery of this unique organoiron complex, several other transition metal analogs were prepared opening the door to an exciting new field in organotransition metal chemistry.^{182,183} Today, substituted metallocenes find a wide range of applications¹⁸⁴ in such areas as organic synthesis,¹⁸⁵ asymmetric catalysis,¹⁸⁶ and materials

science.^{187,188} Some ferrocene molecules have been shown to have substantial biological activity and possible therapeutic value.¹⁸⁹

With the presence of two aromatic rings it is perhaps not surprising that ferrocene reactivity often parallels that of benzene. It was quickly established that ferrocene undergoes electrophilic aromatic substitution reactions, such as Friedel-Crafts acylations, in one or both rings.¹⁹⁰ Metalation chemistry is no exception, and has been a mainstay in synthesis of ferrocene derivatives since the first reports by Benkeser and Nesmeyanov in 1954.^{191,192} Though their early attempts at preparation of 1-lithioferrocene met with limited success, due primarily to contamination by 1,1'-dilithioferrocene, they provided the basis for modern methods. Various modifications in solvent, temperature and reaction conditions have allowed for optimization such that 1-lithioferrocene, and hence 1-substituted ferrocene derivatives, may be prepared in as high as 70% yield with minimal interference of 1,1'-disubstituted products.¹⁸⁶ Furthermore, Guillaneux and Kagan have developed a method whereby 1-lithioferrocene can be prepared without detectable contamination by 1,1'-dilithioferrocene.¹⁹³ Accordingly, ferrocene (**1.96**) was metalated (2.0 equiv. *t*-BuLi / 0 °C / 30 min / THF:hexane 1:1) to give an intermediate mixture of ferrocene, 1-lithioferrocene (**1.97**) and 1,1'-dilithioferrocene (**1.98**). Quench of the reactive intermediates with Bu₃SnCl gave a mixture of unreacted ferrocene, and stannyl derivatives **1.99** and **1.100** (Scheme 1.33). Purification by distillation under reduced pressure gave **1.99** as a dark red oil in 70 % yield. Transmetalation of **1.99** (*n*-BuLi / THF / -78 °C), generates pure monolithioferrocene which may then be quenched with various electrophiles to provide pure monosubstituted ferrocenes **1.101**. While the obvious utility of this method lies in the ability to prepare pure monolithioferrocene, the long term stability of **1.99** towards air and light make it even more attractive. Similar approaches to monolithioferrocene by transmetalation of chloromercurioferrocene,¹⁹⁴ or by halogen metal exchange with bromo- or iodoferrocene¹⁹⁵ have also been reported but these methods are less attractive owing to the instability and difficulty in preparation of the starting

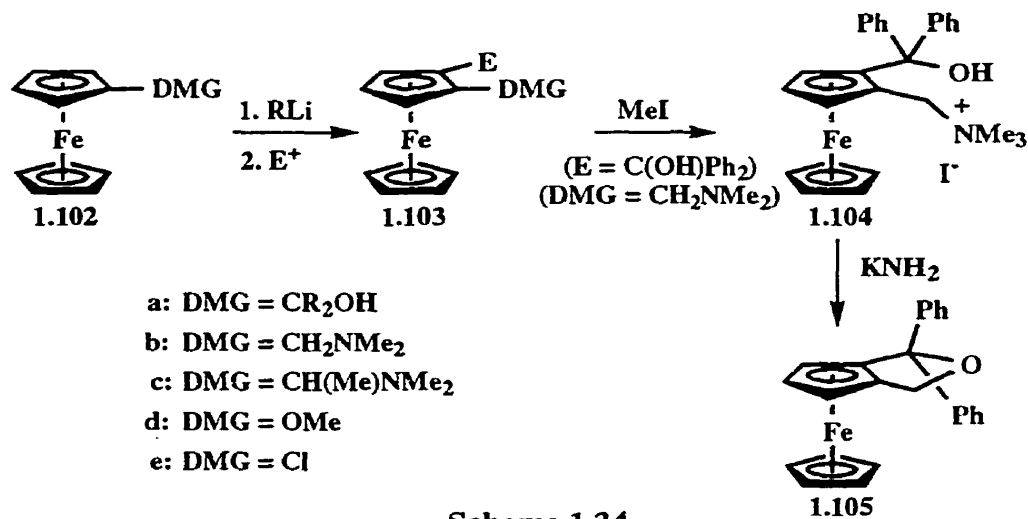
materials. Straightforward procedures are also available for the preparation of **1.98** devoid of any contamination by **1.97**.^{196,197}



1.3.1 Directed *ortho* Metalation of Ferrocene Derivatives

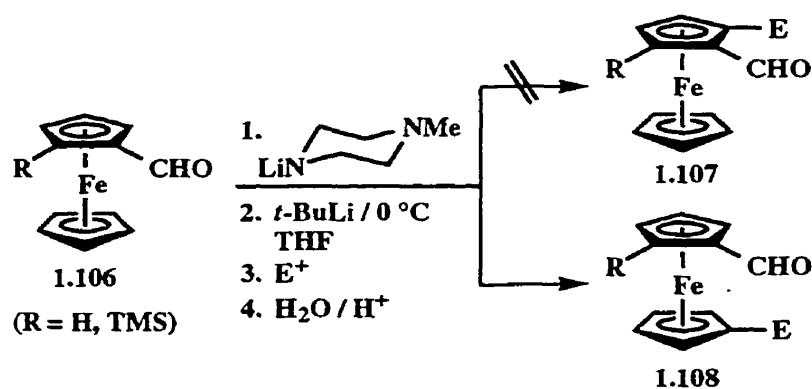
Application of DoM methodology to ferrocene substrates soon followed initial lithioferrocene experiments, perhaps in part due to the rapid evolution of both DoM chemistry and ferrocene chemistry during the same time period. In 1961, Benkeser and co-workers first described the DoM reaction in a ferrocene using $-CPh_2OH$ as the DMG.¹⁹⁸ Subsequently, the methodology steadily expanded to encompass other DMG-bearing ferrocenes (Scheme 1.34). Arguably the most important case was the metalation of dimethylaminomethylferrocene (**1.102b**)¹⁹⁹ which proceeded to completion in only 1 h compared to *N,N*-dimethylbenzylamine metalation which was known to require about 16 h.^{200,201} The importance of **1.102b** and its evolution into closely related amine **1.102c** will become evident in Section 1.3.2.2. Since sophisticated spectroscopic experiments were unavailable at the time the regioselectivity of the reactions often had to be proved by further derivatization or correlation experiments. For DMG = CH_2NMe_2 , this was accomplished by quenching the lithiated intermediate with benzophenone to give the tertiary alcohol **1.103b** ($E = C(OH)Ph_2$), quaternization to **1.104**, and cyclization to ether **1.105** (Scheme 1.34). Similarly, regioselectivity of methoxyferrocene (**1.102d**)^{202,203} and chloroferrocene (**1.102e**)²⁰⁴

metalation was widely speculated to occur in the 2-position, but firm proof of the 1,2-relationship of substituents was not established until some years after the initial work.²⁰² Smooth metalation of chloroferrocene also provided a notable exception to the tendency of ferrocene DoM chemistry to parallel benzene chemistry since chlorobenzene metalation is not a facile process, a result which implies increased acidity of ferrocene protons compared to benzene protons. Several other ferrocene DMG systems have since been developed including -C(O)NHR,²⁰⁵ -P(O)Ar₂,^{89,206,207} -OTHP,²⁰⁸ -S(O)R,³⁹ -CH(OR)₂,¹⁸⁶ and oxazolines.²⁰⁹



Scheme 1.34

Iftime²¹⁰ and co-workers reported an interesting regioselective C-1' directed metalation of ferrocenes. Thus, treatment of aldehydes **1.106** according to the method of Comins⁴⁶ surprisingly afforded, after quench with various electrophiles, 1,1'-disubstituted products **1.108** (R = H) with only minor contamination by the 1,2-disubstituted analogs **1.107** (R = H). The method has also been applied to the synthesis of 1,2,1'-trisubstituted systems **1.108** (R = TMS) where the regioselectivity in favour of heteroannular metalation is even more pronounced (Scheme 1.35).²¹¹ An extension of this methodology has recently been developed and applied to the synthesis of chiral ferrocene derivatives.²¹² This method, along with others, will be discussed in the following section.



Scheme 1.35

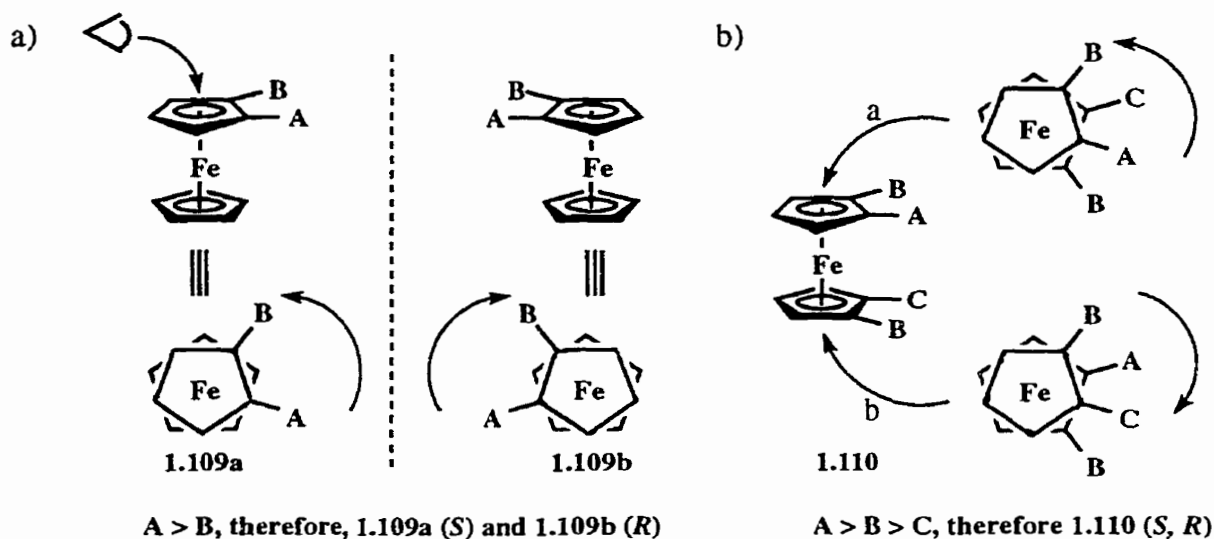
1.3.2 Planar Chiral Ferrocenes

Substituted ferrocenes and related metallocene derivatives have the unique ability to possess *planar chirality*, that is, chiral by virtue of an asymmetric plane.²¹³ This property is the driving force for much of the modern research in ferrocene chemistry.^{81,82,186} Methods for synthesis of ferrocenyl substrates possessing centres of chirality are not significantly different than other asymmetric methods normally employed in asymmetric synthesis. For this reason, discussion here will be limited to planar chirality and how it may be incorporated into substituted ferrocenes.

In order for planar chirality to exist in a ferrocene template, there must be at least two different substituents in the *same ring* of the molecule (eg. **1.106-1.108** [$\text{R} \neq \text{H}$]). Since there are two rings, it is possible for two chiral planes, and hence diastereomers, to exist based on planar chirality only. *Meso* compounds may result when the substituents on both rings are equivalent.

Assignment of absolute configuration in planar chiral derivatives is performed in a similar way to tetrahedral centres of chirality. As shown for enantiomers **1.109a** and **1.109b** in Scheme 1.36a, the molecule is turned such that it is viewed from *above* the chiral plane, and along the Cp-Fe-Cp axis. The substituents are then prioritized according to the standard Cahn-Ingold-Prelog rules.²¹⁴ Determination of the absolute configuration is accomplished by tracing the substituents around the ring from the highest priority substituent to the next highest and

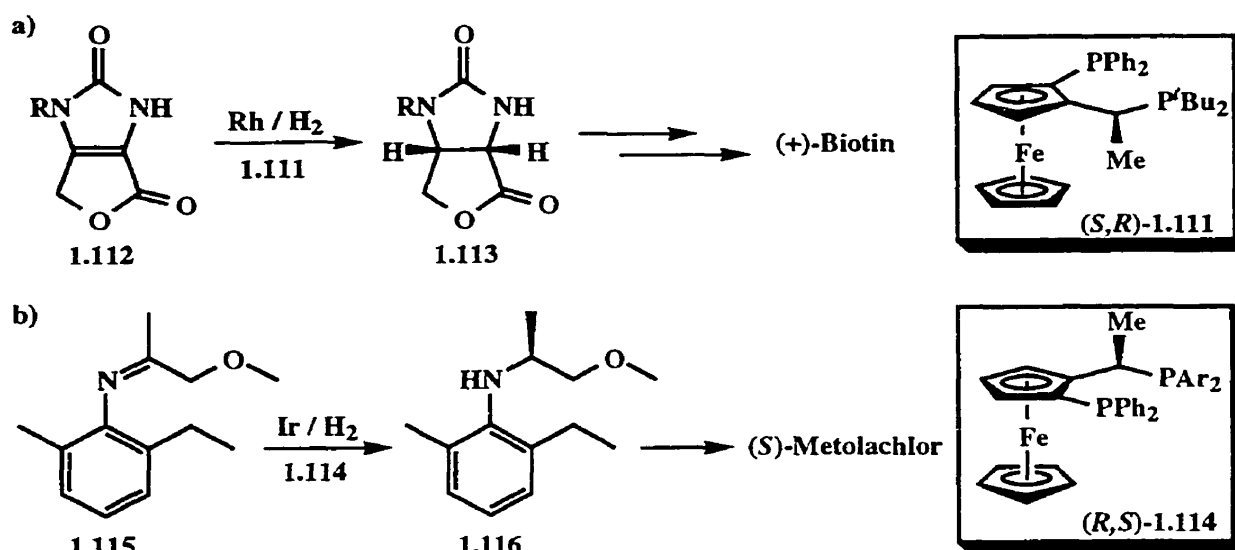
correlating the direction of travel around the ring either clockwise (*R*), or anti-clockwise (*S*). Similarly, where two chiral planes exist (1.110, Scheme 1.36b), the assignment is first made for the ring containing the highest priority substituent (substituent A > B, path a), then, in the same way, for the second ring (substituent B > C, path b). The same rules apply for 1,3-disubstituted systems and other polysubstituted systems which have at least two substituents in the same ring.



Scheme 1.36

Many chiral ferrocene systems find practical applications as chiral ligands for numerous metal catalyzed processes.^{81,82,184} The importance of this broad class of ligands is powerfully demonstrated in current industrial applications. Indeed, bis-phosphine ligands based upon ferrocene skeletons provide the chiral component for two commercially important syntheses (Scheme 1.37). In the first example, ligand 1.111 is applied to the asymmetric hydrogenation of the tetrasubstituted bond in 1.112 ($R = (S)\text{-PhCHMe}$), the key step in Lonza's commercial production of (+)-biotin, an important naturally occurring growth factor. Similarly, CIBA (Novartis) developed the related ligand 1.114 ($\text{Ar} = 3,5\text{-dimethylphenyl}$) which proved highly effective when used in conjunction with iridium for the asymmetric hydrogenation of imine 1.115. Though the mechanism of this crucial step in the synthesis of the selective pre-

emergence herbicide (*S*)-Metolachlor is not well understood, it is clear that the chiral ligand is responsible for providing the only chiral centre in the target molecule. Little significance is attached to the moderate (80%) enantiomeric excess since Metolachlor is an agrochemical product and the low ee is compensated for by the extremely high activity (substrate: catalyst $\geq 1 \times 10^6$).



Scheme 1.37

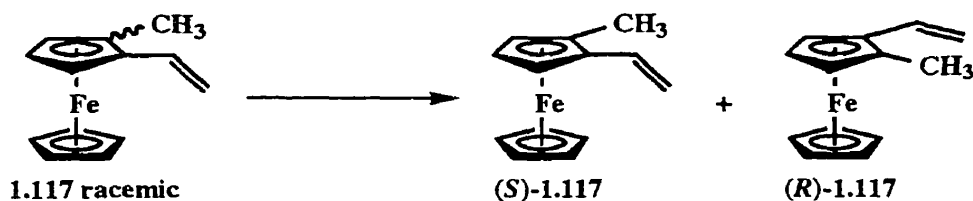
Each of the ligands presented in Scheme 1.37 contains a chiral centre as well as a chiral plane. Whether the chiral environment responsible for induction in these catalytic systems is derived from the chiral plane or from the chiral centre is unknown, and the overall importance of planar vs. central chirality in such systems is still a matter of debate. There is strong evidence suggesting that both elements of chirality play an important role in chiral induction.²¹⁵

Since the phenomenon of planar chirality in ferrocenes was recognized,^{216,217} chemists have sought methods to impart planar chirality into such systems. Techniques employed for creating chiral planes include chemical or enzymatic resolution techniques and metalation chemistry.²¹⁸ Metalation approaches may be further classified into diastereoselective approaches and enantioselective approaches as described below.

1.3.2.1 Planar Chiral Ferrocenes *via* Resolution

As with many chiral molecules, racemic mixtures of ferrocene derivatives possessing planar chirality may be separated and isolated by resolution techniques. Although chiral ferrocenes have been resolved by both chemical and enzymatic techniques, the latter technique has been most prevalent for resolution of planar chiral ferrocene derivatives.

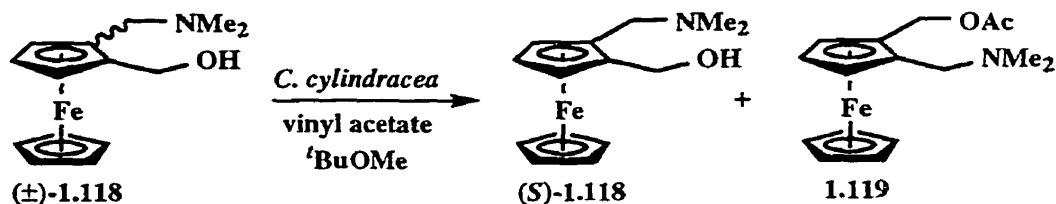
There are only a few scattered reports of resolution of planar chiral ferrocenes by chemical methods. Metalation of *N,N*-dimethylaminomethylferrocene (**1.102b**, Scheme 1.34) followed by quench with chlorodiphenylphosphine resulted in isolation of racemic **1.103b** ($E = PPh_2$), which was resolved by conversion into the corresponding phosphine sulfide dibenzoyl tartaric acid salt.^{219,220} Similarly, enantiomeric vinylferrocenes **1.117** (Scheme 1.38) were resolved, although the optical purity was subsequently shown to be only 86% ee.^{213,221}



Scheme 1.38

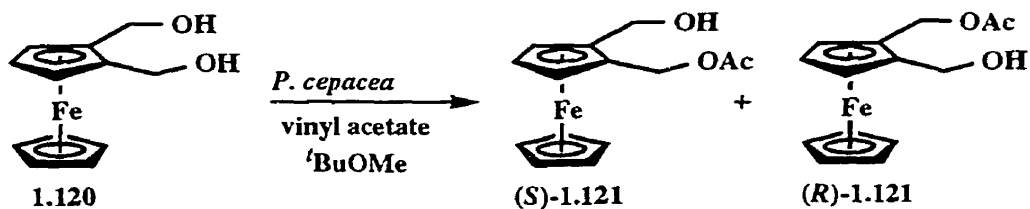
More frequently, racemic ferrocenes have been resolved by enzyme promoted kinetic resolution. Racemic amino alcohol **1.118** (Scheme 1.39) was subjected to enzyme catalyzed trans-esterification in which vinyl acetate was used as an acyl source.²²² A series of five enzymes was employed, converting the racemic mixture into acetate (*R*)-**1.119** and unreacted (*S*)-**1.118** with varying degrees of selectivity. Subsequent alkaline hydrolysis of (*R*)-**1.119** provided the enantiomeric aminoalcohol (*R*)-**1.118**. Optimal conditions (92% ee of **1.119**) were found using *Candida cylindracea* lipase and *tert*-butyl methyl ether solvent. A maximum 38% ee was obtained using any of the other lipases, although the use of immobilized *Mucor miehei* lipase (Lipozyme®) produced a mixture with the opposite selectivity, that is, (*R*)-**1.118** and (*S*)-**1.119**, with 35% ee. As an alternative to alkaline hydrolysis of (*R*)-**1.119**,

treatment of *rac*-**1.119** under alcoholysis conditions (*C. cylindracea* / *n*-butanol / *tert*-butyl methyl ether) provided (*R*)-**1.118** in as high as 98% ee.



Scheme 1.39

A similar transesterification reported by Nicolosi and co-workers involves enzymatic desymmetrization. Thus diol **1.120** was treated with vinyl acetate and *Pseudomonas cepacea* to provide alcohol (*S*)-**1.121** in 80% yield and 100% ee (Scheme 1.40).²²³ Attempts to produce the enantiomer (*R*)-**1.121** by similar enzyme catalyzed hydrolysis of the corresponding diacetate were unsuccessful. By contrast, the use of *Chromobacterium viscosum* allowed production of (*R*)-**1.121** selectively from **1.120** in 57% yield and with 100% ee. Whereas the remainder of the starting material was left unreacted in the *P. cepacea* case, yield in this example was sacrificed due to production of the *meso* diacetate.

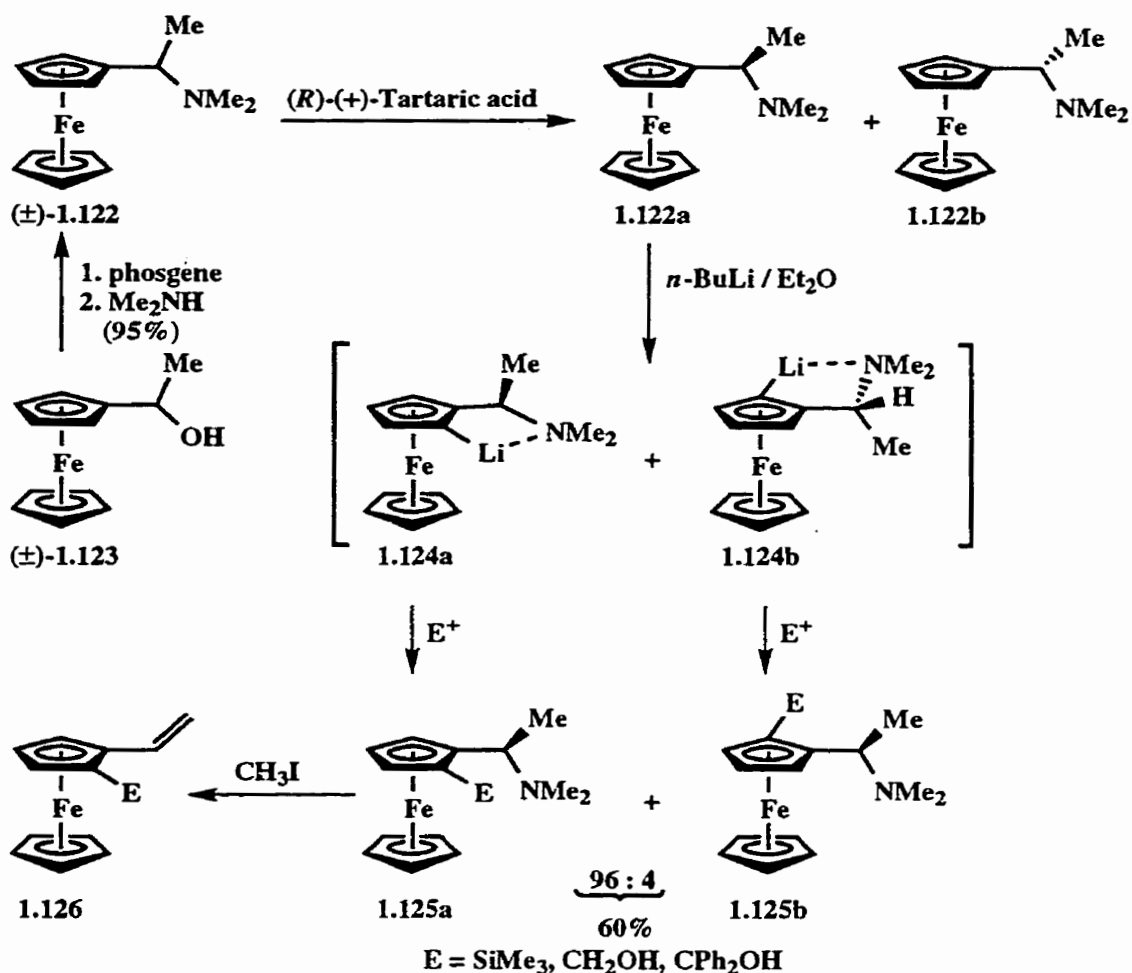


Scheme 1.40

Simple chemical transformations have also been applied to generation of ferrocenes with *only* the planar element of chirality by taking advantage of the facile substitution reactions which occur in the α -position or of chiral auxiliary use. This approach will be covered in more detail in Section 1.3.2.2 since the precursors have most frequently been formed *via* a diastereoselective metalation approach.

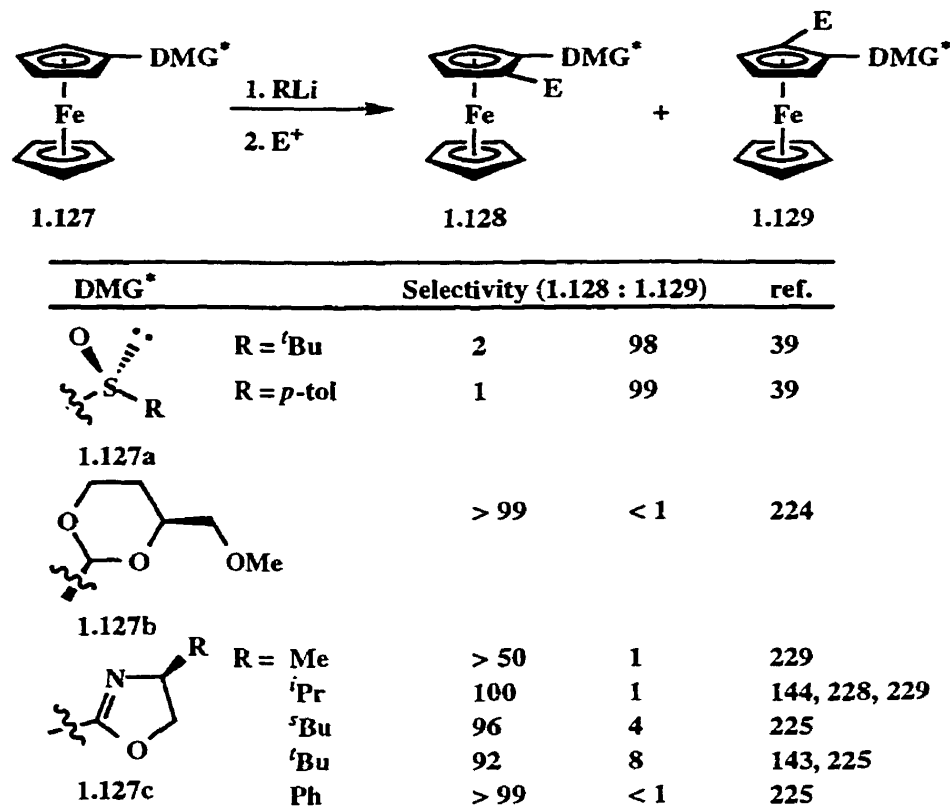
1.3.2.2 Planar Chiral Ferrocenes *via* Diastereoselective Metalation

During the early development of ferrocene metalation, it was recognized that the dimethylaminomethyl substituent acted as a powerful DMG for ferrocene systems (**1.102b** → **1.103b**, Scheme 1.34).¹⁹⁹ Ugi and co-workers, in a salient contribution, provided the first diastereoselective metalation approach.²²¹ Incorporation of an α -methyl group in **1.102b** provided an analogue containing a chiral centre which could be used to advantage in metalation. Thus, (\pm)-**1.122** was easily prepared from (\pm)- α -ferrocenylethanol (**1.123**) by reaction with phosgene followed by dimethylamine. Resolution of **1.122** with (*R*)-(+)-tartaric acid was accomplished to provide both enantiomers of **1.122** in high yield (Scheme 1.41). Metalation of **1.122a** proceeded smoothly in accordance with the analogous metalation of **1.102b** to provide 1,2-disubstituted ferrocenes **1.125** in a diastereoselective manner. The chiral environment created by the α -methyl group dictates the regioselectivity, and consequently the diastereoselectivity of the reaction. The high diastereoselectivity (96:4) observed, which is independent of electrophile, suggests that diastereoselectivity is induced in the deprotonation step. Unlike many stereoselective metalation reactions, there is little or no interconversion between diastereomers of the carbanionic intermediates **1.124a** and **1.124b** since this would necessitate a reprotonation / deprotonation sequence. Furthermore, no interconversion of diastereomers is expected in the substitution step since diastereomeric products differing in planar chirality (eg. **1.125a** and **1.125b**) arise from substitution at *different* carbon atoms in the ferrocene ring. That is, interconversion between diastereomeric products would require cleavage of the electrophile and reattachment at the diastereomeric carbon. Analogous metalation / substitution reactions using **1.122b** as the substrate proceed to give products **1.125** with the correspondingly opposite diastereoselectivity. Since both enantiomers of **1.122** are readily available, this procedure represents a powerful method for utilizing central chirality to induce planar chirality. In addition, treatment of chiral products **1.125** with methyl iodide leads to elimination and formation of vinylferrocenes **1.126** which contain *only* the planar element of chirality.



Scheme 1.41

This pioneering study by Ugi and co-workers led the way for several other groups to investigate metalation of ferrocenyl-DMG systems involving DMGs with chiral centres (1.127) to produce 1.128 or 1.129 selectively (Scheme 1.42). Kagan and co-workers¹⁸⁶ reported diastereoselective metalation of chiral sulfoxides³⁹ and acetals.²²⁴ Both of these methods avoid resolution of substrates and rely on asymmetric synthesis of starting materials. More recently, several groups have studied the diastereoselective metalation of ferrocenes bearing a chiral oxazoline DMG.^{143,144,225-229} While the achievement of highly diastereoselective results in these studies are impressive, certain aspects require further discussion, particularly in reference to the oxazoline DMG (Scheme 1.42).



Scheme 1.42

Using several different oxazolines with varying R groups, results have been reported which suggest a strong dependence on reaction conditions, particularly with respect to choice of alkyl lithium base and solvent. Richards reported²²⁸ that metalation of **1.127c** (R = ⁱPr) with *n*-BuLi in Et₂O gave a 2.5:1 ratio of products **1.128** and **1.129** after quench with ClPPh₂ (E = PPh₂). Concurrent reports by Sammakia and co-workers noted that under the same conditions, but in the presence of TMEDA, a diastereoselectivity ratio as high as 100:1 was observed.^{143,144} This provides yet another example of the profound effect of TMEDA on metalation reactions.

A further study by Sammakia and co-workers¹⁴³ showed that when **1.127c** (R = ⁱPr) was treated with each of *n*-BuLi, *s*-BuLi, and *t*-BuLi, products **1.128c** and **1.129c** (E = TMS) were formed in ratios of 2:1, 8:1, and 16:1, respectively. This suggests that there is a strong interaction between the oxazoline and the alkyl lithium which becomes more pronounced

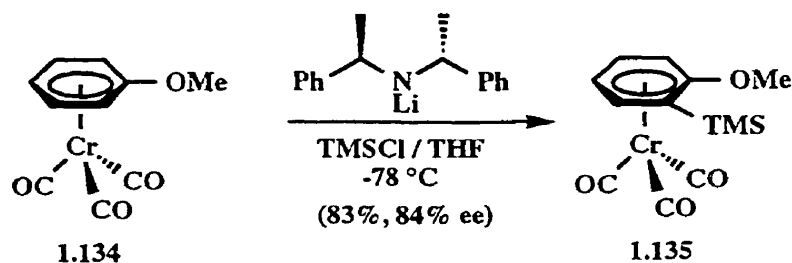
as the steric bulk of the base is increased. The critical role of the solvent in these reactions was also explored, and it was shown that metalation (*n*-BuLi in the absence of TMEDA) in hexane, THF, or Et₂O resulted in diastereomer ratios of 1:1, 2:1, and 6:1, respectively. Addition of TMEDA to the reaction mixture greatly improved the diastereomer ratios for reactions in hexane and Et₂O solvents (100:1), but the effect was much less pronounced in the case of THF (3:1).

The predominance of **1.128c** as the major diastereomer in these reactions was contrary to a prediction based on the following argument. It was proposed that a steric interaction between the R group on the oxazoline moiety and the rest of the ferrocene molecule would orient the oxazoline in such a way that the R group was forced up and away from the iron atom (**1.130b**, Scheme 1.43). If this was indeed the case, one of two conditions must hold in order to explain the predominance of **1.128**. Either the oxygen atom, and not the nitrogen is responsible for directing the deprotonation, or a conformation results in which the R group is oriented towards the iron and the rest of the ferrocene molecule. In order to investigate this further, the constrained ferrocenyl oxazoline **1.65** (Scheme 1.22) was prepared and treated under identical metalation conditions. The formation of **1.66** as the sole product provided firm evidence that the nitrogen is responsible for directing the metalation reaction. As a consequence, the transition state leading to the major product must involve a structure in which the R group on the oxazoline is oriented towards the iron atom (**1.130a**). It is then reasonable to conclude that an R / alkyl lithium steric interaction (**1.130b**) is the driving force which provides the observed selectivity, at least for the range of R groups tested (Scheme 1.42), and that the initially proposed R / ferrocene steric interaction is less important in determining the stereochemical outcome.^{143,228} This hypothesis also provides some rationalization for the variation in selectivity when different bases are employed.

yield. The silyl intermediate **1.131b**, upon a second metalation-electrophile quench produced trisubstituted ferrocene **1.132**. Smooth desilylation by treatment with TBAF provided **1.133**, the planar diastereomer of **1.131a**, in good overall yield. Alternatively a two step, one pot metalation procedure was applied to give an improved overall yield of **1.132** without compromising the optical integrity of the product.

1.3.2.3 Planar Chiral Ferrocenes *via* Enantioselective Metalation

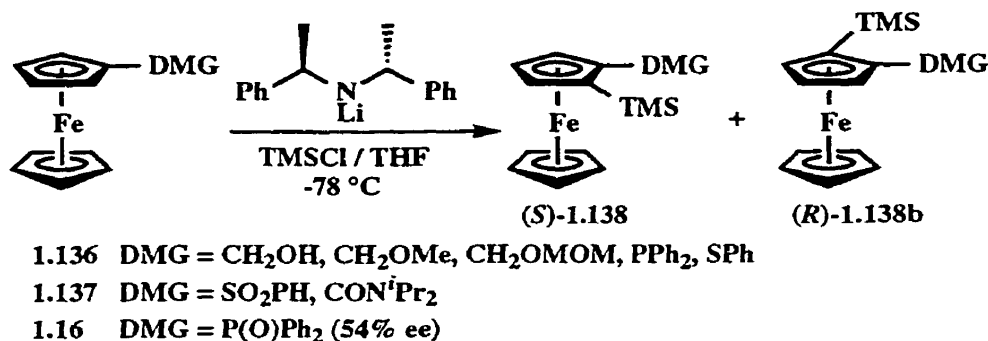
Although the utility of the diastereoselective procedures described above has been amply demonstrated, the requirement for substrate specific resolution or chiral auxiliary removal still persisted. The first attempts to circumvent these requirements were reported by Price and Simpkins in 1995.⁸⁹ This protocol, which has already been briefly described (Scheme 1.5, Section 1.2.3.1), borrows from established methodology for the asymmetric metalation of planar chiral tricarbonyl(η^6 -arene)chromium (0) complexes such as **1.134** (Scheme 1.45).²³⁰⁻²³³ The underlying principle in this approach is to provide a chiral environment in the transition state by employing a chiral lithium amide base as the metalating



Scheme 1.45

agent, thus inducing an asymmetric deprotonation. While the chromium complex **1.134** provided chiral products **1.135** in good yields and with reasonable enantioselectivity, extension to ferrocenyl DMG systems proved quite difficult and gave disappointing results (Scheme 1.46). Most of the DMG systems (**1.136**) evaluated failed to give any metalation products, and those that did undergo metalation (**1.137**), provided the expected 1,2-disubstituted ferrocenes **1.138** with no enantioselectivity. The single exception was diphenylphosphinylferrocene (**1.16**) which furnished a good yield of product (95%) with

poor, yet significant, enantiomeric excess (54%, major (*S*)-**1.138**). Although ineffective, this method represents the first reported enantioselective metalation procedure for the induction of planar chirality in ferrocene systems and circumvents the need for chiral DMGs.

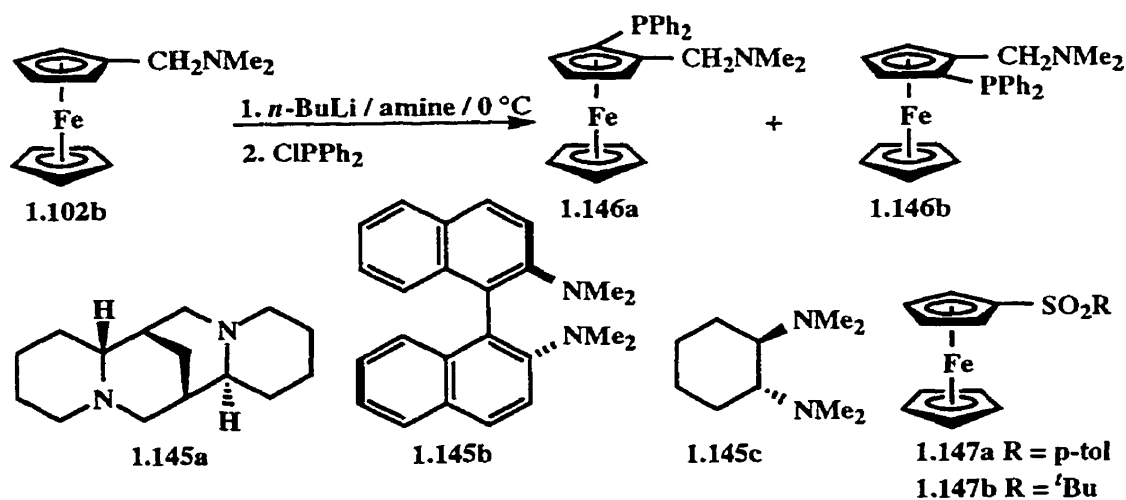
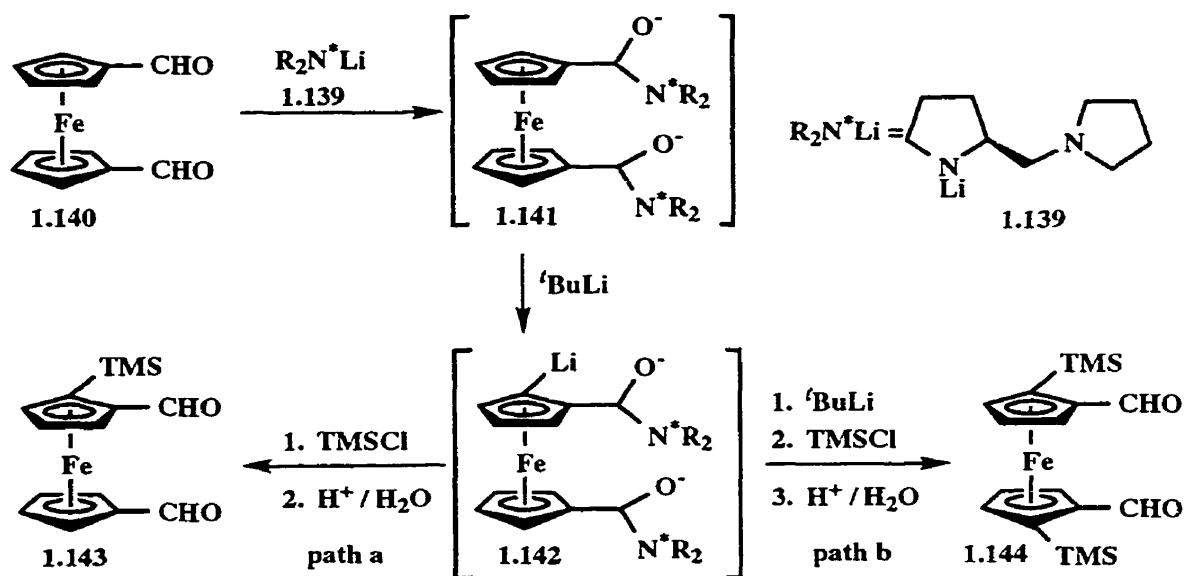


Scheme 1.46

As an extension of their approach to 1,1'-disubstituted ferrocenes (Section 1.3.1),²¹² Iftime and co-workers reported a synthesis of planar chiral ferrocenes (Scheme 1.47). Chiral amide base **1.139**, formed *in situ*, serves as a diastereoselective DMG while simultaneously protecting the aldehyde functionality. Addition of the amide base to 1,1'-ferrocenedicarbaldehyde (**1.140**) provided the protected intermediate **1.141** which, when treated with *t*-BuLi, formed the *ortho* lithiated species **1.142**. Subsequent quench with an electrophile and hydrolysis (path a) provided 1,2,1'-trisubstituted planar chiral ferrocenes (**1.143**), while treatment with excess *t*-BuLi before electrophile quench and hydrolysis (path b) led to 1,1',2,2'-tetrasubstituted planar chiral ferrocenes exhibiting C₂-symmetry (**1.144**). Although yields for this overall process are low (13-29%), up to 99% ee was achieved.

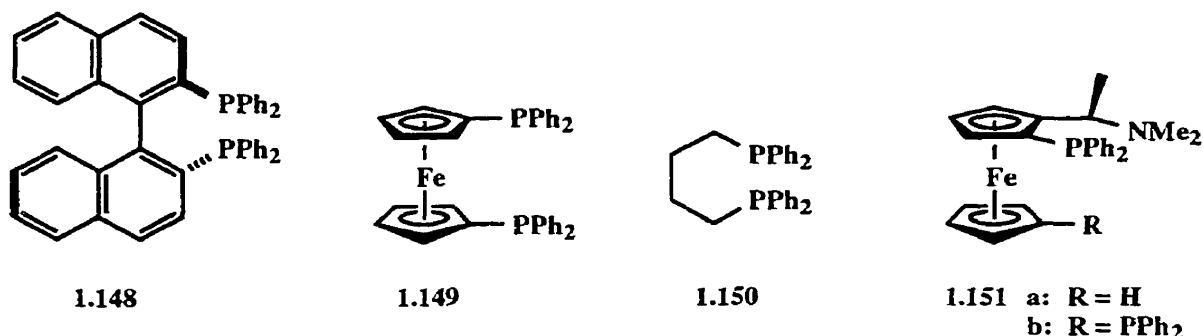
A similar approach was reported by Nishibayashi and co-workers in which chiral diamine ligands were used in conjunction with organolithium reagents in the hope of creating a chiral environment during the deprotonation step.²³⁴ Thus, *N,N*-dimethylaminomethylferrocene (**1.102b**) was treated with *n*-BuLi in the presence of tertiary diamines **1.145a-c**, and quenched with chlorodiphenylphosphine to give aminophosphines **1.146a** and **1.146b**. Optimized metalation conditions for the three ligands gave only trace amounts of products when (-)-sparteine (**1.145a**) was used and a 40% yield of product with

no enantioselectivity when **1.145b** was used. The use of **1.145c**, however, gave a 49% yield of desired products in 62% ee (major **1.146a**). Substituting pyrrolidino, morpholino, or diisopropylamino for the dimethylamino moiety in the directing group led to decreased yield and/or enantioselectivity for the reaction. Application of this procedure to sulfonylferrocenes **1.147a** and **1.147b** led to undetectable enantioinduction.²³⁴



1.4 Phosphine Ligands

Directed *ortho* Metalation provides just one of many available methods for the synthesis of elaborate phosphine ligand systems. The importance of phosphine ligands continues to grow as more and more metal catalyzed processes are developed. Variations in steric and electronic considerations about the phosphine moiety have allowed for the design of ligands for numerous specific applications. Among the most exploited classes of ligands are those based on bidentate bisphosphine systems such as 2,2'-bis(diphenylphosphino)-1,1'-binaphthyl (BINAP, **1.148**), 1,1'-bis(diphenylphosphino)ferrocene (dppf, **1.149**), 1,4-bis(diphenylphosphino)-butane (**1.150**) and their derivatives. The subject of bidentate phosphorus ligands has recently been reviewed by van Leeuwen and co-workers.²³⁵



A complete survey of organophosphine systems and their application to transition metal catalyzed processes would be impractical to consider here. Discussion here will be limited to the smaller class of phosphines characterized by large sterically demanding groups. The increasing importance of sterically compromised arylphosphines^{79,81} is steadily being appreciated. In particular, asymmetric processes catalyzed by transition metal phosphine complexes often show increased selectivity as a result of the steric environment provided by the phosphine component.

1.4.1 Di-*tert*-butylphosphines

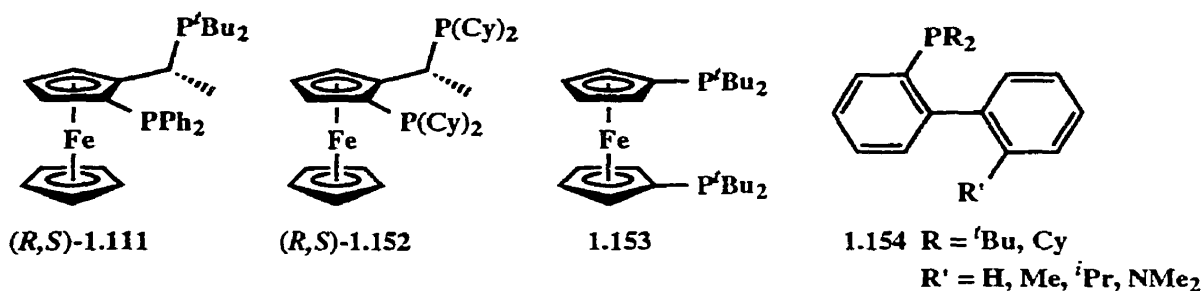
Ligands with ferrocene backbones have been applied to metal catalyzed reactions with remarkable success. Ligand **1.111** (Scheme 1.37, Section 1.3.2) incorporating the highly crowded di-*tert*-butylphosphine moiety as an integral part of the chelating structure is one of

several chiral ferrocene ligands which have evolved from the well known phosphines (*R*)-*N,N*-dimethyl-1-[(*S*)-2-(diphenylphosphino)ferrocenyl]ethylamine ((*R*)-(*S*)-PPFA) **1.151a** and (*R*)-*N,N*-dimethyl-1-[(*S*)-1',2-bis(diphenylphosphino)ferrocenyl]ethylamine (((*R*)-(*S*)-BPPFA) **1.151b** developed by Hayashi and co-workers.²¹⁹ While the specific role of the crowded phosphine moiety is not fully understood, it is clear that the steric environment has important implications. Indeed, the reaction of Scheme 1.37a proceeds with a high degree of stereoselectivity when ligand **1.111** is employed, while use of other less sterically demanding ligands produces inferior results.^{236,237} The nature of the R group also played a role as evidenced by the increased selectivity when a chiral R group was used (R = CH₂Ph, 90% ee; R = (*R*)-CH(Me)Ph, 99% de).⁸¹

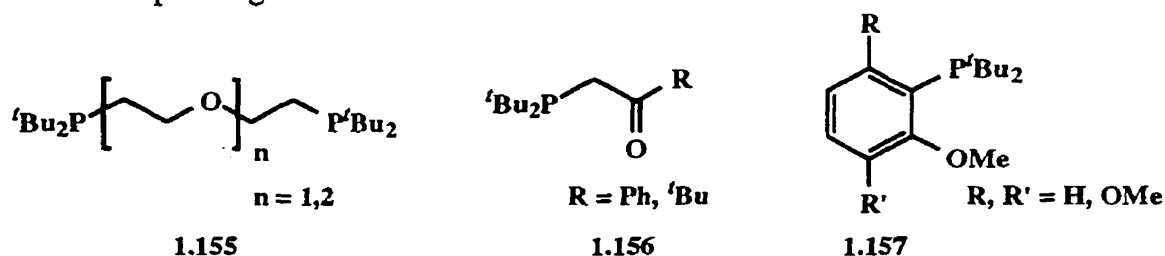
Hamann and Hartwig have recently reported large rate accelerations in certain palladium-catalyzed cross coupling reactions using highly hindered alkyl phosphines as ligands.²³⁸ Increased reaction rates are attributed to two factors working in unison. First, the use of alkyl rather than aryl phosphines increases electron density at the metal centre, a property which should aid in the rate limiting oxidative addition step of the reaction mechanism. Secondly, the inactive tetrahedral Pd(0) ligated by two chelating bisphosphines must undergo complete dissociation of one of the chelating ligands in order for the catalytic cycle to proceed. For this reason, ligands which are too tightly bound to the metal would be counterproductive in the catalytic process. Incorporation of highly crowded alkyl phosphines provides the added electron density while accomplishing the second goal of favouring dissociation by virtue of overcrowding around the metal. Indeed, Pd-catalyzed aryl aminations proceed with highly enhanced reaction rates when the usual BINAP (**1.148**) or dppf (**1.149**) ligands are replaced with chelating phosphines (*R,S*)-**1.111**, (*R,S*)-**1.152**, and **1.153** with **1.153** providing the best results. Effective amination was accomplished with the use of aryl triflates or chlorides where previously success had been limited to aryl bromides and iodides.

Buchwald and co-workers have recently reported an improved synthesis of biphenyl-based phosphine ligands with bulky substituents.²³⁹ Ligands such as **1.154** have been

employed in several transition metal catalyzed processes showing remarkable performance compared to more traditional ligands (e.g. PPh₃). For example, ligand **1.154** (R = Cy; R' = NMe₂), when combined with a source of Pd, efficiently catalyzes aryl aminations and Suzuki cross coupling reactions (Section 3.2). Catalysts based on monodentate versions of **1.154** (R = ^tBu, Cy; R' = H) are, in many cases, just as effective as their bidentate counterparts when used in similar catalytic processes.²⁴⁰⁻²⁴²



The importance of a crowded steric environment has also been demonstrated in the use of oxygen-phosphorus chelating ligands.⁷⁹ Ligands of this nature provide dual functionality in that the tertiary phosphine is used to control the selectivity of the desired product while the oxygen serves as a labile donor that leaves an empty coordination site about the catalytically active metal. Examples of such ligands containing a di-*tert*-butylphosphine group include ethers **1.155**,²⁴³ ketones **1.156**,²⁴⁴ and anisoles **1.157**.^{245,246} Ethers **1.155**, and ketones **1.156** are prepared by reaction of the corresponding alkyl bromides or chlorides with a nucleophilic phosphorus (phosphine or lithiated phosphine) while anisoles **1.157** are usually prepared by D₂O_M reaction using electrophilic chlorophosphines. The range of aromatic phosphines available by this pathway is therefore limited to those which can easily be derived from the corresponding lithiated substrates.



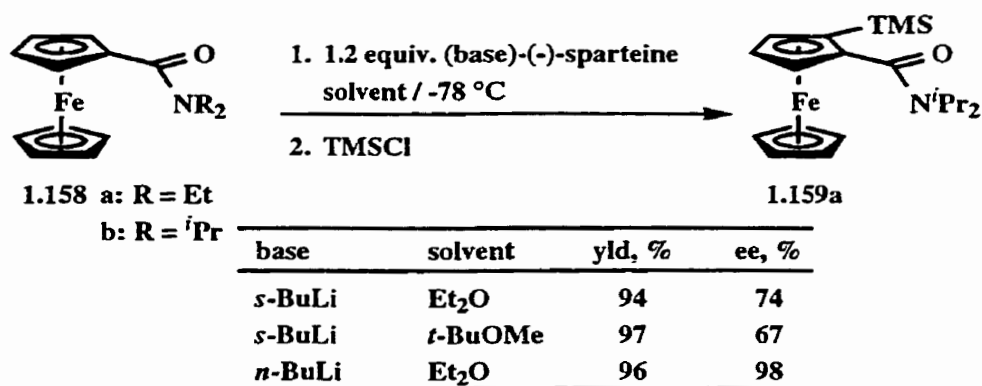
1.5 Results and Discussion

1.5.1 (-)-Sparteine-mediated Enantioselective DoM of *N,N*-Diisopropyl Ferrocenecarboxamide

Work in the Snieckus laboratories on enantioselective metalation of ferrocenecarboxamides developed as a rational extension of aromatic DoM chemistry. Initial experiments by Tsukazaki²⁴⁷ centered around the use of (-)-sparteine (**1.145a**, Scheme 1.48) as a chiral ligand and were stimulated by the results of Hoppe²⁴⁸ and Beak,^{249,250} demonstrating that (-)-sparteine is an effective ligand for high asymmetric induction in lithiation-substitution reactions. The superior properties of this naturally-occurring diamine as it applies to lithiation chemistry have been nicely summarized by Hoppe.²⁵¹

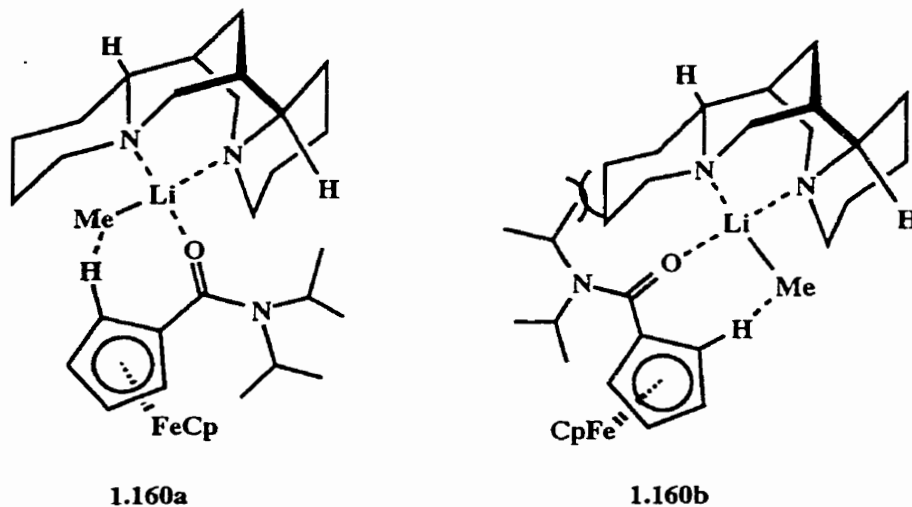
Tsukazaki's initial observations²⁴⁷ that *N,N*-diethyl ferrocenecarboxamide (**1.158a**) had limited solubility in suitable metalation solvents led to the attempted metalation of *N,N*-diisopropyl ferrocenecarboxamide (**1.158b**). It was rapidly established that DoM reaction on **1.158b** proceeded not only in high yield, but that the reaction in the presence of (-)-sparteine as a chiral additive proceeded with a high degree of enantioselectivity.²⁵² Thus, treatment of **1.158b** with a slight excess of *n*-BuLi / (-)-sparteine complex and subsequent quench with chlorotrimethylsilane (TMSCl) led to the isolation of *N,N*-diisopropyl (*R*)-2-trimethylsilylferrocenecarboxamide (**1.159a**) in 96% yield and 98% ee as established by chiral HPLC analysis (Scheme 1.49).

Enantioselectivity in this sequence is almost certainly achieved in the deprotonation stage of the reaction since enantiomeric products are derived from regioselective substitution at one of two different *ortho* positions. While the selectivity in many enantioselective metalation processes can best be explained by a non-selective deprotonation followed by enantioselective substitution (e.g., (-)-sparteine-induced enantioselectivity in lateral metalation of *o*-ethylbenzamides²⁵⁰), such a process in this case would necessitate a reprotonation-deprotonation sequence to take place during the substitution phase of the reaction.

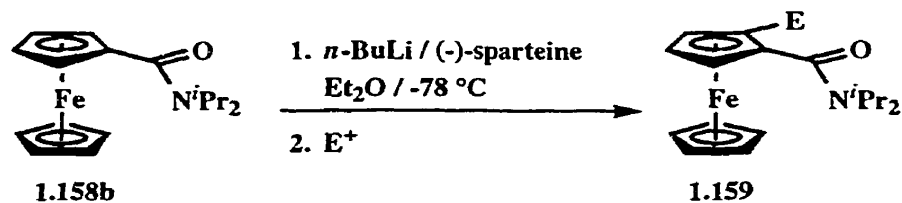


Scheme 1.49

Molecular modeling²⁵³ provided useful insight into the origin of the stereoselective deprotonation. Using MeLi as a model for *n*-BuLi, calculations showed that complexation between the MeLi / (-)-sparteine reagent and the amide carbonyl leads to a complex in which the base is in close proximity with the pro-(*S*) hydrogen (**1.160a**). Conversely, orientation of the amide functionality towards the pro-(*R*) hydrogen is impossible to achieve without a concomitant steric interaction between the amide isopropyl groups and the associated ligand (**1.160b**).



A collaborative effort was undertaken by several group members in order to further exploit the metalation of **1.158b**. Thus, using Tsukazaki's conditions, a number of planar chiral ferrocene derivatives showing a range of functionality including carbon, halogen, sulfur, silicon, selenium, boron, and phosphorus electrophiles were prepared (Scheme 1.50).²⁵²

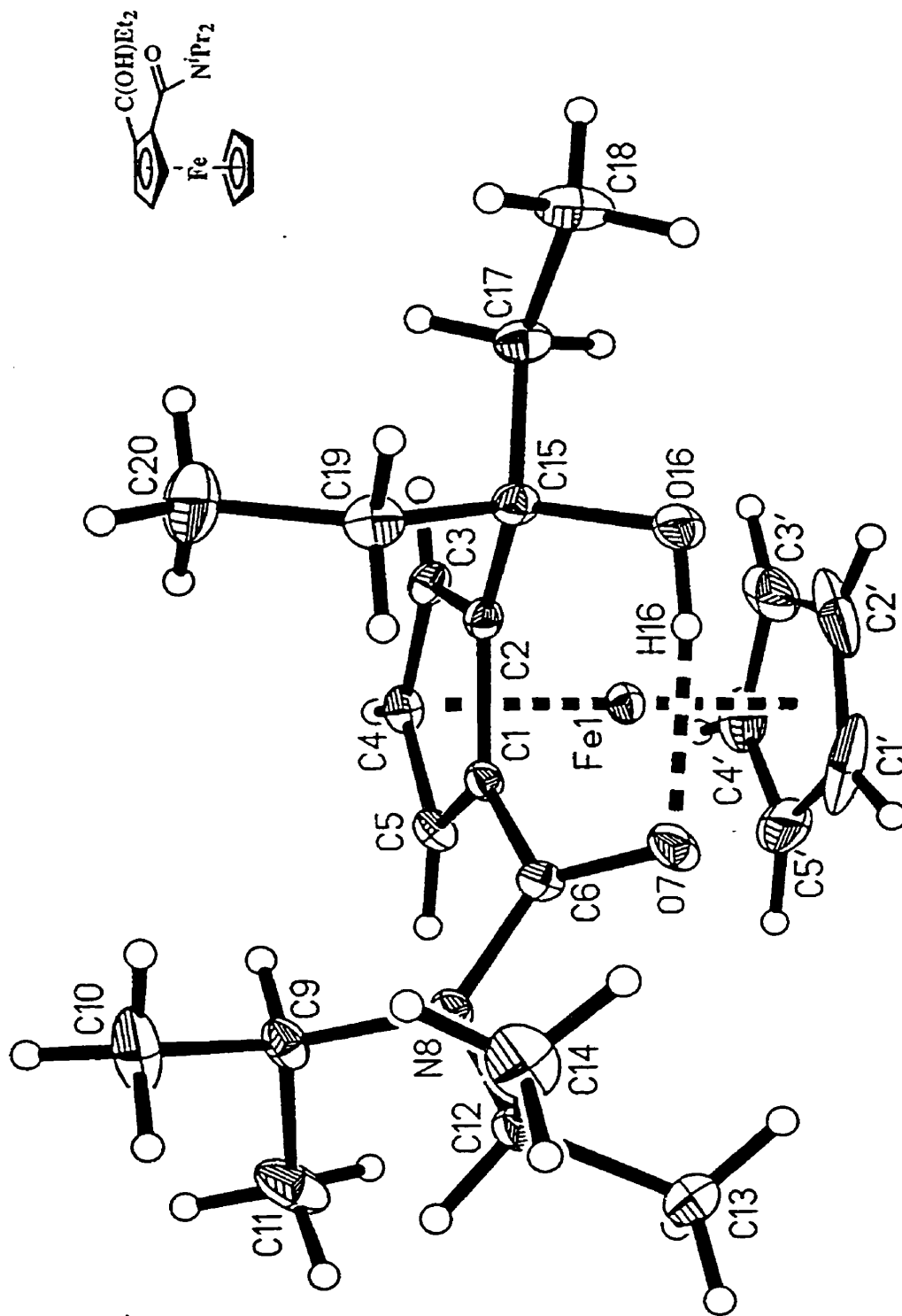


entry	E ⁺	E	product	yld, %	ee, %
1	MeI	Me	b	91	94
2	ClCH ₂ OCH ₃	CH ₂ OCH ₃	c	62	81
3	Et ₂ CO	Et ₂ C(OH)	d	45	99
4	Ph ₂ CO	Ph ₂ C(OH)	e	91	99
5	B(OMe) ₃	B(OH) ₂	f	89	85
6	TMSCl	TMS	a	96	98
7	Ph ₂ PCl	PPh ₂	g	82	90
8	(PhS) ₂	SPh	h	90	98
9	(PhSe) ₂	SePh	i	92	93
10	I ₂	I	j	85	96

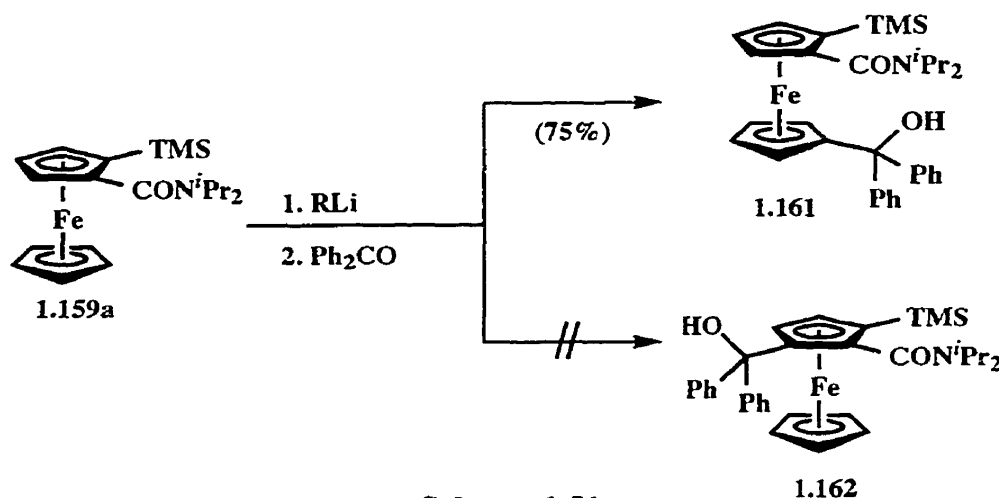
Scheme 1.50

Although the absolute configuration of the products **1.159** had been predicted based on molecular modeling studies, proof of the absolute configuration was achieved by single crystal X-ray analysis on **1.159d** (Figure 1.1). Anomalous scattering showed convincingly that the stereochemistry was indeed the same as what was predicted based on the computer modeling. Solution and refinement of the crystal data gave R indices of 2.83 % (R) and 2.98 % (wR) while the corresponding indices for the enantiomeric product were 4.30 %, and 4.67 %, respectively (Appendix 1). Further confirmation of stereochemistry was provided by chiral HPLC analysis of the actual crystal used in the X-ray experiment which confirmed that the crystal used represented the major enantiomer. Another interesting feature of the solid state structure is the hydrogen bond between the tertiary alcohol (O16-H16) and the amide carbonyl (O7) (see also the hydrogen bond in the solid state structure of **1.161**).

Figure 1.1 - Single Crystal X-ray Analysis of 1.159d.



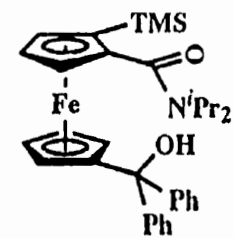
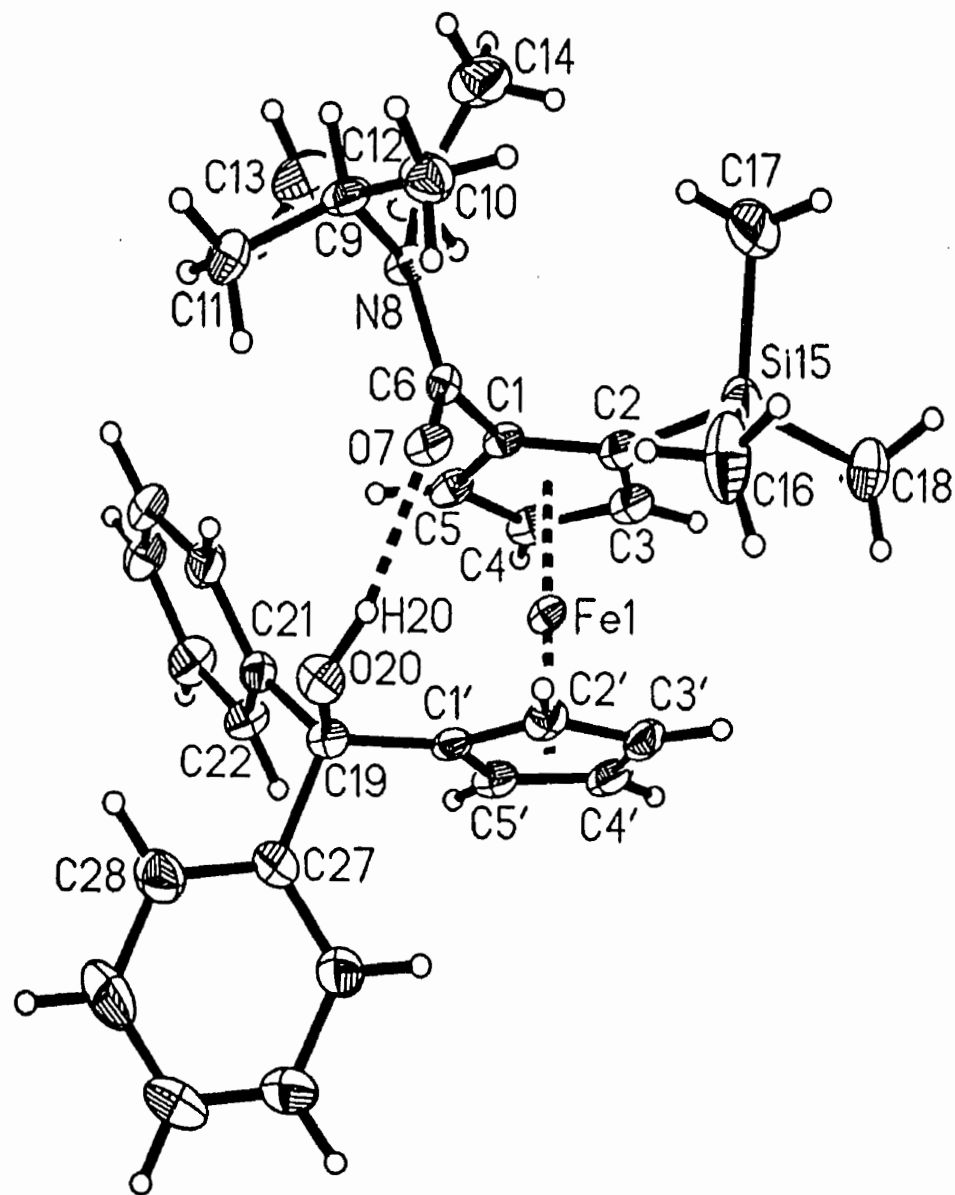
In order to produce structures with the opposite stereochemistry, a procedure analogous to Scheme 1.44 was attempted.²⁵⁴ Thus, trimethylsilyl substituted amide **1.159a** was treated with either *n*-BuLi or *s*-BuLi followed by quench with benzophenone. Surprisingly, heteroannular metalation occurred resulting in the isolation of 1,2,1'-trisubstituted ferrocene **1.161** rather than the expected 1,2,3-trisubstituted product **1.162** (Scheme 1.51). X-ray analysis of **1.161** (Figure 1.2) confirmed the heteroannular substitution but perhaps more importantly it demonstrated that the stereochemical outcome of the initial deprotonation was consistent with that demonstrated by the X-ray analysis of **1.159d**. Again, anomalous scattering results were quite convincing. Solution and refinement of the structure gave R and wR values of 2.79 % and 2.91 % respectively compared with corresponding values of 4.35 % and 4.72 % for the enantiomer (Appendix 2). A strong transannular intramolecular hydrogen bond (H(20)-O(7) = 1.91 Å) is also evident in structure **1.161**.



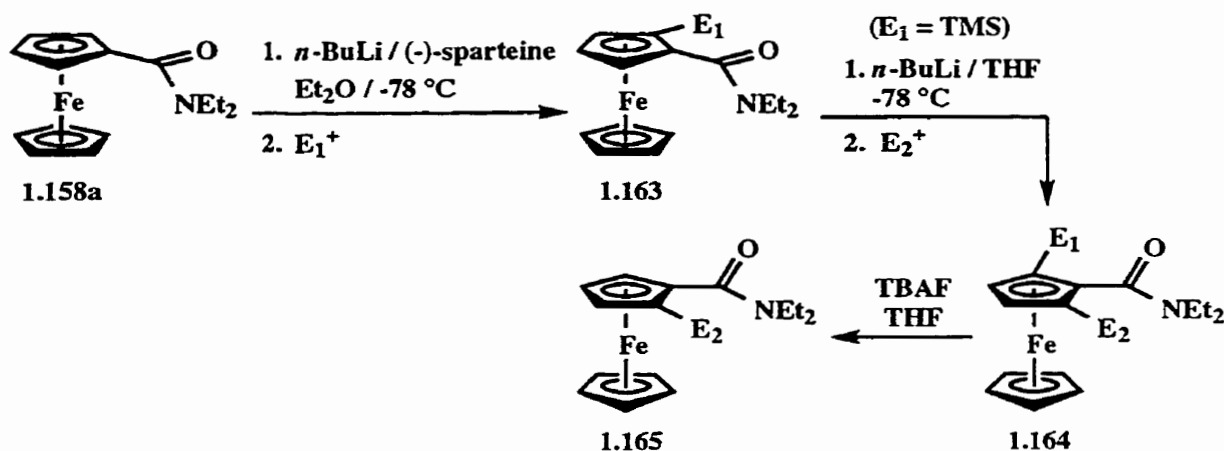
Scheme 1.51

Subsequent re-examination of the asymmetric metalation and electrophile quench of *N,N*-diethyl ferrocenecarboxamide²⁵⁵ (**1.158a**) led to products **1.163** (Scheme 1.52) in chemical yield and enantiomeric excess which were only marginally lower than those observed with the diisopropyl amide **1.158b**. Furthermore, metalation of *N,N*-diethyl 2-trimethylsilylferrocenecarboxamide (**1.163**, E₁ = TMS) proceeded smoothly to produce the

Figure 1.2 - Single Crystal X-ray Analysis of 1.161.



desired 1,2,3-trisubstituted products (**1.164**), which were desilylated to form enantiomerically enriched products (**1.165**).²⁵⁵ This sequence circumvents the unavailability of (+)-sparteine.



Scheme 1.52

As a final note, choice of solvent in the asymmetric metalation reactions proved to be crucial. While both chemical yield and enantiomeric excess were quite high using Et₂O as the solvent, significant erosion of enantiomeric excess was observed when THF was employed. The effect has been rationalized based on the coordinating ability of the solvent which competes with (-)-sparteine in occupying the coordination sites at lithium, thus removing the asymmetric environment responsible for induction. The superior ligating properties of THF have already been noted and have been found to compete significantly with other diamines such as TMEDA.¹⁴

1.5.2 DoM of Ferrocenes bearing other DMGs

With the success of the amide directing group, effort was concentrated on expanding the enantioselective DoM methodology to encompass other directing groups. Several DMGs were investigated²⁵⁶ with the focus of this work being phosphorus-based DMGs.

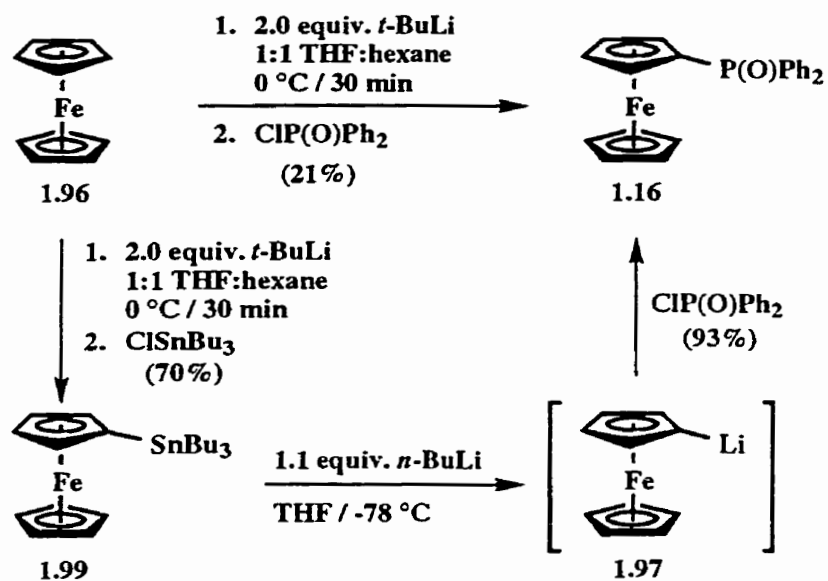
Within the realm of phosphorus-based DMGs, the diphenylphosphinyl group has received the most attention. Based on this factor, and encouraged by the results of Price and Simpkins (Scheme 1.46),⁸⁹ diphenylphosphinylferrocene (**1.16**) was chosen as a starting

point. Initial experiments were performed in order to evaluate the directing ability of this group in an achiral sense.

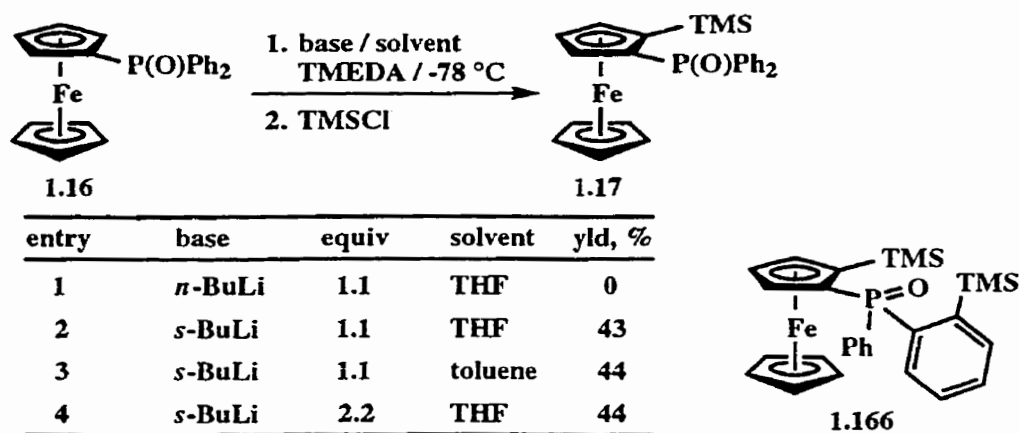
Synthesis of the starting material was approached by two similar routes (Scheme 1.53). In the first approach, ferrocene (**1.96**) was treated with 2.0 equiv. of *t*-BuLi in a 1:1 THF:hexane mixture at 0 °C for 30 minutes, conditions used to optimize the monolithioferrocene / dilithioferrocene ratio.¹⁹³ The resulting anion was treated with diphenylphosphinyl chloride to give the desired diphenylphosphinylferrocene (**1.16**) which, unfortunately, was obtained in low yield (21%) in spite of repeated attempts to optimize the reaction. Alternatively, the method of Guillaneaux and Kagan¹⁹³ was employed (Scheme 1.33) to form tri-*n*-butylstannylferrocene (**1.99**), which, upon transmetalation to **1.97** followed by ClP(O)Ph₂ quench led to **1.16**. Although this method is a two step procedure, it has the advantage of excellent yield in the transmetalation / substitution step. Furthermore, the precursor **1.99** may be produced in relatively large quantities and stored for extended periods of time without deterioration thus providing a convenient and efficient means for the synthesis of **1.16**. The discrepancy in yield between the two methods is quite striking, yet not unprecedented. Guillaneux noted that this electrophile and others gave poor yields upon the direct lithiation of ferrocene while the transmetalation route proceeded smoothly to afford the monosubstituted products.²⁵⁷ It has been suggested²⁵⁷ that the transmetalation proceeds *via* a five-coordinate tin species whose reactivity may be different from the corresponding lithium carbanion.

With the starting material in hand, some simple DoM reactions were carried out using TMSCl quench as a probe for determining optimal reaction conditions (Scheme 1.54). Due to the low solubility of **1.16** in Et₂O, THF was chosen as a substitute. Although treatment of **1.16** with *n*-BuLi resulted in complete recovery of starting material (entry 1), the use of *s*-BuLi allowed isolation of **1.17** in 44% yield after column chromatography (entry 2). Switching the solvent to toluene had no effect on the overall yield (entry 3), and solubility problems were again encountered at low temperature. The use of excess base (entry 4) did not enhance the yield of **1.17** but also led to a small amount of a new compound whose ¹H-NMR

spectrum suggested the disilylated ferrocene **1.166**. Complete characterization was not possible and an attempt to repeat the synthesis was unsuccessful (see Experimental Section).



Scheme 1.53



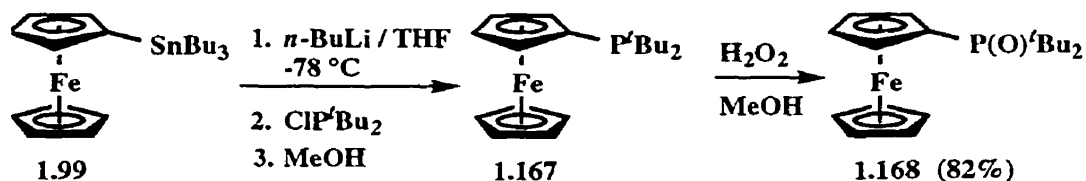
Scheme 1.54

Thus, although the DoM chemistry of **1.16** was established, several problems (poor solubility, low yield, and interfering by-products) required solution. With these aims in mind, other phosphine oxide DMGs were considered.

The previously uninvestigated di-*tert*-butylphosphinyl group was considered as a reasonable alternative to the diphenylphosphinyl moiety. Among the benefits of the DMG

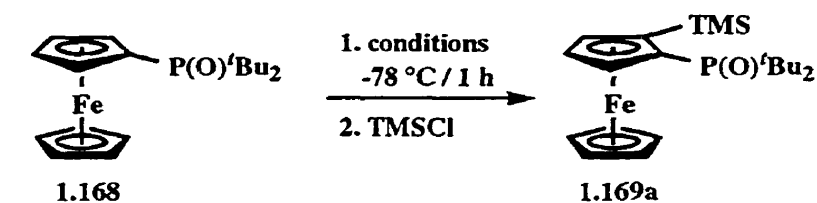
expected were: *i*) added solubility, particularly in hydrocarbon solvents, due to the alkyl groups; *ii*) reduced interference of by-products since no aromatic hydrogens are present; *iii*) steric protection against alkyllithium reagent attack at phosphorus (Section 1.2.3.1); *iv*) suitable geometry for promoting *ortho* deprotonation (Section 1.5.3); and *v*) potential access to a wide range of new and interesting phosphines. The synthesis and metalation of di-*tert*-butylphosphinylferrocene (**1.168**) was pursued to determine if any of the above advantages could be realized.

The synthesis of **1.168** was accomplished in an analogous manner to that of **1.16** starting from tributylstannylferrocene (**1.99**, Scheme 1.53). To this end, tin-lithium exchange with *n*-BuLi at -78 °C in THF, followed by quench with chlorodi-*tert*-butylphosphine gave the crude phosphine (**1.167**) by simple quench with MeOH and removal of solvent under reduced pressure. Immediate oxidation according to the method of Schmid and co-workers⁹⁵ gave the required phosphine oxide **1.168** in 82% overall yield from **1.99** (Scheme 1.55).



Scheme 1.55

As predicted, the solubility of **1.168** was substantially greater than for the diphenyl analogue and it dissolved freely in either THF or Et₂O. Preliminary results of DoM on **1.168** (Scheme 1.56) demonstrated that any of the common alkyllithiums were effective with the best results being achieved using *t*-BuLi (entry 3), and that ethereal solvents were suitable, with or without the presence of a chelating ligand (entry 2,4). Interestingly, *s*-BuLi (2 equiv) in THF afforded a modest yield of product (entry 2) while this base in Et₂O in the presence of TMEDA (entry 4) afforded **1.169a** in high yield. The best yield was obtained using *t*-BuLi (entry 3).



entry	base	TMEDA	equiv	solvent	ylid, %
1	<i>n</i> -BuLi	no	2.0	THF	80
2	<i>s</i> -BuLi	no	2.0	THF	49
3	<i>t</i> -BuLi	no	2.0	THF	92
4	<i>s</i> -BuLi*	yes	1.2	Et ₂ O	74

* Inverse addition

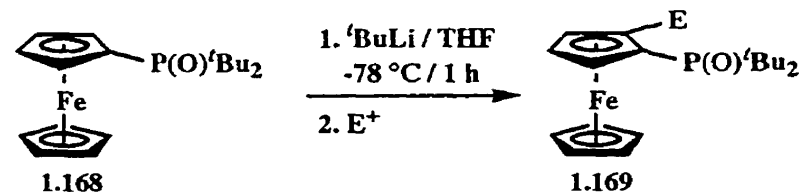
Scheme 1.56

The influence of the 2-substituent in **1.169a** was clear from the examination of its ¹H-NMR spectrum. The starting material **1.168** exhibits a large doublet at δ 1.26, $^3J_{H-P} = 13.5$ Hz integrating for the expected 18 H. The inclusion of a 2-substituent incurs a dramatic change by rendering the two *tert*-butyl groups diastereotopic. Presumably, the bulk of the *tert*-butyl groups precludes free rotation which previously existed about the Cp-P bond, isolating each of the *tert*-butyl groups in a different chemical environment. This is quite clear from the NMR spectrum of **1.169a** which shows two doublets, each integrating for 9 H, at δ 1.54, and δ 0.91 with $^3J_{H-P} = 13.6$ Hz and 13.3 Hz, respectively (Appendix 3).

Using the best available conditions (normal addition, *t*-BuLi / -78 °C / THF / 1 h), a series of derivatives **1.169b-f** was prepared representing a range of functionality including carbon, halogen, and other heteroatom electrophiles (Scheme 1.57). Notably, the sulfur²⁵⁸ substituted derivative **1.169e** was cleanly prepared, but rapidly decomposed upon flash chromatography to give unidentifiable products.

In an effort to further develop the enantioselective metalation of phosphinyl ferrocenes parallel to that achieved with the corresponding tertiary amides (Scheme 1.50), asymmetric synthesis of silyl substituted ferrocene **1.169a** was pursued using the *s*-BuLi / (-)-sparteine complex. Addition of a solution of the substrate at -78 °C to the complex followed by one hour reaction time and quench with trimethylsilyl chloride furnished the desired product **1.169a** in a

yield of 43-46%. Attempts to increase the yield by changing solvent to toluene, increasing the amount of base (2.2 equiv), or using *n*-BuLi were unsuccessful.



entry	E ⁺	E	product	yld, %
1	MeI	Me	b	72
2	Ph ₂ CO	C(OH)Ph ₂	c	97
3	B(OMe) ₃	B(OH) ₂	d	65
4	TMSCl	TMS	a	92
5	<i>p</i> -TolSO ₂ S ^t Bu	S ^t Bu	e	68
6	I ₂	I	f	76

Scheme 1.57

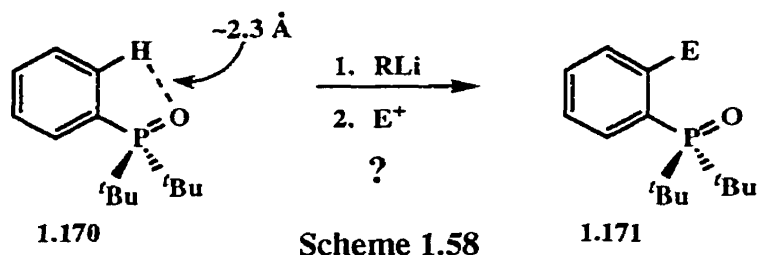
Determination of enantiomeric excess of **1.169a** proved to be an insurmountable task. Racemic **1.169a** was subjected to numerous sets of chiral HPLC conditions using available chiral columns (Chiralcel OD, Chiralcel OJ, Chiralcel OK) and a host of solvent mixtures (various combinations of hexane, ether, diethylamine, isopropanol, *tert*-butyl methyl ether). Unfortunately, conditions for effective separation of the enantiomers were never achieved. Although separation of peaks was observed, there was substantial overlap and quantitation of results was not possible. HPLC analysis of **1.169a** produced from the (-)-sparteine mediated reactions showed a similar chromatogram to the racemic material, which indicated that, if any chiral induction had occurred, it was not substantial. The optical activity of **1.169a** derived from the (-)-sparteine mediated reactions was analyzed and it was found that only a miniscule optical rotation was present. Optical rotations ranged from -0.025 to -2.43° (*c* = 90.8 mg / 10.0 mL, CHCl₃) depending on the source used, with the Hg³⁶⁵ source providing the highest rotation. While the low optical rotation is not a firm indication of low enantiomeric excess, it seems likely that the enantioinduction from these experiments was low (compare with e.g. (*R*)-

N,N-diisopropyl 2-trimethylsilylferrocenecarboxamide at +20.2° (c = 0.97 mg / 10.0 mL, CHCl₃), especially when coupled with the HPLC results.

With the disappointing results of enantioselective metalation of the phosphinyl DMG in ferrocene systems, focus was returned to further development of this DMG in other aromatic systems.

1.5.3 DoM of Di-*tert*-butylphenylphosphine Oxide

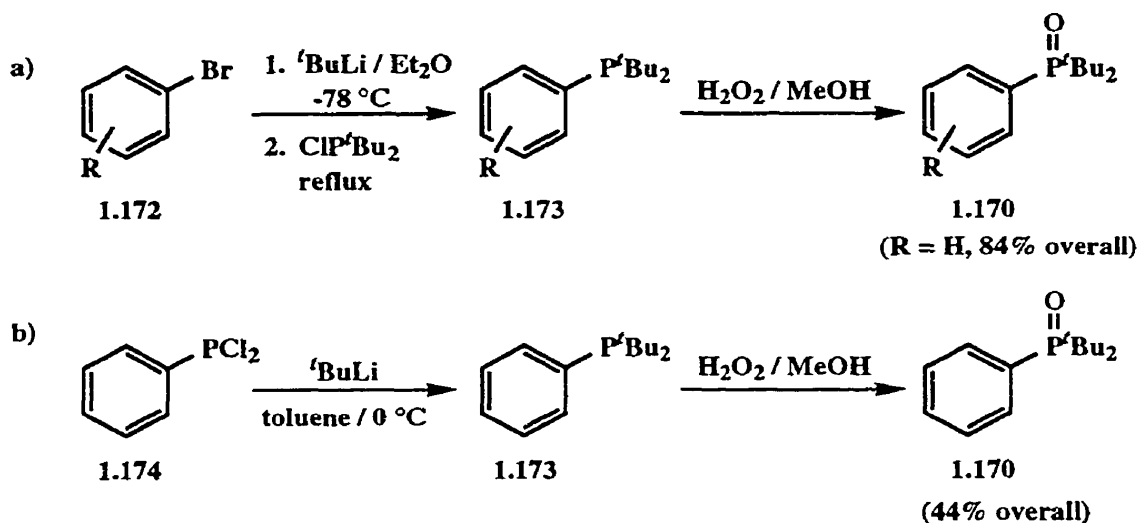
During initial stages of investigation of the metalation behaviour of **1.168** (Scheme 1.56), the possibility of metalating di-*tert*-butylphenylphosphine oxide (**1.170**) was also considered. Initially, molecular modeling (MM2 force field) was performed to determine if DoM might be a viable process for this substrate.²⁵³ The lowest energy conformation indicated a proximal oxygen-*ortho*-hydrogen distance of approximately 2.3 Å which seemed favourable to promote *ortho*-deprotonation. The successful *ortho* metalation of this substrate was considered valuable for several reasons. First, after metalation and substitution with



electrophiles, reduction of the phosphine oxide functionality gives access to a wide variety of substituted hindered phosphines whose importance in ligand chemistry has already been established (Section 1.4.1). Second, the inclusion of bulky *tert*-butyl groups was expected to prevent attack of alkyllithium reagent at the phosphorus atom, a problem associated with several other P-DMGs (Section 1.2.3). Furthermore, the use of *t*-BuLi as a metalating agent would make any such attack at phosphorus degenerate. Third, it was expected that the large alkyl groups would reduce hygroscopic character of the substrate, while minimizing the risk of side reactions due to non-regioselective metalation at competing sites on other aromatic rings.

With these goals and the results of the molecular modeling study in mind, synthetic efforts were undertaken.

Synthesis of the desired substrate **1.170** was easily accomplished by two methods. The first method (Scheme 1.59a), an adaptation of a literature procedure,^{95,259} involved the addition of phenyllithium (generated by lithium / bromine exchange of bromobenzene **1.172** (R = H) with *t*-BuLi) to commercially available chlorodi-*tert*-butylphosphine at low temperature and warming to reflux in Et₂O. The resulting phosphine **1.173** was isolated by removal of the solvent *in vacuo* and subjected to immediate oxidation with hydrogen peroxide to give a good overall yield (84 %) of **1.170** (R = H). This method offers the advantage of applicability to a wide range of aryllithium substrates.

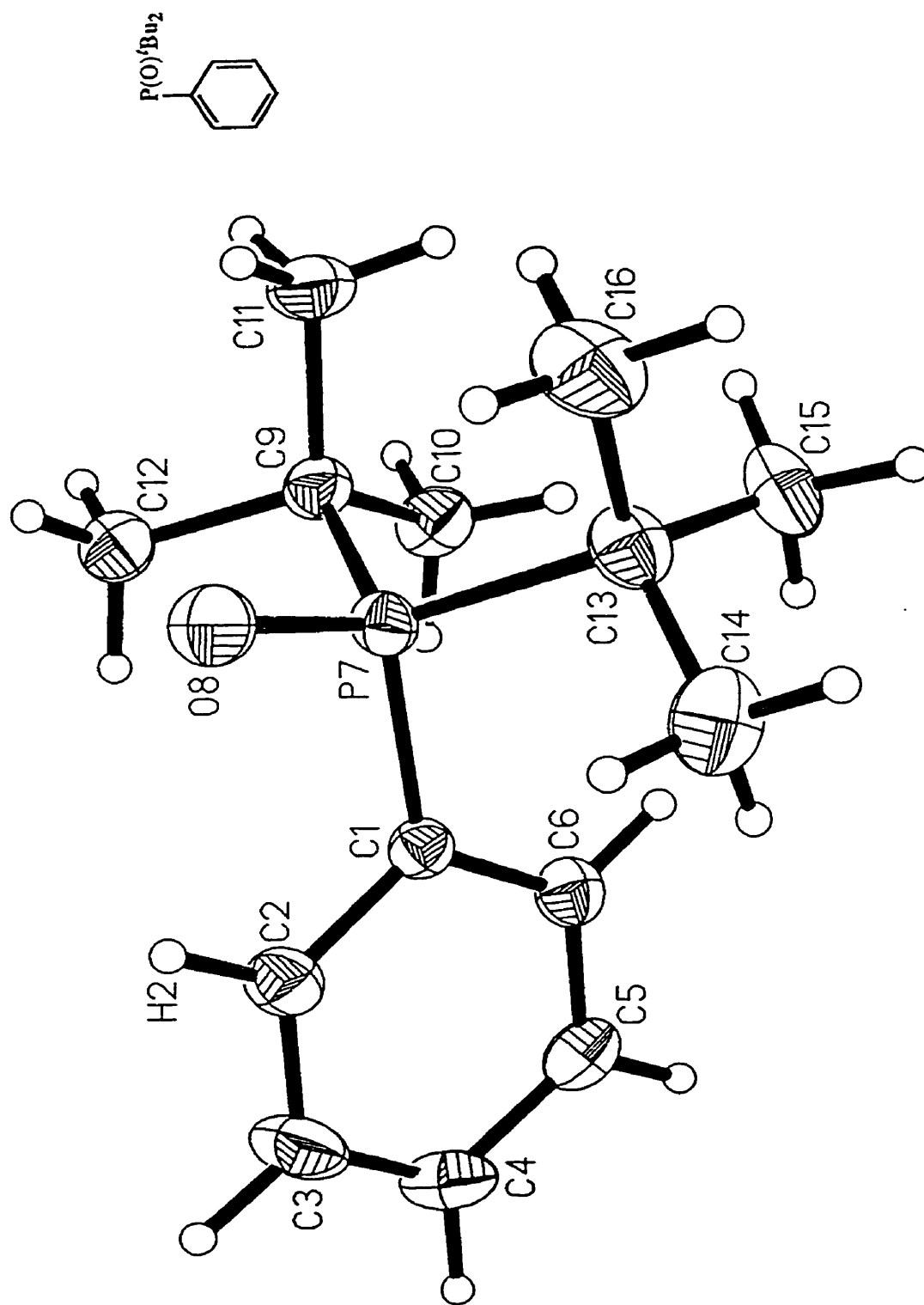


Scheme 1.59

The second method (Scheme 1.59b) involved the direct addition of *t*-BuLi to dichlorophenylphosphine (**1.174**) followed by an analogous oxidation of the crude phosphine intermediate **1.173** to give **1.170**.²⁶⁰ Although this method is lower yielding and less general, it is particularly convenient for the synthesis of large quantities of **1.170** since **1.174** is readily available in large quantities and at a relatively low price.²⁶¹

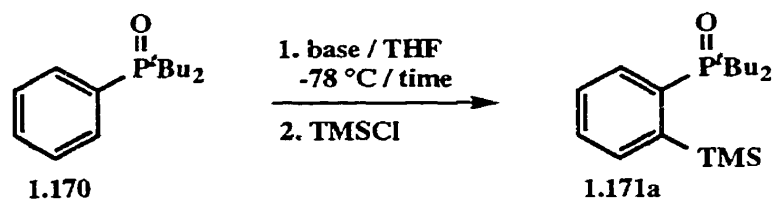
Crystallization of **1.170** from hexane provided single crystals which were suitable for X-ray analysis (Appendix 4). Information provided by the solid state structure (Figure 1.3)

Figure 1.3 - Single Crystal X-ray Analysis of 1.170.



supported the results of the MM2 study. The compound crystallizes with two molecules per asymmetric unit, both with very similar geometry, and an average oxygen-*ortho*-hydrogen distance of 2.498 Å. Not surprisingly, the bulky *tert*-butyl groups are oriented in such a way that they straddle the plane of the aromatic ring, the result being that the oxygen is aimed directly at an *ortho* hydrogen (Figure 1.3).

Exploration of suitable metalation conditions for **1.170** began with a survey of alkyllithium bases (Scheme 1.60) using the TMS-substituted derivative **1.171a** as an indicator. *t*-BuLi provided the best yield (entry 3), marginally better than *n*-BuLi (entry 1). In agreement with the result in the corresponding ferrocenyl substrate (Scheme 1.56), the lowest yield was observed with the use of *s*-BuLi (entry 2), a result which may be rationalized based on a combination of steric demand and base strength. Increased steric demands of the secondary alkyllithium compared to the primary may render it less suitable for metalation of the highly crowded substrate. Conversely, the more sterically demanding tertiary base compensates for steric shortcomings with increased base strength. Certainly the aggregation states of alkyllithium bases would contribute to the steric interactions in a detrimental way.

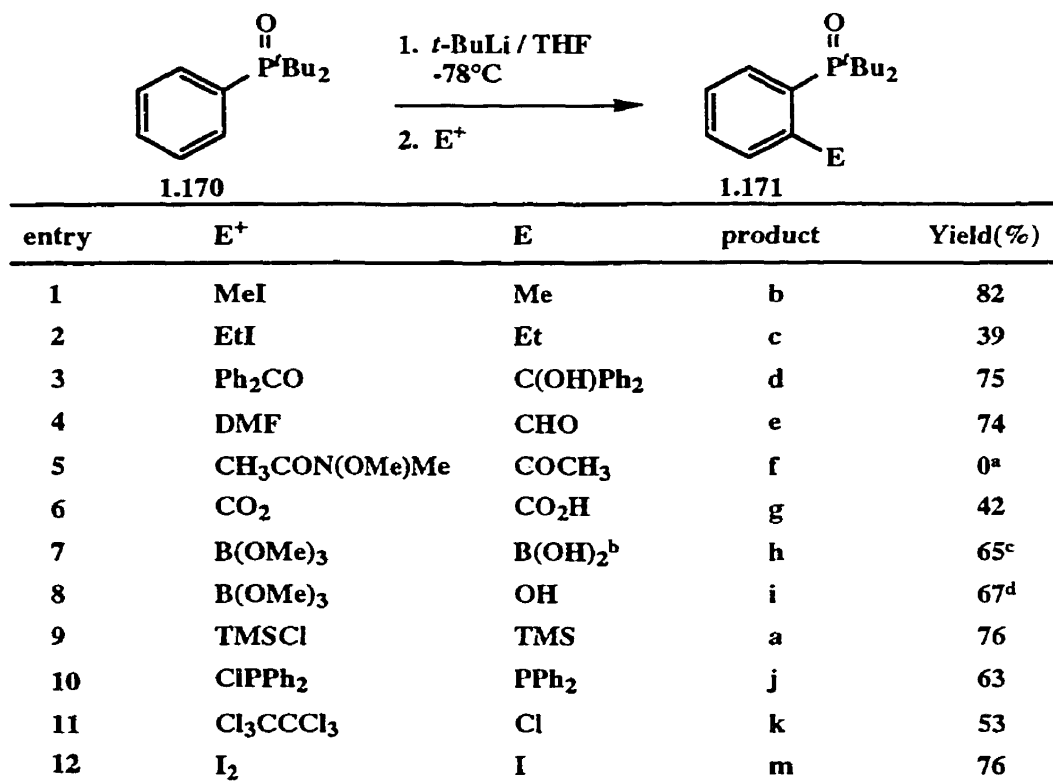


entry	base	time (min)	yield (%)
1	<i>n</i> -BuLi	120	73
2	<i>s</i> -BuLi	120	21
3	<i>t</i> -BuLi	120	76
4	<i>t</i> -BuLi	5	37
5	<i>t</i> -BuLi	60	48
6	<i>t</i> -BuLi	90	47
7	<i>t</i> -BuLi	240	75

Scheme 1.60

Metalation as a function of time was also investigated using *t*-BuLi as base. A metalation time of only 5 minutes produced a substantial yield of product; however, 120 minutes appeared to be the optimal time (Scheme 1.60, entries 3-7). For generalization studies, the standard metalation conditions adopted were *t*-BuLi / THF / -78 °C / 120 min.

Using these standard conditions, a series of 2-substituted aryl phosphines **1.171** representing a broad range of functionality was prepared in 39-82 % yield (Scheme 1.61). While several carbon electrophiles were included (entries 1-6) resulting in alkyl, carbinol, and carbonyl substituents, the use of a Weinreb amide (CH₃CON(OMe)Me) resulted only in quantitative recovery of starting material (entry 5). The amide has the ability to react as an

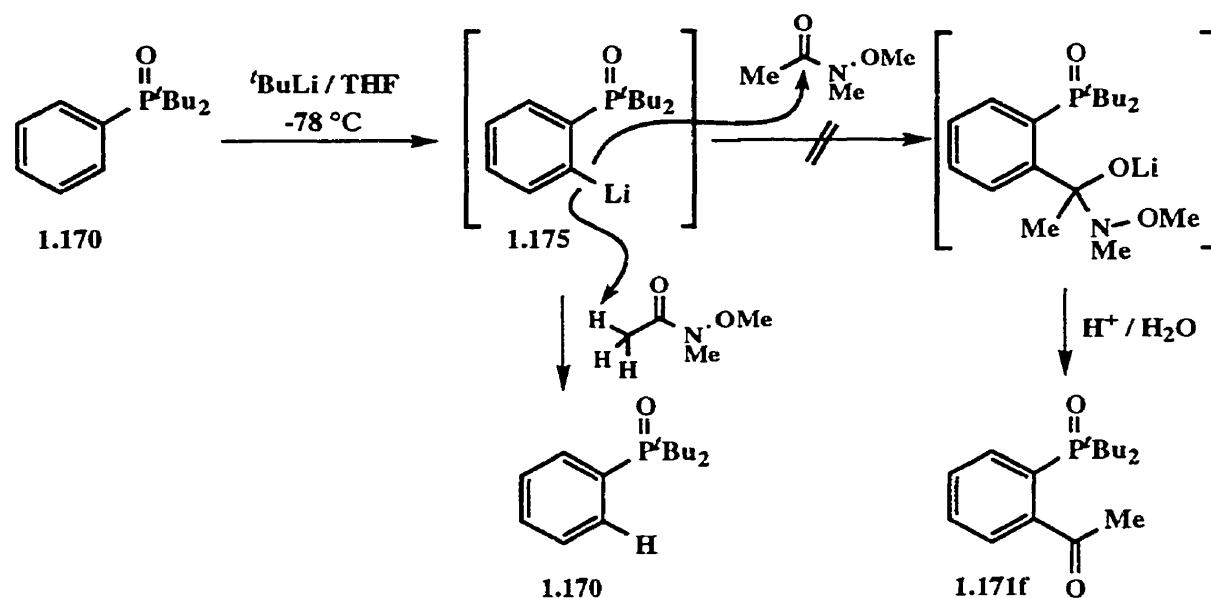


^a Recovered starting material (90%). ^b Isolated as the corresponding 1,3-propanediol boronate ester. ^c Overall yield of boronate ester. ^dAfter treatment with H₂O₂ / OH⁻

Scheme 1.61

electrophile at the carbonyl carbon, or to act as a proton donor with the relatively acidic α-protons. Since formation of the anion (**1.175**) appeared to proceed as usual, as indicated by

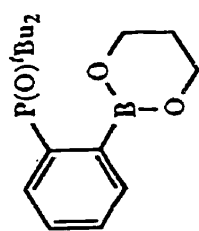
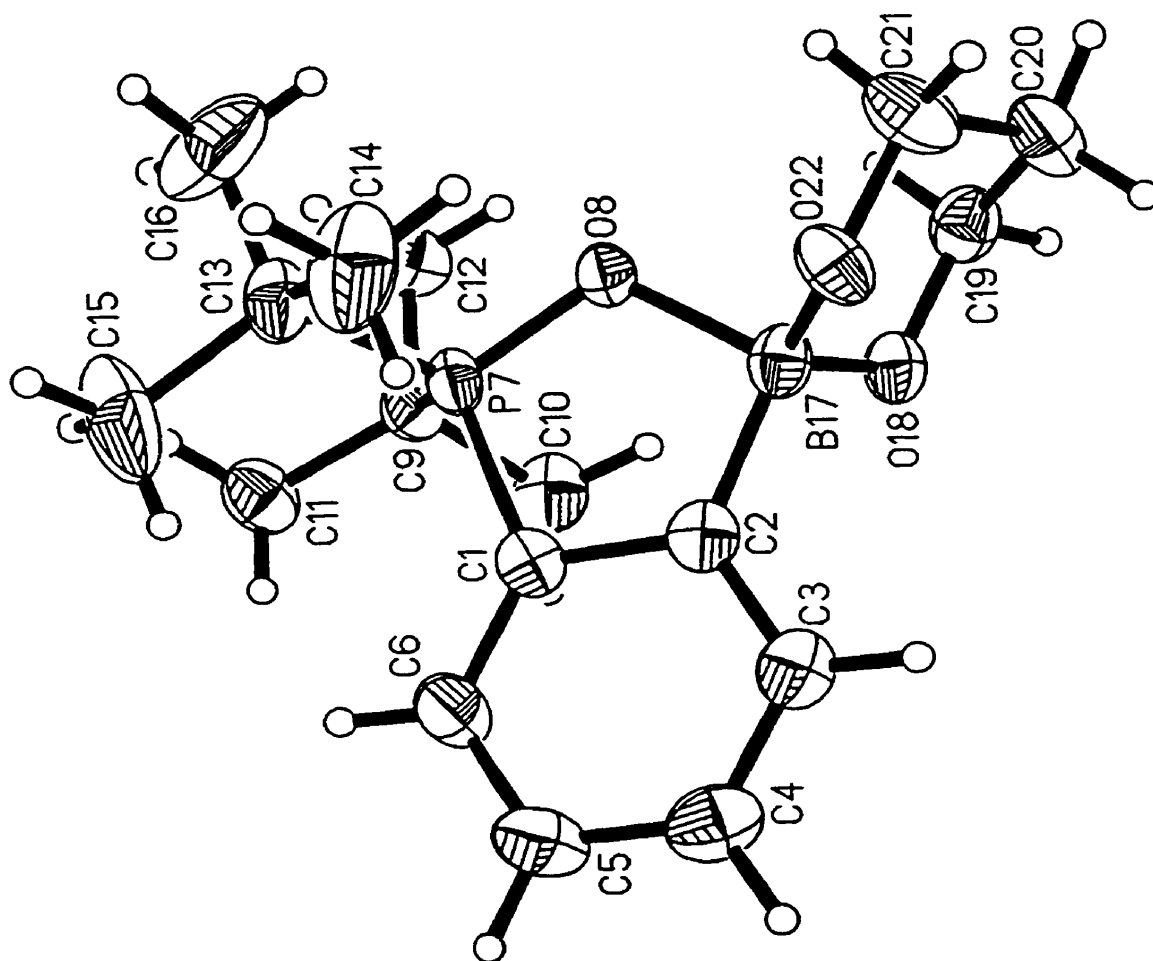
the formation of a bright yellow suspension, it is believed that approach of the electrophile determines the outcome of the reaction. The approach is somewhat limited due to the steric interference of the *tert*-butyl groups and as a result, the less demanding path of proton donation is followed (Scheme 1.62). In order to shed light on this possibility, the corresponding benzamide (PhCON(OMe)Me) was prepared and used as an electrophile. However, the results of this experiment were inconclusive as the reaction produced an intractable mixture of products. Although reprotonation seems to be a plausible explanation for the recovered starting material, more evidence is needed before any conclusions can be drawn.



Scheme 1.62

Several heteroatom based electrophiles were also included providing oxygen, halogen, phosphorus, silicon and boron substituted products (entries 7-12). Perhaps the most interesting of these products, boronic acid derivative **1.171h**, was condensed with 1,3-propanediol in the presence of MgSO₄ affording the corresponding boronate ester **1.171n** in 65% overall yield. The boronate product was crystallized from hexane to provide single crystals suitable for X-ray diffraction studies (Appendix 5). As seen in the solid state structure (Figure 1.4), there is a strong interaction between the boron atom and the oxygen from the phosphine oxide moiety

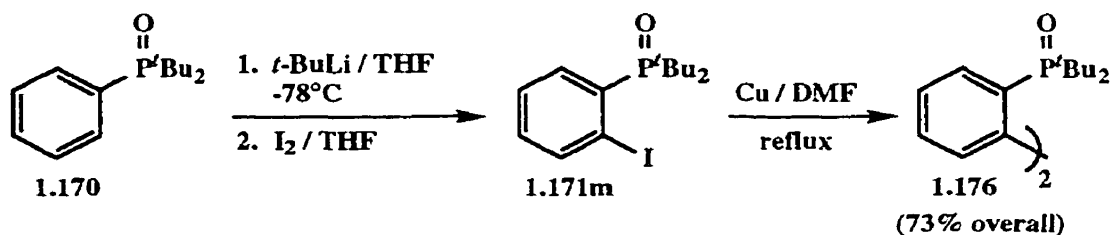
Figure 1.4 - Single Crystal X-ray Analysis of 1.171n.



with an interatomic distance of only 1.666 Å and inducing a tetrahedral arrangement about the boron atom. Comparing this X-ray structure with other phosphine oxides^{262,263} shows that the P-O bond length is only slightly longer than average at 1.533 Å while the B-O ester bond lengths (1.429 Å, 1.434 Å) are longer than would be expected for trigonal planar boronates and are more in line with a tetrahedral arrangement.²⁶⁴⁻²⁶⁶ Analysis of the ³¹P NMR spectrum shows a signal which is significantly downfield compared with other phosphine oxides (**1.171**) in the series, which strongly suggests that a B-O-P interaction probably also exists in solution.

1.5.4 Synthesis of Hindered Biaryl Bisphosphine Oxides

In order to further demonstrate practical applications of the new P-based DoM methodology, the iodo derivative **1.171m** (Scheme 1.63) was prepared for homocoupling studies. Treatment of **1.170** with standard metalation conditions followed by quench with a solution of I₂ led to **1.171m** in 76% yield. A DMF solution of **1.171m** with excess copper powder heated at reflux afforded 96% of the homocoupling product **1.176**. The sequence of metalation / iodination / homocoupling was achieved in 73% overall yield.



Scheme 1.63

X-ray crystal structure analysis of **1.176** revealed a dihedral angle between phenyl rings of nearly 90° as a result of the strong steric interaction between the 2- and 2'-substituents (Appendix 6). The orientation of the two phosphine oxide groups is such that the oxygen points towards the centre of the opposing phenyl ring (Figures 1.5a and 1.5b). Not surprisingly, the limited mobility of the *tert*-butyl groups in this system results in two distinct

Figure 1.5a - Single Crystal X-ray Analysis of 1.176.

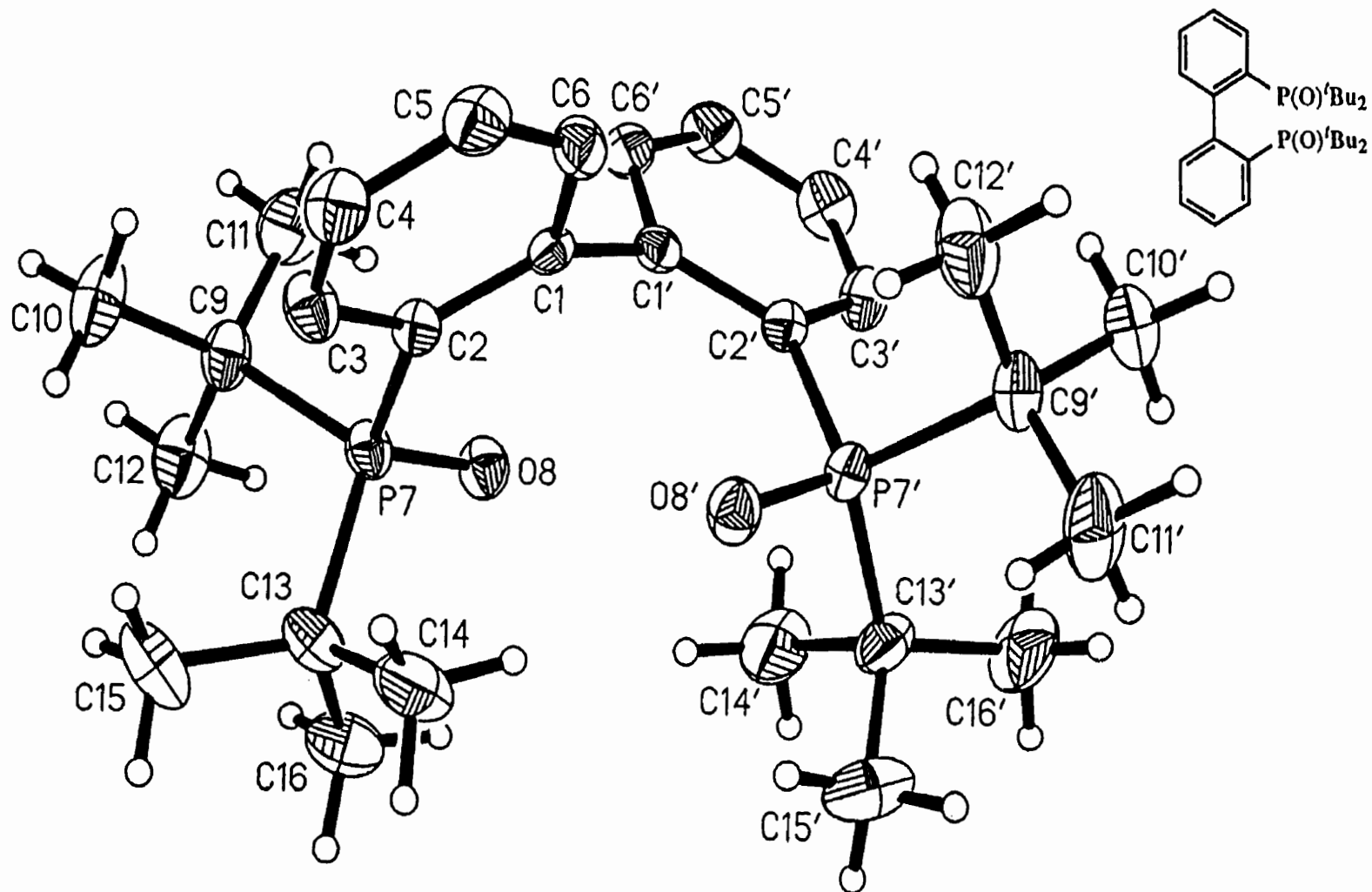
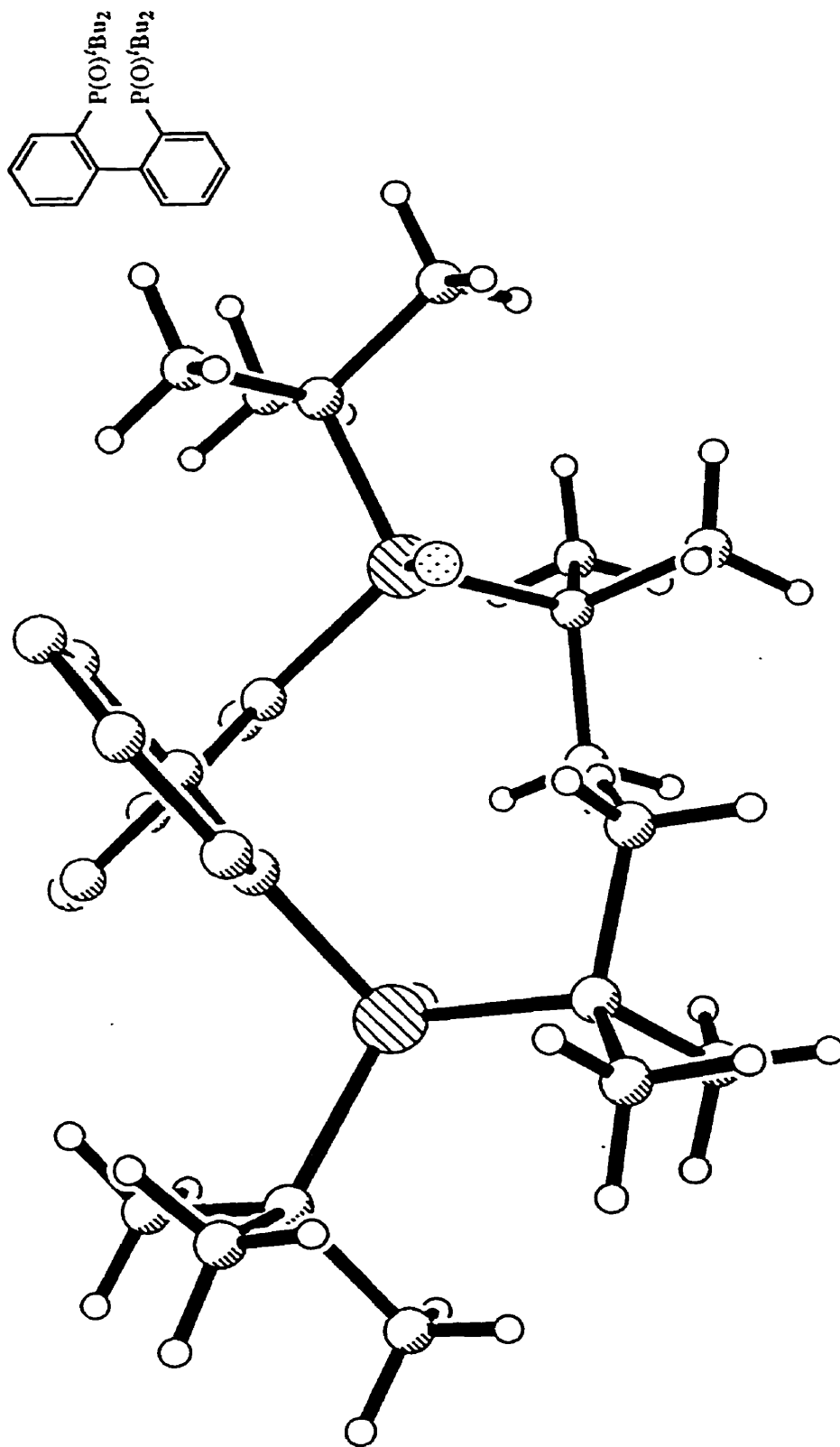


Figure 1.5b - Single Crystal X-ray Analysis of 1.176.

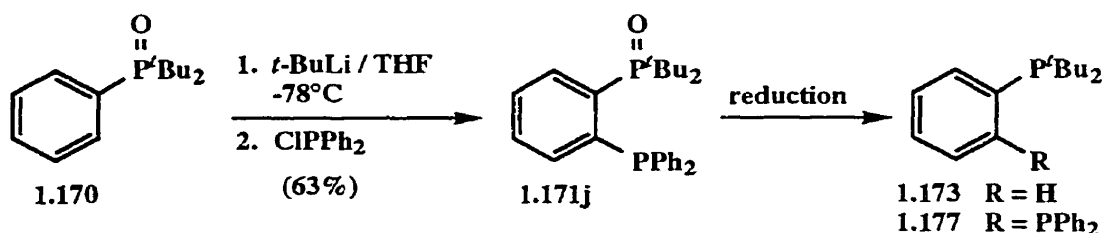


tert-butyl doublets in the $^1\text{H-NMR}$ spectrum centred at δ 1.37 and δ 1.25 respectively, similar to what was observed for ferrocenyl derivatives **1.169** (Scheme 1.57). In the case of **1.176**, the difference in chemical environment probably arises as a result of *tert*-butyl groups oriented towards the "inside" or the "outside" of the molecule.

1.5.5 Aryl Phosphine Oxide Reduction

In order to synthesize new phosphine ligands, the phosphine oxide **1.171j** was subjected to reductive conditions (Scheme 1.64) and afforded the interesting unsymmetrical bisphosphine **1.177**. Literature protocols for the $\text{R}_3\text{P}(\text{O}) \rightarrow \text{R}_3\text{P}$ transformation are limited to two methods; *i*) reduction with aluminum hydrides; and *ii*) silane / Et_3N reducing conditions.

Treatment of a solution of **1.171j** with an excess of LAH in toluene at reflux cleanly produced a new compound which was shown to be phosphine **1.173** (Scheme 1.64) in 71% yield. In contrast, treatment of the phosphine oxide with trichlorosilane in the presence of triethylamine in toluene at reflux proceeded smoothly to give the desired bisphosphine **1.177** in 78% yield. The synthesis of **1.177** provides access to an interesting new unsymmetrical bisphosphine but, more importantly, may constitute a new route to interesting phosphines.



entry	reduction conditions	product	yield, %
1	LAH / toluene / reflux	1.173	71
2	Cl_3SiH / NEt_3 / toluene / reflux	1.177	78

Scheme 1.64

Reduction of biaryl **1.176** under the Cl_3SiH / Et_3N conditions was attempted to further generalize the reduction while producing an interesting bisphosphine which would be difficult to prepare by other means. However, under a variety of conditions, this robust phosphine

oxide remained untouched, even when heated to reflux in xylene (Table 1.2). The inability to reduce the phosphine oxide groups is likely a result of the guarded orientation of the oxygen atoms as discussed previously (Figure 1.5), and imposes a limitation on the application of the methodology.

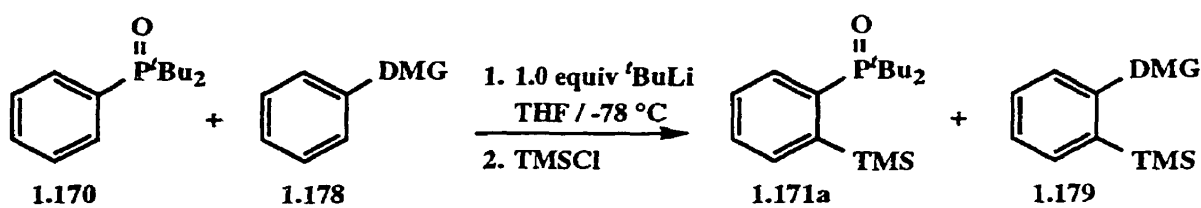
Table 1.2 - Attempted Reduction of 2,2'-Bis(di-*tert*-butylphosphinyl)biphenyl (1.176)

Reduction Conditions	Result
LAH / toluene / room temp	starting material
LAH / toluene / reflux	starting material
Cl ₃ SiH / NEt ₃ / toluene / room temp	starting material
Cl ₃ SiH / NEt ₃ / toluene / reflux	starting material
Cl ₃ SiH / NEt ₃ / xylene / reflux	starting material

1.5.6 Relative DMG Hierarchy of the P(O)*t*Bu₂ DMG

Intermolecular and intramolecular competition studies were performed to pit the P(O)P*t*Bu₂ group against other well established DMGs (CONEt₂, OCONEt₂, and OMe) in order to establish its relative DoM effect.

To test the metalating ability of the di-*tert*-butylphosphinyl group in intermolecular competition against the powerful tertiary carbamate,⁷ equimolar amounts of *N,N*-diethyl-*O*-phenyl carbamate (**1.178a**) and di-*tert*-butylphenylphosphine oxide (**1.170**) were allowed to compete for one equivalent of *t*-BuLi. Using the respective *ortho*-silyl derivatives **1.171a** and **1.179a** (Scheme 1.65) as a measure of the relative amounts of the respective metalated intermediates, the metalation ratios were analyzed. As expected, based on the well known metalation ability of the tertiary carbamate, the only isolated product of the reaction was silyl derivative **1.179a**. The result, isolation of **1.179a** (entry 1, DMG = OCONEt₂) as the sole product with no detectable amount of **1.171a**, demonstrates again the power of the OCONEt₂ DMG.



entry	DMG	substrate 1.178	ratio 1.171a : 1.179
1	-OCONEt ₂	a	< 5 : 95
2	-CONEt ₂	b	20 : 80
3	-OMe	c	> 95 : 5

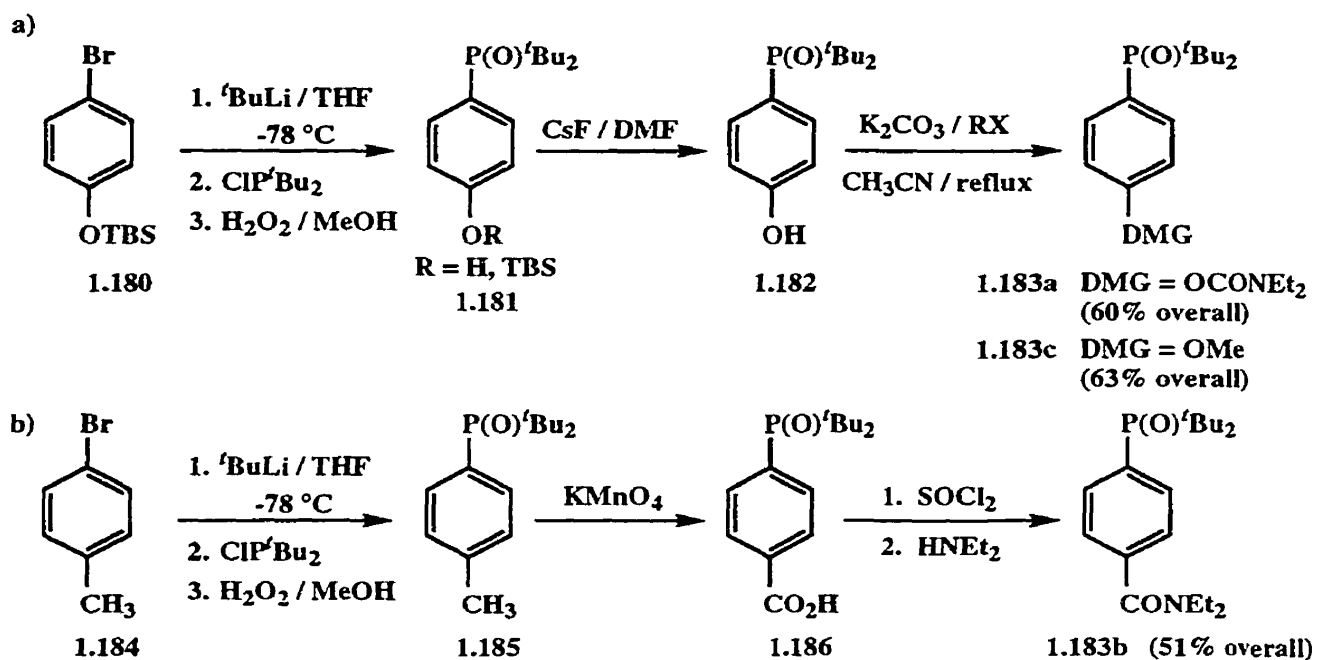
Scheme 1.65

A similar competition experiment carried out between **1.170** and *N,N*-diethyl benzamide (**1.178b**, entry 2) led to products **1.171a** and **1.179b** in a 20:80 ratio. While it may be somewhat optimistic to claim that the di-*tert*-butylphosphinyl moiety is comparable in metalating power to the tertiary amide, it is nonetheless clear that it shows significant directing ability.

The final intermolecular experiment placed **1.170** in competition with anisole (**1.178c**). While tertiary amides and carbamates were the distinct victors in their respective competition experiments, the phosphinyl group showed clear dominance when competing against the methoxy group. The ratio of products strongly favoured **1.171a** with no detectable amount of *ortho*-trimethylsilylanisole (**1.179c**) being formed.

Intramolecular competition experiments were performed by arranging the same three competing DMGs in a 1,4 relationship within the same substrate. For carbamate and methoxy substrates (**1.183a** and **1.183c** respectively), synthesis was accomplished by treating TBS-protected 4-bromophenol (**1.180**) in a metal-halogen exchange reaction and quenching with chlorodi-*tert*-butylphosphine followed by oxidation to produce phosphine oxide **1.181** (R = TBS, Scheme 1.66b) in a sequence analogous to the preparation of **1.170** (Scheme 1.59a). Since the silyl protecting group was partially cleaved during this sequence, the mixture of products was treated with CsF in DMF to obtain pure **1.182**. Standard conditions (ClCONEt₂

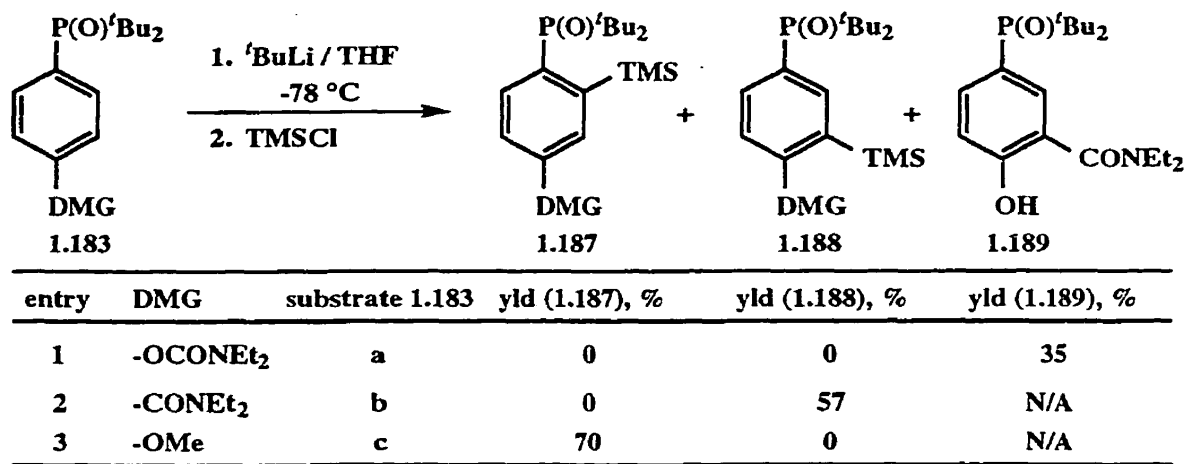
or MeI / CH₃CN / K₂CO₃) were employed to prepare the required 1,4-bisDMG systems **1.183a** and **1.183c** (Scheme 1.66a). The desired amide substrate **1.183b** was easily obtained from the corresponding carboxylic acid **1.186** which was prepared in three steps in 51% overall yield from 4-bromotoluene (**1.184**) by modification of a literature procedure (Scheme 1.66a).^{267,268}



Scheme 1.66

With the desired substrates **1.183a-c** in hand, intramolecular competition experiments were performed (Scheme 1.67). Metalation-silylation of **1.183a** led not to the TMS incorporated products **1.187a** and **1.188a**, but to salicylamide **1.189**, the result of an anionic *ortho* Fries rearrangement, despite quenching the reaction mixture at -78 °C. Although the anionic Fries rearrangement is well documented,⁷ the migration reaction generally is not spontaneous at -78 °C and usually requires warming of the reaction mixture.⁷⁴ In some cases it has been known to occur at low temperature when another *ortho* substituent is present placing undue steric demands on the tertiary carbamate.⁷⁵ The low temperature migration in

this case may simply be the result of the electron withdrawing characteristics of the phosphine oxide making the phenolate a more favourable leaving group.



Scheme 1.67

Intramolecular competition on **1.183b** gave amide **1.188b** as the only discernable product in 57% yield. The product resulting from metalation *ortho* to the phosphinoyl DMG (**1.187b**) was not observed despite the modest competitiveness observed in the intermolecular experiments.

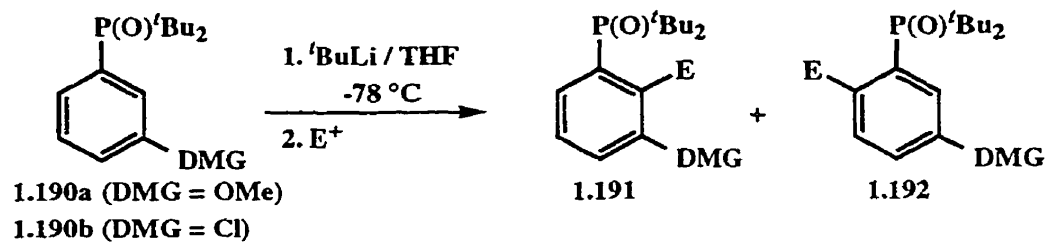
Consistent with the intermolecular results, the phosphinoyl DMG significantly outperformed the OMe DMG in the intramolecular experiment. Treatment of **1.183c** with *t*-BuLi followed by quench with TMSCl resulted in the isolation of **1.187c** in 70% yield while the corresponding product resulting from metalation *ortho* to the methoxy group (**1.188c**) was not detected.

The combination of the above competition studies provides some insight to the relative position of the new DMG in the DMG hierarchy. Based on these results, the relative order of metalating ability DMG = OCONEt₂ > CONEt₂ > P(O)*t*Bu₂ > OMe has been qualitatively established. It is important to recognize that the order of metalating ability thus established assumes that the electrophile reacts with the *ortho*-metalated species faster than inter- or intramolecular equilibration of anions.

1.5.7 Cooperative Metalation of the P(O)^tBu₂ DMG

In DoM chemistry, two directing substituents present in a 1,3 relationship will generally cooperate to direct the metalation to the 2, or "in-between" position. Two cases have been investigated as a preliminary assessment of cooperative DMG effects as they apply to the P(O)^tBu₂ DMG.

In the first cooperative metalation experiment (entry 1, Scheme 1.68), the phosphinyl DMG and the methoxy DMG were used in concert to direct metalation between the two directing groups. This substrate (prepared in 58% overall yield by metal-halogen exchange of 3-bromoanisole followed by quench with chlorodi-*tert*-butylphosphine and oxidation) may be expected to provide as many as three regioisomeric DoM products resulting from metalation *ortho* to phosphorus (**1.192a**), *ortho* to methoxy, or in between (**1.191a**). Having already established the superiority of the phosphinyl DMG, metalation adjacent to methoxy seemed unlikely. Experimental results supported this prediction as treatment of **1.190a** with *t*-BuLi in THF at -78 °C followed by quench with TMSCl resulted in isolation of only **1.191a** in 67% yield.



entry	DMG	E	yld, %	ratio 1.191:1.192
1	-OMe	TMS	67	> 95 : 5
2	-Cl	CONH ^t Bu	56	8 : 1

Scheme 1.68

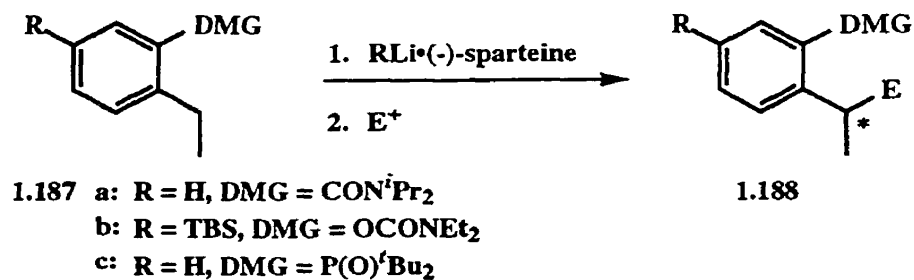
The second cooperative DMG experiment (entry 2), contributed by another group member,²⁶⁹ utilized the noted ability of a chlorine substituent in cooperative metalation. While product distribution was restricted to a single compound in the OMe example, this experiment provided an inseparable mixture of products **1.191b** and **1.192b** in a 8:1 ratio (NMR). The

somewhat lower selectivity may be rationalized based on the much weaker directing ability of the chlorine substituent²⁷⁰ resulting in formation of the small amount of **1.192b**.

1.6 Future Work

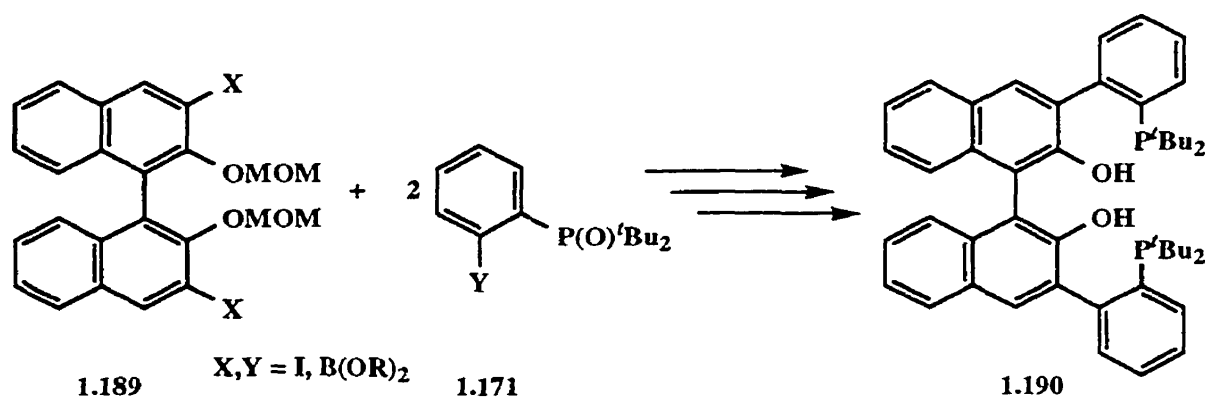
The di-*tert*-butylphosphinyl group has been shown to be an effective DMG in the synthesis of diverse phosphinyl aromatics and its relative position in the DMG hierarchy *vis a vis* OCONEt₂, CONEt₂, and OMe, has been established. With a straightforward synthesis of 2-substituted aryldi-*tert*-butylphosphines now available, future work may include design and synthesis of specific ligands for various catalytic processes. While the reduction of the phosphine oxides to provide tertiary phosphines was demonstrated, despite the relatively high P=O bond energy, it is clear that the *tert*-butyl groups pose some limitations on the reduction (e.g. biaryl **1.176**, Table 1.2). A systematic survey of reduction methods for such systems would be advantageous and would offer a facile route to highly hindered biphenyl-based bidentate phosphine ligands, a class of ligands whose importance has been demonstrated.^{235,239}

Gray and Snieckus have initiated studies on the (-)-sparteine mediated enantioselective lateral metalation of di-*tert*-butyl(2-ethylphenyl)phosphine oxide (**1.187c**)²⁷¹ as an extension of established methodology for other directing groups such as amides **1.187a**²⁵⁰ and carbamates **1.187b**²⁷² (Scheme 1.67). Preliminary experiments have shown modest enantioinduction and further optimization of this chemistry may allow preparation of phosphine ligands incorporating a chiral element and opening the door to applications in asymmetric catalysis.

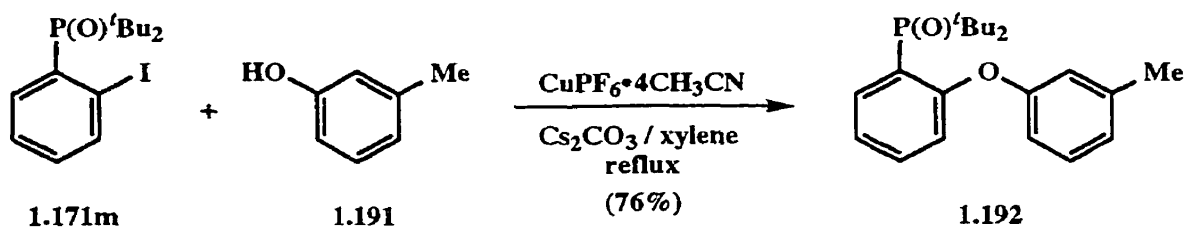


Scheme 1.67

The preparation of derivatives such as iodide **1.171m** and boronate **1.171h** (Scheme 1.61) suggests that Suzuki aryl-aryl cross coupling chemistry of such derivatives should be investigated. Quinn and Snieckus have initiated cross coupling studies towards the synthesis of polydentate ligand systems such as **1.189** (Scheme 1.68).^{273,274} The accessibility of both halide and boron derivatives by the new methodology provides flexibility for coupling reactions. In addition, Felding and Snieckus have coupled iodide **1.171m** with *m*-cresol (**1.191**) providing diaryl ether **1.192** and potentially providing access to novel heterocyclic compounds (Scheme 1.69).²⁷⁵



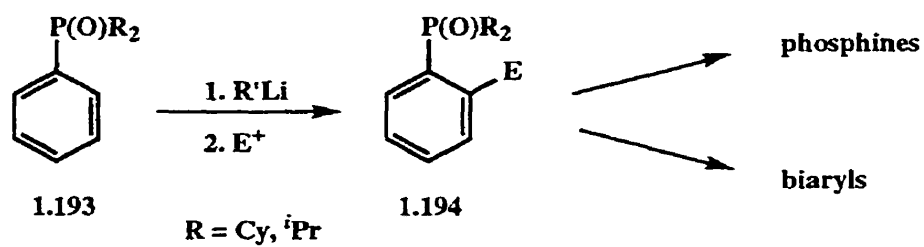
Scheme 1.68



Scheme 1.69

Finally, while metalation of **1.170** (Scheme 1.61) was quite successful and led to synthesis of novel phosphines, the problem of phosphine oxide reduction in highly hindered molecules places a limitation on the utility of this method. In this context, investigation of the metalation of other phosphinyl-containing systems may be appropriate. With this in mind, substrates such as **1.193** (Scheme 1.70) warrant some attention. Analogous metalation /

electrophile quench with such substrates could lead to substituted phosphine oxides **1.194**, molecules whose reduction is expected to be more facile due to the reduced steric demands.

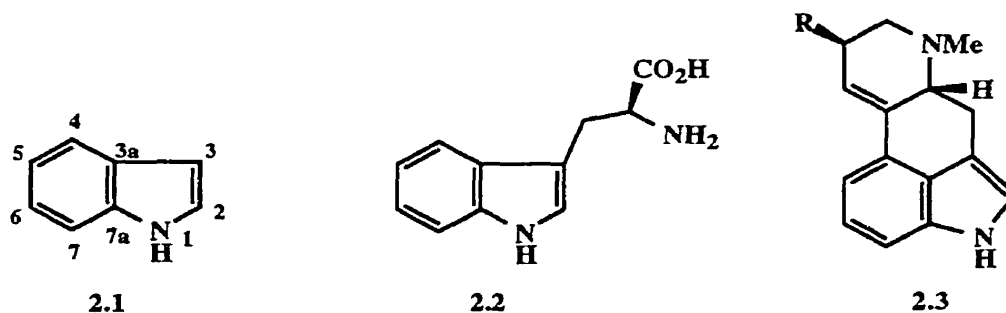


Scheme 1.70

2.0 Regioselective C-7 Metalation of Indoles

2.1 Introduction

The indole ring (2.1), constitutes part of the structure of essential compounds such as the amino acid tryptophan (2.2), and more complex natural products such as the ergot alkaloids (2.3),²⁷⁶ some of which are psychoactive. Indole natural products represent a large class of alkaloids^{277,278} and have long been a source of synthetic targets for chemists due to their wide range of biological activity.

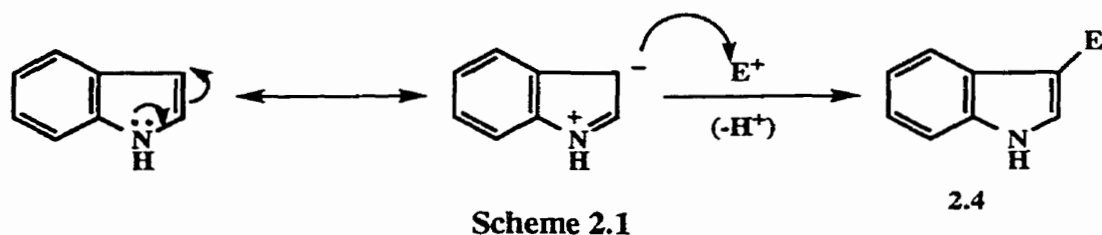


Synthesis of functionalized indoles²⁷⁹ may be accomplished through *de novo* ring construction of the indole nucleus from substituted benzene precursors.²⁸⁰⁻²⁸⁴ Alternatively, functionalization of a pre-existing indole nucleus may be conveniently divided into two categories: *i*) derivatization of the pyrrole ring; and *ii*) derivatization of the benzenoid ring. Although strategies for substitution of the pyrrole ring by electrophilic substitution and DoM are well established, general methods for direct functionalization of the benzene ring are much less prevalent.²⁸⁵ Section 2.2 will address the various synthetic methods available for functionalization of a pre-existing indole nucleus.

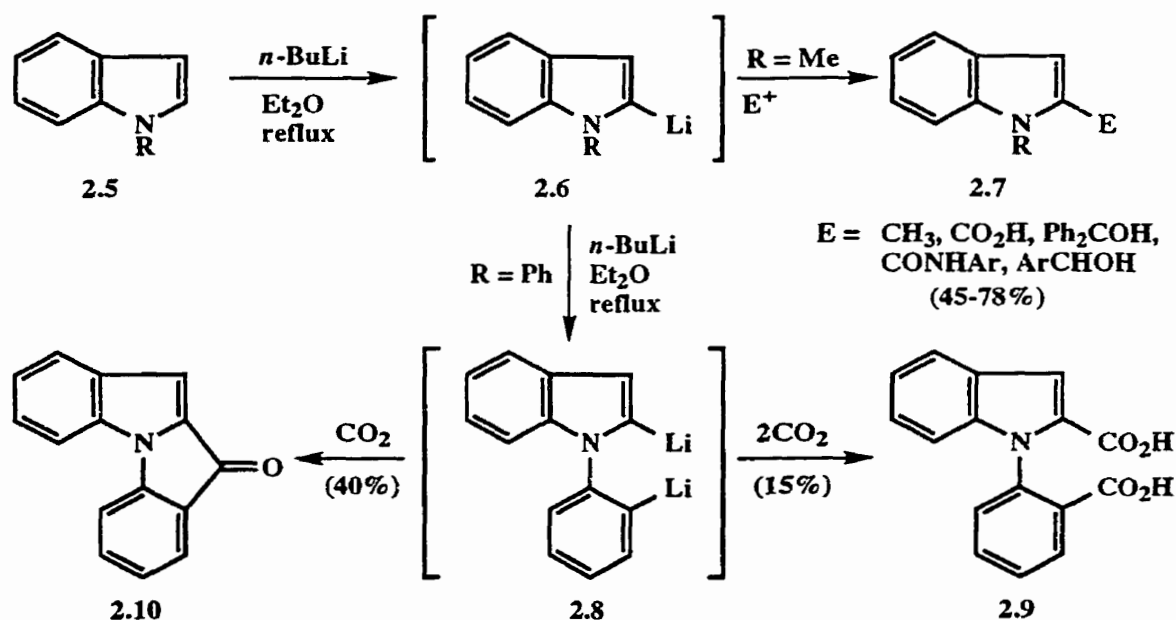
2.2 Functionalization of Indoles

2.2.1 2- and 3-Substituted Indoles

While the utility of electrophilic substitution in formation 3-substituted indoles 2.4 is well documented (Scheme 2.1),²⁷⁹ discussion here will be limited to metalation chemistry of indole systems.



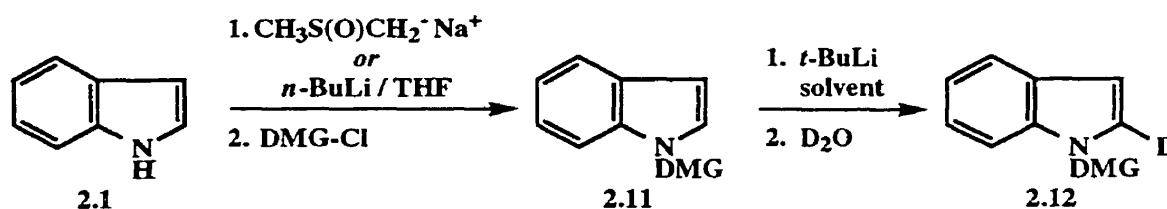
Metalation chemistry has played an important role in the derivatization of indoles at the 2-position. In *N*-substituted indoles, the 2-H is more acidic than any of the other ring protons, and thus metalation / electrophile quench in the 2-position is a facile process. A range of indole-*N* protecting / directing groups have been employed for the synthesis of 2-substituted indoles. Shirley and Roussel, after finding that unprotected indole could not be dimetalated, reported the first lithiation of protected indoles in the 2-position.²⁸⁶ Thus, treatment of *N*-methylindole (**2.5**, R = Me, Scheme 2.2) with *n*-BuLi proceeded smoothly to give *N*-methyl-2-lithioindole (**2.6**) and, after quench with an electrophile, 2-substituted indoles **2.7**. The regioselectivity of this reaction is governed by the thermodynamic acidity of the 2-H rather than



any directing ability of the *N*-substituent since there is clearly no coordinative stabilization provided by the alkyl group. While 1-methyl-2-lithioindole is efficiently prepared in this

manner, synthetic application is limited due to the difficulty in removing the *N*-alkyl group. In the same study, metalation of *N*-phenylindole (**2.5**, R = Ph) was attempted. Although metalation occurred in the 2-position as expected, a substantial portion of the product was derived from dimetalation forming **2.8** such that quench with CO₂ afforded dicarboxylic acid **2.9** (15%) and ketone **2.10** (40%).

Early efforts to find a suitably labile *N*-directed metalation group were reported by Sundberg and Russell.²⁸⁷ Thus, a series of *N*-substituted indoles **2.11** were prepared and their metalation / deuteration reactions using *t*-BuLi as the metalating agent were studied (Scheme 2.3). Treatment of **2.1** with the dimsilyl sodium followed by appropriate electrophiles allowed preparation of **2.11a-d** in good yields (80-92%), while **2.11e-f** were prepared by treating a THF solution of **2.1** with *n*-BuLi followed by the appropriate silyl chloride. Each of the *N*-substituted indoles was then subjected to metalation and the best results were achieved

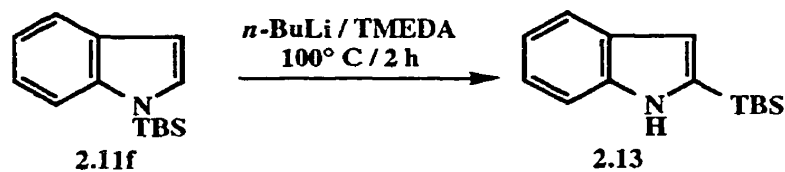


entry	SM	DMG	solvent	% recovery	% D	% D at C-2
1	2.11a	MOM	Et ₂ O	77	95	95
2	2.11b	CH ₂ OCH ₂ Ph	Et ₂ O	35	40	30
3	2.11c	CH ₂ Ph	THF	90	70	15
4	2.11d	SO ₂ Ph	THF	90	97	86
5	2.11d	SO ₂ Ph	TMEDA	85	90	88
6	2.11e	TMS	TMEDA	0	0	0
7	2.11f	TBS	THF	85	0	0
8	2.11f	TBS	TMEDA	60	0	0

Scheme 2.3

using *N*-MOM (**2.11a**) and *N*-SO₂Ph (**2.11d**) indoles (entries 1,4,5), which provided corresponding 2-deuterio derivatives **2.12** in excellent yield using *t*-BuLi for deprotonation.

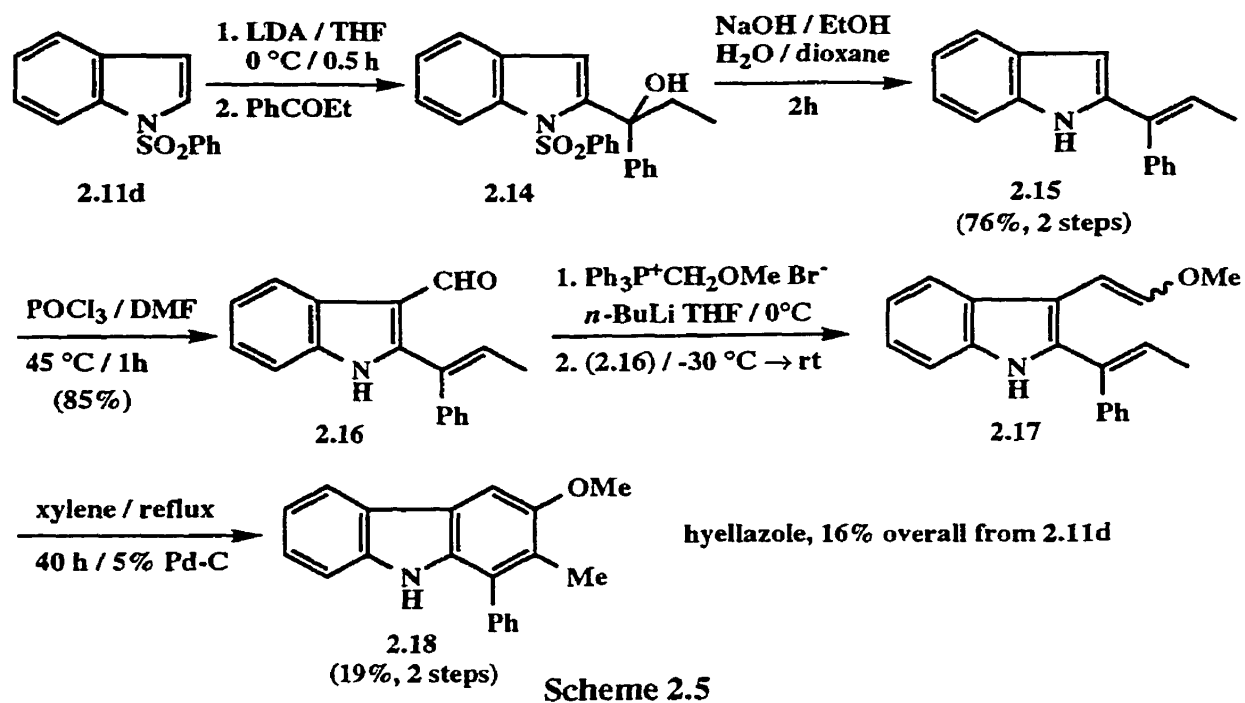
N-Benzyloxymethylindole (**2.11b**) underwent metalation but provided the desired 2-deuterio derivative **2.12d** in only 30% yield (entry 2); benzylic metalation and Wittig migration was the predominant reaction pathway. Benzylic metalation was also the major reaction when *N*-benzylindole (**2.11c**) was treated with *t*-BuLi (entry 3); incorporation of deuterium in the 2-position accounted for only 15% of the product mixture. *N*-Trimethylsilylindole (**2.11e**) was deprotected under the reaction conditions to give indole (**2.1**) as the only detectable product (entry 6) while *N*-(*tert*-butyldimethylsilyl)indole (**2.11f**) failed to provide any products with 2-deuterium incorporation (entries 7,8), probably due to the steric effect of the TBS group. Reaction of **2.11f** with the less sterically demanding *n*-BuLi, however, resulted in metalation in the 2-position as evidenced by the isolation of silicon-migrated product **2.13** (Scheme 2.4) along with unreacted starting material. Although the isolation of **2.13** is a clear indication that 2-metalation was achieved, harsh reaction conditions were required and there is little synthetic utility in the migration.



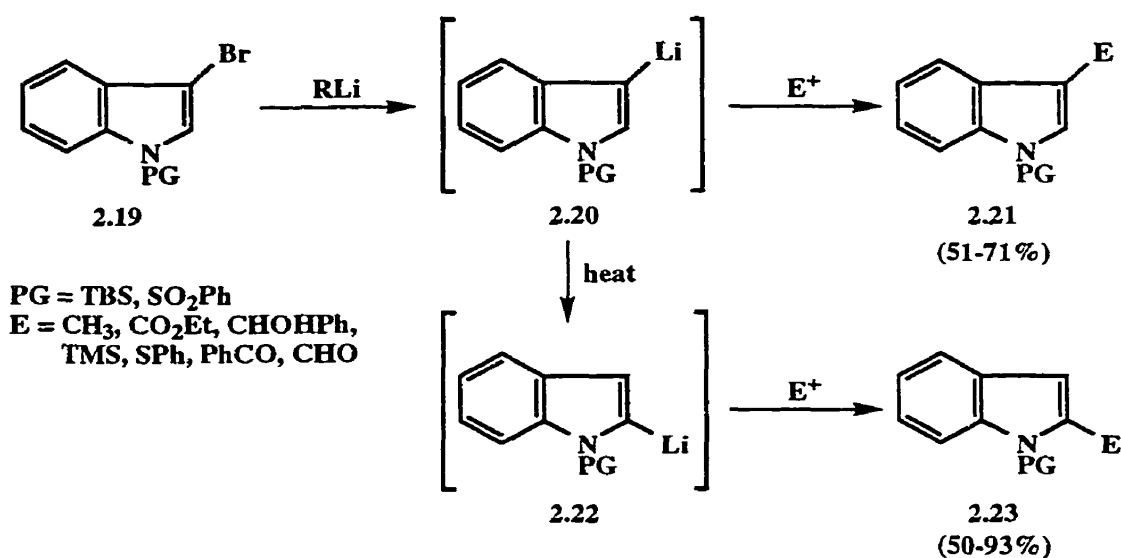
Scheme 2.4

Subsequently, several other labile *N*-directing groups have proven effective in 2-metalation of indoles and/or pyrroles, including Boc,²⁸⁸⁻²⁹⁰ OSEM,^{289,291-293} CO₂⁻,²⁹⁴⁻²⁹⁶ CH₂NMe₂,^{297,298} OMe,²⁸⁹ and CON(*t*Bu)Li.²⁹⁹ Effective manipulation of the protecting / directing groups has led to numerous natural product syntheses involving indole-2-metalation as a key step. In an instructive example of metalation used in conjunction with electrophilic substitution, Kano and co-workers reported a concise synthesis of the alkaloid hyellazole (Scheme 2.5).³⁰⁰ Thus, *N*-(phenylsulfonyl)indole (**2.11d**) was treated with LDA followed by propiophenone affording the tertiary alcohol **2.14**. Basic hydrolysis of the phenylsulfonyl DMG proceeded with concomitant dehydration of the alcohol to give olefin **2.15**, exclusively

as the *E*-isomer. Vilsmeier reaction of **2.15** gave aldehyde **2.16**, which was reacted without purification to provide the olefin **2.17** as a mixture of isomers. Finally, thermal cyclization in the presence of Pd on carbon produced hyellazole (**2.18**) in 16% overall yield from **2.11d**.



Several groups have demonstrated that metalation approaches may indirectly be applied to the synthesis of 3-substituted indoles. Treatment of suitably protected (e.g. PG = TBS) 3-bromoindoles **2.19**, easily accessible by electrophilic bromination,^{301,302} with an alkyllithium reagent promoted a metal-halogen exchange producing the *N*-protected-3-lithioindole **2.20** (Scheme 2.6). Subsequent quench with an electrophile afforded the corresponding 3-substituted products **2.21**. Over extended periods of time or upon warming, some intermediates **2.20** underwent rearrangement to the corresponding 2-lithio derivatives **2.22** owing to the thermodynamic stability of the 2-Li species and thereby lead to **2.23**.³⁰³⁻³⁰⁸ Certain *N*-(benzenesulfonyl)-3-lithioindoles have also been shown to undergo a ring fragmentation forming 2-aminophenylacetylene derivatives.³⁰⁹⁻³¹¹

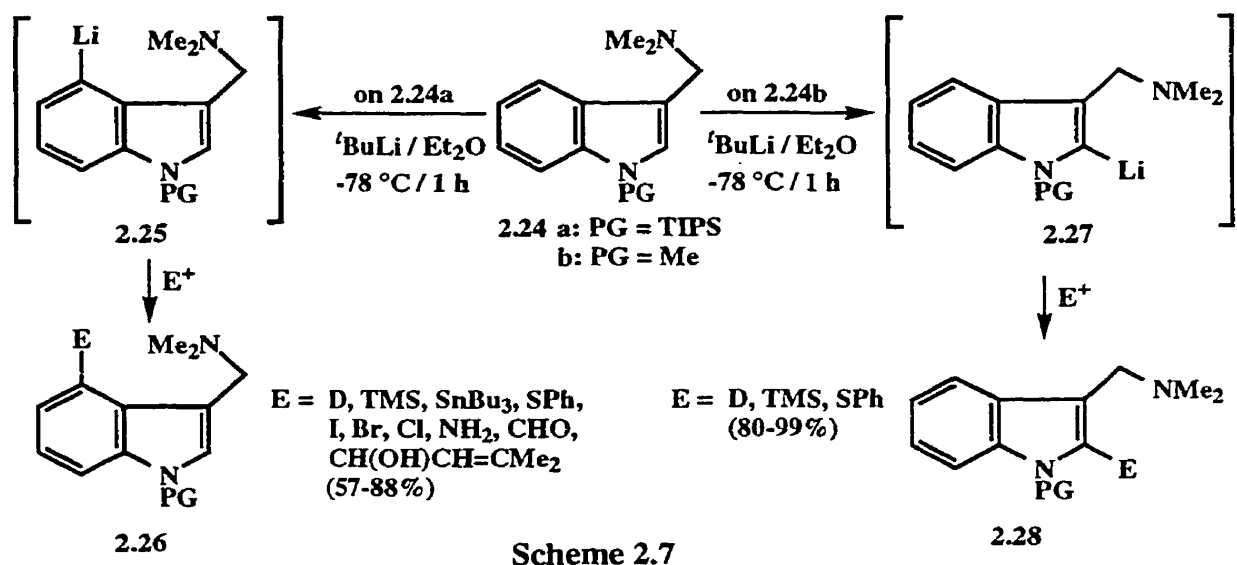


Scheme 2.6

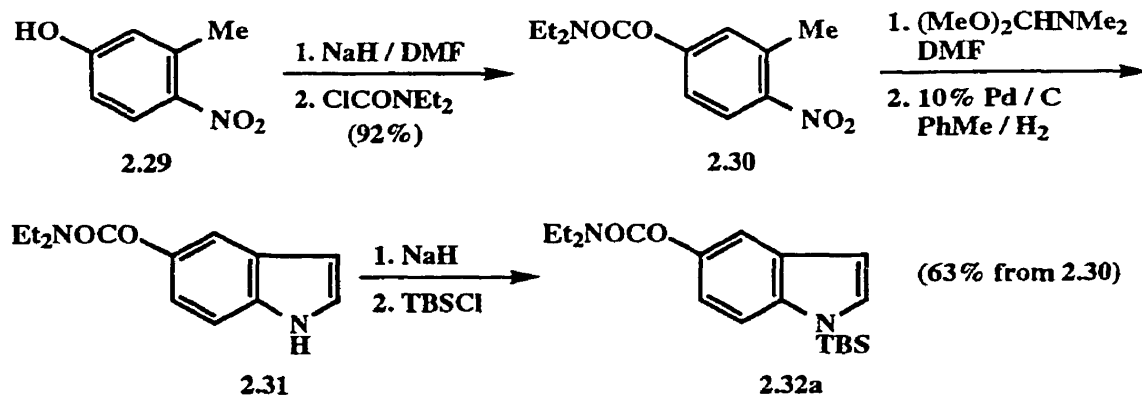
2.2.2 Benzenoid Substitution

In contrast to the plethora of conditions available for pyrrole ring functionalization in indoles, the few available methods for functionalization of the benzenoid portion invariably rely on classical electrophilic substitution or incorporation of functionality prior to indole ring construction.²⁷⁹ However, metalation of the benzenoid ring is indeed a viable process despite receiving limited attention. Accordingly, Iwao demonstrated³¹² that *N*-TIPS-gramine (**2.24a**) was smoothly metalated with *t*-BuLi to afford the corresponding 4-lithio derivative **2.25** (Scheme 2.7). Subsequent quench with an electrophile led to good yields of 4-substituted indoles **2.26**. Again, the silicon functionality serves not only as an NH protecting group, but also to sterically block deprotonation at the 2-position. This transformation represented the first example of regioselective metalation in the benzenoid ring of an indole system where the thermodynamic acidity of the ring protons is clearly greater than that in the pyrrole ring. While the dimethylaminomethyl functionality undoubtedly contributes to the regioselectivity of the reaction, the importance of the steric contribution of the silicon protecting group is demonstrated by metalation of the related indole **2.24b**. When this *N*-methyl analogue was treated under identical conditions, 2-substituted indoles **2.28** were the only isolated products,

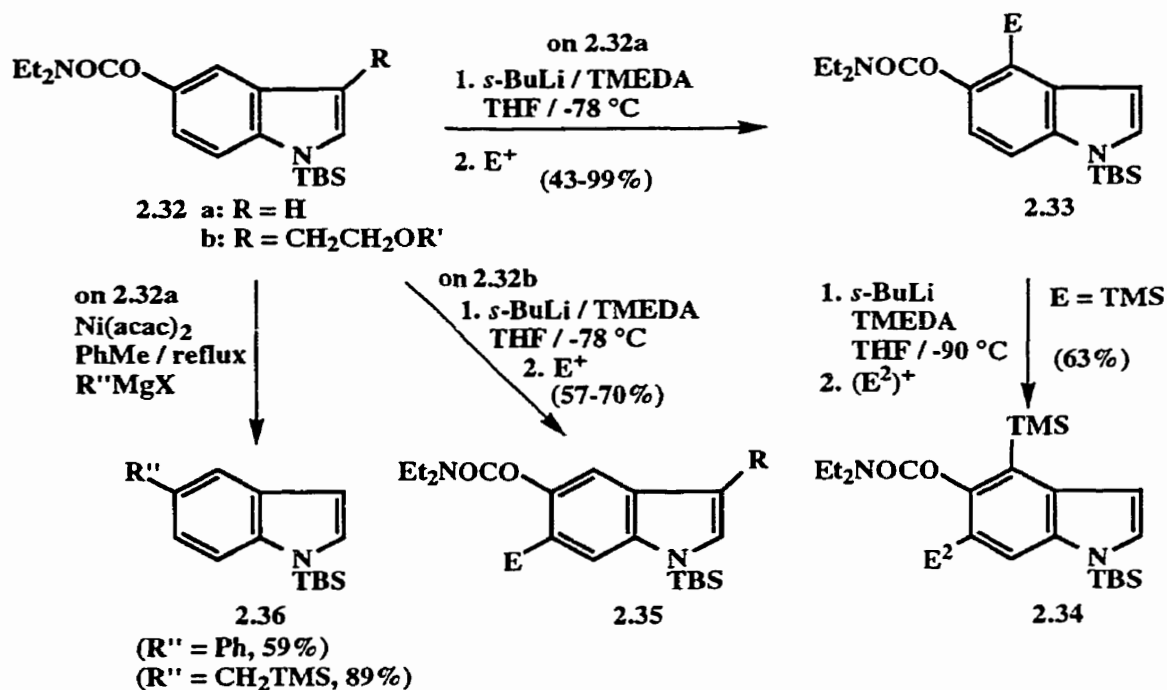
perhaps suggesting that the 2-H is more thermodynamically acidic but inaccessible when the bulky silicon protecting group is in place.



Snieckus and co-workers have contributed to benzenoid metalation in indoles by taking advantage of *O*-indolyl carbamate **2.32a**, easily accessible by the Leimgruber-Batcho indole synthesis (Scheme 2.8).^{282,302} Thus, after phenol protection, the *ortho*-nitrotoluene **2.30** was treated with DMF-dimethyl acetal followed by catalytic hydrogenation to provide indole **2.31**. Silicon protection provided the desired indole **2.32a** in 63% overall yield from commercially available **2.29**. Metalation of this versatile intermediate under standard



carbamate metalation conditions (*s*-BuLi / TMEDA / THF / -78 °C) proceeded cleanly to provide 4,5-disubstituted products **2.33** in modest to excellent yield (Scheme 2.9). This protocol provides direct access to 5-hydroxyindole derivatives, compounds which have been implicated in a broad range of physiological processes,^{313,314} while avoiding the necessity of a DMG in the 3-position. This regioselective metalation process also allows selective preparation

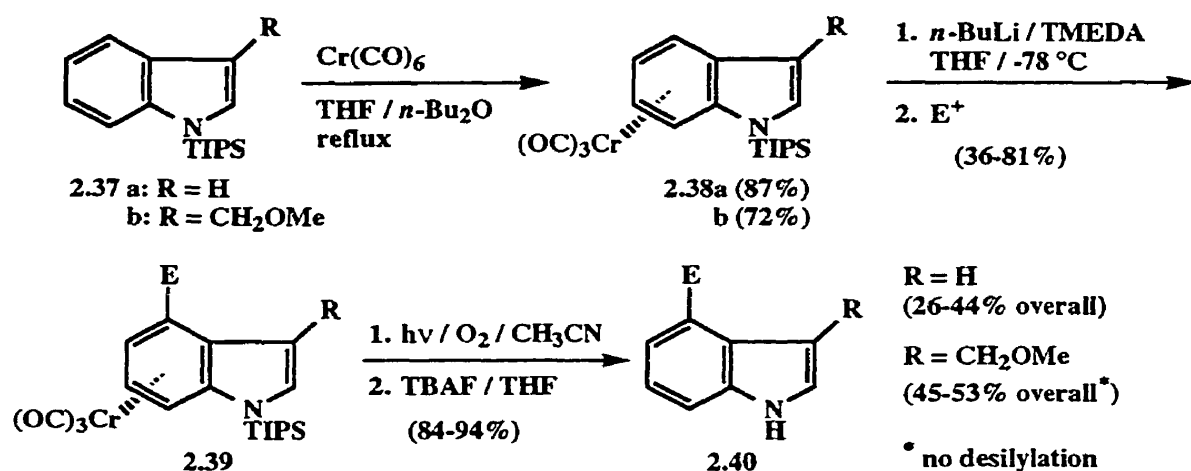


Scheme 2.9

of 6-substituted indoles. Thus, treatment of **2.32a** under standard metalation conditions (Scheme 2.9) and quenching the resulting anion with TMSCl gave **2.33** (E = TMS) in 90% yield. The silyl substituted indole was then treated under similar metalation conditions, maintaining the temperature at -90 °C to avoid an anionic Fries rearrangement of the carbamate moiety,⁷⁴ and quenched with an electrophile to afford the corresponding 4,5,6-trisubstituted indoles **2.34** (Scheme 2.9). The presence of a substituent in the 3-position was shown to have a drastic effect on regioselectivity. While metalation of TBS-indole **2.32a** cleanly gave 4-substituted products, treatment of related indoles **2.32b** (R' = H, TBS) under the same conditions yielded the corresponding 6-substituted indoles **2.35** rather than the expected 4-

substituted products. Although no acidity data is available, the remarkable 4- vs. 6-regioselectivity in these processes may be due to a subtle difference in kinetic acidity favouring the 4-position since the presence of less sterically demanding 3-substituents including TMS and Me had the same effect on regioselectivity.^{302,315} Finally, the carbamate moiety may be utilized in Ni-catalyzed cross-coupling reactions to further functionalize the indole nucleus. Thus, treatment of **2.32a** with a Grignard reagent in the presence of Ni(acac)₂ proceeded to provide the corresponding 5-substituted indoles **2.36** in good to excellent yield.^{302,315,316}

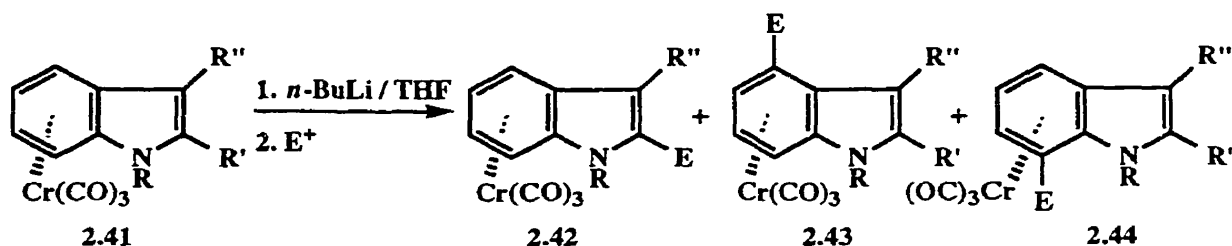
Widdowson and co-workers,^{317,318} taking advantage of increased ring proton acidity supplied by tricarbonylchromium(0) complexation, have applied metalation chemistry to the synthesis of 4-substituted indoles. Thus, *N*-TIPS-indole (**2.37a**) was treated with chromium hexacarbonyl to provide arene complex **2.38a** in 87% yield (Scheme 2.10). Upon treatment with *n*-BuLi / TMEDA, followed by treatment with an electrophile, 4-substituted complexes **2.39** were isolated in acceptable yield (36-69%). Subsequent photolytic decomplexation and TBAF-promoted desilylation provided the corresponding indoles **2.40** with overall yields for the 4 step procedure ranging from 26-44%. Alternatively, the deprotection sequence could be reversed, with desilylation preceding thermal decomplexation of the chromium moiety. Although the TIPS group effectively blocked the 2- and 7-positions, some products were observed which resulted from metalation in the 5- and 6-positions. The methoxymethyl substituted indole **2.37b**, despite giving a lower yield of complexation product **2.38b** (72%), led to better yields of metalation products **2.39** (61-81%) since the presence of the methoxymethyl group in the 3-position aided in CIPE and coordination of the lithiated intermediate. Furthermore, the extra coordination offered better regioselectivity since no products resulting from 5- or 6- metalation were observed (Scheme 2.10). Thus, **2.37b** offered better overall yields of 4-substituted indoles although the desilylation procedure was not demonstrated for this series.



Scheme 2.10

As also demonstrated by Widdowson, the tricarbonylchromium approach to indole metalation has also found application to the synthesis of other substituted indoles.^{319,320} While the TIPS group was effective at precluding any 2- or 7-metalation, other *N*-substituents provided products of varying substitution. Since metalation of *N*-methylindole was already known (2.5, Scheme 2.2),^{286,287} the corresponding chromium(0) tricarbonyl complex **2.41a** (Scheme 2.11) was prepared to determine the regioselectivity of metalation. It was observed (entry 1) that, similar to the uncomplexed case, metalation in the 2-position was the only discernable process, providing moderate yields of the 2-substituted indole complexes **2.42**. However, in contrast to the uncomplexed indoles, treatment of the silicon-protected intermediate **2.41b** with *n*-BuLi (entries 3-8) resulted in metalation in the 4- and 7-positions leading to substituted complexes **2.43** and **2.44**. In most cases, the isomers were separable by column chromatography and the 7-substituted derivatives were obtained in favour of the 4-substituted derivatives but with poor selectivity. Reasoning that the methoxymethyl substituent would aid in metalation processes due to its coordinating ability, complex **2.41c** was prepared and treated under similar conditions (entries 9,10). Although 7-substituted products were obtained directly, without any blocking of the 2-position, the 2-substituted isomers were still produced in substantial quantities. Similarly, use of the SEM DMG without C-2 protection (**2.41d**) led to a mixture of 2- and 7-isomers which could not be separated (entry 11). In

marked contrast to *N*-methylindole-Cr(CO)₃ complex **2.41b**; however, the corresponding *N*-SEM complex **2.41e** underwent metalation regioselectively in the 7-position providing indoles **2.44** in moderate yields (entries 12-14). Presumably, the coordinating ability of the SEM substituent, which is unavailable in the methyl derivative, is at least partially responsible



entry	2.41	R	R'	R''	E	2.42 (%)	2.43 (%)	2.44 (%)
1	a	Me	H	H	TMS	60	0	0
2	a	Me	H	H	CO ₂ Et	78	0	0
3	b	Me	TMS	H	CO ₂ Et	-	17	67
4	b	Me	TMS	H	Me	-	64*	64*
5	b	Me	TMS	H	PhCH(OH)	-	20	63
6	b	Me	TMS	H	CH ₂ =CHCH(OH)	-	14	60
7	b	Me	TMS	H	SPh	-	22	51
8	b	Me	TMS	H	Me ₂ C=CHCH ₂	-	18	43
9	c	CH ₂ OMe	H	H	TMS	†	-	66
10	c	CH ₂ OMe	H	H	Me ₂ C=CHCH ₂	†	-	49
11	d	SEM	H	H	TMS	‡	-	‡
12	e	SEM	TMS	H	Me	-	-	95
13	e	SEM	TMS	H	CHO	-	-	70
14	e	SEM	TMS	H	CH ₂ =CHCH ₂	-	-	69
15	f	SEM	H	Me	TMS	-	-	88
16	f	SEM	H	Me	CO ₂ Et	-	-	66
17	f	SEM	H	Me	SnMe ₃	-	-	65
18	f	SEM	H	Me	CH ₂ =CHCH ₂	-	-	69

* combined yield of inseparable 4- and 7-isomers; † 2-isomer was present but not isolated; ‡ inseparable mixture of 2- and 7-isomers.

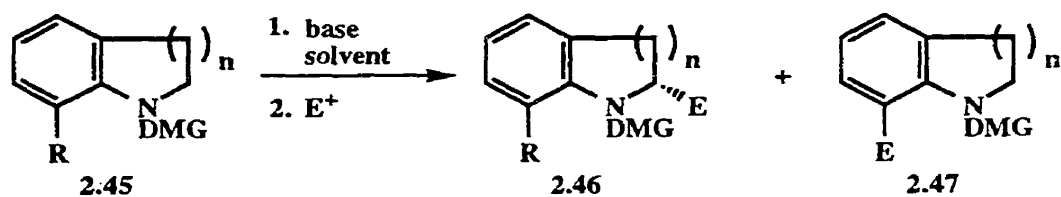
Scheme 2.11

for the observed regioselectivity. These results suggest that, unlike uncomplexed indoles, the H-7 acidity is of similar order to that of H-2. Further evidence is provided by metalation of *N*-SEM-3-methylindole (**2.41f**) which proceeded to afford 7-substituted products **2.44** (entries

15-18) regioselectively and in moderate yield, despite the lack of a protecting group in the 2-position. In these cases, the modest steric protection provided by the methyl group appears to be sufficient to induce metalation in the 7-position. While it is clear that benzenoid ring functionalization is a viable process through arenetricarbonylchromium (0) complexes, it is equally evident that many limitations exist, including poor regioselectivity, the necessity of introducing protecting groups, and the complexation / decomplexation process. Toxicity of chromium (0) compounds and the reluctance of industry to utilize chromium complexes as intermediates further limits the application of these procedures.

An interesting approach to 7-substituted indoles was provided by Iwao and co-workers.³²¹ Recognizing the relative ease of interconversion of indoles and indolines,³²²⁻³²⁵ Iwao focused on 7-position functionalization in indolines. Meyers and Hellring had previously shown³²⁶ that formamidine protected indoline and 1,2,3,4-tetrahydroquinoline (**2.45a** and **2.45b**) could be functionalized in the 2-position when treated with *t*-BuLi followed by an electrophile (**2.46**, Scheme 2.12 entries 1-2). Beak and Lee, on the other hand, had reported³²⁷ that *N*-Boc-1,2,3,4-tetrahydroquinoline (**2.45c**) undergoes metalation in the aromatic ring producing the corresponding 8-substituted product **2.47** (entry 3). This result stimulated Iwao to apply the same reaction conditions to *N*-Boc-indoline (**2.45d**) in an effort to functionalize the 7-position. Indeed, treatment of **2.45d** with *s*-BuLi / TMEDA in Et₂O at -78 °C followed by quench with an electrophile led to 7-substituted products **2.47** in moderate to excellent yield (entries 4-7). Although Iwao observed no products resulting from 2-lithiation, Meyers re-examined the reaction and found that 2-deprotonation was possible for the Boc substrates if the 7-position was unavailable.³²⁸ Thus, treatment of *N*-Boc-7-deuteroindoline (**2.45e**) and *N*-Boc-8-deuterio-1,2,3,4-tetrahydroquinoline (**2.45f**) under Iwao's conditions, followed by quench with MeOD led to incorporation of deuterium in the 2-position in 50% and 90% respectively (entries 8,9). Interestingly, Beak's studies on (-)-sparteine-mediated asymmetric α -metalation of amines³²⁹ demonstrated that regioselectivity of *N*-Boc-indoline metalation could be controlled by only slight variation of conditions. Thus,

when **2.45d** was treated with *s*-BuLi / (-)-sparteine in cumene rather than *s*-BuLi / TMEDA in Et₂O, 2-substituted indolines **2.46** were prepared in moderate yield and in most cases with excellent enantioselectivity (entries 10-13), in contrast to Iwao's regioselective 7-substitution. Treatment of 7-chloroindoline **2.45f** under similar conditions provided chiral 2-substituted indolines **2.46** as expected since the 7-position was unavailable (entry 14). The results in Scheme 2.12 are representative examples of these methods.

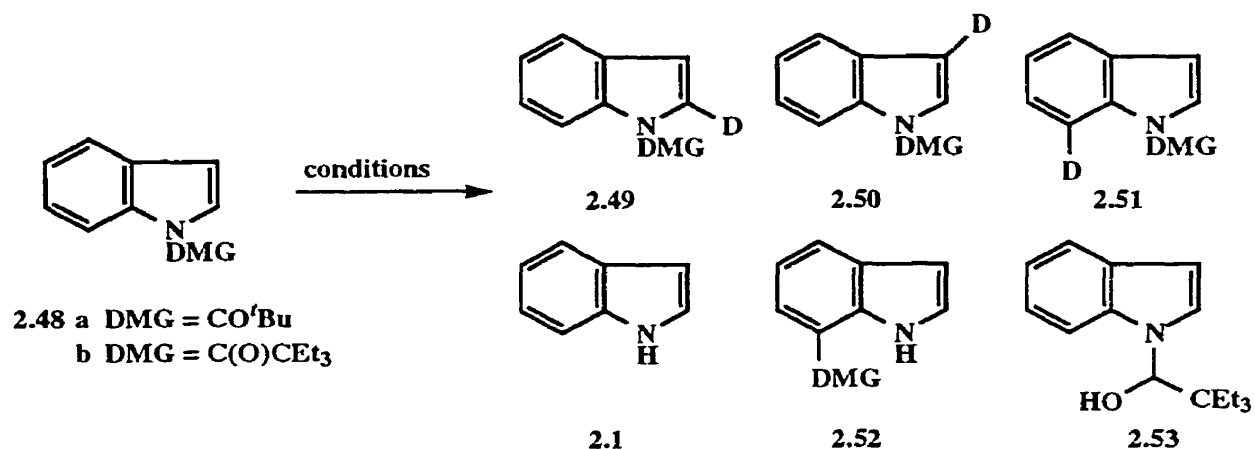


entry	2.45	DMG	n	R	E	2.46, % (ee%)	2.47 (%)
1	a	CH=N ^t Bu	1	H	D	90 (-)	-
2	b	CH=N ^t Bu	2	H	D	90 (-)	-
3	c	Boc	2	H	D	-	-
4	d	Boc	1	H	Me	-	91
5	d	Boc	1	H	CO ₂ H	-	56
6	d	Boc	1	H	TMS	-	83
7	d	Boc	1	H	I	-	59
8	e	Boc	1	D	D	50 (-)	-
9	f	Boc	2	D	D	90 (-)	-
10	d	Boc	1	H	Me	52 (97)	-
11	d	Boc	1	H	CH ₂ CH=CH ₂	28 (36)	-
12	d	Boc	1	H	TMS	57 (95)	-
13	d	Boc	1	H	SnMe ₃	70 (98)	-
14	g	Boc	1	Cl	SnMe ₃	75 (74)	-

Scheme 2.12

More recently, Iwao and co-workers have contributed to the direct C-7 functionalization of indoles.³³⁰ Noting that 1-acylindoles are known to exist as planar mixtures of *E* and *Z* conformers,³³¹ their approach involved the use of bulky acyl substituents with the intention of taking advantage of steric interactions between the alkyl groups and the *peri*-hydrogen. A

substantial interaction would orient the acyl carbonyl such that it pointed towards the C-7 hydrogen, possibly directing lithiation to that position. Thus, treatment of *N*-pivaloylindole (**2.48a**) was attempted and it was found that indole (**2.1**) was the only isolable product, presumably due to attack of the alkyllithium at the carbonyl of the acyl group (Scheme 2.13). Alternatively, when *N*-(2,2-diethylbutanoyl)indole (**2.48b**) was treated under a variety of metalation conditions, followed by quench with MeOD, mixtures of indole (**2.1**), and deuterated indoles **2.49**, **2.50**, and **2.51** (Scheme 2.13) were isolated. In addition, migrated product **2.52** and alcohol **2.53** were isolated as minor side products. Although the C-7 metalation was achieved, selectivity for the 7-position is poor and it is clear that the need still exists for methods of direct functionalization at C-7.



entry	2.48	solvent	base (equiv)	TMEDA (equiv)	2.1 (%)	2.49 (%)	2.50 (%)	2.51 (%)
1	a	Et ₂ O	<i>s</i> -BuLi	1.5	79	0	0	0
2	b	Et ₂ O	<i>s</i> -BuLi	2.3	0	49	0	52
3*	b	Et ₂ O	<i>s</i> -BuLi	0	0	51	0	12
4	b	Et ₂ O	<i>n</i> -BuLi	2.3	40	0	0	0
5	b	Et ₂ O	<i>t</i> -BuLi	2.3	0	80	0	13
6	b	THF	<i>s</i> -BuLi	2.3	24	44	15	39

* 30% of **2.53** was also isolated.

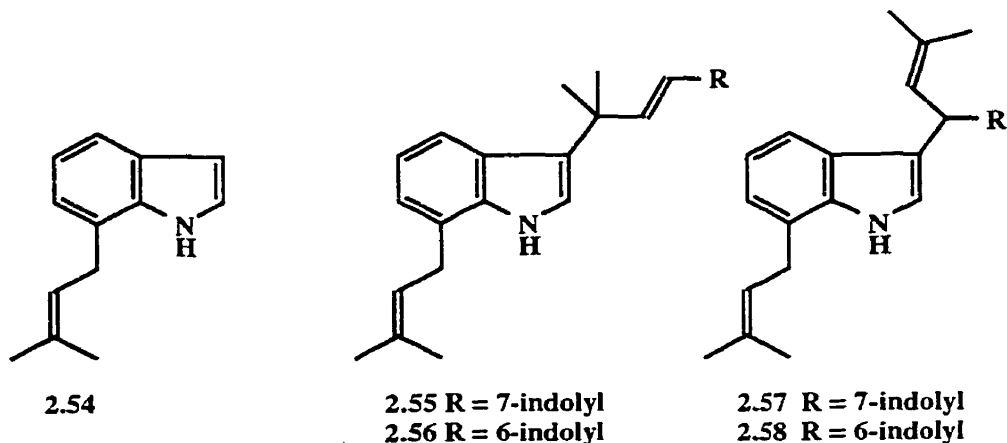
Scheme 2.13

2.3 Indole Natural Products

While indole natural product chemistry has been practiced for decades, new natural products continue to be discovered thus providing a constant source of challenging synthetic targets. The vast number of indoles found in nature²⁷⁷ precludes the possibility of a comprehensive summary, thus only relevant natural products will be discussed.

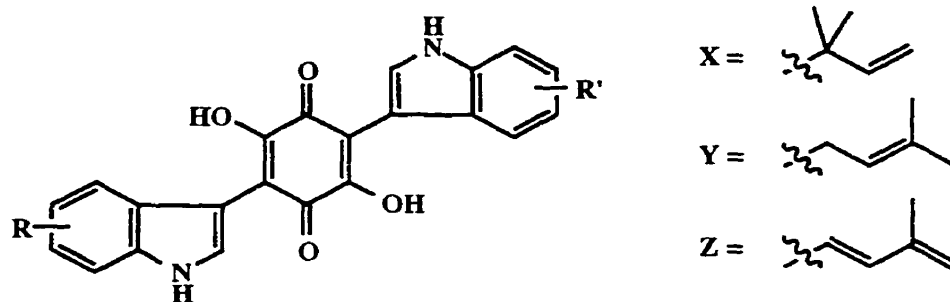
2.3.1 Prenyl Substituted Indoles

Of the many classes of indoles found in nature, many contain a prenyl (3-methylbut-2-enyl) substituent. Natural sources are varied and include bark, soil, and fungi. Many members of this large group of indoles have shown medicinal properties and plant sources have seen application as tribal medicines. The stem bark of the West African *Annonidium mannii* yielded, among other compounds, the simple indole **2.54** along with the more complex bisindoles **2.55-2.58**, each containing the prenyl substituent in the 7-position.³³² Structures **2.55-2.58**, annonidines, each contain two indole ring structures linked together by a C₅ isoprenoid unit.



The first reported compound in a group of related bisindole natural products having the general structure **2.59**, was cochliodinol (**2.59a**), isolated from *Chaetomium cochliodes* in 1968.³³³⁻³³⁶ Although the chemical structure was not deciphered until some years later (Section 2.3.2),^{337,338} it was recognized that cochliodinol and related metabolites possessed significant biological activity (Section 2.3.4). Several related compounds have since been

isolated and characterized,³³⁹⁻³⁴³ and many are now commonly referred to as asterriquinones having been also isolated from *Aspergillus terreus*.^{341,344} The structural similarity among asterriquinones is apparent, each having a dihydroxyquinone nucleus with two prenylated indole appendages.



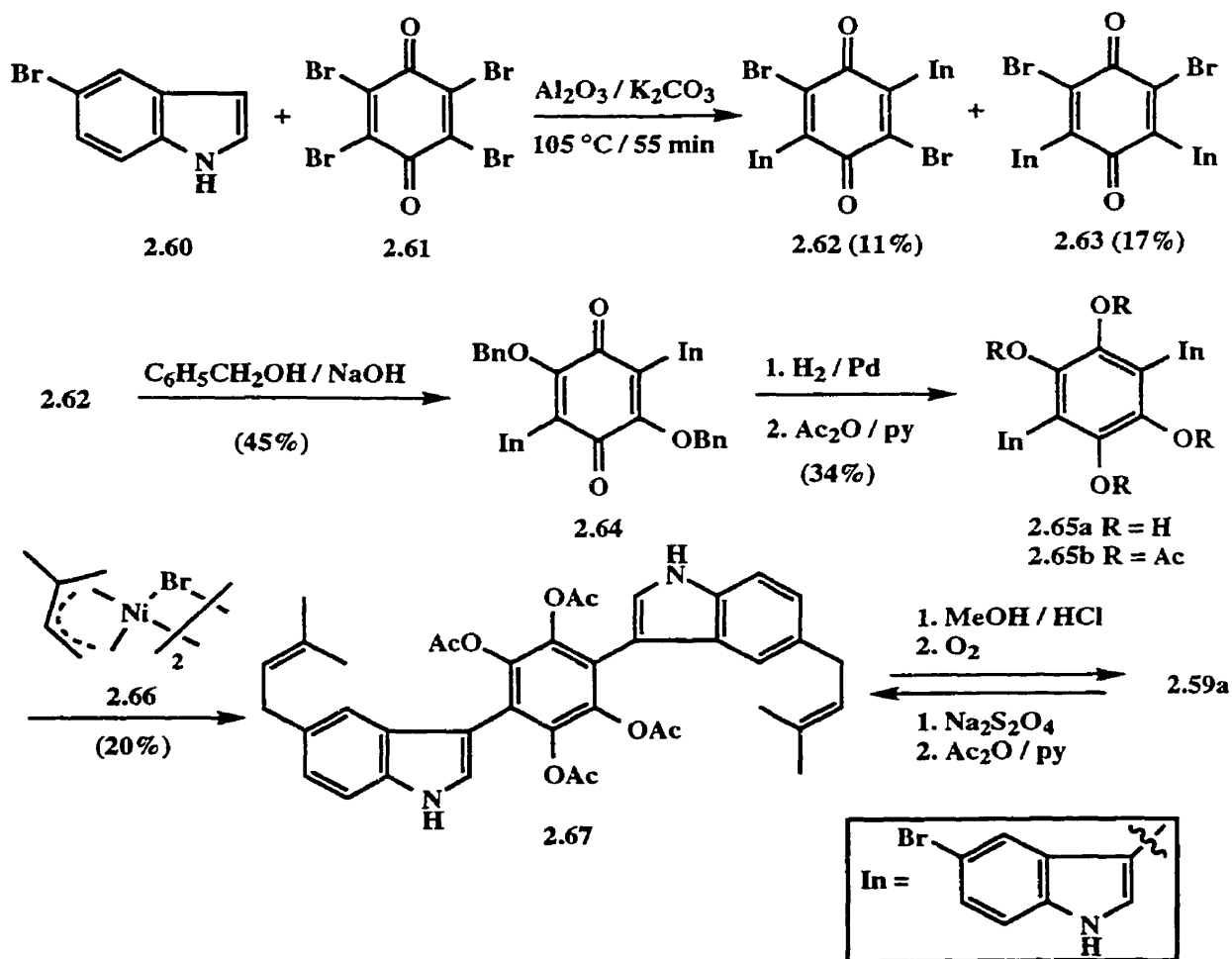
2.59	a: Cochliodinol	R = R' = 5-Y
	b: Asterriquinone	R = R' = 1-X
	c: Asterriquinone CT1	R = R' = 6-Z
	d: Asterriquinone CT2	R = 6-Z; R' = 6-Y
	e: Asterriquinone CT3	R = R' = 6-Y
	f: Asterriquinone CT4	R = R' = 7-Y
	g: Asterriquinone CT5	R = R' = 2-Y
	h: Hinnuliquinone	R = R' = 2-X
	i: Isoasterriquinone	R = 1-X; R' = 2-Y

2.3.2 Syntheses of Asterriquinones

Total synthesis of asterriquinones and related bisindolylbenzoquinone natural products has received some attention. Jerram and co-workers^{337,338} established the structure of cochliodinol, the first isolated member of the family, through chemical derivatization and spectral analysis. The dihydroxyquinone moiety was proposed based on the ease of reduction / oxidation, established previously by Meiler and Taylor.³³⁵ Corresponding dimethyl and diacetyl derivatives were readily prepared and the analysis of spectral data for the three compounds led to the proposed structure **2.59a**.

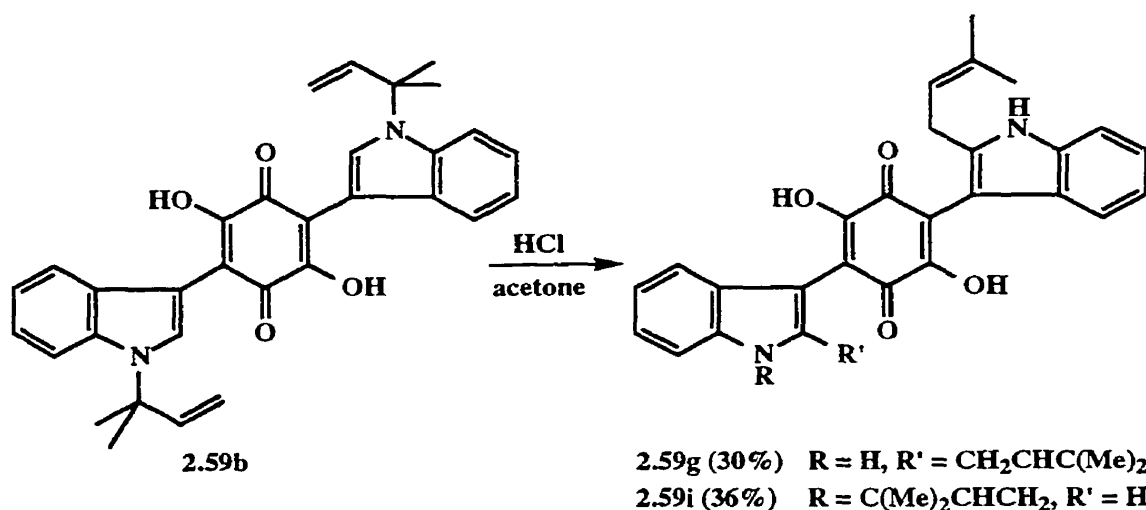
Hörcher and co-workers confirmed the structure of cochliodinol by total synthesis³⁴⁵ (Scheme 2.14). Thus, 5-bromoindole (**2.60**) and 2,3,5,6-tetrabromobenzoquinone (**2.61**) were condensed in the presence of $\text{Al}_2\text{O}_3 / \text{K}_2\text{CO}_3$ to form the two isomeric bisindolylbenzoquinones **2.62** (11%) and **2.63** (17%). Though the reaction was non-

selective and low-yielding, it provided the desired quinone for further functionalization. Benzylation of **2.62** led to **2.64** in 45% yield. Cleavage of the benzyl protecting groups by hydrogenation occurred with concomitant reduction of the quinone moiety to give **2.65a** which was immediately protected by acetylation to provide the tetraacetate **2.65b** (34% overall from **2.64**). Double incorporation of the prenyl moiety was accomplished by reaction of **2.64** with nickel complex **2.66** (generated by reaction of $\text{Ni}(\text{CO})_4$ with 1-bromo-3-methyl-2-butene) to give **2.67** (20%). The final step in the total synthesis involved simple deprotection and oxidation to form cochliodinol (**2.59a**) in 35% yield. Further confirmation of structure was achieved by converting natural cochliodinol by reduction and acetylation to the corresponding tetraacetate derivative **2.67** (56%).



Scheme 2.14

Other asterriquinones and related molecules have been synthesized through manipulation of isolated natural products. For example, asterriquinone CT5 (**2.59g**) was prepared by *N*- to C-2 prenyl migration of asterriquinone (**2.59b**) with HCl in acetone.³⁴⁶ The mono-rearrangement product (isoasterriquinone, **2.59i**) was also isolated in approximately the same yield (Scheme 2.15). Numerous other examples of such functional group manipulations exist in this alkaloid series, including formation of methyl ethers and acetates, redox of the benzoquinone moiety, and reductive cyclization.^{337-339,342,346-348}



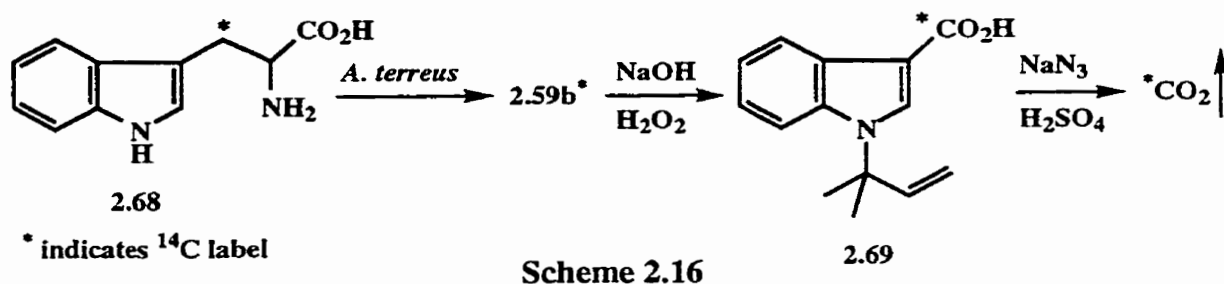
Scheme 2.15

Manipulation of functional groups on the benzoquinone moiety has been investigated by Kaji and co-workers.³⁴⁷ In particular, methods have been developed for the individual derivatization of the hydroxy groups.^{349,350} The selective manipulation of these groups has proven important in SAR studies for asterriquinones (Section 2.3.4).

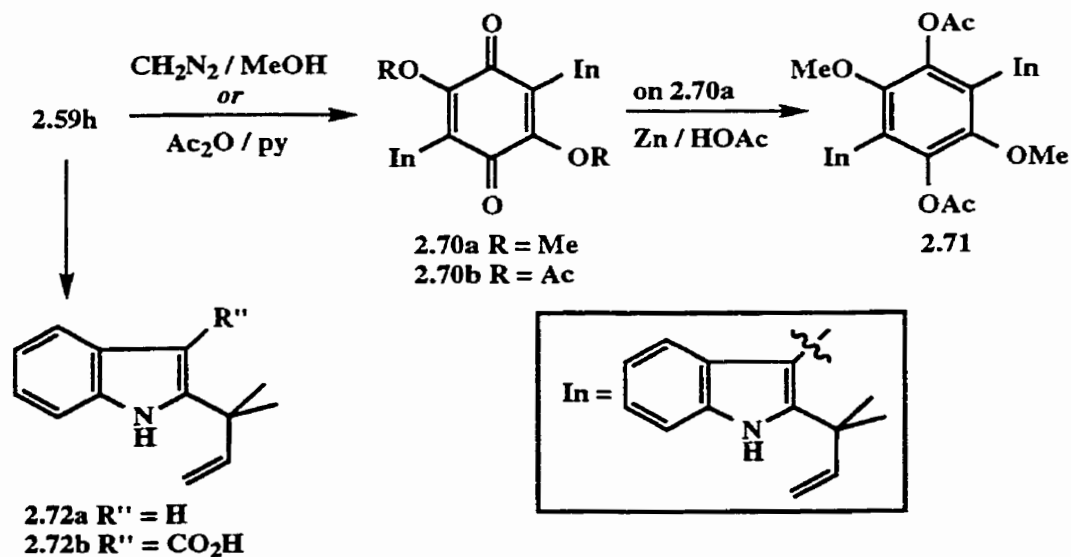
2.3.3 Biosynthesis

Little effort has been expended in studying the biosynthesis of the asterriquinones. Yamamoto³⁴⁴ provided an initial study on the biosynthesis of asterriquinone (**2.59b**), which proved that asterriquinone is derived from tryptophan and mevalonate. Administration of DL-[3-¹⁴C]tryptophan (**2.68**) to cultures of *Aspergillus terreus* resulted in isolation of radioactive (13.6%) asterriquinone after 7 days of fermentation. Upon oxidative degradation, the

radioactive asterriquinone provided *N*-substituted indole-3-carboxylic acid (**2.69**), which displayed almost all of the radioactivity detected in the natural product. Finally, Curtius rearrangement of **2.69** yielded carbon dioxide with 90% of the radioactivity (Scheme 2.16). Mevalonate was also incorporated into asterriquinone although at a very low level (0.07%). While incorporation was limited, the result nonetheless provided evidence that the prenyl functionality was mevalonate derived.

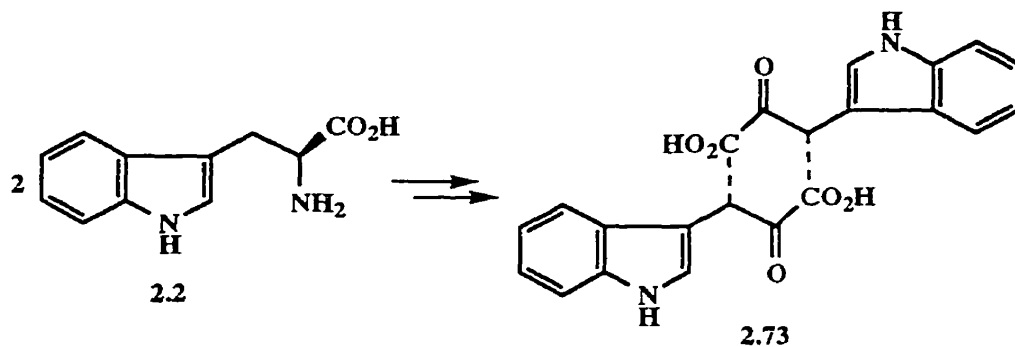


O'Leary and co-workers^{342,343} studied the biosynthesis of the dark red pigment hinnuliquinone (**2.59h**), which differs from asterriquinone CT-5 only in the attachment of the C₅ appendage. O'Leary's study began by confirmation of the chemical structure through chemical degradation and analysis of spectral data (Scheme 2.17).³⁴²



Scheme 2.17

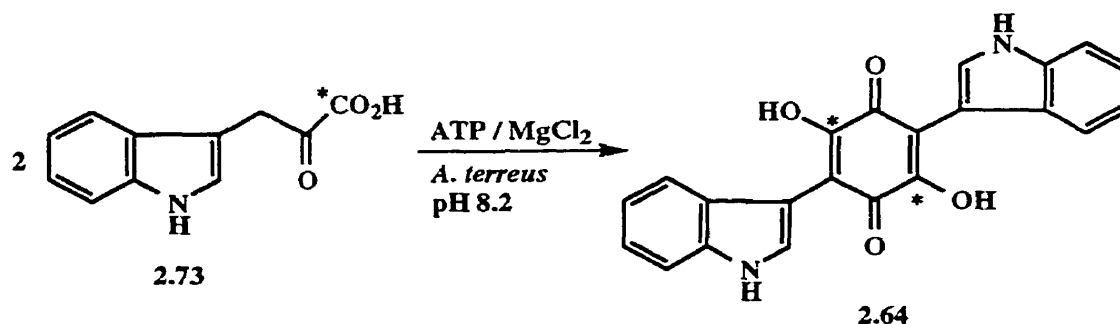
O'Leary proposed that the bis(indolyl)-2,5-dihydroxybenzoquinone structure resulted from the self condensation of 2 moles indolylpyruvic acid (**2.73**),^{343,344} which was derived from tryptophan (Scheme 2.18). Support for this proposal was provided by radiolabeling experiments in which cultures of *Nodulisporium hinnuleum* were treated with [U-³H]tryptophan and [2-¹⁴C]mevalonate. Incorporation, though modest (0.8% and 0.2% respectively), was observed in the natural product after a 7 day fermentation period. Similarly, [1-¹⁴C]tryptophan was incorporated, implying that the tryptophan side chain is incorporated in the benzoquinone portion of the natural product. The proposed self condensation was investigated by treatment of *N. hinnuleum* with indolylpyruvic acid which had been obtained synthetically from [3-¹⁴C]tryptophan. Again, modest incorporation (0.35%) was observed, suggesting that while this pathway is plausible, another derivative of tryptophan is perhaps more likely to be the intermediate. Notably, attempts in the laboratory to perform the self-condensation reaction were unsuccessful.



Scheme 2.18

Arai and co-workers,³⁵¹ building on earlier results from Yamamoto and O'Leary, and their respective co-workers, undertook studies on the biogenesis of other asterriquinones. Initially, cell cultures were treated with asterriquinones in order to elucidate possible metabolic relationships between members of the family. With only a few exceptions, no interconversions of asterriquinones were noted. The low interconversion of compounds was attributed to poor water solubility of asterriquinones and/or inability of added compounds to permeate fungi cells.

The possibility of an indolylpyruvic acid intermediate was also investigated by Arai. Unlike O'Leary's study, dimerization of [1-¹⁴C]indolepyruvic acid to form the asterriquinone skeleton was achieved in the laboratory upon exposure of the former to crude cell extracts (*A. terreus*) in the presence of buffer and ATP (Scheme 2.19). Several experiments were also performed in order to evaluate prenylation pathways. Enzyme-promoted prenylation experiments using dimethylallylpyrophosphate led to the conclusion that prenylation occurs simultaneously at C-2, C-7, and N-1 of indole.



2.3.4 Biological Activity

Shortly after the discovery of cochliodinol (**2.59a**), Brewer and co-workers investigated its biological activity³³⁶ and showed that it inhibited growth and germination of spores of several species of *Fusarium*, and perhaps more importantly, that it is relatively non-toxic to various mammalian cell lines. A related investigation by Meiler and Taylor subsequently showed that respiration of microspores of *F. oxysporum* was inhibited by cochliodinol³³⁵ and suggested that the inhibition was a result of cochliodinol interfering with respiratory oxidation pathway(s). Clearly the benzoquinone moiety would be involved in this mode of activity.

In the first studies on the biological activity of asterriquinone (**2.59b**), Yamamoto and co-workers found that this antibiotic had significant ability to inhibit tumour growth.³⁵² Similar to cochliodinol, asterriquinone was relatively low in toxicity, having an LD₅₀ of greater than 400 mg/kg for intraperitoneal administration in mice. Various transplantable tumours

were implanted in mice and the mice were treated with varying dosages of asterriquinone daily over a 7 day period. For Ehrlich ascites carcinoma, control mice exhibited 100% fatality 23 days after implantation. By contrast, mice treated with 10 mg/kg/day of asterriquinone exhibited only 50% fatality 50 days after implantation, while those treated with 20 mg/kg/day and 40 mg/kg/day of asterriquinone exhibited less than 20% fatality 50 days after implantation. Activity varied depending on the type of tumour cells. Ascites hepatoma AH-13 gave results similar to those above, while AH-109A was largely unaffected. Moderate effectiveness was noted for Yoshida sarcoma and L-1210 mouse leukemia. In an early SAR investigation,³⁵² it was found that all antitumour activity was lost if the hydroxyl groups were converted to the corresponding methyl ethers, or if the isopentenyl groups were hydrogenated.

Further SAR studies involved investigation of antitumour activity of chemically modified asterriquinones.³⁵³ The first series of compounds prepared involved modification of the benzoquinone moiety giving derivatives **2.74**, **2.75**, and **2.76**. These chemical modifications failed to improve upon the antitumour activity of asterriquinone. Modification of **2.77** by introduction of 3-methyl-2-butenyl substituents to give isomer **2.78** was also ineffective. Finally, unsymmetrical derivative **2.79** (prepared from **2.80**) was ineffective in tumour reduction, but close relative **2.81** (also prepared from **2.80**) showed moderate antitumour activity.

compound	R	R'	R''	R'''
2.74	OMe	X	H	X
2.75	NH ₂	X	H	X
2.76		X	H	X
2.77	OMe	H	H	H
2.78	OH	Y	H	Y
2.79	OH	Z	X	Z
2.80	OH	H	X	H
2.81	OH	Y	X	Y

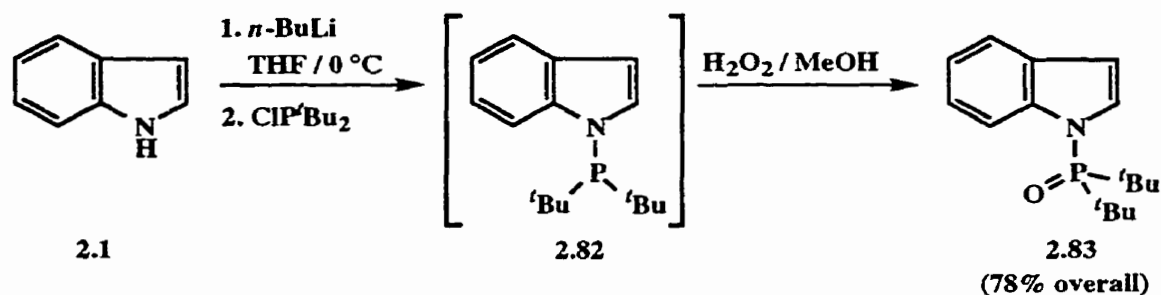
Cytotoxicity of a series of asterriquinones against mouse leukemia P388 cells was investigated and modest activity was found.³⁵⁴ Based on these and previous results, Kaji and co-workers have reached 4 conclusions regarding cytotoxicity of asterriquinones against such cells: *i*) at least one OH or OAc group in the benzoquinone moiety is required for activity; *ii*) one OMe and/or one OAc in the benzoquinone moiety results in higher activity than two OH substituents; *iii*) the indole component is important for biological activity; and *iv*) the 1,1-dimethyl-2-propenyl substituent, present in many asterriquinones, is not crucial for the activity. These conclusions, as well as the results of Yamamoto and co-workers clearly indicate that this class of alkaloids have wide ranging biological activity.

2.4 Results and Discussion

2.4.1 Metalation of *N*-(Di-*tert*-butylphosphinyl)indole

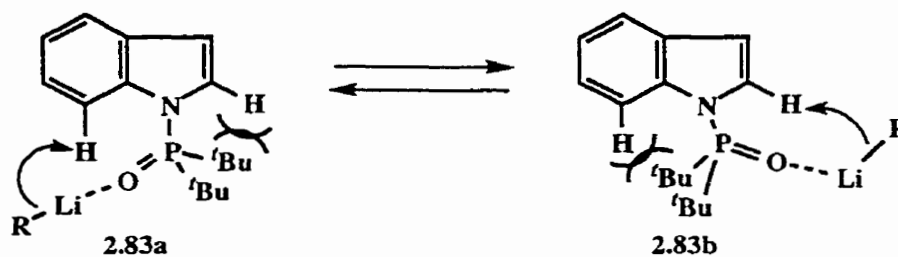
Despite the numerous DMGs available for regioselective 2-indole metalation, there remains a lack of satisfactory methods for direct and regioselective functionalization of the 7-position. While phosphorus-based groups are known for indole-*N*-protection,³⁵⁵ there have been no reports of indole-*N*-phosphorus-based DMGs. Accordingly, it was proposed that nucleophilic substitution at phosphorus by an indole-derived anion should be a facile process leading to a P-protected indole derivative. With the success of the di-*tert*-butylphosphinyl DMG in both ferrocene (Section 1.5.2) and benzene (Section 1.5.3)³⁵⁶ systems, indole substitution was a logical progression and *N*-di-*tert*-butylphosphinylindole (**2.83**) was chosen as the desired starting material.

Numerous protocols are known²⁷⁹ for *N*-substitution in indoles; thus, the initially chosen method was based on previous experience and remained consistent with formation of phosphinyl benzenes (see Section 1.5.3). A solution of indole (**2.1**) in THF was successively treated with a slight excess of *n*-BuLi and chlorodi-*tert*-butylphosphine. Treatment of the crude phosphinoindole **2.82** with aqueous H₂O₂ in MeOH led, after purification, to the desired phosphinylindole **2.83** in 78% overall yield (Scheme 2.20).



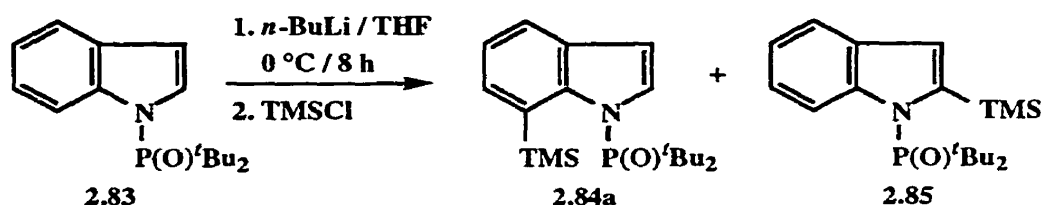
Scheme 2.20

With the starting material in hand, focus turned to metalation studies on **2.83**. Working on the assumption that a CIPE would be operating,⁸ two reasonable pathways for deprotonation could be envisioned. The bulky *tert*-butyl groups would be expected to align the N-P-O moiety in the same plane as the indole ring due to steric repulsion, consistent with the X-ray results found for **1.170** (Section 1.5.3 and Appendix 4). This being the case, the phosphinoyl group could align with the oxygen pointing towards either the C-7 or C-2 hydrogen. It was proposed that the high steric demand of the *tert*-butyl groups would provide enough of an energetic difference to favour complex **2.83a** over **2.83b** and thus direct deprotonation to the C-7 hydrogen.



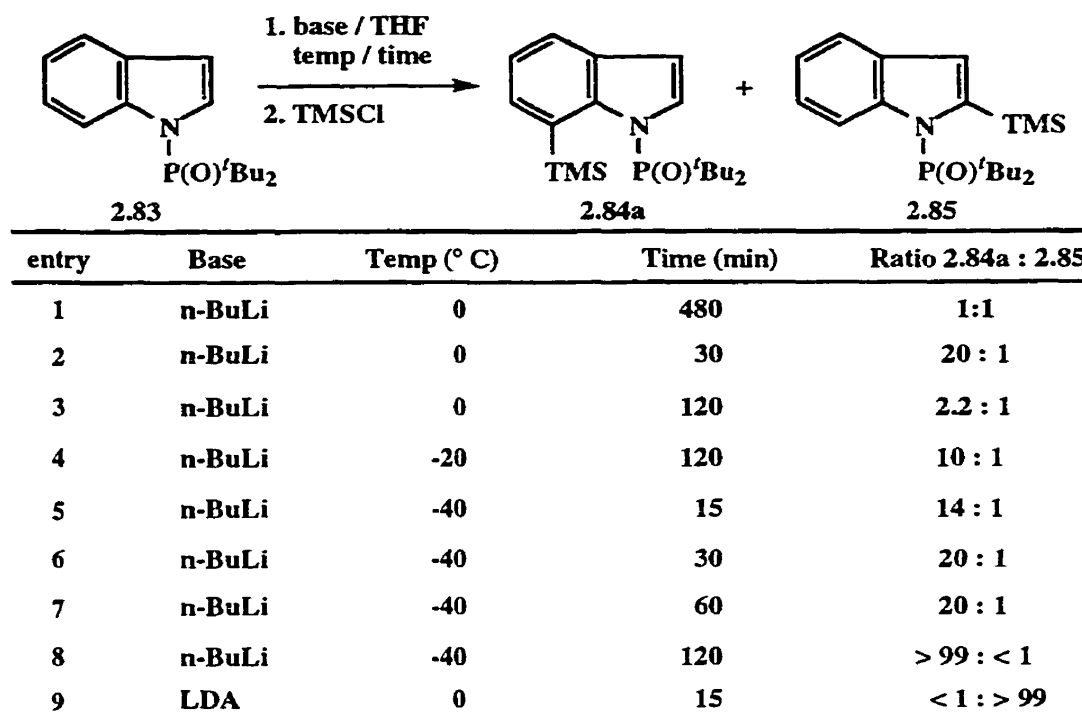
Scheme 2.21

Initially *n*-BuLi was chosen as the metalating agent in order to explore metalation behaviour of **2.83**. Although no reaction occurred in THF at -78 °C, a higher temperature (0 °C) of metalation followed by quench with TMSCl afforded, after purification, the monosilylated compounds **2.84a** and **2.85** in 42% and 47% yield, respectively (Scheme 2.22).



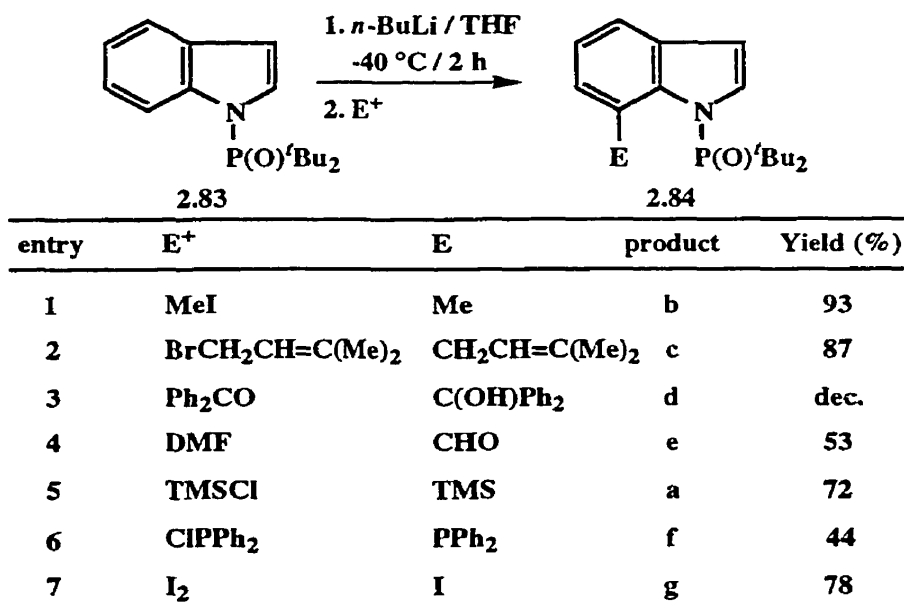
Scheme 2.22

Following this encouraging result, a series of experiments were performed in order to establish optimal conditions for metalation in the 7-position. Using TMSCl quench as a probe for regioselectivity of metalation, various metalation times and temperatures were explored and relative amounts of C-7 and C-2 metalated products were determined by GC analysis (Scheme 2.23). Initially, the temperature was maintained at 0°C and the length of metalation time was varied (entries 1-3). As can be seen in the table, shorter metalation times favoured C-7 metalation while longer periods showed less selectivity. Lowering the temperature to -20°C resulted in greater C-7 selectivity (entry 4). At -40°C , metalation times were again varied and product ratios were analyzed (entries 5-8). A short metalation period (entry 5) showed good selectivity, however, increasing the metalation time to 2 h greatly improved the regioselectivity providing a $> 99:1$ ratio of products in favour of C-7 metalation (entry 8). These standard conditions were adopted for regioselective C-7 metalation. Interestingly, when LDA was employed instead of $n\text{-BuLi}$, the regioselectivity was completely reversed, providing the C-2 product after only 15 minutes of metalation. The regioselectivity may perhaps be explained on the basis of equilibration of thermodynamically and kinetically favoured anions. The preference for C-7 metalation at lower temperatures indicates that the 7-position is probably the kinetically favoured metalation site. Conversely, as the temperature is increased, some anion scrambling takes place, thus lowering the regioselectivity. In the extreme case, LDA allows for facile equilibration of the two anions and, after only a short metalation period, the thermodynamically favoured anion dominates. This model assumes that the monosilylated products are an accurate representation of the anion distribution in the reaction mixture.



Scheme 2.23

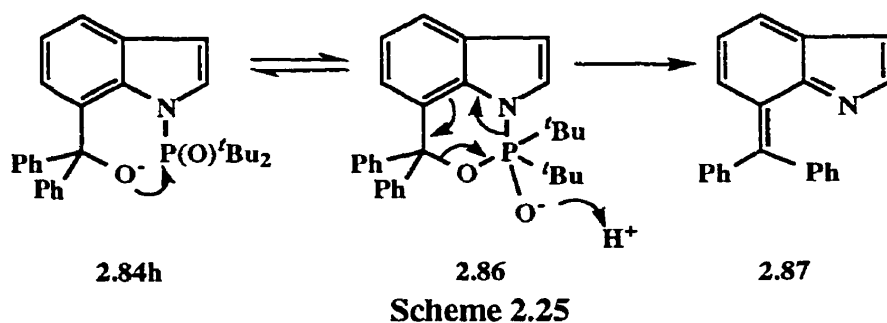
With optimum reaction conditions established, a series of derivatives were prepared representing a range of electrophiles including carbon (entries 1-4), silicon (entry 5), phosphorus (entry 6), and iodine (entry 7, Scheme 2.24). Products were formed in moderate



Scheme 2.24

to excellent yield providing direct access to 7-substituted indoles, which were previously difficult to achieve. Many of the products would be expected to have substantial steric interaction between the C-7 substituent and the phosphinyl moiety. Single crystal X-ray analysis on **2.84c** (Appendix 7) clearly demonstrates this situation (Figure 2.1). As can be seen in Figure 2.1, a methylene proton from the prenyl functionality is almost in contact with the phosphinyl oxygen.

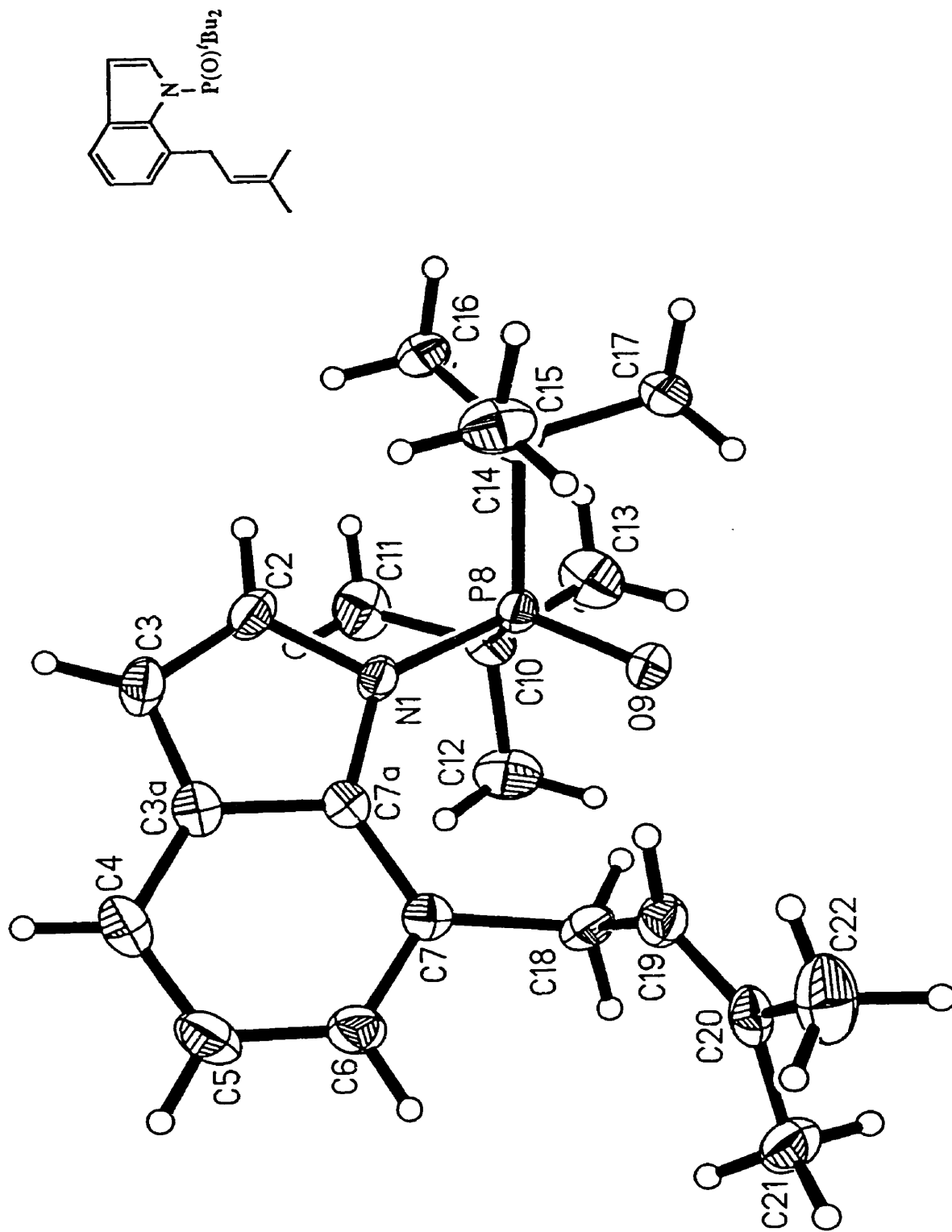
Carbon electrophiles were successfully incorporated in alkyl and aldehyde oxidation states (entries 1,2,4); however, when benzophenone was employed as the electrophile (entry 3), no product was isolated. Although a new compound was detected by TLC, standard workup of the reaction resulted in development of a deep green colour suggesting decomposition. A plausible explanation for this decomposition is demonstrated in Scheme 2.25. After initial formation of alkoxy anion **2.84h**, intramolecular attack occurs at phosphorus resulting in cyclic intermediate **2.86**. Upon acidic workup, degradation is accompanied by loss of aromaticity resulting in **2.87**. This conjugated polyene has several available reaction pathways which could result in polymerization and/or re-aromatization. The proposed pathway also results in the loss of the phosphinyl group (see Section 2.4.2) as the phosphinic acid $(t\text{Bu})_2\text{P}(\text{O})\text{OH}$, the presence of which may further catalyze the decomposition of **2.86**.



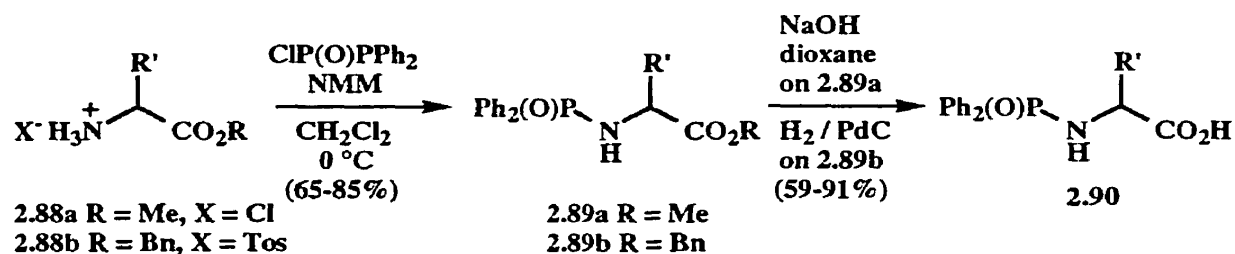
2.4.2 DMG Cleavage

Having successfully introduced substituents into the C-7 position, attention turned to removal of the phosphinyl DMG. While phosphorus-based protecting groups are known for

Figure 2.1 - Single Crystal X-ray Analysis of 2.84c.



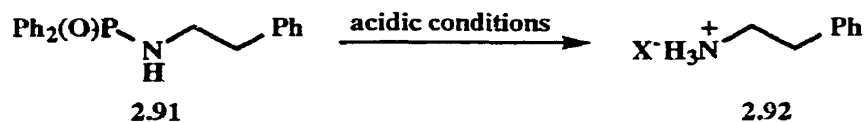
amines,^{355,357-359} their application to indoles has not been explored. Ramage and co-workers³⁵⁵ have applied phosphinamides as protecting groups in peptide synthesis, noting the acid lability of P-N bonds in such molecules. Methyl or benzyl protected amino acids **2.88** were treated with diphenylphosphinic chloride in the presence of *N*-methylmorpholine providing doubly protected amino acids **2.89** in good yields. Removal of the acid protecting group by either mild alkaline hydrolysis (on methyl esters **2.89a**) or standard hydrogenolysis (on benzyl esters **2.89b**) provided the desired *N*-protected amino acids **2.90** (Scheme 2.26). The newly formed *N*-protected amino acids were found to be effective in peptide forming reactions with the diphenylphosphinyl moiety providing suitable stability and protection of nitrogen.



Scheme 2.26

Previous studies had shown that the rate of acid cleavage of phosphinamide groups is highly dependent on the substituents on phosphorus. Thus, cleavage of the protecting group was studied using diphenylphosphinyl-protected 2-phenylethylamine (**2.91**) as a model (Scheme 2.27). Several mildly acidic conditions were evaluated and it was found that, with one exception, successful removal of the diphenylphosphinyl group providing **2.92** in near quantitative yields was achieved. Furthermore, simple peptides were tested and selective cleavage was possible (entries 6,7). Methanolic HCl (entry 5) proved to be the method of choice for diphenylphosphinyl removal for reasons of convenience and simplicity. However, in situations where stability with this reagent could pose potential difficulties (e.g. peptides with a phenyl ester at the C-terminus), alternative conditions were investigated including the use of weaker acids and different solvents. All sets of conditions allowed for complete

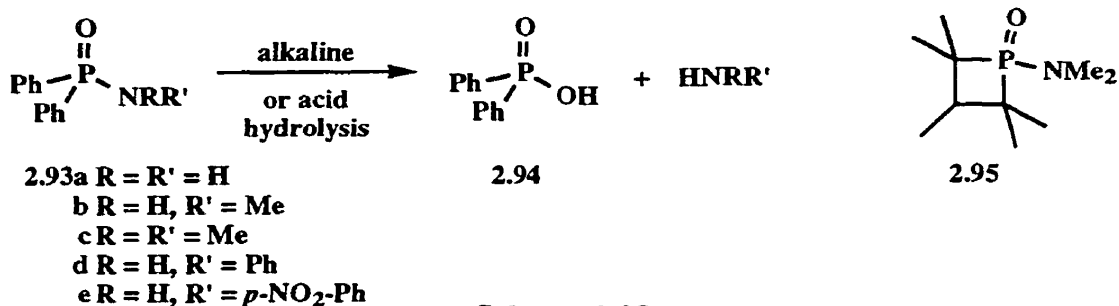
deprotection of amines in 24 h or less, with the exception of 80% aqueous acetic acid (entry 3), for which cleavage was incomplete after 72 h.



entry	Starting Material	Conditions	Complete Deprotection
1	2.91	95% TFA	10 min
2	2.91	TFA / CH ₂ Cl ₂ (1:1)	40 min
3	2.91	80% aq. CH ₃ CO ₂ H	72 h (incomplete)
4	2.91	CH ₃ CO ₂ H / HCO ₂ H / H ₂ O (7:1:2)	24 h
5	2.91	HCl / MeOH	30 min
6	Ph ₂ P(O)GlyGlyO ^t Bu	15% TFA / CDCl ₃	2 h
7	Ph ₂ P(O)Lys(Z)GlyOMe	HCl in dioxane / H ₂ O (2:1)	3 h

Scheme 2.27

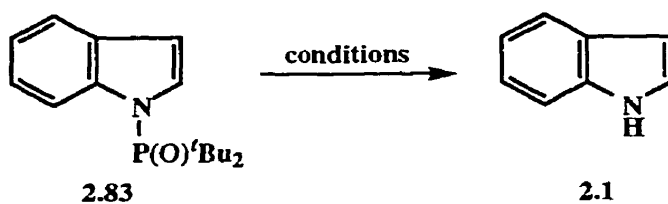
Koizumi and co-workers,³⁵⁷ and Tyssee and co-workers³⁵⁸ have also studied the hydrolysis of P-N bonds in phosphinamides. Koizumi's study focused on the kinetics of acidic and alkaline hydrolysis of phosphinamides with various P- and N-substituents. Rates were found to depend linearly on acid concentration for hydrolysis of simple phosphinamides such as **2.93a-c** to form the corresponding phosphinic acid **2.94**. Phosphinamides with more sterically demanding P-substituents (e.g. **2.95**) required the use of stronger acids to effect hydrolysis of the P-N bond. Alkaline hydrolysis reactions were equally successful for phosphinamides **2.93a-c** and displayed first order kinetics with respect to both amide and hydroxide concentration (Scheme 2.28).



Scheme 2.28

Studies by Tyssee and co-workers on the acid hydrolysis of phosphinamides **2.93a**, **2.93d**, and **2.93e** showed that the mechanism varied according to the substituents on nitrogen (Scheme 2.28). Strongly electron-withdrawing nitrogen substituents, such as in **2.93e**, favoured a dissociative mechanism while the corresponding primary amide **2.93a** proceeded *via* an associative route indicating that the group on nitrogen exerts some influence on the P-N bond cleavage.

Using **2.83** as a model, we investigated various methods for the removal of the di-*tert*-butylphosphinyl moiety from the indole nucleus. Initially, HCl / MeOH (Scheme 2.29, entry 1) was chosen based on the results of Ramage;³⁵⁵ however, in this substrate no deprotection was observed. These results are consistent with Koizumi's conclusion³⁵⁷ that hydrolysis is substantially hindered when large substituents are present on phosphorus. Several other options were investigated; notably, LiOH in MeOH and neat TFA (entries 2,3) failed to deprotect the indole nitrogen. Reductive cleavage of the phosphinyl moiety was attempted using LiAlH₄ in CH₂Cl₂ (entry 4), and, again, no deprotection was observed. Finally, reductive removal was again attempted with LiAlH₄ in refluxing toluene (entry 5). This combination proved successful and provided indole (**2.1**) in quantitative yield. Although this method of *N*-dephosphinylation places limitations on the range of useful electrophiles, it nonetheless demonstrates that DMG removal is feasible.



entry	Conditions	Result
1	HCl / MeOH	N.R.
2	LiOH / MeOH	N.R.
3	TFA	N.R.
4	LiAlH ₄ / CH ₂ Cl ₂	N.R.
5	LiAlH ₄ / toluene	quantitative

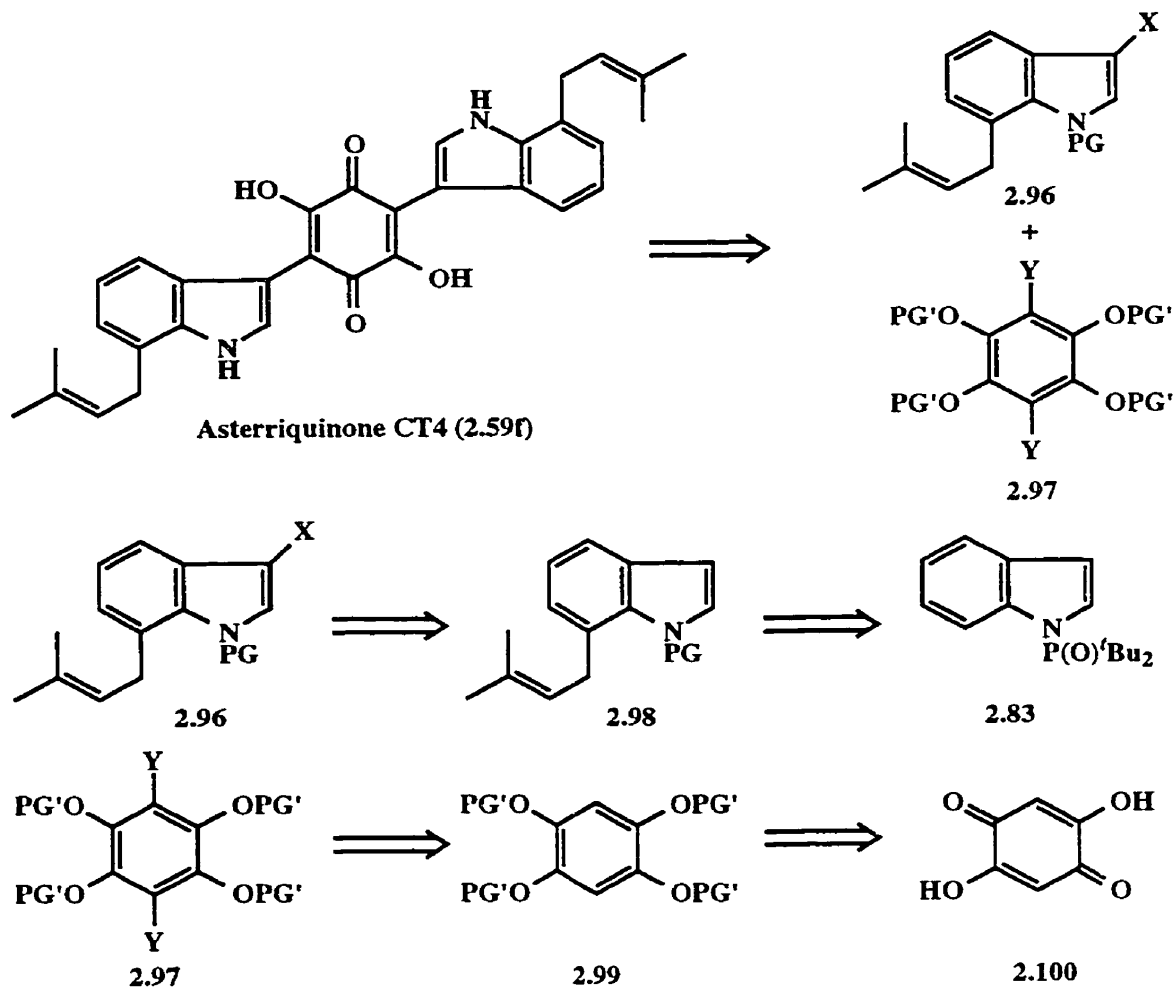
Scheme 2.29

2.4.3 Application to Natural Products

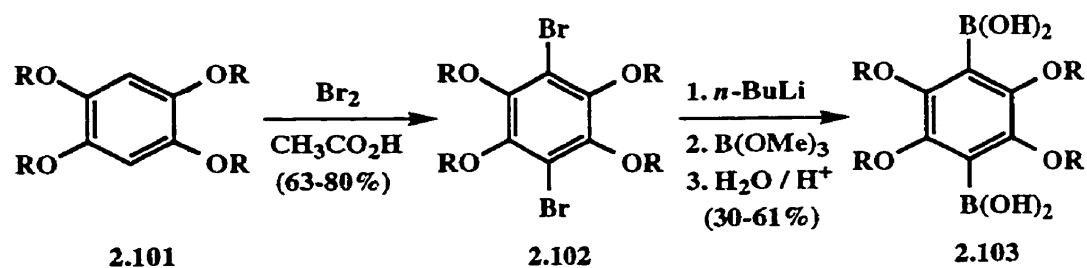
With the plethora of known natural products centred around an indole framework, candidates for application of this new methodology were readily available. Members of the asterriquinone family seemed particularly appropriate since several displayed substituents in the 7 position, and, in some cases, molecular symmetry contributed to a concise synthetic strategy. A retrosynthetic analysis of asterriquinone CT4 (**2.59f**) provided a rapid, convergent approach to this system (Scheme 2.30). Thus, **2.59f**, consisting of 3 independent aromatic systems, can be envisioned to arise from a 2:1 coupling of **2.96** and **2.97**. The ease of conversion between the oxidized and reduced forms of the dihydroxybenzoquinone moiety makes a symmetrical hexasubstituted benzene such as **2.97** ideal for this application. The relatively simple indole coupling partner **2.96** is ideally suited for application of the new methodology for regioselective C-7 metalation, while incorporating a coupling component in the 3-position. Hexasubstituted benzene **2.97**, containing 2 coupling components, is conceptually achievable from suitably protected tetrahydroxybenzene derivative **2.99**, which may be derived from commercially available 2,5-dihydroxybenzoquinone (**2.100**). The synthetic focus thus turned to the preparation of coupling partners **2.96** and **2.97** with the intention of utilizing a modified Suzuki aryl cross coupling reaction (Section 3.2) as the key step in formation of the asterriquinone ring system. As such, an aryl bromide or iodide was required for one coupling partner and an aryl boronic acid for the other. Thus, **2.96** (X = Br) and **2.97** (Y = B(OH)₂) were chosen as the targets.

The approach to **2.97** required selection of an appropriate protecting group for the four hydroxy substituents. It was envisioned that *DoM* chemistry would be a suitable way to introduce the desired boronic acid functionality, thus a protecting group resistant to attack by alkyllithium reagents would be required. Furthermore, the known ability of alkoxy substituents to direct metalation to the *ortho* position suggested that this would be a favourable pathway. Jennekens and co-workers³⁶⁰ had established that tetraalkoxybenzenes **2.101** could easily be dibrominated providing hexasubstituted benzenes **2.102**. Furthermore,

lithium halogen exchange on this system with an excess of *n*-BuLi, followed by quench with trimethyl borate and acidic workup was shown to provide bis-boronic acids **2.103** in good yields (Scheme 2.31).



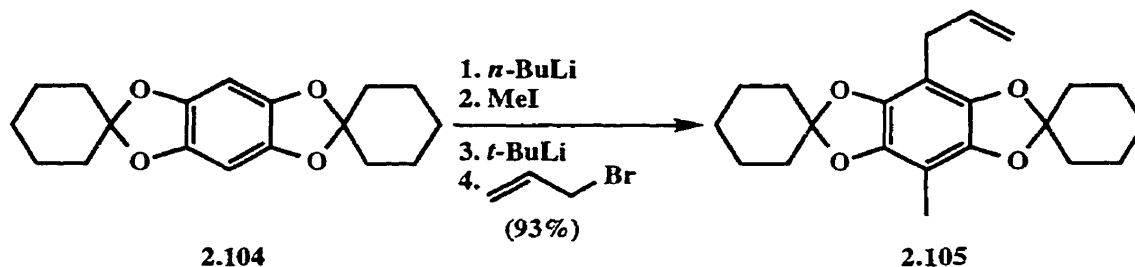
Scheme 2.30



$\text{R} = n\text{-C}_3\text{H}_7, n\text{-C}_6\text{H}_{13}, n\text{-C}_8\text{H}_{17}, n\text{-C}_{10}\text{H}_{21}$

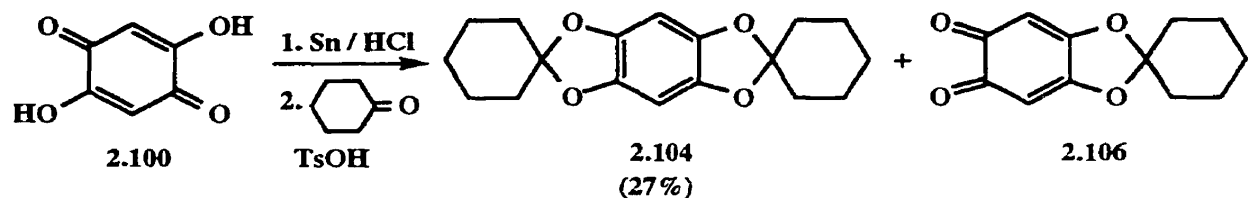
Scheme 2.31

In contrast to the metal halogen exchange approach, Hegedus and co-workers³⁶¹ showed that stepwise direct metalation of bisketal **2.104** was a facile process allowing introduction of two distinct electrophiles. Thus, treatment of **2.104** with *n*-BuLi followed by MeI and then *t*-BuLi followed by allyl bromide gave fully substituted benzene **2.105** in a high yielding one-pot reaction (Scheme 2.32).



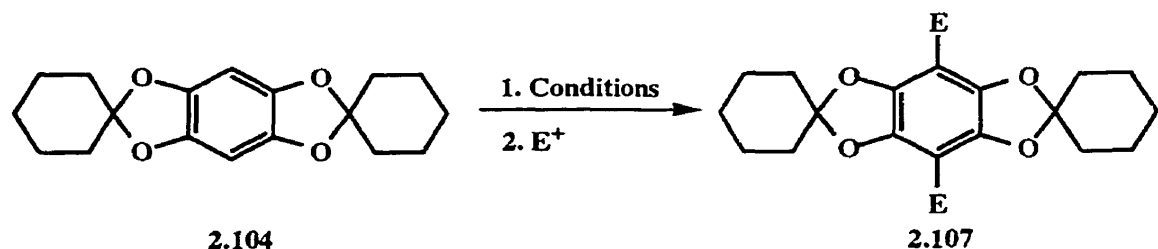
Scheme 2.32

It was proposed that the cyclohexylidene ketal would provide ideal protection for several reasons; *i*) it is an easily removable, acid labile protecting group; *ii*) metalation has proven to be a facile process; *iii*) since the ketal is secured to two oxygen atoms, it is not freely rotating and therefore should provide little steric interference in the cross coupling step. In addition, Jenneskens' work had shown that formation of a bis-anion was feasible while Hegedus' work clearly showed that direct metalation was possible. Direct double metalation of **2.104** was then proposed as a rapid, direct route to desired bisboronic acid **2.97**. Initial attempts at catalytic hydrogenation of 2,5-dihydroxybenzoquinone (**2.100**) according to a literature procedure³⁶⁰ were unsuccessful; however, treatment with Sn / HCl provided 1,2,4,5-tetrahydroxybenzene in 91% yield.^{361,362} Reaction with cyclohexanone in the presence of a catalytic amount of *p*-toluenesulfonic acid with removal of water provided desired bisketal **2.104**, in a yield which was significantly lower than that (61%) quoted in the literature.³⁶¹ A small amount of reoxidized quinone monoketal **2.106** was also isolated.



Scheme 2.33

Metalation of bisboreal **2.104** was then investigated as a possible route to the desired bisboronic acid. In order to evaluate the extent of metalation, **2.104** was treated under a variety of metalating conditions and quenched with MeOD. Deuteration in conjunction with $^1\text{H-NMR}$ provides an excellent measure of the extent of metalation since the desired product has no remaining aromatic protons. Initially, **2.104** was treated with an excess of *t*-BuLi in THF at room temperature (Scheme 2.34, entry 1). From integration of the $^1\text{H-NMR}$ signal, deuterium incorporation was determined to be 77%. Increasing the number of equivalents of base slightly increased deuterium incorporation (entry 2); however, when the solvent was changed to Et₂O and metalation time was extended, incorporation was increased to 94% (see Appendix 8 for $^1\text{H-NMR}$ spectra of **2.107a** with varying D incorporation). Using these conditions, **2.104** was converted to bisboronic acid **2.107b** in moderate yield (entry 4).

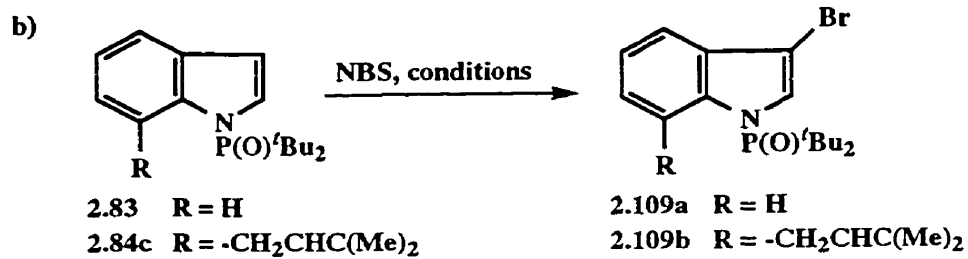
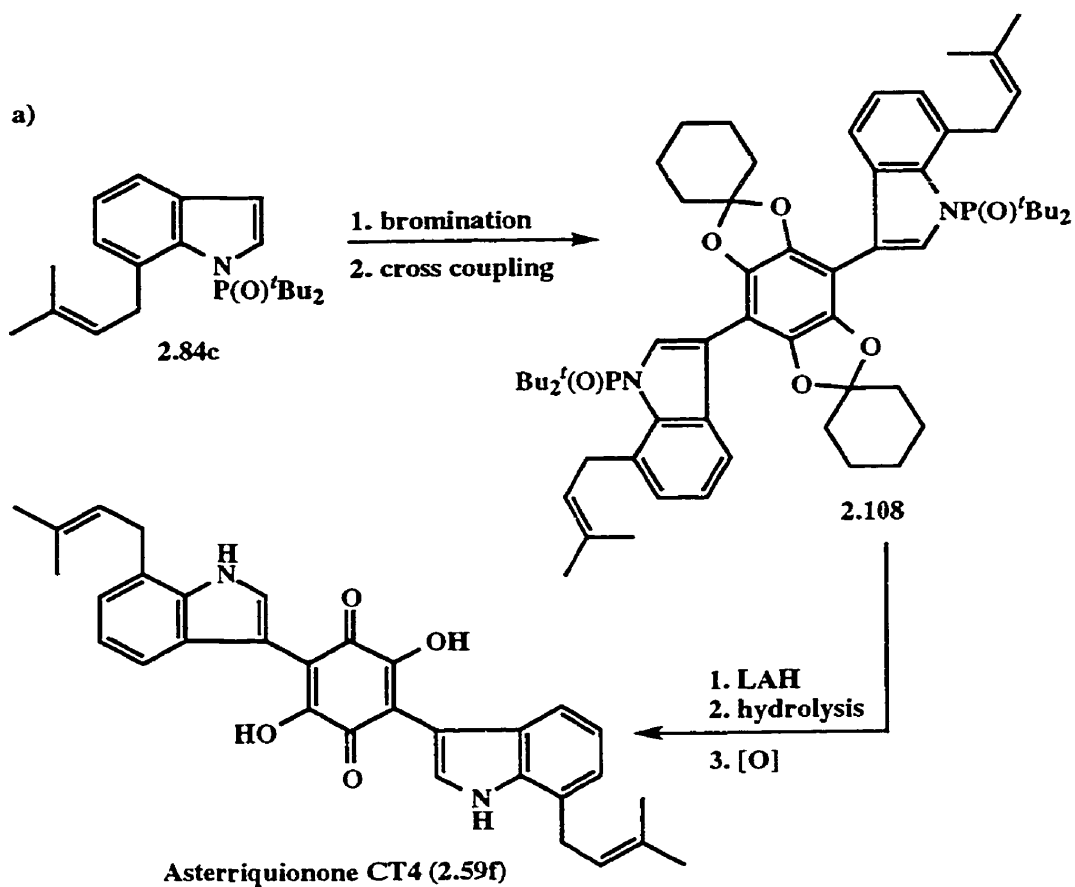


entry	Conditions	E+	E	Product	D inc* / Yield (%)
1	<i>t</i> -BuLi (3 equiv.) / THF / rt / 3.5 h	MeOD	D	a	77
2	<i>t</i> -BuLi (5 equiv.) / THF / rt / 3.5 h	MeOD	D	a	85
3	<i>t</i> -BuLi (3 equiv.) / Et ₂ O / rt / 18 h	MeOD	D	a	94
4	<i>t</i> -BuLi (3 equiv.) / Et ₂ O / rt / 18 h	B(OMe) ₃	B(OH) ₂	b	68

* %D incorporation determined by $^1\text{H-NMR}$ integration

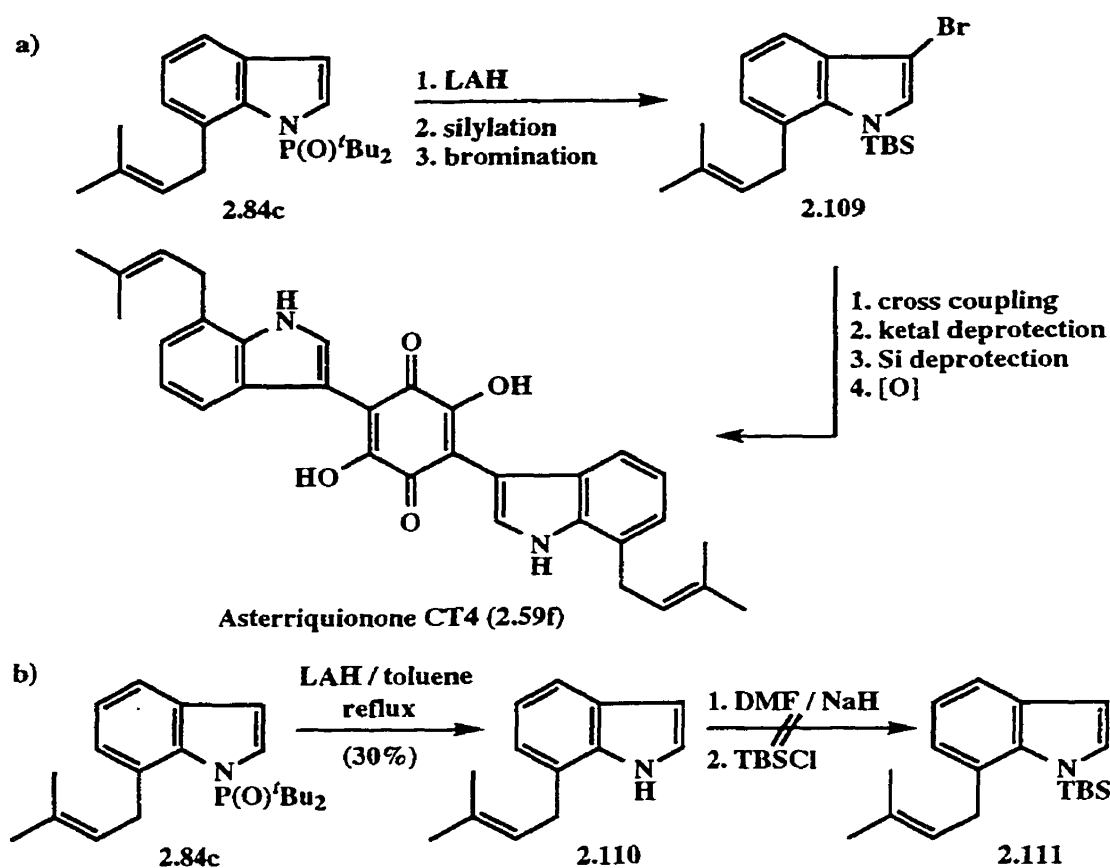
Scheme 2.34

Having achieved the preparation of one of the desired cross coupling partners, attention was turned to synthesis of the indole portion. According to the established procedure, **2.84c** was prepared from **2.83** in 87% yield. Two options were then considered for further functionalization of **2.84c**. In the first proposed route (Scheme 2.35a), the phosphinyl protecting group would be carried through to the cross coupled product (**2.108**) and then reductively removed as previously established (Section 2.4.2). This would require bromination of **2.84c** followed by cross coupling with **2.107b** and finally phosphinyl removal with LAH. Simple acid hydrolysis of the cyclohexylidene ketal protecting groups and air oxidation would then provide the desired natural product **2.59f**. In pursuit of this approach, bromination was first attempted on model *N*-phosphinylindole **2.83** to establish conditions. Thus, treatment of **2.83** with NBS in either DMF or cyclohexane at room temperature provided the desired monobromo derivative in high yield (95% and 94% respectively, Scheme 2.35b, entries 1,2). Unfortunately, under these conditions **2.84c** failed to undergo reaction, even after extended periods of time (entry 4) and at elevated temperatures (entry 5). This result led to the decision that early removal of the phosphinyl group would be more advantageous and thus the second approach, removal of the phosphinyl moiety immediately after incorporation of the prenyl group, was examined (Scheme 2.36a). Further protection of the indole with an acid labile protecting group would be followed by bromination and cross coupling. Subsequent simultaneous removal of the indole protecting group and the cyclohexylidene ketal protecting groups, followed by air oxidation, would provide the natural product. Thus, **2.84c** (Scheme 2.36b) was treated with LAH in toluene at reflux providing indole **2.110** in modest yield. Although the yield was disappointingly low, this two step procedure is representative of a new regioselective route to 7-substituted indoles. All attempts to silylate (TBSCl) **2.110** were unsuccessful, resulting in partial recovery of starting material.



entry	Reactant	Solvent	Temp	Time	Product	Yield (%)
1	2.83	DMF	rt	24 h	2.109a	95
2	2.83	cyclohexane	rt	12 h	2.109a	94
3	2.84c	CH ₃ CN	rt	12 h	2.109b	0
4	2.84c	cyclohexane	rt	7 d	2.109b	0
5	2.84c	cyclohexane	reflux	24h	2.109b	0

Scheme 2.35



Scheme 2.36

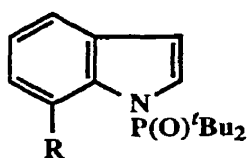
A plausible explanation for the lack of reactivity involves the steric interaction between the prenyl moiety and the incoming silyl group. As was demonstrated in the solid state structure of **2.84c**, bulky substituents in the 1- and 7- positions have strong steric interactions and thus the C₅ side chain may be hindering the approach of the TBSCl to a substantial degree. Further work in this area could lead to effective indole N-H protection (Section 2.5) and appropriate functionalization for cross coupling. Unfortunately, time constraints prevented further pursuit of the synthesis.

2.5 Future Work

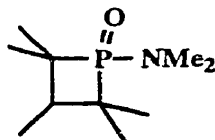
2.5.1 DMG Cleavage

The value of this new methodology clearly lies in the ability to regioselectively prepare 7-substituted indoles directly. Despite the direct entry into a traditionally difficult to achieve substitution pattern, the range of useful electrophiles is severely restricted by the necessary

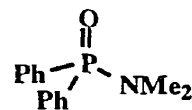
conditions for removal of the electrophile. Clearly, a milder method for removal of the directing group from **2.83** and its derivatives would facilitate much broader application of this methodology. Thus far, the only successful method of removal relies upon the LAH reduction of the phosphine moiety. With this in mind, other reductive methods for phosphine oxides may be appropriate. Reaction of phosphine oxides with chlorosilane reagents³⁶³ (Section 1.5.5) is a well established method of reduction, and may be applicable to this system. Alternatively, Griffin and co-workers³⁶⁴ have reported AlH_3 as a highly effective reagent for reduction of phosphine oxides to the corresponding phosphines. The advantage of this method lies in the ability to perform the reduction while avoiding the requirement of an aqueous workup procedure, a step which often results in partial reoxidation.³⁶⁵ While reoxidation during workup is of little consequence for the present study, this method may still prove to be advantageous. In order to avoid reductive conditions, which impose limitations on the range of useful electrophiles, alternative acidic and basic procedures should be investigated. As reported by Koizumi and co-workers, hindered phosphine oxides such as **2.95** require more vigorous conditions for hydrolysis than their less hindered counterparts (e.g. **2.93c**). Nonetheless, acidic hydrolysis of such systems is achievable and similar conditions may be applicable to the present system. Similarly, more vigorous alkaline conditions may aid in the hydrolysis of **2.83** and its 7-substituted derivatives.



2.83 R = H
2.84 R = E



2.95



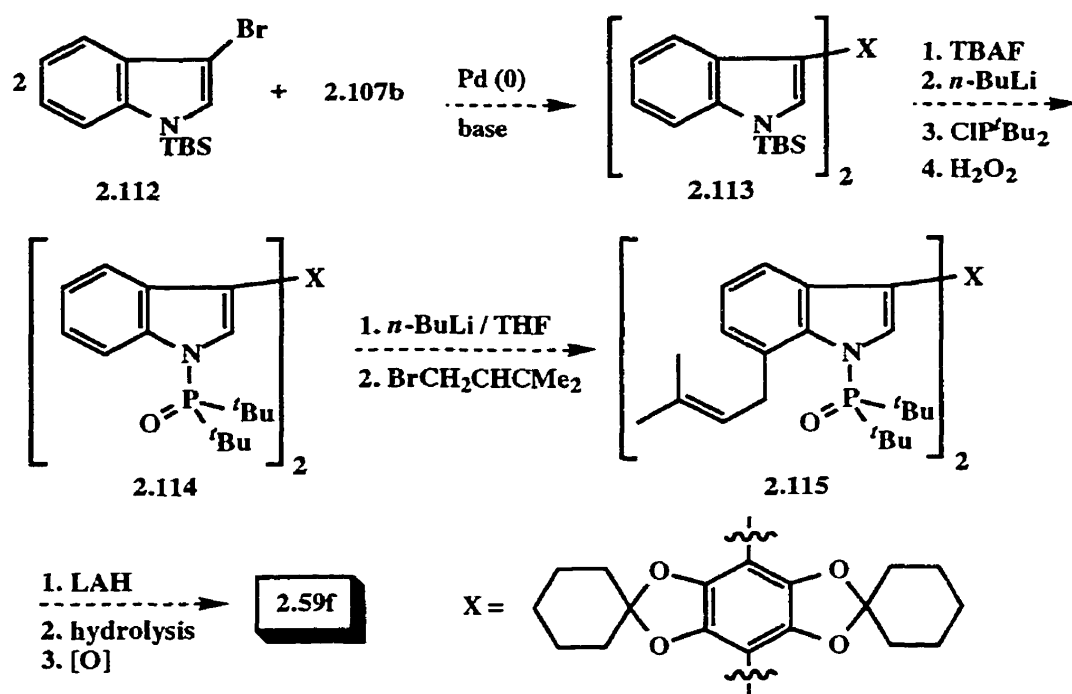
2.93c

2.5.2 Total Synthesis of Asterriquinone CT4

The initial progress towards the total synthesis of Asterriquinone CT4 (**2.59f**) is encouraging, as good syntheses of cross coupling partners **2.107b** and prenylated indole **2.110** have been achieved. Although the approach in Scheme 2.35 gave difficulty and was

ultimately abandoned, the approach in Scheme 2.36 may still be achievable. Currently, the limitation is the silylation of **2.110** to give **2.111**. If this silylation step can be conquered, the success of the synthesis will rely primarily on the cross coupling step, as all other steps in the synthesis involve well established deprotection steps. Only one silyl group has been investigated thus far, and success may lie in the choice of a different, and perhaps less sterically demanding, silyl protecting group for the indole nitrogen.

A third approach to this natural product involves introduction of the prenyl moiety by metalation at a later stage (Scheme 2.37). In this approach, a simpler indole cross coupling partner (**2.112**) may be utilized in conjunction with previously synthesized bisboronic acid **2.107b** to provide the required triaryl ring system (**2.113**) of the natural product. Desilylation of **2.113**, and reprotection of the indole nitrogens would provide bisphosphinyltriaryl **2.114**. In a key step, metalation of **2.114** under established conditions, followed by quench with prenyl bromide would afford prenylated derivative **2.115**. Finishing steps would then involve cleavage of the phosphinyl groups, removal of the cyclohexylidene ketal protecting groups, and finally air oxidation of the benzoquinone moiety providing the natural product **2.59f**. This straightforward approach seems reasonable, but has several potential pitfalls: *i*) solubility of some intermediates may be limited due to the size of the molecules, though the protecting groups should aid with solubility in most cases; *ii*) introduction of the two phosphinyl groups requires formation of a dianion, which may have poor solubility and/or reactivity; *iii*) introduction of the prenyl groups requires either a double metalation, requiring formation of a dianion, or a stepwise metalation procedure introducing the two groups sequentially and adding another step to the synthesis and adding the possibility of allyl C-H deprotonation; and *iv*) the regioselectivity of metalation may be sacrificed since the proposed metalation substrate **2.114** is clearly more complex than **2.83**. Despite these potentially troublesome areas, this third approach may still be viable as a total synthesis of asterriquinone CT4.

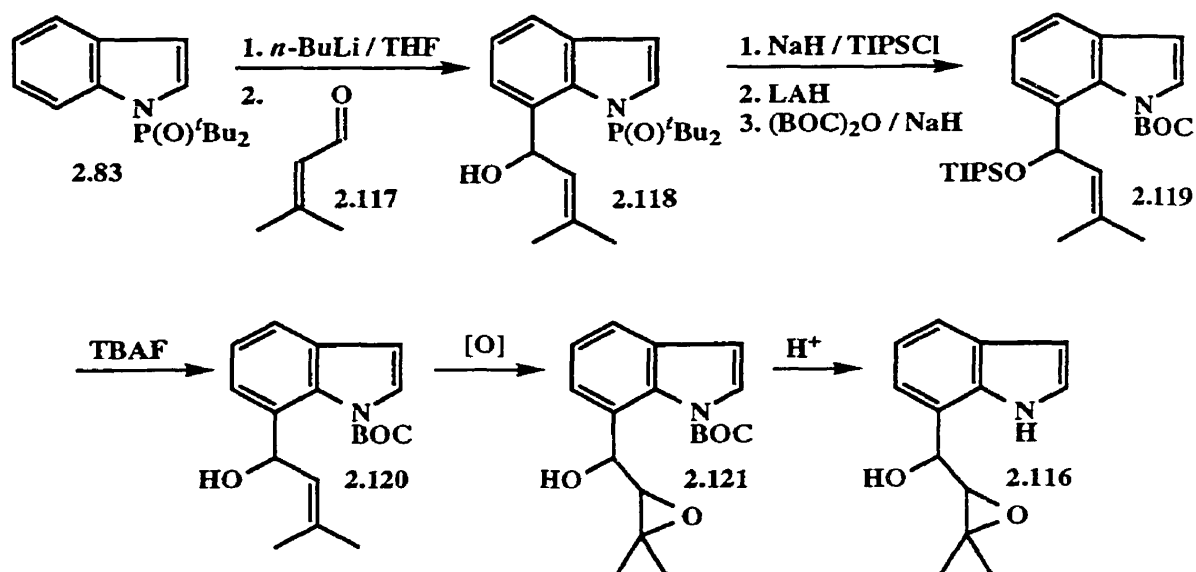


Scheme 2.37

2.5.3 Total Synthesis of Leiocarpol

During the course of isolation and structure determination of the components from the roots of *Esenbeckia leiocarpa*, Monache and co-workers isolated several indole derivatives, constituting the first indole natural products isolated from this genus.³⁶⁶ Among those isolated was the interesting epoxy alcohol leiocarpol (2.116) whose relative and absolute stereochemistry remain unknown. Consideration of this natural product shows that it is a good candidate for application of the new methodology for introduction of the substituent in the 7-position. Accordingly, exposure of 2.83 to established conditions followed by quench with 3-methyl-2-butenal (2.117) would be expected to lead to [1,2]-addition product 2.118. In order to proceed from this intermediate alcohol to the desired natural product, careful manipulation of protecting groups is required to allow: *i*) removal of the phosphinyl directing group; *ii*) differential protection of the alcohol and the indole nitrogen; *iii*) selective removal of the protecting groups; and *iv*) epoxidation of the double bond. One possible approach to this protection / deprotection sequence (Scheme 2.38) involves TIPS protection of the alcohol

functionality before removal of the phosphinyl group and finally protection with an acid sensitive group such as *tert*-butoxycarbonyl (Boc) giving fully protected indole **2.119**. Selective removal of the silicon protecting group using TBAF then provides the necessary epoxidation precursor **2.120**. After epoxidation of the double bond to form epoxy alcohol **2.121**, acid catalyzed cleavage of the Boc protecting group leads to leiocarpol (**2.116**). This synthesis also allows one to take advantage of asymmetric epoxidation techniques for selective preparation of the various stereoisomers.

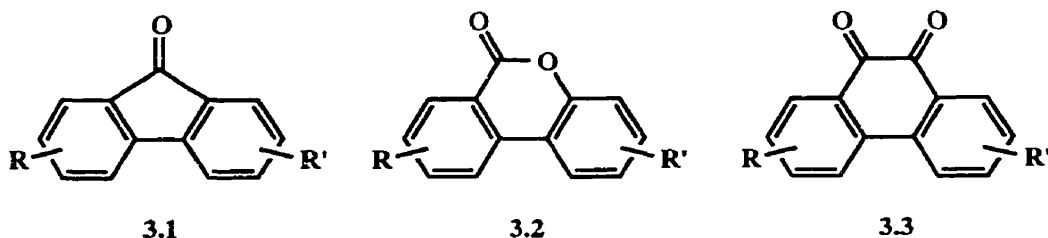


Scheme 2.38

3.0 Studies Directed Toward the Total Synthesis of Biruloquinone

3.1 Introduction

Condensed aromatic carbocyclic and heterocyclic natural products from a variety of sources provide interesting and challenging synthetic targets. As potential targets continue to grow in complexity, so does the range of techniques available for their construction. DoM chemistry in conjunction with aryl-aryl cross-coupling reactions has proven to be a successful strategy in the construction of several naturally occurring condensed aromatic ring systems^{5,7,161,367} including fluorenones (3.1),^{169,170} dibenzo-[*b,d*]pyranones (3.2),^{176,368,369} and phenanthrene-9,10-quinones (3.3).^{172,370-372}



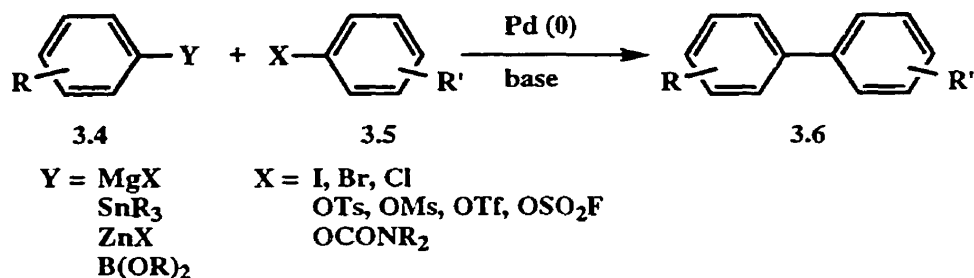
The combination of DoM chemistry and aryl-aryl cross-coupling is well documented^{161,367} and has been applied to numerous ring systems and natural products.

3.2 Transition Metal Catalyzed Aryl-Aryl Cross-Coupling

Transition metal catalyzed aryl-aryl cross-coupling methodology performs the classically difficult task of joining two aromatic rings providing complex biaryl systems. Since the first reports by Corriu³⁷³ and Kumada^{374,375} and their respective co-workers, several groups have contributed to the area providing numerous strategies in formation of biaryls.^{45,376-379}

Cross-coupling involves the combination an aryl organometallic species (3.4) and a second aryl species (3.5) containing a leaving group (Scheme 3.1). Several variations on this reaction are known incorporating a halogen (usually Br or I, but more recently Cl) as the leaving group, though other leaving groups have been investigated (e.g. -OTf,^{380,381} -OCONR₂,^{382,383}). The principle feature in distinguishing the various coupling techniques is

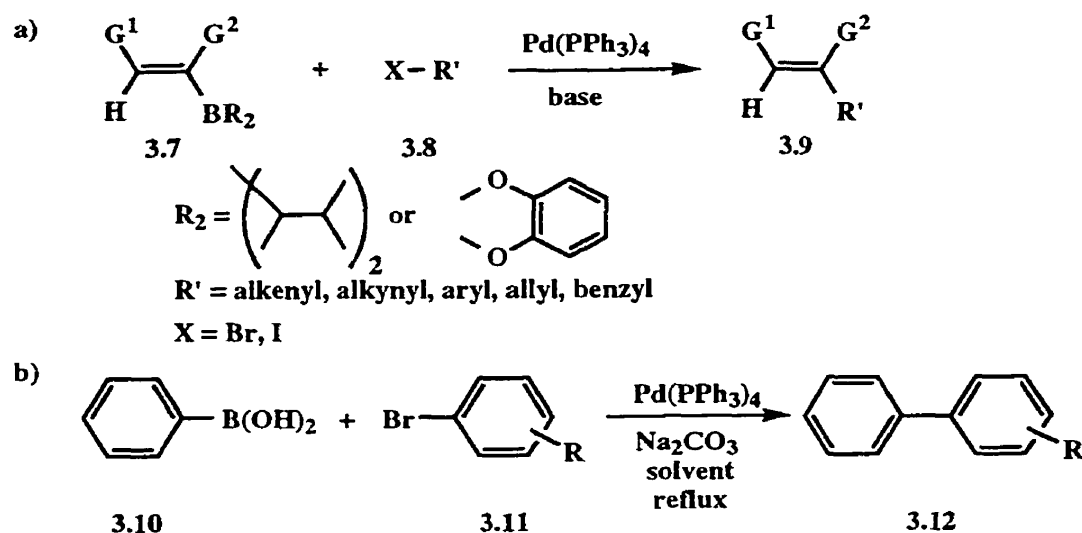
the nature of the organometallic coupling partner; the four main categories are referred to as Kumada ($Y = MgX$),^{374,375} Stille ($Y = SnR_3$),³⁸⁴ Negishi ($Y = ZnX$),³⁸⁵ and Suzuki-Miyaura ($Y = B(OR)_2$).³⁷⁹ While each of the different methods has its own advantages and disadvantages,^{45,376} all are effective in the construction of substituted biaryls. The focus of this section will be the Suzuki-Miyaura-type cross-coupling reaction.



Scheme 3.1

In 1981, Suzuki and co-workers first reported that phenylboronic acid and haloarenes could be efficiently coupled under basic conditions and with palladium catalysis.³⁸⁶ This method evolved as an extension of Davidson and Triggs' results³⁸⁷ in which symmetrical biaryls were formed by dimerization of the corresponding boronic acids with sodium palladate, and Suzuki's prior work in the coupling of alkenylboranes with various organic halides (Scheme 3.2a).³⁸⁸⁻³⁹⁰ Suzuki's procedure had two significant advantages: *i*) only a catalytic amount of palladium reagent is required whereas the dimerization reaction requires a stoichiometric amount of sodium palladate, and *ii*) the reaction is not limited to the formation of symmetrical biaryls. Thus, conditions were investigated for coupling chloro-, bromo-, and iodobenzene with phenylboronic acid (**3.10**) in the presence of base and a catalytic (3 mol%) amount of $Pd(PPh_3)_4$. Best results were obtained when aqueous Na_2CO_3 was employed as the base and an excess of $PhB(OH)_2$ was used. Iodobenzene and bromobenzene provided good yields of products; however, chlorobenzene failed to participate in the coupling reaction. A range of biaryls (**3.12**) was prepared according to the new procedure from their corresponding bromobenzene derivatives (**3.11**, Scheme 3.2b). Simple bromotoluenes and

bromoanisoles smoothly underwent coupling (Table 3.1, entries 1-4) in good yield providing the expected biaryls. Since the inability of chloro substituents to undergo reaction had already been established, *p*-bromochlorobenzene provided *p*-chlorobiphenyl as the only product (entry 5). Conversely, *p*-dibromobenzene underwent coupling at both sites to provide a moderate yield of *p*-terphenyl (entry 6). More sterically demanding substrates such as mesityl bromide (entry 7) and 1-naphthyl bromide (entry 8) led to the expected products in moderate to good yield; albeit at higher temperatures and longer reaction times. Finally, reaction with methyl *p*-bromobenzoate provided the expected biaryl demonstrating further scope as the sensitive methyl ester was not affected under the reaction conditions (entry 9).³⁹¹

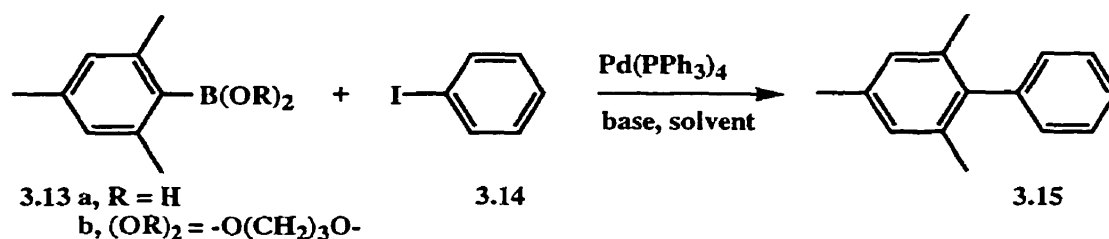


Scheme 3.2

Table 3.1 - Coupling of Aryl Bromides with Phenylboronic Acid (Scheme 3.2b)

entry	Bromide (3.11)	Solvent	Time (h)	Yield (%)
1	R = 2-Me	C ₆ H ₆	6	94
2	R = 4-Me	C ₆ H ₆	6	88
3	R = 2-OMe	C ₆ H ₆	6	99
4	R = 4-OMe	C ₆ H ₆	6	66
5	R = 4-Cl	C ₆ H ₆	6	89
6	R = 4-Br	PhCH ₃	12	40
7	R = 2,4,6-Me	PhCH ₃	17	80
8	1-naphthyl	PhCH ₃	10	49
9	R = 4-CO ₂ Me	C ₆ H ₆	6	94

Subsequent modifications to Suzuki's procedure have allowed for greater versatility and broader scope of the reaction. Aryl triflates proved to be equally effective coupling partners as the corresponding halides.³⁹² Modifications by Gronowitz^{393,394} and Snieckus^{395,396} employed 1,2-dimethoxyethane (DME) as the solvent, which reduced the amount of protodeboronation as a side reaction. Noting the difficulty in the preparation of sterically hindered biaryls³⁹⁷ and the fact that arylboronic acids containing electron withdrawing groups provided unsatisfactory results,^{393,394} Suzuki and co-workers sought methods for improving the reaction conditions.^{398,399} Numerous bases were identified and their effect on the coupling of mesitylboronic acid (**3.13a**) and iodobenzene (**3.14**) was investigated. Best results were obtained with Ba(OH)₂ in aqueous DME, and Cs₂CO₃ or K₃PO₄ in DMF, each of which produced the desired biaryl in > 98% yield after 8 hours at reflux (Scheme 3.3). When Cs₂CO₃ and K₃PO₄ were used, the 1,3-propanediol boronate ester of mesitylboronic acid (**3.13b**) was the coupling partner.



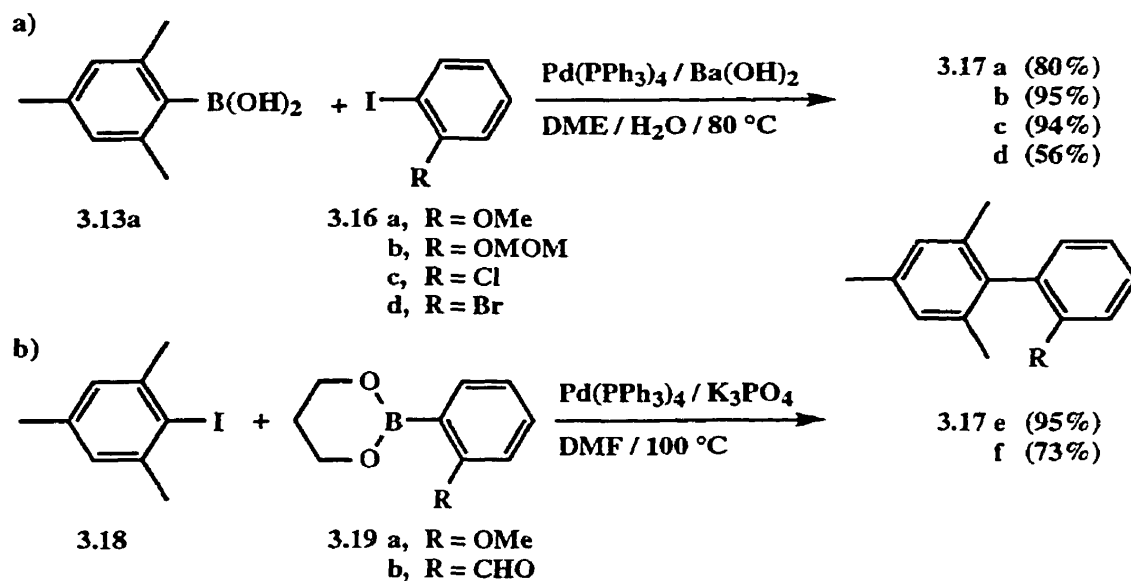
substrate	base	solvent	temp (°C)	yield (%)
3.13a	Ba(OH) ₂	DME/H ₂ O	80	99
3.13b	Cs ₂ CO ₃	DMF	100	98
3.13b	K ₃ PO ₄	DMF	100	98

Scheme 3.3

Using the newly developed conditions, several hindered biaryls were generated under either protic (Ba(OH)₂ / DME / H₂O) or aprotic (K₃PO₄ / DMF) conditions (Scheme 3.4). Using mesitylboronic acid (**3.13a**), iodobenzenes with *ortho* substituents were effectively coupled, providing biaryls **3.17a-c** in good yield and **3.17d** in modest yield, probably due to competitive coupling of the iodide and bromide in **3.16d**, or further coupling of **3.17d** with

excess mesitylboronic acid (Scheme 3.4a). Noting that both electron withdrawing and electron donating substituents contributed to hydrolytic deboronation,⁴⁰⁰ the aprotic procedure was applied to boronate esters **3.18** providing good to excellent yields of hindered biaryls **3.17e-f** (Scheme 3.4b).

While Suzuki coupling reactions involving aryl iodides and bromides are well documented, the corresponding reactions for aryl chlorides have, until recently, been unavailable. Development of new ligand systems such as those discussed²³⁹ in Section 1.4.1 have helped to make such couplings more accessible⁴⁰¹ and numerous examples have been reported.⁴⁰²⁻⁴⁰⁵

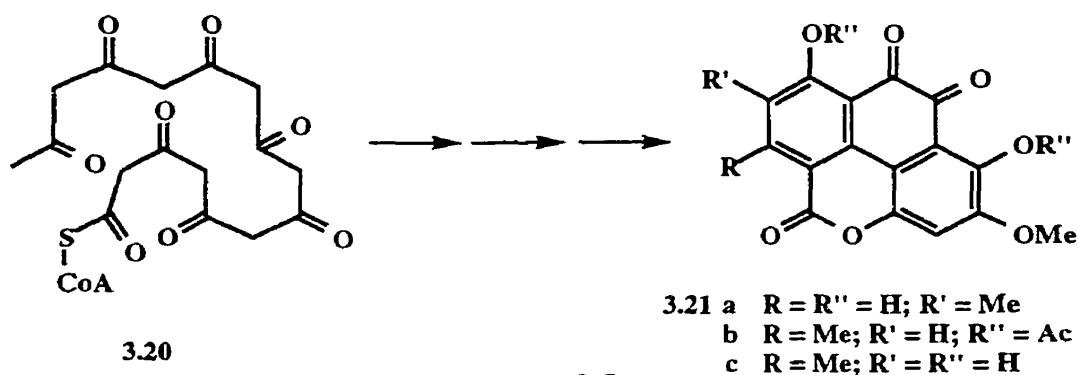


Scheme 3.4

The versatility of the Suzuki cross-coupling reaction is enhanced by its connection with DoM chemistry.³⁶⁷ In most cases, the required boronic acids are easily derived from metalation followed by quench with B(OMe)₃ or a similar borate. Furthermore, many of the DMGs in the boronic acid coupling partners may be utilized for further functionalization of the biaryl product (see Section 1.2.5).

3.3 Biruloquinone and Related Natural Products

In 1983, Krivoschekova and co-workers reported the isolation of the main pigment of *Parmelia birulae*.⁴⁰⁶ The purple compound was the first phenanthraquinone isolated from lichens and the structure **3.21a** was proposed based on spectral data. Among the evidence for the structural assignment was the observation that conversion of the natural product to the corresponding diacetate (**3.21b**) resulted in minimal upfield shifts for the aromatic protons, which led to the conclusion that neither proton was adjacent to a hydroxy group. While the analysis seemed logical, Thomson later suggested⁴⁰⁷ that the structure **3.21c** was more consistent with the spectral data and, significantly, fit the acetate-malonate biogenesis (Scheme 3.5).



Arnone and co-workers, while studying the metabolites of *Mycosphaerella rubella*,^{408,409} found that a compound in the ethyl acetate extracts had a melting point, and IR, UV, mass and ¹H-NMR spectra identical with those reported for biruloquinone. In order to firmly establish the structure of biruloquinone, a detailed ¹³C-NMR study was undertaken.⁴¹⁰ To overcome poor solubility, the natural product was reductively acetylated in the presence of Zn to give the corresponding tetraacetate **3.22**, which showed much greater solubility and was amenable to a ¹³C-NMR study. Despite the complexity of the molecule, the ¹H-NMR spectrum of **3.22** (DMSO-*d*₆) was relatively simple showing four singlets for the acetyl methyl groups, a singlet for the methoxy, a singlet for H-3, and doublets (J = 0.9 Hz) for the methyl and H-7 signals. Similarly, the ¹³C-NMR spectrum was straightforward showing 25

distinct resonances with multiplicities consistent with the structure shown. Extensive heteronuclear $^{13}\text{C}\{-^1\text{H}\}$ selective decoupling was then used to establish the two and three-bond connectivity (Figure 3.1). The ^{13}C resonance at δ 114.74 was assigned to C-5 based on the three bond couplings of 7.5 and 3.5 Hz with H-7 and H₃-13, respectively. The methyl group showed a second three-bond coupling to the aromatic methine signal (δ 126.89, $^3J_{\text{CH}} = 5.5$ Hz) as well as a two-bond coupling to the quaternary aromatic carbon (δ 145.68, $^2J_{\text{CH}} = 6.5$ Hz), thus establishing the position of the methyl group at C-6. Further evidence of the connectivity was provided by the two-bond coupling from H-7 to C-8 (δ 148.68, $^2J_{\text{CH}} = 4.0$ Hz) and the three-bond coupling from H-7 and C-8a (δ 115.21, $^3J_{\text{CH}} = 6.0$ Hz). Finally, long range coupling from the C-12 carbonyl to H-7 and H₃-13 (δ 158.80, $^4J_{\text{CH}} = 1.4$ Hz and 1.2 Hz respectively) precluded the possibility of the initially proposed structure (3.21a) and firmly established 3.21c as the structure of biruloquinone, confirming Thomson's insightful suggestion.

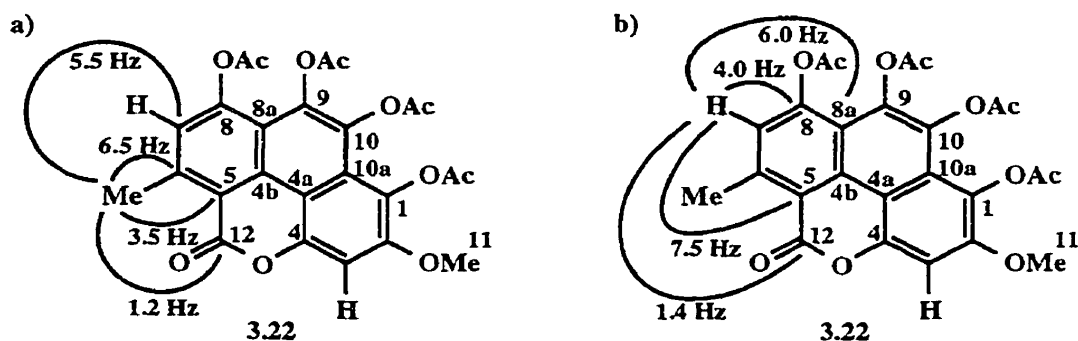


Figure 3.1 - Selected two-, three-, and four-bond C-H couplings in biruloquinol tetraacetate (3.22) for (a) H₃-13; and (b) H-7

From a structural standpoint, biruloquinone presents a truly unique ring construction. While the 9,10-phenanthraquinone and dibenzopyranone ring systems are both known to exist in nature, no other natural product can boast both ring systems in the same structure (Figure 3.2).

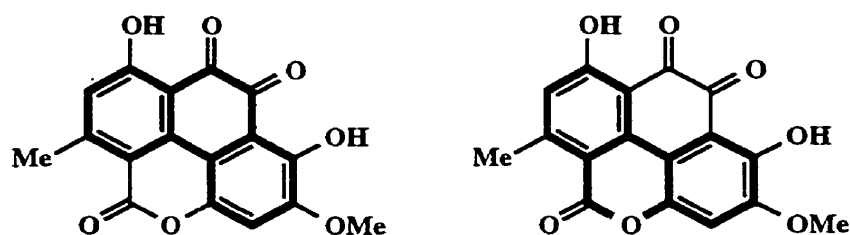
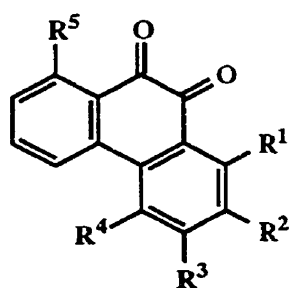


Figure 3.2 - Ring systems within the structure of biruloquinone
(a) 9,10-phenanthrenequinone; and (b) dibenzo-[*b,d*]pyranone

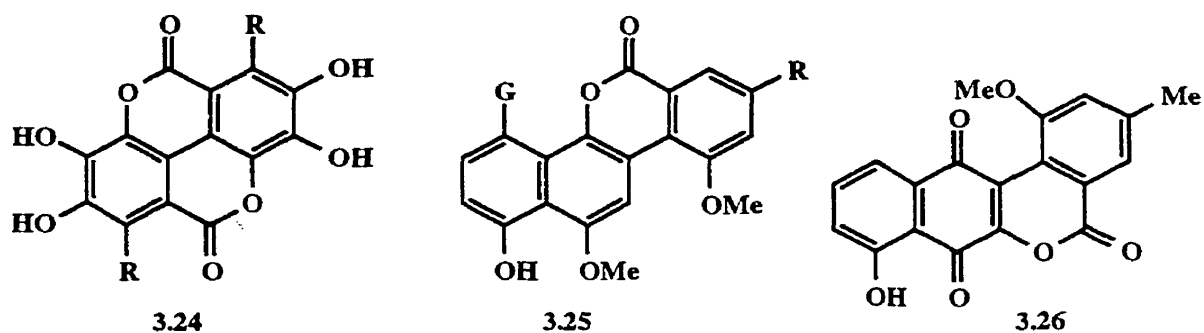
Naturally occurring phenanthraquinones are known in a variety of forms including *ortho* and *para* quinone isomers; however, the 9,10-phenanthraquinone structure is relatively scarce.^{411,412} Chi and co-workers reported denticulatol as the first example;⁴¹³ however, Sargent and co-workers demonstrated by total synthesis that the two proposed structures (3.23a, 3.23b) are incorrect.⁴¹⁴ Sachihiko confirmed the incorrect assignment of denticulatol by an independent total synthesis.⁴¹⁵ The small population of known 9,10-phenanthraquinones includes the related compounds haloquinone (3.23c) from *Streptomyces venezuela*,^{416,417} piloquinone (3.23d) from *S. pilosus*,^{411,418,419} 4-hydroxypiloquinone (3.23e),^{420,421} and murayaquinone (3.23f) from *S. murayamaensis*.⁴¹²

Table 3.2 - Naturally occurring 9,10-phenanthraquinones

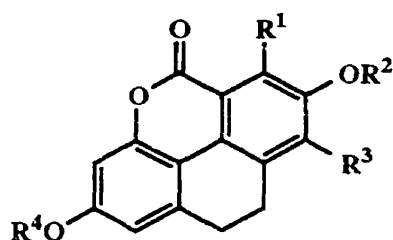


3.23	R ¹	R ²	R ³	R ⁴	R ⁵
a	H	OH	H	OH	Me
b	OH	H	OH	H	Me
c	OH	Me	C(O)Me	H	OH
d	OH	Me	C(O)CH ₂ CH ₂ CH(Me) ₂	H	OH
e	OH	Me	C(O)CH ₂ CH ₂ CH(Me) ₂	OH	OH
f	OH	Me	C(O)CH ₂ CH ₂ CH ₃	H	OH

In contrast to the 9,10-phenanthraquinones, dibenzopyranones are much more common in nature. Several examples display an interesting range of biological activity and include such diverse molecules as ellagic acid (3.24, R=H) and coruleoellagic acid (3.24, R = OH),⁴²² gilvocarcins (3.25, G = glycoside, R = Me, Et, vinyl),⁷² and WS 5995A (3.26).⁴²³



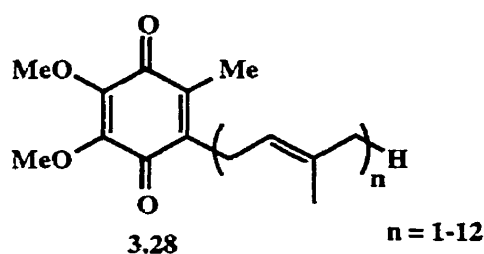
Perhaps the most structurally relevant examples of naturally occurring dibenzopyranones are the series of related dihydrophenanthropyranones **3.27a-d** isolated from various species of Himalayan orchid. While not identical to biruloquinone, its similarity in the underlying ring structure of coeloginin (**3.27a**),⁴²⁴ oxoflavidinin (**3.27b**),⁴²⁵ isooxoflavidinin (**3.27c**),⁴²⁶ and oxoflavidin (**3.27d**)⁴²⁷ is clearly evident and differs only in the oxidation state of the phenanthrene.



3.27	R ¹	R ²	R ³	R ⁴
a	OH	Me	OMe	H
b	H	Me	H	H
c	H	H	H	Me
d	H	H	H	H

3.3.1 Biological Activity

To date, no biological activity studies on biruloquinone have been published. Quinones are widely known to readily undergo redox processes, converting between the quinone and dihydroquinone forms.⁴²⁸ Indeed, this property has been amply documented in Chapter 2 for asterriquinones and related molecules. The ability of quinones to take part in such processes generally makes them willing candidates for participation in numerous metabolic pathways.⁴²⁹ This is clearly evident with well known biological molecules such as ubiquinones (**3.28**) which readily participate in electron transport processes.



While biruloquinone itself has never been subjected to bioscreening, related compounds have demonstrated their potential biological activity. Halobacteria, which possess a special kind of cell wall containing a glycoprotein very similar to that of eucariotic cells, showed very low sensitivity to a group of 50 known antibiotics.⁴¹⁶ Haloquinone (3.23c, Table 3.2) was tested against a series of almost 40 different bacteria and it was found that, while haloquinone was not active against all tested strains, it was active against several strains of halobacteria and arthrobacteria. The mode of action of haloquinone on *Halobacterium cutirubrum* cells appears to be through DNA and/or RNA interaction based on drastic and immediate inhibition of ¹⁴C-thymidine and ¹⁴C-uracil incorporation. Though no reports exist on similar testing of the related compounds piloquinone (3.23d, Table 3.2), 4-hydroxypiloquinone (3.23e), or murayaquinone (3.23f), the structural similarity to haloquinone suggests that some antibiotic activity should be expected.

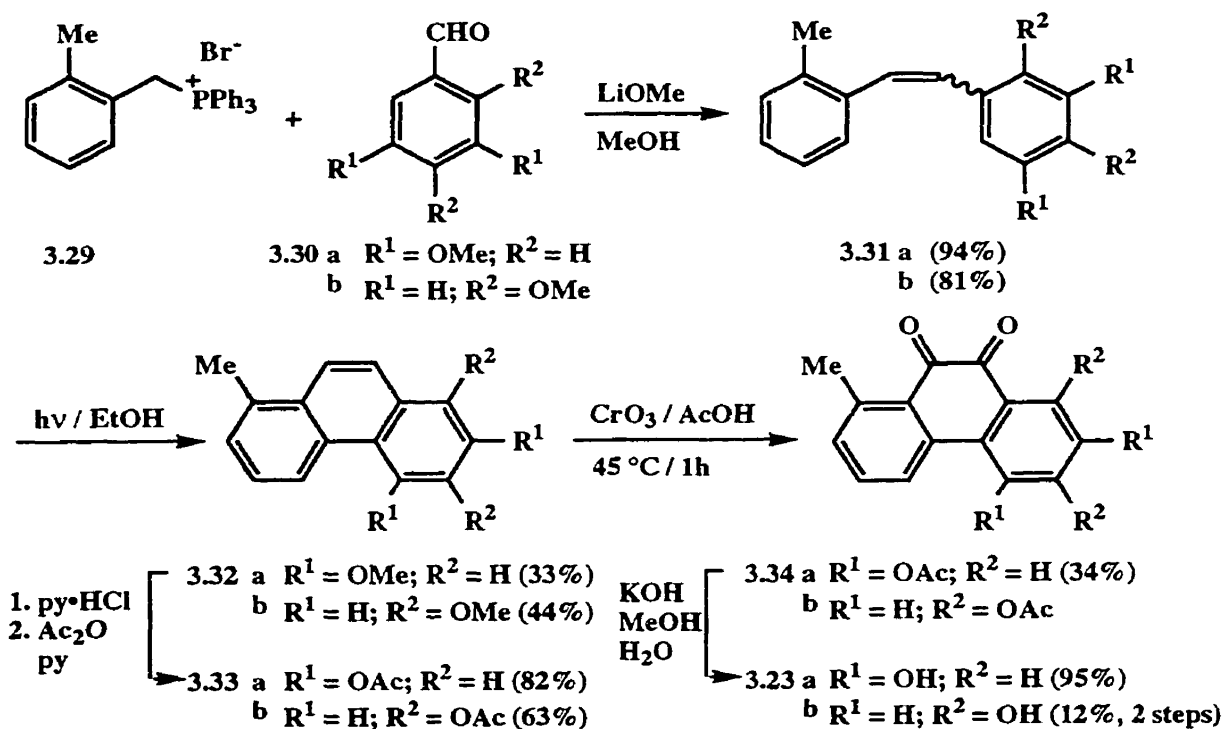
Several members of the dibenzo-[*b,d*]pyranone class of natural products exhibit different modes of biological activity. Ellagic acid (3.24) and its derivatives have shown antitumour activity⁴²² as have the gilvocarcins (3.25) which also exhibit antibiotic properties.^{72,422,430}

The range of possible biological activity for a molecule as diversely functionalized as biruloquinone adds to its allure as an attractive synthetic target.

3.3.2 Previous Syntheses of 9,10-Phenanthraquinones

Although little attention has been devoted to the synthesis of biruloquinone since its discovery in 1983, synthetic efforts towards related natural products are notable. Few methods are available for the construction of the 9,10-phenanthraquinone ring system, and most rely on

oxidation of a phenanthrene. Sargent and co-workers have applied the classical strategy of stilbene photocyclization followed by phenanthrene oxidation in the synthesis of quinones **3.23a** and **3.23b**⁴¹⁴ as well as the total synthesis of piloquinone (**3.23d**).⁴¹¹ Stilbenes were prepared *via* Wittig reaction of an appropriate benzaldehyde and a benzyltriphenylphosphonium halide. Accordingly, **3.29** was condensed with 3,5-dimethoxybenzaldehyde (**3.30a**) in the presence of lithium methoxide providing stilbene **3.31a** as a mixture of *E,Z*-isomers (Scheme 3.6).⁴¹⁴ Photocyclodehydrogenation of **3.31a** proceeded in modest yield to afford 2,4-dimethoxy-8-methylphenanthrene (**3.32a**).^{431,432} Cleavage of the methyl ethers and replacement with acetyl groups provided **3.33a** which, upon treatment with CrO₃ in glacial acetic acid, afforded 9,10-phenanthraquinone **3.34a** in 34% yield. Simple alkaline hydrolysis

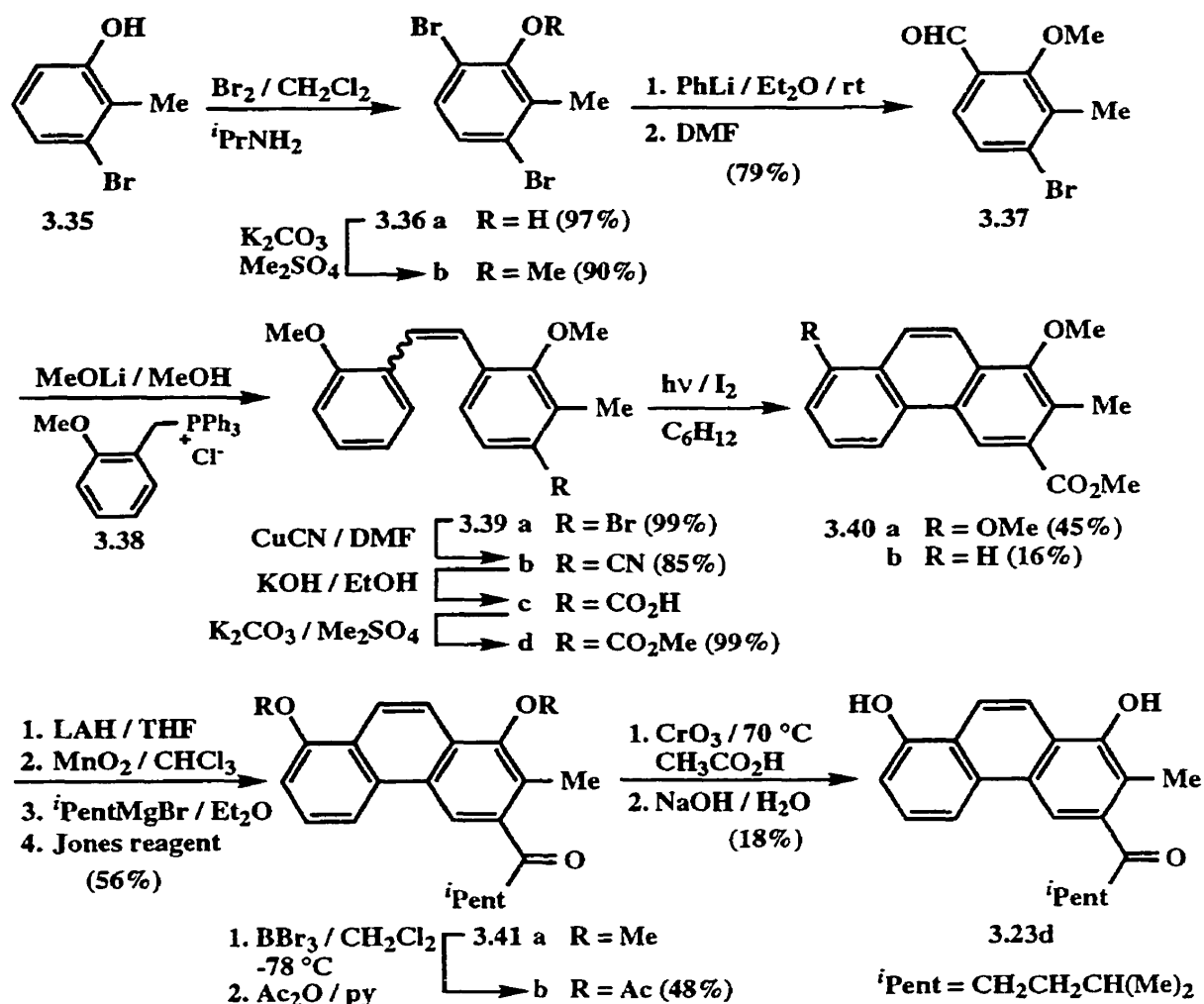


Scheme 3.6

of the acetyl protecting groups gave the desired quinone **3.23a** in 8.2% overall yield and 7 steps from benzaldehyde **3.30a**. An identical sequence of reactions was executed starting with

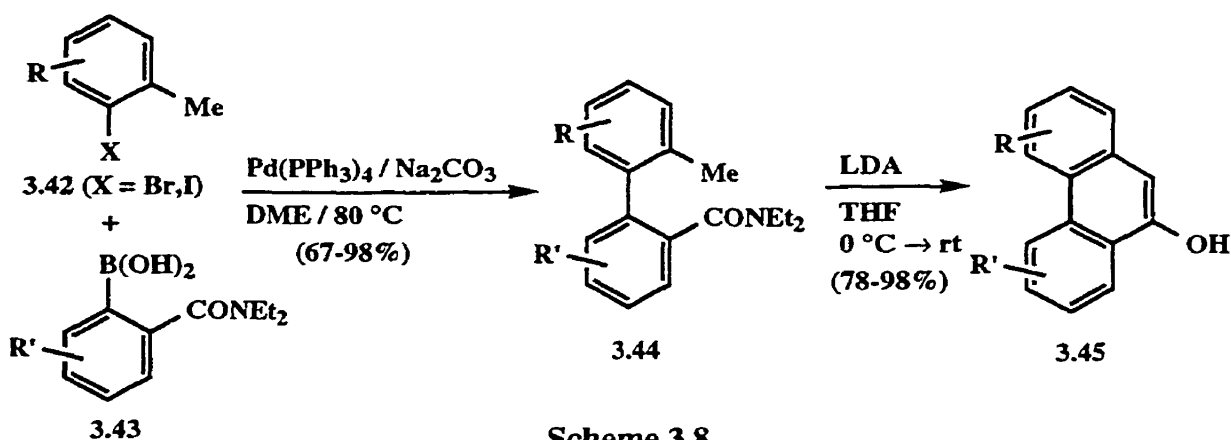
2,4-dimethoxybenzaldehyde (**3.30b**), affording the isomeric quinone **3.23b** in 2.7% overall yield and 7 steps.

In a similar approach for the synthesis of piloquinone (Scheme 3.7), bromination of bromophenol **3.35** under Pearson's conditions for monobromination *ortho* to phenols⁴³³ gave an excellent yield of dibromophenol **3.36a**, which was easily converted into the corresponding methyl ether **3.36b** by treatment with dimethyl sulfate. A selective lithium-halogen exchange was then performed using phenyllithium, and subsequent quench with DMF yielded aldehyde **3.37**, the regioselectivity being ascribed to the coordinating ability of the *ortho* methoxy group. Aldehyde **3.37** was treated with (2-methoxybenzyl)triphenylphosphonium chloride (**3.38**) in the presence of lithium methoxide to give stilbene **3.39a**. The distribution of the *E/Z*-isomers of **3.39a** was highly dependant on solvent choice providing predominantly the *trans* stilbene when MeOH was used and the *cis* stilbene when DMF was used. Treatment with CuCN, followed by hydrolysis and methylation led sequentially to cyanostilbene **3.39b**, carboxylic acid **3.39c**, and finally ester **3.39d**. The mixture of *E/Z*-isomers was then irradiated providing the desired phenanthrene **3.40a** in modest yield (45 %) along with a significant amount (16 %) of phenanthrene **3.40b** arising from cyclization with concomitant loss of MeOH.⁴³⁴ Conversion of the ester functionality to the desired 4-methylpentanoyl side chain was accomplished by reduction of the ester to the corresponding primary alcohol, MnO₂ oxidation to the aldehyde, addition of isopentylmagnesium bromide, and Jones oxidation of the resulting secondary alcohol, giving the desired ketone **3.41a** in 56% overall yield from **3.40a**. Finally, oxygen protecting groups were exchanged by demethylation using BBr₃ followed by immediate acetylation of the crude phenol to give diacetate **3.41b**. Oxidation with CrO₃, followed by hydrolysis provided piloquinone (**3.23d**) in 1.4 % overall yield. An analogous sequence was applied to the synthesis of the trimethyl ether of 4-hydroxypiloquinone (**3.23e**).⁴²¹



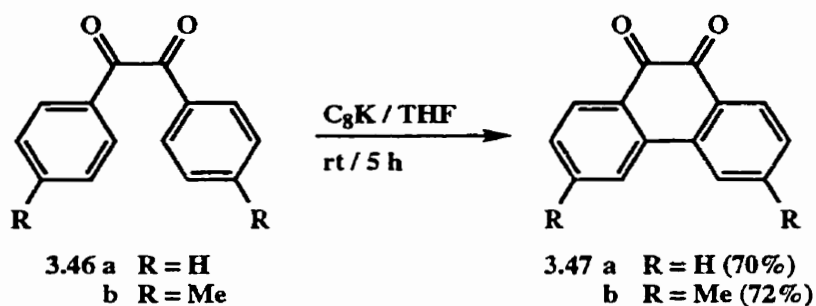
Scheme 3.7

Snieckus and co-workers reported a regioselective cross-coupling / directed remote metalation (DreM) route to 9-phenanthrols, immediate precursors to 9,10-phenanthraquinones.^{172,173} Thus, Suzuki-Miyaura coupling of *ortho*-halotoluene derivatives **3.42** with the benzamide-*ortho*-boronic acids **3.43**, easily derived from DoM on the parent amide and quench with B(OMe)₃, provided good yields of biaryls **3.44** (Scheme 3.8). Addition of LDA to the biaryls at 0 °C, followed by warming to room temperature resulted in smooth conversion to 9-phenanthrols **3.45**, which were subsequently oxidized to the corresponding 9,10-phenanthraquinones.^{70,370,372}



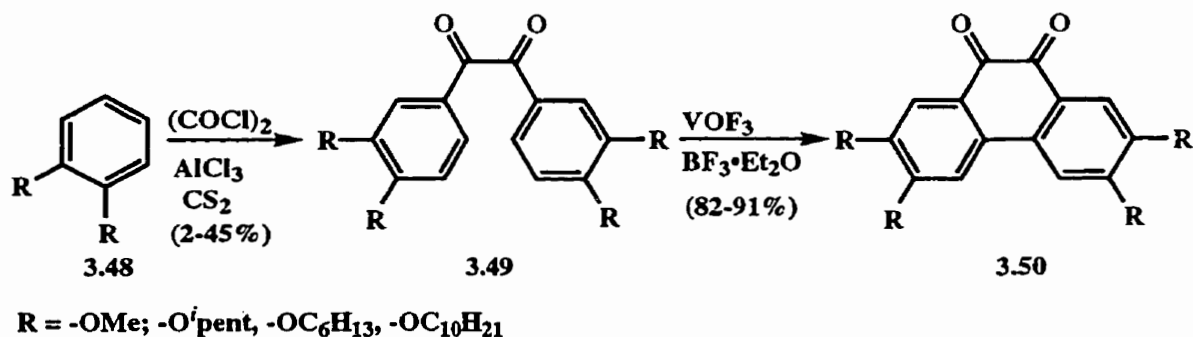
With an aim towards industrial application, Kharlampovich and Morotskii have reported the synthesis of 9,10-phenanthraquinone by aerial oxidation of phenanthrene using a V_2O_5 - K_2SO_4 -silica gel catalyst system.⁴³⁵ Although the method successfully provided the desired quinone product, the reaction is carried out at extremely high temperature in the vapour phase and proceeds in low yield (25-27%). Wenxiang, investigating the use of 9,10-phenanthraquinone as a photosensitizer and fungicide, approached its synthesis by phenanthrene oxidation using alkyl peroxides.⁴³⁶ In this approach, the peroxide (e.g. t BuOOH) was added to a mixture of phenanthrene and a Mo or V catalyst (e.g. $VO(acac)_2$) producing the desired *ortho*-quinone in 90% yield. Other oxidizing agents that have been successfully employed in synthesis of phenanthraquinones include $Pb(OAc)_4$,⁴³⁷ CrO_3 / H_2SO_4 ,⁴³⁸ bis(2,2'-bipyridyl)copper(II) permanganate,⁴³⁹ salcomine,^{70,440} barium permanganate,⁴⁴¹ dihydroxy phenylselenonium benzenesulfonate,⁴⁴² and ceric ammonium nitrate.¹⁷³

Rabinovitz and co-workers have reported a novel application of the graphite-potassium intercalate C_8K to the preparation of substituted 9,10-phenanthraquinones.⁴⁴³ Thus, benzil (**3.46a**) or 3,3'-dimethylbenzil (**3.46b**) was added to a large excess of freshly prepared C_8K in THF and, after evolution of hydrogen, the corresponding phenanthraquinone (**3.47**) was isolated in good yield (Scheme 3.9). Extension of this methodology allows formation of phenanthraquinones from benzoin derivatives or benzoate esters.⁴⁴⁴



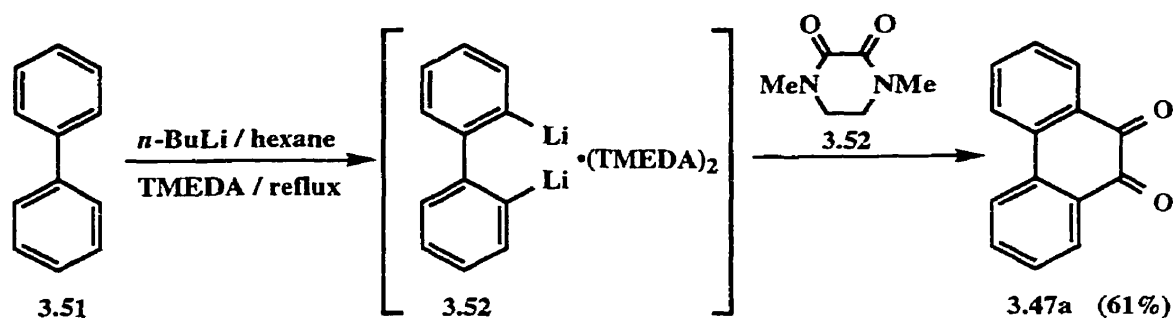
Scheme 3.9

In a similar approach, Wegner and co-workers have prepared a variety of symmetrical 9,10-phenanthraquinones.⁴⁴⁵ After preparation of the symmetrical benzils **3.49** (Scheme 3.10) by double Friedel-Crafts reaction of substrates **3.48** (2 equiv) with oxalyl chloride, intramolecular coupling was accomplished using vanadium (V) oxyfluoride. The desired coupling was also accomplished using thallium (III) oxide, although in considerably lower yield. Interestingly, benzil substrates with a 3,3',4,4'-tetraalkoxy substitution pattern gave excellent yields of the corresponding quinones whereas those with other substitution patterns (e.g. 4,4'-dialkoxy, 2,2',4,4'-tetraalkoxy, and 2,2',5,5'-tetraalkoxy) failed to undergo reaction. It was also observed that the double Friedel-Crafts reaction on 1,2-dimethoxybenzene (**3.48**, R = OMe) gave a very poor yield of the corresponding benzil. The low yield in this case was attributed to the poor solubility of the intermediate Friedel-Crafts complex, a problem which was avoided when long chain or branched alkoxy groups were employed.



Scheme 3.10

9,10-Phenanthraquinone (**3.47a**) has also been prepared by double lithiation of biphenyl (**3.51**) according to the method of Schleyer,^{121,446} followed by quench of the resulting dilithio-bis-TMEDA complex **3.52** with *N,N*-dimethylpiperazine-2,3-dione (**3.53**).⁴⁴⁷ Compound **3.47a** was obtained in modest yield, but the scope of the reaction appears to be limited to a single example.⁴⁴⁸

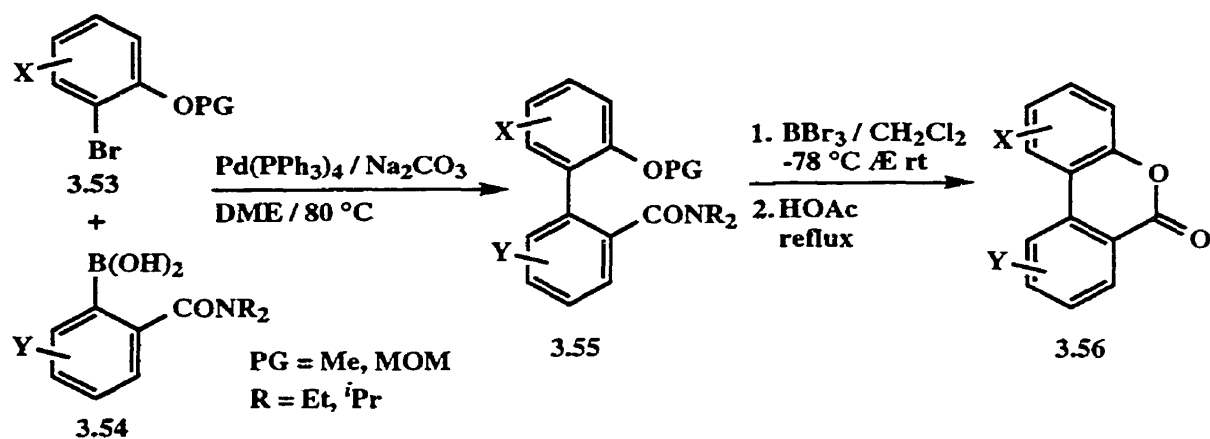


Scheme 3.11

3.3.3 Previous Syntheses of Dibenzo-*[b,d]*pyranones

The powerful combination of DoM and cross-coupling reactions is also been useful for the construction of the dibenzopyranone framework. Cross-coupling of protected (e.g. methyl or methoxymethyl ethers) *ortho*-hydroxyhaloarenes **3.53** with tertiary benzamide-*ortho*boronic acids (**3.54**) provides biaryl substrates **3.55** which, upon deprotection and treatment with acid, easily cyclize to the corresponding dibenzo-*[b,d]*pyranones **3.56** in high yield (Scheme 3.12).^{368,369} The subsequent discovery of the remote anionic Fries rearrangement (Scheme 1.30, Section 1.2.5.2) has allowed for greater diversity of substrates and access to a broader range of dibenzopyranones.¹⁷⁶ James and Snieckus recently reported the use of this strategy in the total synthesis of gilvocarcins.⁷²

The combination of the 9,10-phenanthraquinone ring system and the dibenzopyranone moiety in biruloquinone makes for an interesting and challenging synthetic target. The synthetic challenge lies in incorporating both ring systems in an efficient and practical manner. Several synthetic approaches are known for both ring systems, and application of established methodology to biruloquinone is the focus of the next section.

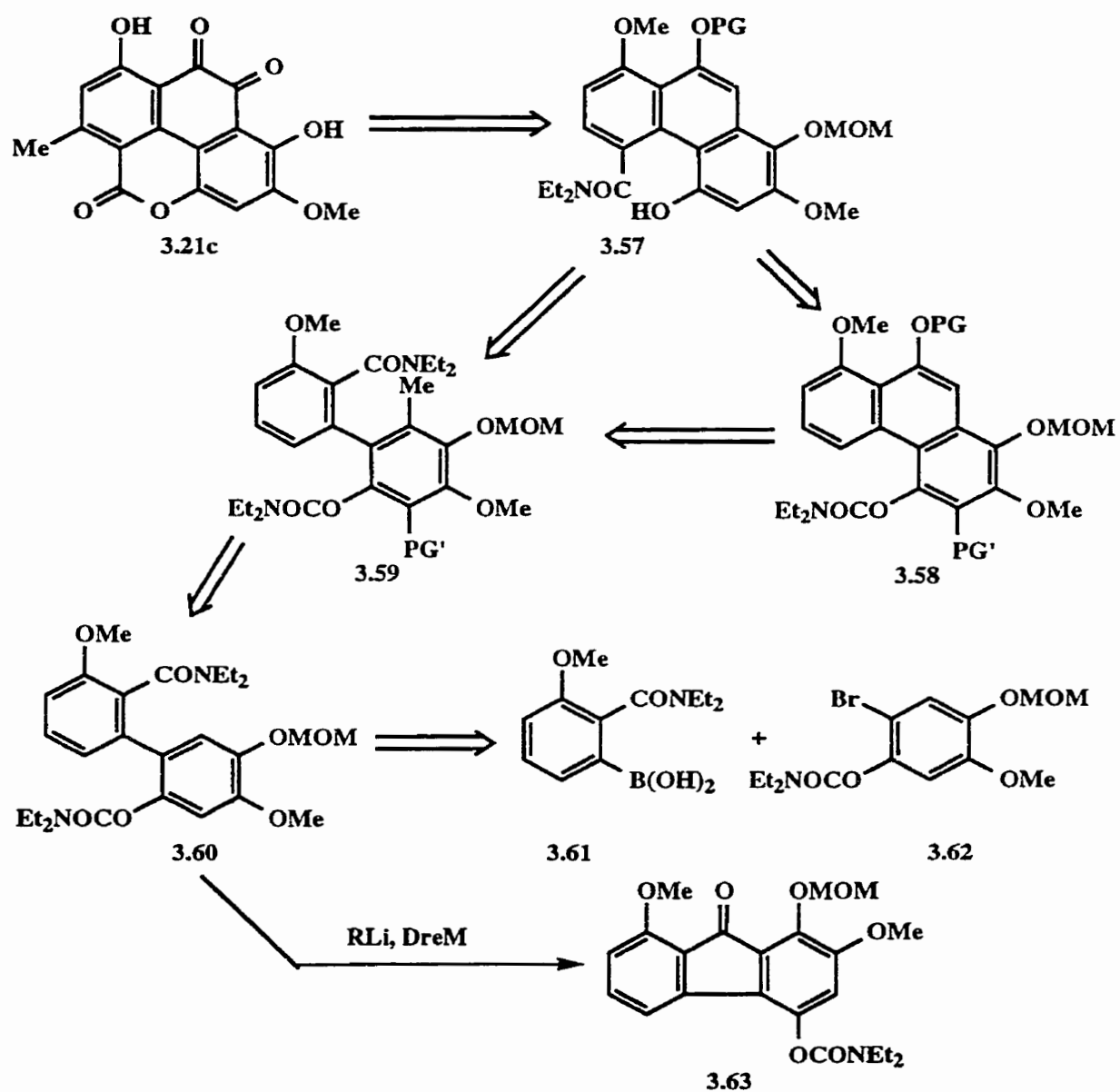


Scheme 3.12

3.4 Synthetic Strategy

A retrosynthetic analysis of the initial approach (Strategy A) towards biruloquinone is shown in Scheme 3.13a. In this strategy, DoM and directed remote metalation (DreM) are proposed in conjunction with cross-coupling to form the key bonds and incorporate the appropriate substituents. The lactone and quinone functionalities in biruloquinone (**3.21c**) are accessible by cyclization and oxidation of the key protected phenanthrol **3.57**. The formation of **3.57** hinges upon successful DreM / carbamoyl migration of the appropriately protected precursor **3.58**. While similar remote anionic Fries rearrangements are well documented,^{72,176} precedent for this system does not exist but could be facilitated by the rigid planar framework. Furthermore, under the strongly basic conditions (LDA) required for formation of phenanthrol **3.58** from highly substituted biaryl **3.59**, carbamoyl migration could also potentially take place allowing direct access to **3.57** in a one-pot reaction. Achieving appropriate substitution in biaryl **3.59**, requires DoM of the biaryl precursor **3.60** containing several DMGs. With five directing groups in the molecule, one is left with the immediate impression that regioselectivity would be difficult, if not impossible, to achieve. Upon closer inspection of **3.60**, however, one may reasonably expect metalation *ortho* to the OCONEt₂ functionality to be the favoured pathway since the carbamate is the most powerful known DMG,^{7,41} especially when compared with the weaker DMGs such as OMe and OMOM

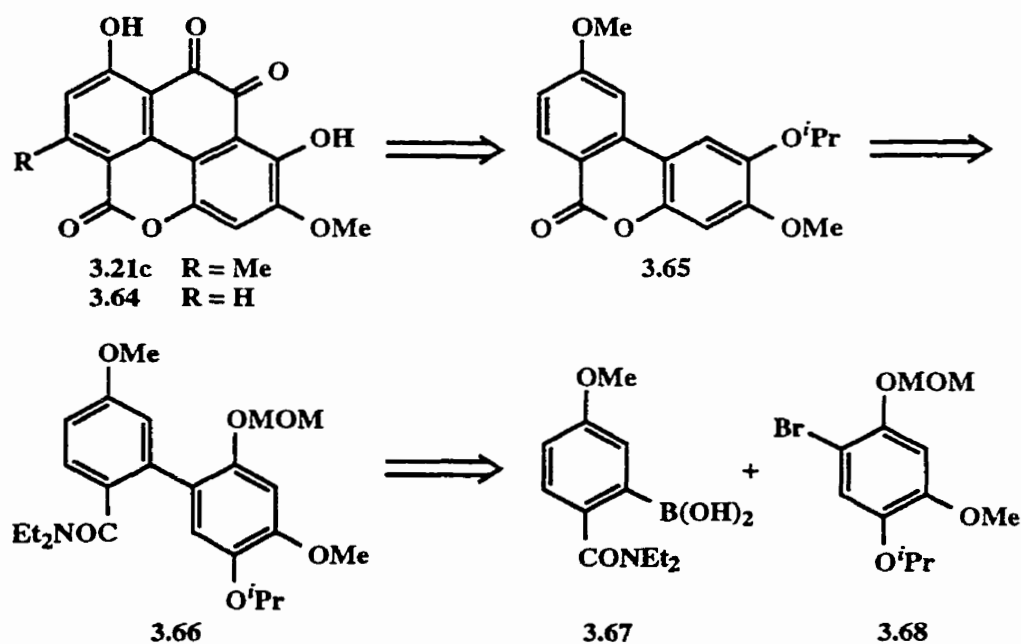
that are present in the molecule. In addition, the presence of the OMe, cooperative to the carbamate DMG, would be expected to further favour the desired metalation site. Likewise, a second DoM reaction for incorporation of the methyl group would be expected to occur regioselectively since the only DMG competing with the OMOM group is the much weaker OMe group. Precursor **3.60** is well suited for synthesis by Suzuki-Miyaura coupling of boronic acid **3.61** and aryl bromide **3.62**. Other than possible regioselectivity problems with



Scheme 3.13 - (Retrosynthetic Strategy A)

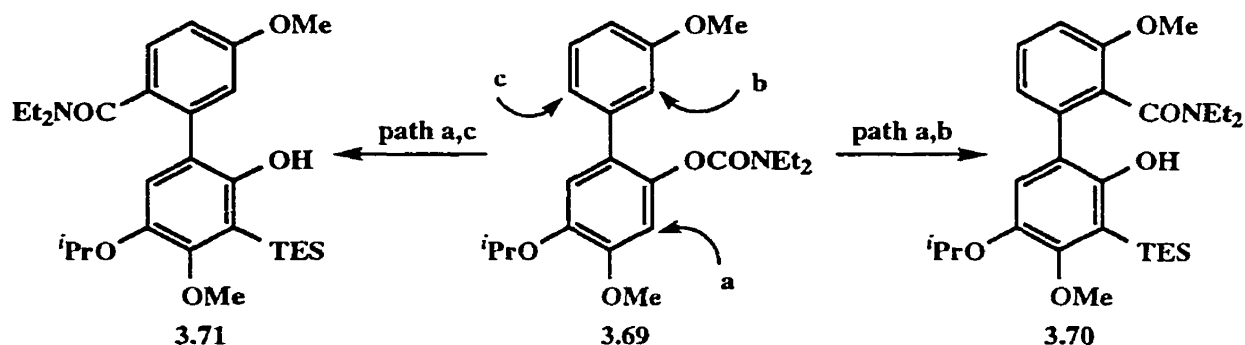
DoM reactions, the only other foreseeable difficulty lies in the possibility of formation of the undesired fluorenone (**3.63**) by a DreM route from **3.60** (Scheme 3.13).^{169,170} Such a reaction is likely avoided by maintaining low temperature throughout the duration of the metalation / electrophile quench sequence.

A second retrosynthetic analysis (Strategy B) of biruloquinone (**3.21c**) revealed an alternative strategy (Scheme 3.14) which could avoid some of the potential pitfalls of the initial approach. As a model system, the demethyl analog of biruloquinone (**3.64**) was considered (see below). The key step in this approach is the incorporation of the quinone portion of the natural product at a late stage in the synthesis. This was envisioned to occur by a double Friedel-Crafts acylation on the pyranone **3.65**. Although such double acylations are rare, both inter-^{449,450} and intramolecular⁴⁵¹⁻⁴⁵⁴ examples have been reported and double acylation of **3.65** is favourable due to the presence of electron donating substituents. The dibenzopyranone **3.65** would be expected to result from deprotection and cyclization of the highly oxygenated biaryl **3.66**,³⁶⁸ an ideal Suzuki-Miyaura cross coupling candidate. With this in mind, cross coupling partners **3.67** and **3.68** became the focus of this approach.



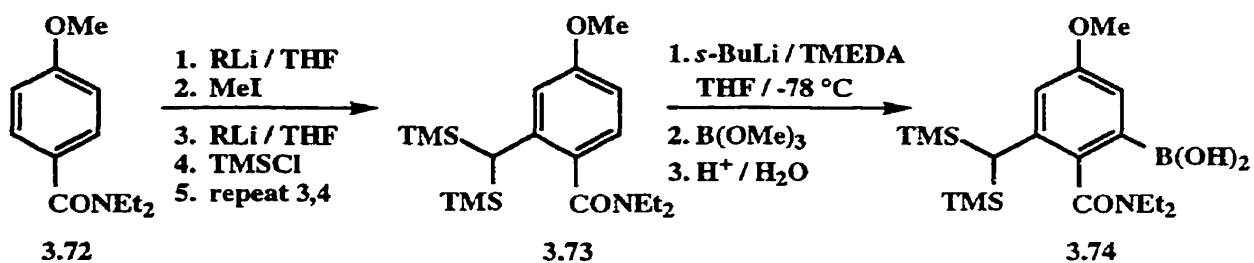
Scheme 3.14 - Retrosynthetic Strategy B

In the above strategy, the ring-to-ring carbamoyl migration approach to the dibenzo-*[b,d]*pyranone is bypassed in favour of direct Suzuki-Miyaura coupling of an amide and protected phenol and thereby avoids potential regioselectivity problems with the migration reaction. The required biaryl (**3.69**), containing the carbamate DMG, is expected to undergo *DoM ortho* to the carbamate (Scheme 3.15, path a), allowing protection with a suitable protecting group (e.g. TES).¹⁷⁶ However, subsequent metalation is preceded to follow path b affording **3.70** rather than the desired path c to give **3.71** based on the cooperative DMG effect exerted by the OMe substituent.¹⁷⁶ By firmly establishing the amide position at an earlier stage, regioselectivity issues during migration are avoided.



Scheme 3.15

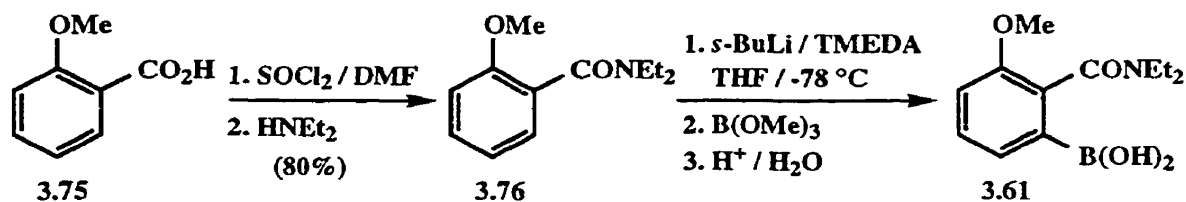
Strategy B provides a good approach to the biruloquinone ring system, but fails to address the methyl group in the 7-position of the natural product. Incorporation of the methyl group is proposed by application of the strategy of Snieckus and Mills for protection of a methyl group *ortho* to an amide (Scheme 3.16).^{455,456} Thus, introduction of the methyl group at an early stage in the synthesis, followed by bis-TMS protection (**3.72** → **3.73**), would be followed by formation of the desired boronic acid **3.74** for cross-coupling. Bis-TMS protected boronic acid **3.74** may then be applied in Strategy B rather than **3.67** (Scheme 3.14) and the protected methyl group may be carried throughout the synthesis. Increased solubility of intermediates may be a possible benefit of this strategy.



Scheme 3.16

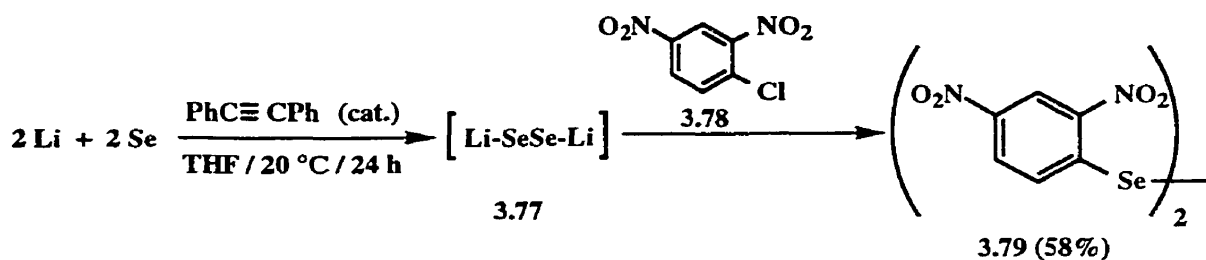
3.5 Results and Discussion

For Strategy A, cross-coupling partners **3.61** and **3.62** (Scheme 3.13) were targeted for synthesis. Thus, **3.61** was prepared in a straightforward manner⁴⁵⁷ by conversion of *ortho*-anisic acid (**3.75**) to the corresponding amide **3.76**, and DoM / borate quench to introduce the boronic acid functionality (Scheme 3.17).



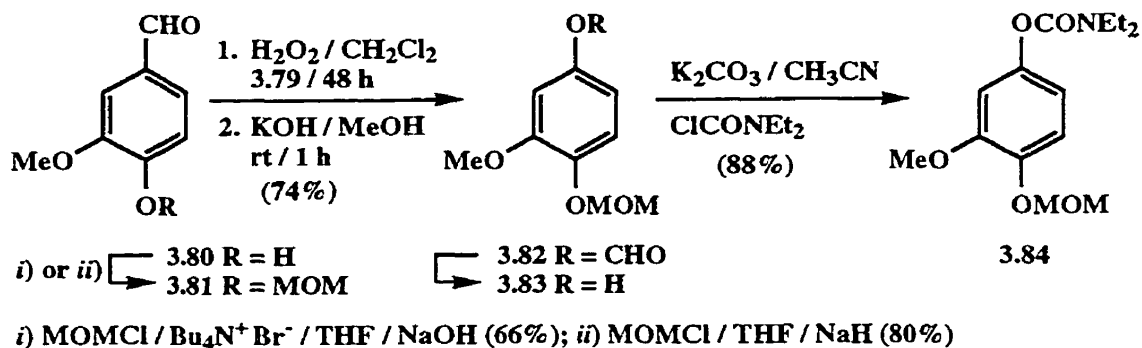
Scheme 3.17

Aryl bromide **3.62** (Scheme 3.13) represents a highly oxygenated system whose synthesis presented a greater challenge. Syper's modified Baeyer-Villiger oxidation for aromatic aldehydes⁴⁵⁸ using hydrogen peroxide and diselenide catalysts seemed to provide an ideal avenue for introduction of the desired oxygen substituents in **3.62** since an appropriate starting material (**3.81**, Scheme 3.19) was readily available and inexpensive. Preparation of the required⁴⁵⁸ diselenide catalyst **3.79** proceeded according to a literature method (Scheme 3.18)⁴⁵⁹ with elemental selenium and elemental lithium combining at room temperature to form the dilithium diselenide species (**3.77**) *in situ*. Reaction with 2,4-dinitrochlorobenzene (**3.78**) produced the required catalyst **3.79** in 58% overall yield.



Scheme 3.18

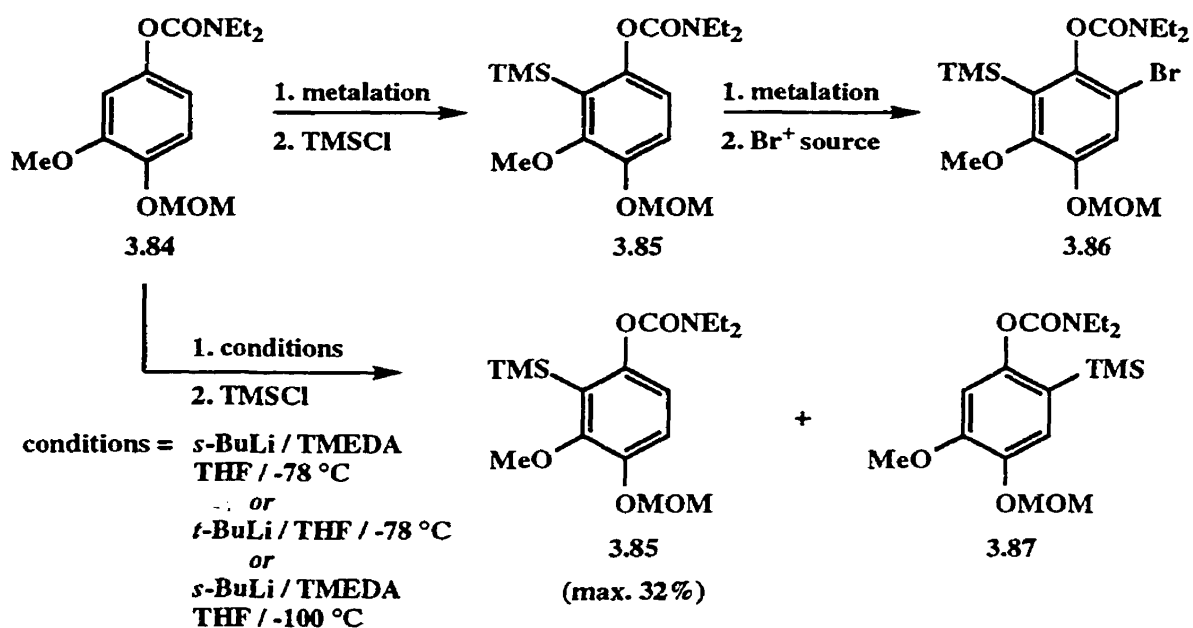
With the required catalyst in hand, vanillin (**3.80**) was treated with chloromethyl methyl ether under phase transfer conditions⁴⁶⁰ to provide MOM ether **3.81** in 66% yield (Scheme 3.19). Alternatively, **3.81** was prepared in 80% yield by addition of vanillin to a mixture of NaH and chloromethyl methyl ether in THF. Oxidation of the resulting ether according to Syper's method proceeded to give formate ester **3.82**, which was hydrolyzed without isolation to give phenol **3.83** in 74% yield. With the intention of using DoM to introduce the bromide substituent for cross-coupling, the resulting phenol was converted to the corresponding *N,N*-diethyl carbamate **3.84** in 88% yield.



Scheme 3.19

Initially it was believed that the powerful directing ability of carbamate DMG in conjunction with the cooperative metalation effect provided by the OMe group in **3.84** would regioselectively direct metalation to the "in-between" position. Quenching of the resulting anion with a suitable electrophile (e.g. TMSCl) would then give tetrasubstituted benzene **3.85**, which could be further metalated to introduce the bromo substituent affording **3.86** (Scheme 3.20). This process would not only give the desired cross-coupling partner, but would put in

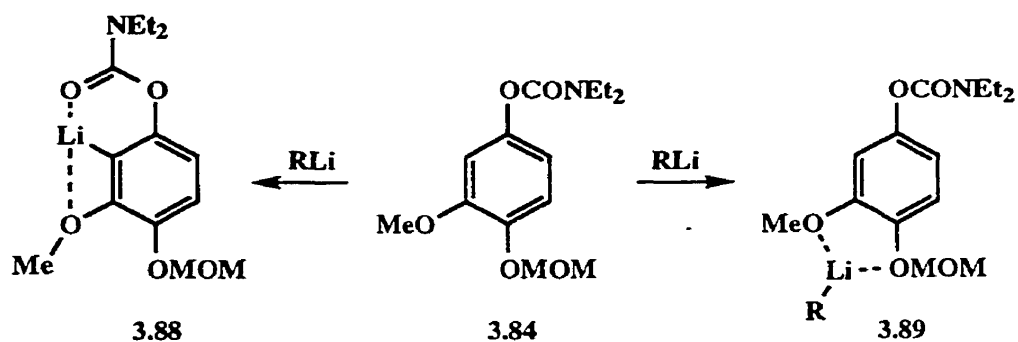
place the necessary protection required further along in the synthesis (PG' in **3.59**, Scheme 3.13), and therefore reduce the possibility of regioselectivity problems at a later stage. In the event, metalation of **3.84** under standard carbamate metalation conditions⁷⁴ showed a surprising lack of regioselectivity, resulting in both the expected product **3.85** (32%) and its isomer **3.87** (< 15%), which was inseparable from starting carbamate **3.84**. Other conditions were attempted (see Experimental Section), but the yield of the desired silyl compound could not be increased and therefore other methods were investigated for the synthesis of the desired cross coupling partner.



Scheme 3.20

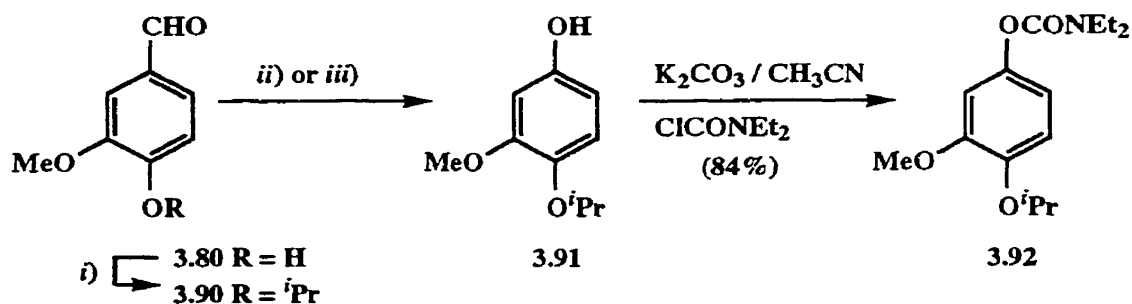
The lack of regioselectivity in the metalation of **3.84** was unexpected since substantial precedent exists for the cooperative metalation between carbamate and methoxy DMGs.^{7,74} Clearly, the presence of the MOM ether is responsible, at least in part, for the unselective metalation. Normally, the OMe substituent would be expected to provide additional coordinative stability of the lithiated intermediate (**3.88**, Scheme 3.21). In substrate **3.84**, the potential exists for coordination of an alkyllithium reagent between the methoxy and OMOM

substituents (**3.89**), thus precluding any additional directing ability which might be expected from the methoxy group (Scheme 3.21).



Scheme 3.21

In an effort to test this hypothesis by reduction of coordination between the oxygen substituents (**3.89**), an analogous set of reactions were performed on **3.92** in which the MOM substituent is replaced by a bulky isopropyl group. Thus, vanillin (**3.80**) was treated with K_2CO_3 and isopropyl iodide to provide ether **3.90** (Scheme 3.22). While Baeyer-Villiger oxidation and alkaline hydrolysis of **3.90** gave a modest yield of phenol **3.91**, a more convenient method⁴⁶¹ involving treatment with acidic hydrogen peroxide in MeOH, provided the desired phenol (**3.91**) in 88% yield. Conversion to the corresponding carbamate was

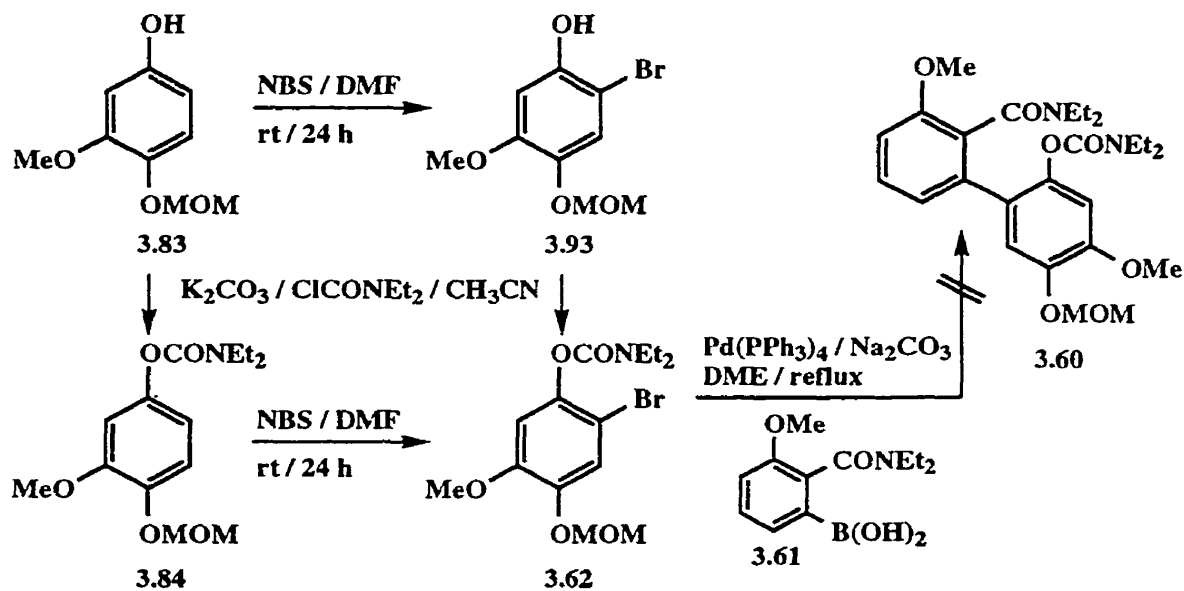


- i) $K_2CO_3 / CH_3CN / CH_3CH(I)CH_3 / \text{reflux} / 10 \text{ h} (89\%)$
 ii) $H_2O_2 / CH_2Cl_2 / 3.79 / 48 \text{ h}$; then $KOH / MeOH / \text{rt} / 1 \text{ h} (65\%)$
 iii) $H_2O_2 / H_2SO_4 / MeOH / \text{rt} / 8 \text{ h} (88\%)$

Scheme 3.22

accomplished as described in Scheme 3.19 affording **3.92** in 84% yield. Unfortunately, metalation of this substrate provided results which were even less encouraging than metalation of **3.84**. Very low yields of products were obtained, and separation from unreacted starting material was not possible.

Still seeking a method for introduction of the bromo substituent for cross-coupling, attention turned to more classical methods. Using Mitchell's method for monobromination of activated aromatics,⁴⁶² electrophilic bromination of phenol **3.83** occurred regioselectively and provided bromophenol **3.93**, which was unstable and was immediately treated with *N,N*-diethyl carbamoyl chloride and K_2CO_3 to give carbamate **3.62** (Scheme 3.23). Alternatively, higher yield could be achieved by electrophilic bromination of carbamate **3.84**, which again proceeded regioselectively to provide bromocarbamate **3.62**. With a suitable cross-coupling

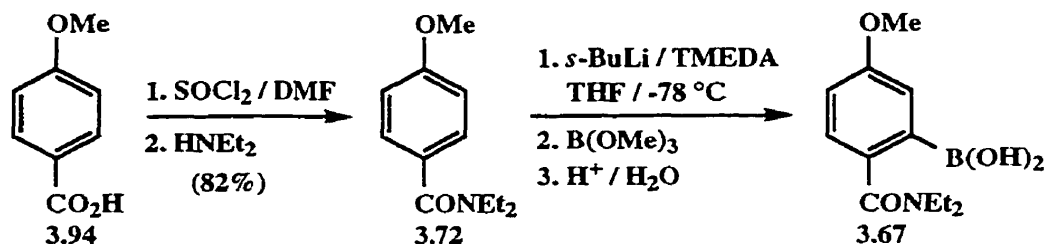


Scheme 3.23

partner now available, **3.62** was treated under modified Suzuki-Miyaura conditions with boronic acid **3.61** in an attempt to prepare the necessary biaryl **3.60**. Surprisingly, the coupling reaction failed resulting in isolation of only small amounts of protodeboronation product (**3.76**, Scheme 3.17), and debrominated carbamate (**3.84**). The synthetic difficulties

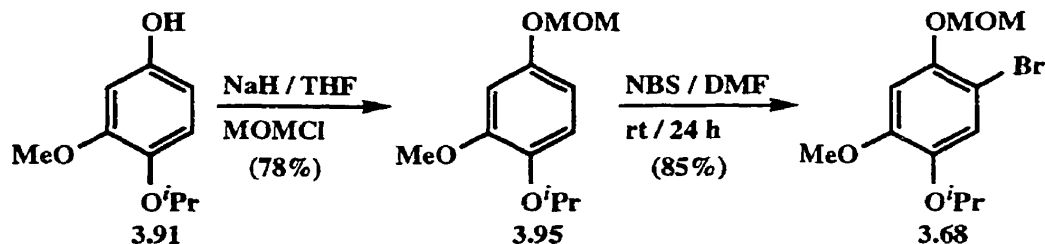
encountered to this stage led us to pursue Strategy B and work began on synthesis of the necessary cross-coupling partners.

Analogous to the preparation of boronic acid **3.61**, *p*-anisic acid (**3.94**) was converted to the corresponding benzamide (**3.72**), and metalation under standard conditions followed by quench with trimethyl borate furnished boronic acid **3.67** required for cross-coupling (Scheme 3.24).



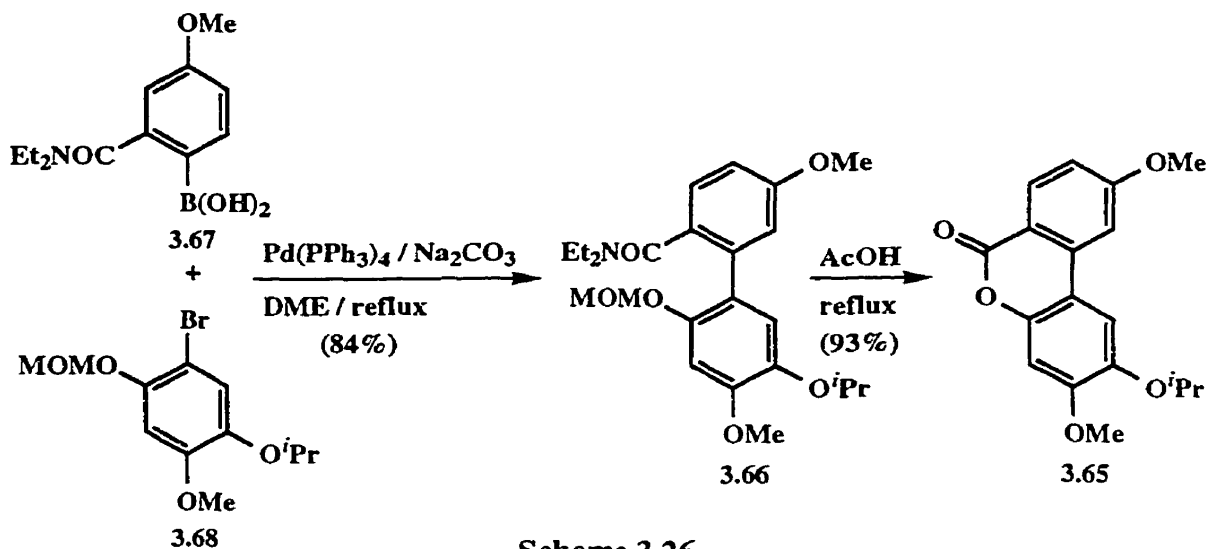
Scheme 3.24

Using knowledge and materials already gained from Strategy A (Scheme 3.22), synthesis of the second cross-coupling partner began with phenol **3.91** (Scheme 3.25). The chosen isopropyl protecting group served two functions in that it allowed a simpler, higher yield oxidation of protected vanillin **3.90** (Scheme 3.22) while providing a means of differentiating the two phenolic oxygens by alternate MOM protection. Accordingly, the hydroxy group was converted to the corresponding MOM ether by treatment with NaH / MOMCl to give **3.95** in good yield. Electrophilic bromination of **3.95** proceeded smoothly as for **3.84** (Scheme 3.23) providing cross coupling partner **3.68**.



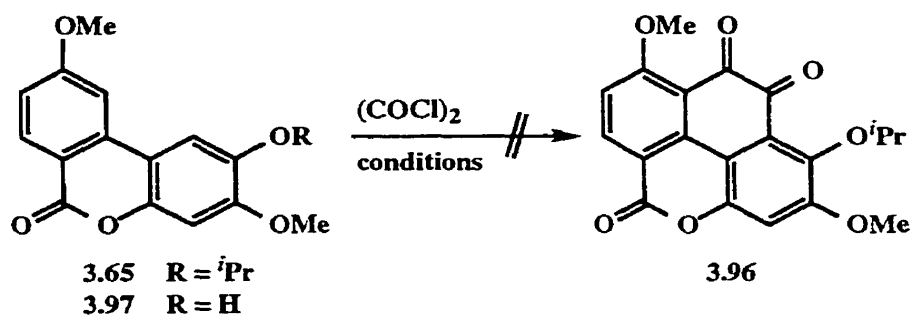
Scheme 3.25

In contrast to the poor cross-coupling results of Strategy A, cross-coupling of partners **3.67** and **3.68** proceeded smoothly under standard conditions providing the highly substituted biaryl **3.66** in 84% yield. The full value of the MOM ether protecting group was then realized since deprotection-cyclization easily occurred in the same pot upon treatment of **3.66** with glacial acetic acid at reflux to give dibenzopyranone **3.65** in excellent yield.



Scheme 3.26

Dibenzopyranone **3.65** lacked the 7-methyl group and the quinone functionality of biruloquinone (**3.21c**). In an effort to convert **3.65** into the quinone, a variety of Friedel-Crafts conditions were employed, using oxalyl chloride as the electrophile (Scheme 3.27). When oxalyl chloride and **3.65** were combined in the presence of AlCl_3 in either CH_2Cl_2 or CH_3NO_2 solvent, only starting material was isolated. Similarly, when $\text{Ti}(\text{O}^i\text{Pr})_4$ was employed as the Lewis acid, no reaction occurred and only starting material was isolated. The use of TiCl_4 as the Lewis acid led to deisopropylation to give phenol **3.97** in 71% yield. While protecting group removal was not the goal of these experiments, it nonetheless provided evidence that manipulation of protecting groups would be possible at a later stage. Further exploration of this pathway is required.



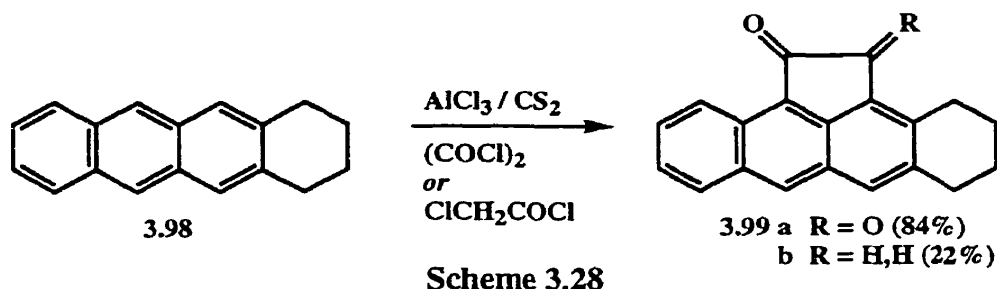
Lewis acid	solvent	temp. (°C)	product
AlCl ₃	CH ₂ Cl ₂	40	SM
AlCl ₃	CH ₃ NO ₂	100	SM
Ti(O ^{<i>i</i>} Pr) ₄	CH ₃ NO ₂	100	SM
TiCl ₄	CH ₃ NO ₂	100	3.97

Scheme 3.27

Both of the synthetic strategies presented have shown some promise towards the total synthesis of biruloquinone (3.21c). Strategy B appears to be more promising at this stage since the dibenzopyranone moiety has been successfully constructed and problems with regioselectivity have been avoided.

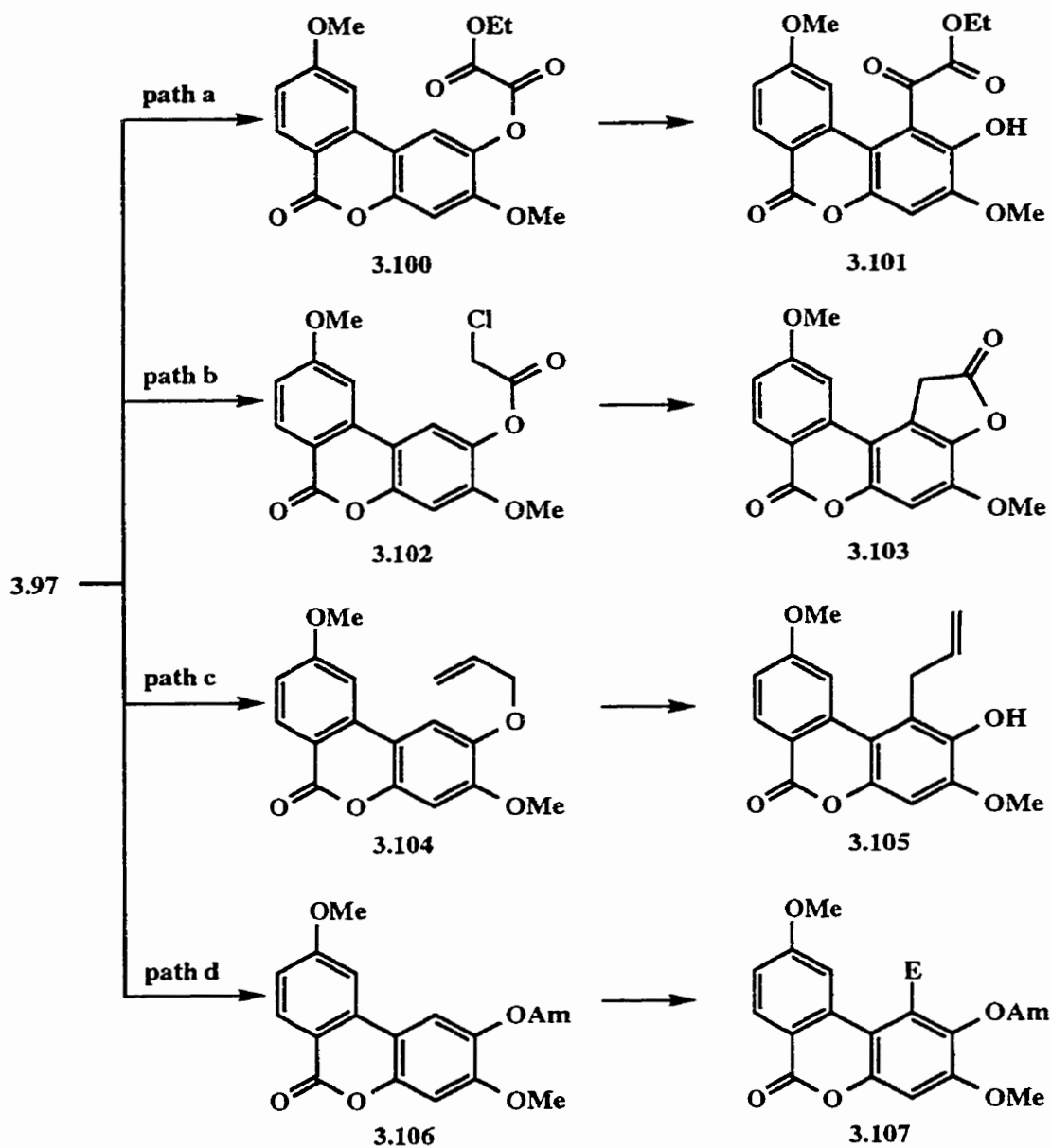
3.6 Future Work

Continuing work on biruloquinone should focus on Strategy B and incorporation of the C₂ unit for the quinone functionality. Although initial results of Friedel-Crafts incorporation of oxalyl chloride were not encouraging, a wider range of Lewis acids and solvents should be tested. Sangaiah and Gold have reported a double Friedel-Crafts reaction of oxalyl chloride on 1,2,3,4-tetrahydronaphthacene 3.98, using AlCl₃ catalyst and CS₂ as the solvent to give diketone 3.99a in high yield (84%).⁴⁵⁴ Similarly, chloroacetyl chloride underwent the same reaction to give ketone 3.99b, though in substantially lower yield (Scheme 3.28). Though not an ideal model, this system provides evidence that a double acylation is possible. The use of chloroacetyl chloride may be advantageous since the present system is clearly more sterically demanding than Gold's example.



If the attempted acylation (**3.65** → **3.96**) is unsuccessful, attention should be turned to introduction of the C₂ unit by other methods. Hydroxypyranone **3.97** (Scheme 3.27) may prove to be a valuable intermediate towards achieving this goal. Esterification with ethyl oxalyl chloride would provide oxalate ester **3.100** (Scheme 3.29, path a), having the potential to undergo an *ortho*-Fries rearrangement providing α -ketoester **3.101**. Although little precedent exists for such rearrangements of oxalates, methyl aryl oxalates have been shown to provide *o*-hydroxyglyoxylates in a photo-Fries rearrangement.⁴⁶³ Attempts at Lewis acid catalyzed rearrangements of the same substrates led to phenols as a result of ester cleavage. Alternatively, condensation with chloroacetyl chloride would lead to ester **3.102**. Intramolecular Friedel-Crafts alkylation would lead to benzofuranone **3.103**, forming one of the requisite carbon-carbon bonds necessary for introduction of the quinone moiety. In a different approach, allyl ether **3.104** could be prepared and subjected to Claisen rearrangement to give allyl phenol **3.105** and again introduce the first of the two necessary carbon-carbon bonds. Ozonolysis of the resulting double bond would leave the necessary C₂ unit in place with only one more bond to form. Finally, carbamate **3.106** could be used in a *D*_oM process incorporating a suitable carbon electrophile to give **3.107**. As in previous examples, the carbamate functionality is expected to be the dominant DMG, and with only one *ortho* site available regioselectivity problems should be avoided. Of course metalation would have to be performed with LDA in order to avoid irreversible addition of an alkyllithium reagent to the dibenzopyranone carbonyl. Each of these four derivatives offers potential for introduction of the quinone moiety. After successful introduction of the quinone, deprotection would provide 7-demethylbiruloquinone. Using the bis-TMS-methyl protected benzamide (**3.74**, Scheme

3.16) in an analogous series of reactions would lead to a total synthesis of biruloquinone (3.21c).



Scheme 3.29

4.0 Experimental Section

¹H-NMR spectra were recorded on Bruker AMX-500, AC-300, AM-250 and AC-200 spectrometers using tetramethylsilane (TMS) as the internal standard. Chemical shifts are reported in parts per million (ppm) relative to TMS. When peak multiplicities are given for NMR spectra, the following abbreviations are used: s, singlet; d, doublet; t, triplet; q, quartet; sp, septet; sx, sextet; dd, doublet of a doublet; dt, doublet of a triplet; ddd, doublet of a doublet of a doublet; m, multiplet; b, broad; bs, broad singlet. ¹³C-NMR spectra were proton decoupled and recorded on Bruker AMX-500, AC-300, AM-250 and AC-200 spectrometers using the carbon signal of the deuterated solvent as the internal standard. ³¹P-NMR spectra were recorded on Bruker AMX-500 and AC-200 spectrometers using phosphoric acid as an external standard. IR spectra were recorded on a BOMEM MB-100 infrared spectrophotometer as KBr disc or liquid film. Electron impact (EI) and chemical ionization (CI) mass spectra were performed on Kratos MS890 and Hewlett-Packard 5890 Series II/5971A MSD instruments. Elemental analyses were performed by M-H-W Laboratories, Phoenix, AZ, U.S.A. Melting points are not corrected and were recorded on a BÜCHI SMP-20. Optical rotations were measured on a Perkin-Elmer 241 Polarimeter. Analytical HPLC was performed on a Waters 600E / 486 unit and the wavelength detector was operated at 254 nm. Chiral HPLC analyses were performed using CHIRALCEL OD, CHIRALCEL OK and CHIRALCEL OJ columns at room temperature unless stated otherwise. Enantiomeric purity assays using chiral HPLC columns were completed with both racemic and enantioenriched materials and repeated at least once in order to ensure reproducibility of the method used. Flash chromatography was performed with silica gel (230-400 mesh, 60 Å) obtained from VWR, Toronto. Analytical thin layer chromatography was performed on Macherey-Nagel Alugram SIL G/UV₂₅₄ aluminium-backed plates and the visualization was accomplished by UV lamp. All reported yields are isolated yields unless specified otherwise.

All solvents were used without further purification unless otherwise indicated. Diethyl ether (Et₂O), *tert*-butyl methyl ether (*t*-BuOMe), and tetrahydrofuran (THF) were distilled from

sodium/benzophenone under a nitrogen atmosphere. Dichloromethane, ethyl acetate (EtOAc) and hexanes used for flash chromatography were distilled from bulk solvent. TMEDA and (-)-sparteine were distilled from CaH₂ under nitrogen atmosphere and stored under argon. Solutions of *n*-BuLi in hexanes and *s*-BuLi in cyclohexane were obtained from FMC Corporation or Aldrich Chemical Co. and titrated periodically according to the method of Watson and Eastham.⁴⁶⁴ Cooling baths were prepared as follows: -78 °C, CO₂ / acetone; -40 °C, CH₃CN / liquid N₂; -15 °C, ice / water / NaCl; 0 °C, ice / water slush.

General Procedures

General Procedure A, lithiation of *N,N*-diisopropyl ferrocenecarboxamide (1.158b) with *n*-BuLi / (-)-sparteine to form 1,2-disubstituted ferrocenes:

Under an inert atmosphere, *n*-BuLi was added to a stirred solution of (-)-sparteine in anhydrous Et₂O at -78 °C and stirring was continued for 15 min at -78 °C. A solution of 1.158b in anhydrous Et₂O was added dropwise *via* cannula and the resulting red suspension was stirred for 1 h at -78 °C. The electrophile (neat or as a solution in anhydrous solvent) was added and the resulting mixture was stirred for 30 min at -78 °C and then allowed to warm to room temperature. The reaction mixture was quenched with saturated NH₄Cl solution and the organic layer was separated. The aqueous phase was extracted three times with Et₂O, and the combined organic extract was washed with H₂O and brine, dried over anhydrous Na₂SO₄ or MgSO₄, filtered and concentrated *in vacuo* to provide the crude product. The molar ratios of reagents and quantities of solvents are specified for each individual procedure. (-)-Sparteine may be recovered by basification of the aqueous extract with 2N NaOH, followed by extraction with Et₂O, separation of the organic layer, drying (anhydrous MgSO₄), concentration and distillation from CaH₂ of the resulting residue.

General Procedure B, lithiation of di-*tert*-butylferrocenylphosphine oxide (1.168) to form 1,2-disubstituted ferrocenes: Under an inert atmosphere, *t*-BuLi was added dropwise to a stirred solution of di-*tert*-butylferrocenylphosphine oxide (1.168) in Et₂O or THF at -78 °C and stirring of the resulting red suspension was continued for 60 min at -78 °C. The electrophile (neat or as a solution in anhydrous THF or Et₂O) was added and the resulting mixture was stirred for 30 min at -78 °C and then allowed to warm to room temperature. The reaction mixture was quenched with saturated NH₄Cl solution and the organic layer was separated. The aqueous phase was extracted three times with Et₂O, and the combined organic extract was washed with H₂O and brine, dried over anhydrous Na₂SO₄ or MgSO₄, filtered and concentrated *in vacuo* to provide the crude product. Molar ratios of reagents and quantities of solvents are specified for each individual procedure.

General Procedure C, preparation of aryldi-*tert*-butylphosphine oxides from aryl halides: In a modification of a literature procedure,⁹⁵ the appropriate aryl halide was dissolved in anhydrous Et₂O, cooled to -78 °C under an inert atmosphere, and treated with *n*-BuLi or *t*-BuLi. In a separate flask, fitted with a reflux condenser, a solution of chloro-di-*tert*-butylphosphine in Et₂O was cooled to 0 °C under an inert atmosphere. After stirring for 20 minutes, the solution of newly formed aryllithium was added to the solution of phosphine *via* cannula. An extra portion of anhydrous ether was used to rinse any remaining aryllithium into the phosphine solution. The mixture was allowed to warm to room temperature and was then heated to reflux for 2-3 h. Upon cooling to room temperature, a small portion of methanol was added to quench any remaining organolithium. Most of the Et₂O was removed under reduced pressure before adding the remainder of the methanol. The resulting suspended residue was cooled to 0 °C and 30% H₂O₂ was added dropwise. Stirring was continued for 1 h, after which Na₂SO₃ (2 M, aqueous) and HCl (10%, aqueous) were added consecutively with 1 h of stirring at each step. Most of the methanol was removed under reduced pressure, the resulting mixture was extracted with three portions of CH₂Cl₂, and the combined organic

extracts were dried (Na_2SO_4 or MgSO_4) and evaporated under reduced pressure to provide the desired arylphosphine oxide. Molar ratios of reagents and quantities of solvents are specified for individual procedures.

General Procedure D, metalation / quench of di-*tert*-butylphenylphosphine oxide (1.170) to form 1,2-disubstituted benzenes: Under an inert atmosphere, *t*-BuLi was added dropwise to a stirred solution of di-*tert*-butylphenylphosphine oxide (1.170) in THF at $-78\text{ }^\circ\text{C}$ and stirring of the resulting brilliant yellow suspension was continued for 120 min at $-78\text{ }^\circ\text{C}$. The electrophile (neat or as a solution in anhydrous solvent) was added and the resulting mixture was stirred for 30 min at $-78\text{ }^\circ\text{C}$ and then allowed to warm to room temperature over 2 h. The reaction mixture was quenched with saturated NH_4Cl solution and the organic layer was separated. The aqueous phase was extracted with three portions of CH_2Cl_2 , and the combined organic extract was washed with H_2O , dried over anhydrous Na_2SO_4 or MgSO_4 , filtered and concentrated *in vacuo* to provide the crude product. The molar ratios of reagents and quantities of solvents are specified for each individual procedure.

General Procedure E, intermolecular competition experiments [$\text{PhPO}'\text{Bu}_2$ (1.170) vs. PhDMG (1.178, DMG = OCONe_2 , CONe_2 , OMe)]: Under an inert atmosphere, one equivalent of *t*-BuLi was added dropwise to a stirred solution of di-*tert*-butylphenylphosphine oxide (1.170) and an equimolar amount of appropriate substrate 1.178 in anhydrous THF at $-78\text{ }^\circ\text{C}$. The resulting solution was stirred for the specified length of time at $-78\text{ }^\circ\text{C}$, after which a slight excess of TMSCl was added in one portion. The resulting mixture was stirred and allowed to warm slowly over several hours. Undecane (60 μL) was added to the reaction mixture as an internal standard for GC analysis of product ratios. The reaction mixture was quenched with saturated NH_4Cl solution and the organic layer was separated. The aqueous phase was extracted with three portions of CH_2Cl_2 , and the combined

organic extracts were washed with H₂O and dried over anhydrous Na₂SO₄ or MgSO₄. A representative sample of the extracted mixture was filtered analyzed by GC.

General Procedure F, preparation of *N,N*-diethyl *O*-arylcabamates from corresponding phenols: To a stirred solution of the appropriate phenol in CH₃CN (approximately 0.1 M - 1.0 M) at room temperature was added a slight excess of K₂CO₃. A mechanical stirrer was required for large scale preparations in order to stir the resulting thick slurry. Freshly distilled ClCONEt₂ was added and the reaction mixture was heated at reflux for the specified period of time or until no starting material remained by TLC. After cooling, the reaction mixture was poured into water and extracted with CH₂Cl₂ or EtOAc. The organic extracts were washed with H₂O, dried over anhydrous Na₂SO₄ or MgSO₄, filtered and concentrated *in vacuo* to provide the crude product. The molar ratios of reagents and quantities of solvents are specified for each individual procedure.

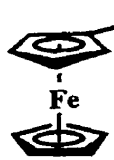
General Procedure G, preparation of *N,N*-diethyl benzamides from corresponding benzoic acids: According to a literature procedure,⁴⁵⁷ the appropriate benzoic acid was placed in a flask and to it was added a large excess of SOCl₂ and a catalytic amount of DMF resulting in rapid effervescence. Stirring was continued until no further evolution of gas was observed, and then approximately half of the SOCl₂ was removed under reduced pressure. An equivalent volume of toluene was added and the mixture of solvents was removed under reduced pressure leaving an oily residue. The addition of toluene and removal under reduced pressure was repeated two more times to remove as much of the SOCl₂ as possible, and the final residue was dissolved in THF and cooled to 0 °C. Addition of excess HNEt₂ with rapid stirring resulted in the formation of a copious white precipitate and evolution of heat. After cooling, the reaction mixture was poured into water and extracted with CH₂Cl₂ or EtOAc. The organic extracts were washed with H₂O, dried over anhydrous Na₂SO₄ or

MgSO₄, filtered and concentrated *in vacuo* to provide the crude product. The molar ratios of reagents and quantities of solvents are specified for each individual procedure.

General Procedure H, intramolecular competition experiments for 4-DMG-di-*tert*-butylphenylphosphine oxide (1.183, DMG = OCONEt₂, CONEt₂, OMe):

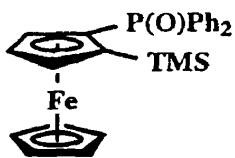
Under an inert atmosphere, a solution of appropriate substrate (1.183) in anhydrous THF at -78 °C was treated with one equivalent of *t*-BuLi and allowed to stir for the specified length of time before a slight excess of TMSCl was added. The mixture was allowed to slowly warm to room temperature before being quenched with saturated NH₄Cl solution. After separating the organic layer and extracting the aqueous layer with three portions of CH₂Cl₂, the combined organic extracts were washed with H₂O and dried over anhydrous Na₂SO₄ or MgSO₄. Product mixtures were separated and analyzed in order to determine regioselectivity of the metalation reaction.

General Procedure I, metalation / quench of *N*-di-*tert*-butylphosphinylindole to form 7-substituted indoles: Under an inert atmosphere, a solution of *N*-di-*tert*-butylphosphinylindole (2.83) in anhydrous THF was cooled to -40 °C (CH₃CN / N₂) and treated by dropwise addition of *n*-BuLi. Stirring was continued for 2 h while maintaining the temperature between -45 °C and -35 °C. The electrophile (neat or as a solution in anhydrous solvent) was added and the resulting mixture was stirred for 30 min at -40 °C and then allowed to warm to room temperature over 2 h. After warming to room temperature, NH₄Cl was added and the mixture was extracted with three portions of CH₂Cl₂. The combined organic layers were washed with H₂O, dried over Na₂SO₄ or MgSO₄, filtered, and concentrated *in vacuo* to provide the crude product. The molar ratios of reagents and quantities of solvents are specified for each individual procedure.



P(O)Ph₂ Diphenylferrocenylphosphine oxide (1.16): According to the method of Kagan,¹⁹³ a solution of tri-*n*-butylstannylferrocene (**1.99**, 475 mg, 1.0 mmol) in anhydrous THF (10 mL) was cooled to -78 °C (dry ice /

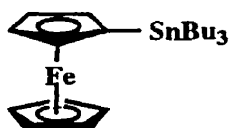
acetone) and treated dropwise with a solution of *n*-BuLi in hexane (1.82 M, 0.60 mL, 1.1 mmol). After 15 min the resulting red / orange suspension was treated with diphenylphosphinyl chloride (260 mg, 1.1 mmol) and stirred for a further 10 min at -78 °C. The solution was allowed to warm to room temperature and stirred for 1 h. The mixture was treated with water (10 mL), and extracted with CH₂Cl₂ (3 x 10 mL). The combined organics were dried (Na₂SO₄) and evaporated to yield an orange solid. Purification by flash chromatography (CH₂Cl₂, then 3% MeOH / CH₂Cl₂) yielded the title compound as an orange solid (342 mg, 88 %): m.p. 163-164 °C (dec.); ¹H-NMR (500 MHz, CDCl₃) δ 4.2 (s, 5H), 4.4 (d, J = 1.4 Hz, 2H), 4.5 (d, J = 1.4 Hz, 2H), 7.4-7.5 (m, 2H), 7.5 (t, J = 7.0 Hz, 1H), 7.7 (m, 2H); ¹³C-NMR (62.9 MHz, CDCl₃) δ 69.6, 71.5 (d, J = 10.2 Hz), 72.3 (d, J = 13.6 Hz), 72.9 (d, J = 117.2 Hz), 128.1 (d, J = 11.9 Hz), 131.3, 131.5, 134.4 (d, J = 106.0 Hz); ³¹P-NMR (81.0 MHz, CDCl₃) δ 29.2; IR (KBr) ν_{max} 3078, 1434, 1202, 1166, 1118, 1105, 1026, 821 cm⁻¹; EI MS *m/z* (rel. intensity) 386 (M⁺, 100), 321 (67), 243 (3), 197 (7), 141 (9), 121 (4), 115 (6); Anal. calcd for C₂₂H₁₉FeOP: C, 68.42; H, 4.96; P, 8.02. found: C, 68.61; H, 4.97; P, 7.93.



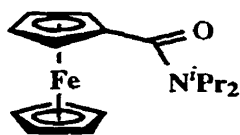
Diphenyl-(2-trimethylsilylferrocenyl)phosphine oxide (1.17): Diphenylferrocenylphosphine oxide (**1.16**, 386 mg, 1.0 mmol) was dissolved in anhydrous THF or toluene (5 mL, see Scheme

1.54). In a separate flask, TMEDA (0.17 mL, 1.1 mmol) or (-)-sparteine (0.26 mL, 1.1 mmol) was dissolved in anhydrous THF or toluene (2 mL) and cooled to -78 °C. To the amine solution was added *s*-BuLi (1.40 M, 0.79 mL, 1.1 mmol) dropwise, and stirring was continued at -78 °C for 15 min. The phosphine oxide solution was then added dropwise over 2 min and the resulting deep orange solution was stirred at -78 °C for 1h. TMSCl (0.19 mL, 1.5

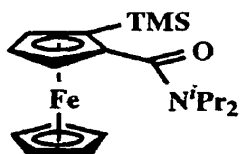
mmol) was added dropwise, and the solution was allowed to warm to room temperature. After 1 h at room temperature, water (3 mL) was added and the mixture was extracted with CH₂Cl₂ (3 x 10 mL). The combined organics were dried (Na₂SO₄) and evaporated to yield an orange solid. Purification by flash chromatography (1% MeOH / CH₂Cl₂) afforded **1.17** (197-202 mg, 43-44%) and recovered starting material (139-147 mg, 36-38%): m.p. 142.5-144 °C; ¹H-NMR (250 MHz, CDCl₃) δ 0.2 (s, 9H), 4.0 (s, 1H), 4.2 (s, 5H), 4.5-4.5 (m, 2H), 7.4-7.6 (m, 8H), 7.8-7.7 (m, 2H); ¹³C-NMR (62.5 MHz, CDCl₃) δ 0.7, 72.6 (d, J = 10.5 Hz), 76.7 (d, J = 11.4 Hz), 78.7, 79.0, 127.9 (d, J = 3.9 Hz), 128.0 (d, J = 7.9 Hz), 131.2, 131.5 (d, J = 9.6 Hz), 131.7 (d, J = 9.7 Hz), 134.5 (d, J = 104.6 Hz), 135.5 (d, J = 104.2 Hz); ³¹P-NMR (81 MHz, CDCl₃) δ 29.0 (s); IR (KBr) ν_{max} 1438, 1247, 1203, 1174, 1119, 1107, 837 cm⁻¹; EI MS *m/z* (rel. intensity) 458 (26), 443 (100), 393 (9), 385 (5), 377 (9), 321 (5); Anal. calcd for C₂₅H₂₇FeOPSi: C, 65.51; H, 5.94. found: C, 65.33; H, 5.75.



(Tri-*n*-butylstannyl)ferrocene (1.99): According to the method of Kagan,¹⁹³ a solution of ferrocene (9.30 g, 50 mmol) in anhydrous THF (25 mL) and hexane (25 mL) was stirred for 30 min at room temperature, then cooled to 0 °C. A solution of *t*-BuLi in pentane (1.64 M, 61.0 mL, 100 mmol) was added dropwise over 30 min, and the mixture was stirred for a further 30 min at 0 °C before tributyltin chloride (20.3 mL, 75 mmol) was added dropwise over 20 min. After 45 min of stirring, the reaction was quenched with aqueous NaOH (2 M, 50 mL). The mixture was extracted with Et₂O (3 x 100 mL), and the combined organic layers were washed with water (100 mL), brine (100 mL), dried (Na₂SO₄), and evaporated to yield a dark orange oil. Distillation under reduced pressure provided the title compound as a dark orange oil (17.88 g, 75%): b.p. 150-152 °C (0.02 mm Hg), [lit.¹⁹³ 140 °C (0.05 mm Hg)]; ¹H-NMR (250 MHz, CDCl₃) δ 0.8-1.1 (m, 15H), 1.4 (dt, J = 7.3 Hz and 7.3 Hz, 6H), 1.5-1.7 (m, 6H), 4.0 (t, J = 1.6 Hz, 2H), 4.1 (s, 5H), 4.3 (t, J = 1.6 Hz, 2H); ¹³C-NMR (62.5 MHz, CDCl₃) δ 10.3, 13.7, 27.4, 29.2, 67.9, 68.7, 70.2, 74.3.

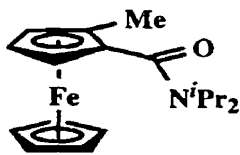


***N,N*-Diisopropyl ferrocenecarboxamide (1.158b)**: To a stirred solution of ferrocenecarboxylic acid (7.95 g, 34.6 mmol) in anhydrous toluene (50 mL) under an argon atmosphere was added oxalyl chloride (6.04 mL, 69.2 mmol) and *N,N*-dimethylformamide (0.50 mL, 6.5 mmol) at room temperature. After stirring at room temperature for 2 h, excess oxalyl chloride was removed *in vacuo*, Et₂O (200 mL) was added, and the solution was cooled to 0 °C. Anhydrous diisopropylamine (13.60 mL, 97.0 mmol) was added and the mixture was stirred at room temperature overnight. The reaction mixture was treated with saturated NH₄Cl solution and extracted with Et₂O (2 x 150 mL). The combined organic extracts were washed with H₂O (2 x 200 mL) and brine (200 mL), dried over anhydrous MgSO₄, and evaporated to give an orange solid. Purification by flash chromatography (9/1 hexane/ethyl acetate), followed by recrystallization (hexane) provided 8.03 g (74%) of **1.158b** as orange needles: m.p. 88-91 °C (hexane); ¹H-NMR (250 MHz, CDCl₃) δ 1.10-1.50 (bs, 12H), 3.15-3.65 (bs, 2H), 4.21 (s, 5H), 4.25 (m, 2H), 4.54 (m, 2H); ¹³C-NMR (62.5 MHz, CDCl₃) δ 21.0, 46.7 (b), 48.9 (b), 68.7, 69.5, 69.8, 81.2, 169.2; IR ν_{max}(KBr) 2977, 2944, 1624, 1461, 1371, 1318, 1034, 814 cm⁻¹; EI MS *m/z* (rel. intensity) 313 (M⁺, 98), 213 (100), 186 (38), 121 (26), 56 (9); HRMS calcd for C₁₇H₂₃FeNO: 313.1129; found: 313.1120; Anal. calcd for C₁₇H₂₃FeNO: C, 65.19; H, 7.40; N, 4.47; found: C, 65.32; H, 7.55; N, 4.50.



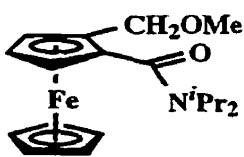
***N,N*-Diisopropyl 2-trimethylsilylferrocenecarboxamide (1.159a)**: According to General Procedure A, a solution of *N,N*-diisopropyl ferrocenecarboxamide (**1.158b**, 313 mg, 1.00 mmol) in Et₂O (2 mL) was added to a mixture of *n*-BuLi (0.73 mL, 1.2 mmol, 1.65 M solution) and (-)-sparteine (0.27 mL, 1.2 mmol) in Et₂O (10 mL). After addition of TMSCl (0.25 mL, 2.0 mmol), the mixture was worked up and purified by flash chromatography (9/1 hexane/Et₂O) to give **1.159a** (370 mg, 96%) as an orange solid (98% ee, determined by HPLC using a

CHIRALCEL OD column at 40 °C with 1.5% *t*-BuOMe in hexane as the mobile phase at a flow rate of 1.5 mL/min): m.p. 102-104 °C; $[\alpha]_D^{25} = +20.2$ (CHCl₃, c = 0.97); ¹H-NMR (250 MHz, CDCl₃) δ 0.25 (s, 9H), 0.90-1.50 (bm, 12H), 3.20-3.65 (bm, 2H), 4.11 (dd, J = 2.2 and 1.1 Hz, 1H), 4.25 (s, 5H), 4.28 (dd, J = 2.3 Hz and unresolved J, 1H), 4.32 (dd, J = 2.4 and 1.1 Hz, 1H); ¹³C-NMR (62.5 MHz, CDCl₃) δ 0.5, 20.4, 20.7, 45.0 (b), 49.0 (b), 69.3, 70.2, 70.3, 72.7, 73.6, 89.9, 167.9; IR ν_{\max} (KBr) 2957, 1621, 1449, 1372, 1330, 1274, 1151, 1036, 840, 814, 757 cm⁻¹; EI MS *m/z* (rel. intensity) 385 (M⁺, 27), 370 (100), 328 (15), 312 (5), 285 (10), 213 (9), 185 (4), 121 (14), 73 (6), 56 (3); HRMS calcd for C₂₀H₃₁FeNOSi: 385.1524; found: 385.1500; Anal. calcd for C₂₀H₃₁FeNOSi: C, 62.32; H, 8.11; N, 3.63; found: C, 61.96; H, 8.14; N, 3.52.



***N,N*-Diisopropyl 2-methylferrocenecarboxamide (1.159b):**

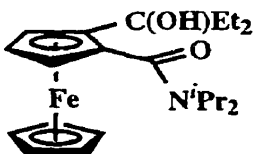
According to General Procedure A, a solution of *N,N*-diisopropyl ferrocenecarboxamide (**1.158b**, 339 mg, 1.1 mmol) in Et₂O (5 mL) was added to a mixture of *n*-BuLi (1.35 mL, 2.4 mmol, 1.76 M solution) and (-)-sparteine (0.55 mL, 2.4 mmol) in Et₂O (10 mL). After addition of iodomethane (0.20 mL, 3.3 mmol) the mixture was worked up and purified by flash chromatography (9/1 hexane/EtOAc) to afford **1.159b** (322 mg, 91%) as an orange solid (94% ee, determined by HPLC using a CHIRACEL OJ column at 5 °C with 5% water in ethanol as the mobile phase at a flow rate of 0.2 mL/min): m.p. 80-81 °C; $[\alpha]_D^{25} = +25.5$ (CHCl₃, c = 0.97); ¹H-NMR (250 MHz, CDCl₃) δ 1.06 (b, 6H), 1.47 (b, 6H), 2.05 (s, 3H), 3.25-3.60 (b, 1H), 3.85-4.30 (b, 1H), 4.00 (dd, J = 2.45 Hz and unresolved J, 1H), 4.10 (m, 1H), 4.14 (dd, J = 2.40 and 1.35 Hz, 1H), 4.22 (s, 5H); ¹³C-NMR (62.5 MHz, CDCl₃) δ 13.3, 20.8, 21.0, 45.7 (b), 49.9 (b), 65.2, 66.3, 68.6, 70.2, 84.1, 87.1, 168.2; IR (KBr) 2969, 1631, 1452, 1312, 813 cm⁻¹; EI MS *m/z* (rel. intensity) 327 (M⁺, 100), 227 (51), 199 (27), 120 (28), 56 (18). Anal. calcd for C₁₈H₂₅NOFe: C, 66.06; H, 7.70; N, 4.28; found: C, 66.05; H, 7.53; N, 4.18.



***N,N*-Diisopropyl 2-(methoxymethyl)ferrocenecarboxamide**

(1.159c): According to General Procedure A, a solution of *N,N*-diisopropyl ferrocenecarboxamide (**1.158b**, 311 mg, 1.0 mmol) in

Et₂O (7 mL) was added to a mixture of *n*-BuLi (1.35 mL, 2.18 mmol, 1.62 M solution) and (-)-sparteine (0.50 mL, 2.2 mmol) in Et₂O (10 mL). After addition of chloromethyl methyl ether (0.22 mL, 3.0 mmol) the mixture was worked up and purified by flash chromatography (19/1 hexane/EtOAc) to afford **1.159c** (213 mg, 62%) as a dark orange oil (81% ee, determined by HPLC using a CHIRALCEL OD column with 10% (Et₂O/Et₂NH 0.5%) in hexane as the mobile phase at a flow rate of 0.9 mL/min): [α]_D²⁵ = +21.9 (CHCl₃, c = 0.91); ¹H-NMR (200 MHz, CDCl₃) δ 1.10 (b, 6H) 1.47 (b, 6H), 3.30 (s, 3H), 3.45 (b, 2H), 4.11-4.51 (m, 5H), 4.26 (s, 5H); ¹³C-NMR (50 MHz, CDCl₃) δ 20.6, 20.8, 57.9, 66.3, 66.9, 68.9, 69.0, 70.2, 84.3, 87.5, 167.5; IR ν_{max}(film) 3093, 2941, 2015, 1627, 1459, 1370, 1324, 1098, 819 cm⁻¹; EI MS m/z (rel. intensity) 357 (M⁺, 96), 327 (10), 292 (100), 262 (35), 235 (10), 205 (5), 176 (5), 156 (8), 121 (12), 105 (42); Anal. calcd for C₁₉H₂₇FeNO₂: C, 63.88; H, 7.62; N, 3.92; found: C, 63.97; H, 7.50; N, 3.78.

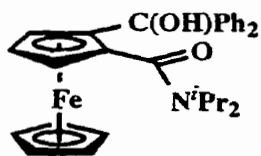


***N,N*-Diisopropyl 2-(diethylhydroxymethyl)ferrocenecarboxamide**

(1.159d): According to General Procedure A, a solution of *N,N*-diisopropyl ferrocenecarboxamide (**1.158b**, 204 mg,

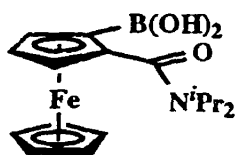
0.7 mmol) in Et₂O (3 mL) was added to a mixture of *n*-BuLi (0.51 mL, 0.78 mmol, 1.53 M solution) and (-)-sparteine (0.18 mL, 0.8 mmol) in Et₂O (10 mL). After addition of diethyl ketone (0.20 mL, 2.0 mmol), the mixture was worked up and purified by flash chromatography (5/1 hexane/Et₂O) to give recovered starting material **1.158b** (85 mg, 42%) together with **1.159d** (117 mg, 45%) as an orange solid (99% ee, determined by HPLC using a CHIRALCEL OD column with 10% (Et₂O/Et₂NH 0.5%) in hexane as the mobile phase at a flow rate of 1.0 mL/min): m.p. 169-171 °C, [α]_D²⁵ = -142.3 (EtOH, c = 1.05); ¹H-NMR (250 MHz, CDCl₃) δ 0.49 (t, 3H, J = 7.5 Hz), 1.11 (t, 3H, J = 7.4 Hz), 1.47 (bm, 16H), 3.43 (b

s, 6H), 4.10 (dd, $J = 2.5$ Hz and unresolved J , 1H), 4.23 (m, 1H), 6.18 (s, 1H); ^{13}C -NMR (62.5 MHz, CDCl_3) δ 7.7, 9.3, 20.9 (b), 29.7, 34.2, 64.9, 65.8, 69.4, 70.7, 72.8, 101.3, C=O not detected; IR ν_{max} (KBr) 3293, 3100, 3004, 2950, 1729, 1587, 1458, 1344, 1134, 851, 817, 765 cm^{-1} ; EI MS m/z (rel. intensity) 399 (M^+ , 19), 381 (100), 334 (11), 316 (32), 281 (8), 167 (7), 149 (220), 121 (13), 57 (11); HRMS calcd for $\text{C}_{22}\text{H}_{33}\text{FeNO}_2$: 399.1861; found: 399.1838. X-ray analysis, Appendix 1.



***N,N*-Diisopropyl 2-(diphenylhydroxymethyl)ferrocenecarboxamide (1.159e)**: According to General Procedure A, a solution of *N,N*-diisopropyl ferrocenecarboxamide (**1.158b**, 484 mg,

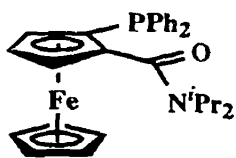
1.6 mmol) in Et_2O (5 mL) was added to a mixture of *n*-BuLi (1.21 mL, 1.9 mmol, 1.53 M solution) and (-)-sparteine (0.43 mL, 1.9 mmol) in Et_2O (15 mL). After addition of a solution of benzophenone (339 mg, 1.9 mmol) in Et_2O (5 mL), the mixture was worked up and purified by flash chromatography (5/1 hexane/ Et_2O) to give **1.159e** (626 mg, 91%) as an orange solid (99% ee, determined by HPLC using a CHIRALCEL OD column with 3% ($\text{Et}_2\text{O}/\text{Et}_2\text{NH}$ 0.5%) in hexane as the mobile phase at a flow rate of 1.5 mL/min): m.p. 180-181 $^\circ\text{C}$, $[\alpha]_{\text{D}}^{25} = +44.5$ (CHCl_3 , $c = 0.96$); ^1H -NMR (250 MHz, CDCl_3) δ 0.67 (bs, 3H), 0.94 (bs, 3H), 1.14 (bs, 3H), 1.36 (bs, 3H), 3.16 (bs, 1H), 3.57 (bs, 1H), 4.06 (dd, $J = 2.4$ Hz and unresolved J , 1H), 4.20 (bs, 1H), 4.34 (bs, 1H), 4.41 (s, 5H), 7.21 (m, 8H), 7.59 (d, 2H, $J = 7.1$ Hz), 7.95 (s, 1H); ^{13}C -NMR (62.5 MHz, CDCl_3) δ 20.0, 20.4, 21.2, 46.0, 50.2, 64.7, 66.2, 70.9, 73.2, 80.1, 105.6, 126.0, 126.5, 127.1, 127.3, 127.5, 145.8, 149.1, 171.1; IR ν_{max} (KBr) 3218, 3075, 2965, 1774, 1587, 1461, 1342, 1134, 818, 765, 756, 702; EI MS m/z (rel. intensity) 495 (M^+ , 18), 430 (78), 357 (24), 313 (24), 285 (6), 257 (72), 228 (19), 183 (16), 121 (7), 105 (30), 77 (16); HRMS calcd for $\text{C}_{30}\text{H}_{33}\text{FeNO}_2$: 495.1861; found: 495.1835.



2-(*N,N*-Diisopropylcarboxamido)ferroceneboronic acid

(1.159f): According to General Procedure A, a solution of *N,N*-diisopropyl ferrocenecarboxamide (**1.158b**, 311 mg, 1.0 mmol) in

Et₂O (7 mL) was added to a mixture of *n*-BuLi (1.35 mL, 2.2 mmol, 1.62 M solution) and (-)-sparteine (0.50 mL, 2.2 mmol) in Et₂O (10 mL). After addition of trimethyl borate (0.34 mL, 3.0 mmol) the mixture was worked up and purified by crystallization (hexane) to afford **1.159f** (315 mg, 89%) as an orange solid (85% ee, determined by HPLC using a CHIRALCEL OK column with 5% H₂O in methanol as the mobile phase at a flow rate of 1.0 mL/min): m.p. 148-150 °C; [α]_D²⁵ = -14.1 (CHCl₃, c = 1.05); ¹H-NMR (250 MHz, CDCl₃) δ 1.42 (b, 12H), 3.50 (b, 2H), 4.22 (s, 5H), 4.44 (t, J = 2.3 Hz, 1H), 4.55 (dd, J = 1.2 and 2.3 Hz, 1H), 4.65 (dd, J = 1.2 and 2.3 Hz, 1H), 7.25 (s, 2H); ¹³C-NMR (62.5 MHz, CDCl₃) δ 21.3, 70.6, 70.8, 71.7, 75.9, 79.0 (b), 84.7, 173.3; IR ν_{max}(KBr) 3331, 2952, 1576, 1385 cm⁻¹; EI MS *m/z* (rel. intensity) 357 (M⁺, 44), 313 (100), 270 (28), 213 (72), 186 (29), 129 (22), 121 (31), 91 (10), 80 (42); Anal. calcd for C₁₇H₂₄BFeNO₃: C, 57.19; H, 6.78; N, 3.92; found: C, 57.31; H, 6.60; N, 3.88.

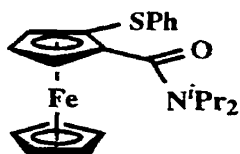


***N,N*-Diisopropyl 2-(diphenylphosphinyl)ferrocenecarbox-**

amide (1.159g): According to General Procedure A, a solution of *N,N*-diisopropyl ferrocenecarboxamide (**1.158b**, 332 mg, 1.1 mmol)

in Et₂O (5 mL) was added to a mixture of *n*-BuLi (1.49 mL, 2.3 mmol, 1.57 M solution) and (-)-sparteine (0.54 mL, 2.3 mmol) in Et₂O (10 mL). After addition of chlorodiphenylphosphine (0.57 mL, 3.2 mmol), the mixture was worked up and purified by flash chromatography (5/1 hexane/EtOAc) to afford **1.159g** (423 mg, 82%) as an orange solid (90% ee, determined by HPLC using a CHIRALCEL OD column with 10% (Et₂O/Et₂NH 0.5%) in hexane as the mobile phase at a flow rate of 1.5 mL/min): m.p. 176-177 °C (dec.); ¹H-NMR (250 MHz, CDCl₃) δ 1.02 (m, 12H), 3.22 (b, 1H), 3.83 (dd, J = 1.0 Hz and unresolved J, 1H), 3.86 (b, 1H), 4.22 (s, 5H), 4.25 (dd, J = 2.4 Hz and unresolved J, 1H),

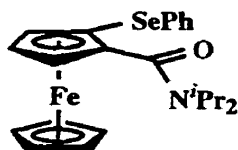
4.45 (dd, $J = 1.1$ Hz and unresolved J , 1H), 7.29 (m, 8H), 7.55 (m, 2H); ^{13}C -NMR (62.5 MHz, CDCl_3) δ 20.3, 20.8, 68.0, 68.7, 70.9, 79.6, 79.8, 90.8, 91.2, 127.8, 127.9, 128.5, 132.8, 133.1, 134.2, 134.5, 138.1, 138.4, 139.5, 139.7, 166.9; IR ν_{max} (KBr) 3089, 3061, 3047, 3012, 2970, 2361, 1739, 1623, 1445, 1433, 1371, 1323, 1040, 1028, 1006, 815, 754, 744 cm^{-1} ; EI MS m/z (rel. intensity) 497 (M^+ , 30), 457 (7), 412 (100), 346 (32), 222 (8), 201 (78), 183 (8), 170 (10), 121 (14), 98 (3), 56 (6); HRMS calcd for $\text{C}_{29}\text{H}_{32}\text{FeNOP}$: 497.1571; found: 497.1569.



***N,N*-Diisopropyl 2-phenylthioferrocenecarboxamide**

(1.159h): According to General Procedure A, a solution of *N,N*-diisopropyl ferrocenecarboxamide (**1.158b**, 339 mg, 1.1 mmol) in

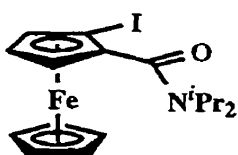
Et_2O (4 mL) was added to a mixture of *n*-BuLi (1.56 mL, 2.4 mmol, 1.53 M solution) and (-)-sparteine (0.55 mL, 2.4 mmol) in Et_2O (10 mL). After addition of phenyl disulfide (0.71g, 3.3 mmol) in anhydrous THF (5 mL) the mixture was worked up and purified by flash chromatography (9/1 hexane/ EtOAc) to afford **1.159h** (410 mg, 90%) as an orange solid (98% ee, determined by HPLC using a CHIRALCEL OD column with 2% 2-propanol in hexane as the mobile phase at a flow rate of 0.5 mL/min): m.p. 154-155 $^\circ\text{C}$; ^1H -NMR (250 MHz, CDCl_3) δ 0.45 (bs, 3H), 0.98 (bs, 3H), 1.37 (bs, 3H), 1.45 (bs, 3H), 3.24 (bs, 1H), 3.68 (bs, 1H), 4.31 (m, 1H), 4.40 (m, 1H), 4.41 (s, 5H), 4.53 (dd, $J = 2.2$ and 1.3 Hz, 2H), 7.00-7.16 (m, 5H); ^1H -NMR (200MHz, DMSO-d_6 , 320 $^\circ\text{K}$) δ 0.91 (d, $J = 8.1$ Hz, 6H), 1.17 (d, $J = 8.3$ Hz, 6H), 3.40-3.60 (m, 2H), 4.33 (s, 5H), 4.41 (m, 1H), 4.52 (m, 2H), 7.08-7.21 (m, 5H); ^{13}C -NMR (62.5 MHz, DMSO-d_6) δ 19.4, 20.4, 44.6, 50.0, 67.9, 68.1, 70.9, 74.5, 76.3, 92.2, 125.1, 126.1, 128.7, 139.3, 164.4; IR ν_{max} (KBr) 2955, 1630, 1580, 1476, 1457, 1321, 814, 742, 690 cm^{-1} ; EI MS m/z (rel. intensity) 421 (M^+ , 100), 321 (50), 292 (52), 171 (36), 121 (57), 56 (17); Anal. calcd for $\text{C}_{23}\text{H}_{27}\text{FeNOS}$: C, 65.56; H, 6.46; N, 3.32; found: C, 65.73; H, 6.29; N, 3.16.



***N,N*-Diisopropyl 2-phenylselenylferrocenecarboxamide**

(1.159i): According to General Procedure A, a solution of *N,N*-diisopropyl ferrocenecarboxamide (**1.158b**, 301 mg, 1.0 mmol) in

Et₂O (7 mL) was added to a mixture of *n*-BuLi (1.56 mL, 2.1 mmol, 1.35 M solution) and (-)-sparteine (0.48 mL, 2.1 mmol) in Et₂O (10 mL). After addition of diphenyl diselenide (0.72 g, 2.3 mmol) in THF (10 mL) the mixture was worked up and purified by flash chromatography (9/1 hexane/EtOAc) to afford **1.159i** (412 mg, 92%) as an orange solid (93% ee, determined by HPLC using a CHIRALCEL OD column with 2% 2-propanol in hexane as the mobile phase at a flow rate of 0.5 mL/min): m.p. 133-135 °C; ¹H-NMR (250 MHz, CDCl₃) δ 0.50 (bs, 3H), 1.00 (bs, 3H), 1.30-1.60 (bs, 6H), 3.20-3.40 (bs, 1H), 3.60-3.85 (bs, 1H), 4.29 (m, 1H), 4.36 (dd, *J* = 2.5 Hz and unresolved *J*, 1H), 4.37 (s, 5H), 4.47 (dd, *J* = 1.3 and 2.2 Hz, 1H), 7.10-7.22 (m, 3H), 7.30-7.40 (m, 2H); ¹³C-NMR (62.5 MHz, CDCl₃) δ 20.8 (b), 45.8 (b), 50.2 (b), 67.9, 68.2, 71.3, 72.8, 75.1, 91.6, 126.0, 128.8, 130.1, 134.0, 166.4; IR ν_{max}(KBr) 2941, 1630, 1577, 1456, 1371, 1317, 1204, 815, 736 cm⁻¹; EI MS *m/z* (rel. intensity) 469 (*M*+1, 100), 369 (8), 340 (14), 268 (10), 213 (13), 121 (13), 56 (6); HRMS calcd for C₂₃H₂₇FeNOSe: 469.0606; found 469.0585; Anal. calcd for C₂₃H₂₇FeNOSe: C, 58.99; H, 5.81; N, 2.99; found: C, 59.16; H, 5.62; N, 2.98.

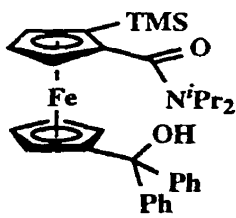


***N,N*-Diisopropyl 2-iodoferrocenecarboxamide** (**1.159j**):

According to General Procedure A, a solution of *N,N*-diisopropyl ferrocenecarboxamide (**1.158b**, 400 mg, 1.3 mmol) in Et₂O (7 mL)

was added to a mixture of *n*-BuLi (2.10 mL, 2.8 mmol, 1.35 M solution) and (-)-sparteine (0.65 mL, 2.8 mmol) in Et₂O (10 mL). After addition of iodine (0.82 g, 3.2 mmol) in THF (10 mL) the mixture was worked up and purified by flash chromatography (17/3 hexane/Et₂O) to afford **1.159j** (478 mg, 85%) as an orange solid (96% ee, determined by HPLC using a CHIRALCEL OD column with 15% (Et₂O/Et₂NH 0.5%) in hexane as the mobile phase at a flow rate of 1.0 mL/min): m.p. 97-99 °C; [α]_D²⁵ = +91.0 (CHCl₃, *c* = 1.06); ¹H-NMR (250

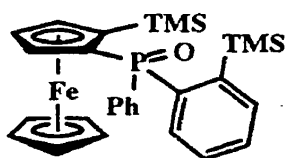
MHz, CDCl₃) δ 0.92-1.05 (bs, 3H), 1.07-1.25 (bs, 3H), 1.40-1.52 (bs, 6H), 3.32-3.50 (bs, 1H), 3.52-3.70 (bs, 1H), 4.18 (dd, J = 2.5 Hz and unresolved J, 1H), 4.28 (dd, J = 2.5 and 1.3 Hz, 1H), 4.35 (s, 5H), 4.43 (dd, J = 2.4 and 1.3 Hz, 1H); ¹³C-NMR (62.5 MHz, CDCl₃) δ 20.8, 40.4, 45.8, 50.7, 66.7, 67.5, 72.7, 73.5, 92.5, 166.2; IR ν_{max}(KBr) 2955, 1622, 1455, 1370, 1316, 1205, 815 cm⁻¹; EI MS m/z (rel. intensity) 440 (M⁺+1, 21), 439 (M⁺, 100), 339 (7), 312 (24), 311 (31), 268 (33), 213 (17), 128 (20), 121 (3), 56 (12); HRMS calcd for C₁₇H₂₂FeNOI: 439.0097; found 439.0080; Anal. calcd for C₁₇H₂₂FeNOI: C, 46.50; H, 5.05; N, 3.19; found: C, 46.34; H, 5.09; N, 3.09.



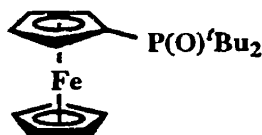
***N,N*-Diisopropyl 2-trimethylsilyl-1'-(diphenylhydroxymethyl)ferrocenecarboxamide (1.161):** To a stirred solution of *N,N*-diisopropyl 2-trimethylsilylferrocenecarboxamide (**1.159a**, 190 mg, 0.5 mmol, 98% ee) in anhydrous Et₂O (8 mL) at -78 °C under a

nitrogen atmosphere, was added dropwise a solution of *s*-BuLi (0.47 mL, 0.6 mmol, 1.28 M). After stirring for 1 h at -78 °C, a solution of benzophenone (120 mg, 0.7 mmol) in anhydrous Et₂O (1 mL) was added and the mixture was stirred for 30 min at -78 °C. After warming to room temperature, the mixture was quenched with saturated aqueous NH₄Cl solution and the organic layer was separated. The aqueous phase was extracted with Et₂O (3 x 15 mL) and the combined organic extract was washed with H₂O (2 x 50 mL) and brine (50 mL), dried over anhydrous MgSO₄ and evaporated to give a brown solid. Purification by flash chromatography (9/1 hexane/Et₂O provided **1.161** (209 mg, 75%) as an orange solid (98% ee, determined by HPLC using a CHIRALCEL OD column with 2% (Et₂O/Et₂NH 0.5%) in hexane as the mobile phase at a flow rate of 1.5 mL/min): m.p. 153-155 °C; [α]_D²⁵ = +295.5 (CHCl₃, c = 1.02); ¹H-NMR (250 MHz, CDCl₃) δ 0.25 (s, 9H), 1.03 (m, 6H), 1.51 (d, J = 6.6 Hz, 3H), 1.75 (d, J = 6.6 Hz, 3H), 3.40-3.57 (m, 2H), 3.63 (dd, J = 2.3 and 1.2 Hz, 1H), 3.93 (m, 1H), 4.01 (dd, J = 2.4 Hz and unresolved J, 1H), 4.09 (dd, J = 2.4 and 1.2 Hz, 1H), 4.19 (m, 1H), 4.36 (m, 1H), 4.68 (m, 1H), 7.06 (s, 1H), 7.09-7.32 (m, 8H), 7.46-

7.50 (m, 2H); ^{13}C -NMR (62.5 MHz, CDCl_3) δ 0.4, 20.1, 20.3, 20.8, 21.1, 46.3, 50.6, 68.4, 68.6, 69.3, 69.7, 70.2, 71.1, 72.9, 73.0, 77.2, 94.8, 98.8, 126.2, 126.3, 126.9, 127.1, 127.3, 148.4, 148.9, 170.4; IR ν_{max} (KBr) 3261, 3088, 3067, 2945, 1597, 1457, 1371, 1332, 1201, 1034, 835 cm^{-1} ; EI MS m/z (rel. intensity) 567 (M^+ , 0.8), 309 (27), 230 (100), 215 (30), 202 (16), 152 (13), 56 (5); HRMS calcd for $\text{C}_{33}\text{H}_{41}\text{FeNOSi}$: 567.2255; found: 567.2246. X-ray analysis, Appendix 2.

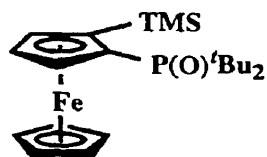


Phenyl(2-trimethylsilylferrocenyl)(2-trimethylsilylphenyl)-phosphine oxide (1.166): To a solution of TMEDA (0.08 mL, 128 mg, 1.1 mmol) in anhydrous toluene (2 mL) at $-78\text{ }^\circ\text{C}$ was added a solution of *s*-BuLi (0.76 mL, 1.1 mmol, 1.45 M). After 20 min, a solution of diphenylferrocenylphosphine oxide (**1.16**, 193 mg, 0.5 mmol) in anhydrous toluene (8 mL) at $-78\text{ }^\circ\text{C}$ was added dropwise to the base mixture via cannula. Stirring was continued at $-78\text{ }^\circ\text{C}$ for 1 h and TMSCl (163 mg, 0.19 mL, 1.5 mmol) was added. The mixture was allowed to warm to room temperature and was stirred for an additional 1 h, then quenched with water (3 mL) and extracted with CH_2Cl_2 (3 x 10 mL). The combined organic layers were dried (Na_2SO_4) and evaporated to give an orange solid. Purification by flash chromatography afforded diphenyl(2-trimethylsilylferrocenyl)-phosphine oxide (**1.17**, 101 mg, 44%) along with a new compound proposed to be **1.166** (80 mg, 30%): ^1H -NMR (200 MHz, CDCl_3) δ 0.08 (s, 9H), 0.27 (s, 9H), 3.75 (s, 1H), 4.33 (s, 5H), 4.45 (s, 2H), 6.99-7.28 (m, 2H), 7.32-7.53 (m, 4H), 7.55-7.76 (m, 3H); EI MS m/z (rel intensity): 530 (M^+ , 30), 515 (100), 457 (9), 379 (22), 193 (21), 121 (40), 73 (24).



Di-*tert*-butylferrocenylphosphine oxide (1.168): To a solution of (tri-*n*-butylstannyl)ferrocene (**1.99**, 950 mg, 2.0 mmol) in anhydrous THF (10 mL) at $-78\text{ }^\circ\text{C}$ was added *n*-BuLi (1.20 mL, 2.1 mmol, 1.76 M) dropwise. After 15 min of stirring at $-78\text{ }^\circ\text{C}$, chlorodi-*tert*-butylphosphine

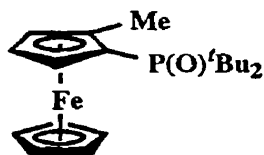
(0.40 mL, 2.1 mmol) was added dropwise and the solution was allowed to warm to room temperature. Stirring was continued for 1 h at room temperature, and water (5 mL) was added. The mixture was extracted with CH₂Cl₂ (3 x 10 mL) and the combined organic layers were dried (Na₂SO₄) and evaporated to afford di-*tert*-butylphosphinoferrocene as an orange oil which was used without further purification. The oil was suspended in MeOH (20 mL) and cooled to 0 °C. Aqueous H₂O₂ (30%, 0.25 mL, 2.2 mmol) was added to the suspension, stirring was continued for 1h, and saturated aqueous Na₂SO₃ (2 mL) was added. Stirring was continued for a further 1h, and aqueous 10% HCl (2 mL) was added. Extraction with CH₂Cl₂ (3 x 10 mL) followed by drying (Na₂SO₄) and concentrating the organic layers resulted in isolation of an orange solid. Purification by flash chromatography (1-4% isopropanol/hexane) afforded **1.168** (567 mg, 82% overall) as an orange solid: m.p. 164-165 °C; ¹H-NMR (250 MHz, CDCl₃) δ 1.26 (d, J = 13.5 Hz, 18H), 4.29 (s, 5H), 4.46 (d, J = 1.2 Hz, 4H); ¹³C-NMR (62.5 MHz, CDCl₃) δ 27.1, 35.8 (d, J = 62.9 Hz), 69.6, 69.9 (d, J = 8.0 Hz), 72.3 (d, J = 9.1 Hz), 72.8 (d, J = 87.7); ³¹P-NMR (81 MHz, CDCl₃) δ 58.7; IR (KBr) ν_{max} 3087, 2950, 2899, 2866, 1476, 1368, 1166, 1144, 1107, 1022, 821 cm⁻¹; EI MS *m/z* (rel intensity): 346 (M⁺, 35), 331 (3), 289 (9), 233 (99), 207 (42), 186 (100), 121 (25), 57 (17); Anal. calcd for C₁₈H₂₇FeOP: C, 62.44; H, 7.86. found: C, 61.94; H, 7.88.



Di-*tert*-butyl-(2-trimethylsilylferrocenyl)phosphine oxide

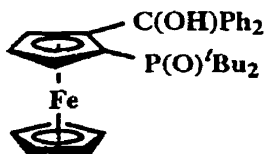
(1.169a): According to General Procedure B, *t*-BuLi (0.68 mL, 1.0 mmol, 1.47 M in pentane) was added to a stirred solution of **1.168** (173 mg, 0.5 mmol) in THF (10 mL) at -78 °C. After addition of TMSCl (0.13 mL, 1.0 mmol) the mixture was worked up and purified by flash chromatography (97/3 CH₂Cl₂/MeOH) to afford **1.169a** as an orange solid (192 mg, 92%): m.p. 138-139 °C; ¹H-NMR (250 MHz, CDCl₃) δ 4.63 (dd, J = 4.0, 2.3 Hz, 1H), 4.51 (t, J = 1.1 Hz, 1H), 4.28 (d, J = 1.8 Hz, 1H), 4.22 (s, 5H), 1.54 (d, J = 13.6 Hz, 9H), 0.91 (d, J = 13.3 Hz, 9H), 0.38 (s, 9H); ³¹P-NMR (81 MHz, CDCl₃) δ 29.3; IR ν_{max} (KBr) 2981, 2950, 2897, 1477,

1239, 1178, 1151, 839, 814 cm^{-1} ; EI MS m/z (rel intensity): 418 (M^+ , 3), 403 (26), 305 (100), 289 (44), 258 (8), 243 (21), 231 (9), 207 (13), 195 (13), 121 (15), 57 (19); Anal. calcd for $\text{C}_{21}\text{H}_{35}\text{FeOPSi}$: C, 60.28; H, 8.43. found: C, 60.35; H, 8.61. $^1\text{H-NMR}$, Appendix 3.



Di-*tert*-butyl-(2-methylferrocenyl)phosphine oxide

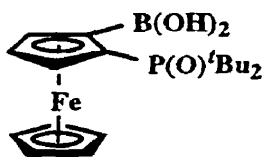
(1.169b): According to General Procedure B, *t*-BuLi (0.63 mL, 1.0 mmol, 1.59 M in pentane) was added to a stirred solution of **1.168** (173 mg, 0.5 mmol) in THF (10 mL) at $-78\text{ }^\circ\text{C}$. After addition of CH_3I (141 mg, 1.0 mmol, 0.06 mL) the mixture was worked up and purified by flash chromatography (95/5 $\text{CH}_2\text{Cl}_2/\text{MeOH}$) to afford **1.169b** as an orange solid (130 mg, 72%): m.p. $132\text{-}134\text{ }^\circ\text{C}$; $^1\text{H-NMR}$ (200 MHz, CDCl_3) δ 0.97 (d, $J = 13.3\text{ Hz}$, 9H), 1.50 (d, $J = 13.4\text{ Hz}$, 9H), 2.23 (s, 3H), 4.02 (s, 1H), 4.17 (s, 5H), 4.32 (s, 2H); $^{13}\text{C-NMR}$ (50.3 MHz, CDCl_3) δ 90.6 (d, $J = 6.6\text{ Hz}$), 72.2 (d, $J = 7.2\text{ Hz}$), 71.3 (d, $J = 12.9\text{ Hz}$), 70.5, 69.8, 69.2 (d, $J = 7.3\text{ Hz}$), 37.5 (d, $J = 63.1\text{ Hz}$), 36.6 (d, $J = 62.2\text{ Hz}$), 27.6, 26.7, 15.9; $^{31}\text{P-NMR}$ (81.0 MHz, CDCl_3) δ 59.6; IR (KBr) ν_{max} 3083, 2950, 2921, 2868, 1478, 1366, 1177, 1150, 1107, 1083, 813 cm^{-1} ; MS (EI) m/z (rel intensity): 360 (88), 320 (6), 303 (22), 248 (15), 247 (100), 200 (90), 181 (12), 149 (13), 134 (14), 121 (20), 119 (11), 78 (24); HRMS calcd for $\text{C}_{19}\text{H}_{29}\text{FeOP}$: 360.0426; found 360.1305.



Di-*tert*-butyl-[2-(diphenylhydroxymethyl)ferrocenyl]-

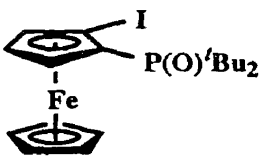
phosphine oxide (1.169c): According to General Procedure B, *t*-BuLi (0.59 mL, 1.0 mmol, 1.70 M in pentane) was added to a stirred solution of **1.168** (173 mg, 0.5 mmol) in THF (10 mL) at $-78\text{ }^\circ\text{C}$. After addition of benzophenone (182 mg, 1.0 mmol), the mixture was worked up and purified by flash chromatography (CH_2Cl_2 followed by 98/2 $\text{CH}_2\text{Cl}_2/\text{MeOH}$) to afford **1.169c** as an orange solid (257 mg, 97%): m.p. $238\text{ }^\circ\text{C}$ (dec.); $^1\text{H-NMR}$ (250 MHz, CDCl_3) δ 0.79 (d, $J = 13.6$

Hz, 9H), 1.63 (d, $J = 13.6$ Hz, 9H), 4.03 (s, 5H), 4.22 (bs, 1H), 4.45 (bs, 1H), 4.51 (bs, 1H), 7.02-7.50 (m, 8H), 7.78 (d, $J = 8.5$ Hz, 2H), 8.50 (s, 1H); ^{31}P -NMR (81.0 MHz, CDCl_3) δ 64.2; IR ν_{max} (KBr) 3429, 1630, 1479, 1450, 1414, 1385, 1151, 1114, 756, 703 cm^{-1} ; EI MS m/z (rel. intensity) 528 (M^+ , 48), 464 (46), 463 (100), 333 (13), 285 (20), 229 (30), 228 (18), 199 (12), 57 (14). HRMS calcd for $\text{C}_{31}\text{H}_{37}\text{FeO}_2\text{P}$: 528.1881; found: 528.1906.



2-Di-*tert*-butylphosphinylderrocenylboronic acid (1.169d):

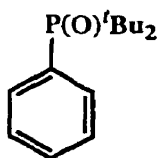
According to General Procedure B, *t*-BuLi (1.02 mL, 1.0 mmol, 0.98 M in pentane) was added to a stirred solution of **1.168** (173 mg, 0.5 mmol) in THF (10 mL) at -78 °C. After addition of $\text{B}(\text{OMe})_3$ (103 mg, 0.11 mL, 1.0 mmol) the mixture was warmed to room temperature. Dropwise addition of HCl (1 M) to pH 1-2 was followed by extraction with CH_2Cl_2 (3 x 10 mL). The combined organic layers were dried (Na_2SO_4) and evaporated to yield a dark orange solid. Recrystallization from hexane gave **1.169d** as an orange solid (118 mg, 65%): m.p. 174 °C (dec.); ^{31}P -NMR (81.0 MHz, CDCl_3) δ 66.3; IR ν_{max} (KBr) 3338, 3097, 2966, 2903, 2872, 1479, 1426, 1400, 1340, 1221, 1107, 815 cm^{-1} ; EI MS m/z (rel. intensity) 390 (M^+ , 37), 346 (100), 325 (37), 290 (10), 277 (35), 259 (30), 233 (48), 212 (29), 186 (46), 167 (17), 121 (39); HRMS calcd for $\text{C}_{21}\text{H}_{32}\text{BFeO}_3\text{P}$: 390.0339; found: 390.0329.



Di-*tert*-butyl-(2-iodoferrocenyl)phosphine oxide (1.169f):

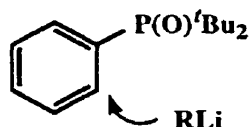
According to General Procedure B, *t*-BuLi (0.66 mL, 1.0 mmol, 1.51 M in pentane) was added to a stirred solution of **1.168** (173 mg, 0.5 mmol) in THF (10 mL) at -78 °C. After addition of I_2 (153 mg, 0.6 mmol) in THF (5 mL) or direct addition of solid I_2 , the mixture was warmed to room temperature. An aqueous solution of $\text{Na}_2\text{S}_2\text{O}_3$ (10 mL, 2 M) was added and the mixture was extracted with CH_2Cl_2 (3 x 10 mL). The combined organic layers were dried (Na_2SO_4) and evaporated to yield a dark orange-

brown solid. Purification by flash chromatography (97/3 CH₂Cl₂/MeOH) gave **1.169f** as an orange solid (179 mg, 76%): m.p. 143 °C (dec.); ¹H-NMR (200 MHz, CDCl₃) δ 1.10 (d, J = 13.4 Hz, 9H), 1.49 (d, J = 13.6 Hz, 9H), 4.30 (bs, 6H), 4.51 (d, J = 1.1 Hz, 1H), 4.79 (d, J = 1.0 Hz, 1H); ¹³C-NMR (50.3 MHz, CDCl₃) δ 73.0, 41.3, 38.3, 37.0, 36.9 (d, J = 62.0 Hz), 29.6, 27.5, 27.1; ³¹P-NMR (81 MHz, CDCl₃) δ 57.32; IR ν_{max}(KBr) 3083, 2950, 2867, 1477, 1351, 1179, 1156, 1107, 824, 814 cm⁻¹; CI MS *m/z* (rel. intensity) 471 (M+1, 100), 343 (50), 311 (6), 289 (20), 231 (33), 185 (39), 163 (10), 121 (10); Anal. calcd for C₁₈H₂₆FeIOP: C, 45.79; H, 5.55. found: C, 45.96; H, 5.43.

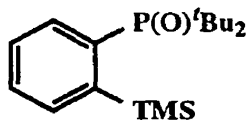


Di-*tert*-butylphenylphosphine oxide (1.170): Method 1: According to General Procedure C, a solution of freshly distilled bromobenzene (4.21 g, 27.0 mmol) in Et₂O (20 mL) was treated with *n*-BuLi (17.7 mL, 26.5 mmol, 1.50 M solution). The newly-formed phenyllithium was added to a solution of chloro-di-*tert*-butylphosphine (4.88 g, 27.0 mmol) in Et₂O (20 mL) and heated to reflux for a period of 2 h. The reaction mixture was cooled and quenched by addition of MeOH (2 mL). After removal of the solvent under reduced pressure, the residue was suspended in MeOH (20 mL) and cooled to 0 °C before H₂O₂ (4.5 mL of a 30% solution, approx. 40 mmol) was added dropwise. Workup with excess Na₂SO₃ (20 mL, 2 M solution) and HCl (20 mL, 10% solution) followed by removal of MeOH, extraction with CH₂Cl₂ (3 x 50 mL), drying with Na₂SO₄, and evaporation of solvent allowed isolation of a white solid. Purification by recrystallization from hexane provided **1.170** as a white crystalline solid (5.47 g, 85%); *or* Method 2: Commercially obtained PhPCl₂ (13.20 g, 73.8 mmol) was dissolved in anhydrous toluene (200 mL), cooled on an acetone/ice bath and treated dropwise with *t*-BuLi (100 mL, 154 mmol, 1.54 M in pentane) over 45 min. The slightly yellow reaction mixture was stirred for 1 hour at room temperature and then heated to reflux for 12 h. The reaction mixture was cooled on an ice bath, quenched by slow addition of water (50 ml), and oxidized by addition of H₂O₂ (30%, 10 mL, 88 mmol, exothermic). After stirring for 3 hours at room temperature, the

mixture was transferred to a separatory funnel, and the organic layer was washed with Na₂S₂O₃ (2 x 50 mL, exothermic) and water (50 mL), dried over MgSO₄, and evaporated yielding a light yellow oil. Crystallization was accomplished by seeding with a small crystal of previously prepared material. Recrystallization from hexane provided **1.170** as a white solid identical to that prepared by Method 1 (7.79 g, 44%): m.p. 102-104 °C (hexane); ¹H-NMR (250 MHz, CDCl₃) δ 1.28 (d, J = 13.5 Hz, 18H), 7.40-7.50 (m, 3H), 7.87 (bs, 2H); ¹³C-NMR (62.5 MHz, CDCl₃) δ 26.9, 35.5 (d, J = 59.7 Hz), 127.5 (d, J = 10.0 Hz), 130.7, 131.1 (d, J = 78.2 Hz), 132.1; ³¹P-NMR (81.0 MHz, CDCl₃) δ 51.8; IR (KBr) ν_{max} 3055, 2937, 1472, 1433, 1155 cm⁻¹; MS (EI) *m/z* (rel intensity): 238 (0.5), 182 (63), 126 (100), 79 (22). Anal. calcd for C₁₄H₂₃OP: C, 70.56; H, 9.73; P, 13.00. found: C, 70.77; H, 9.59; P, 13.23. X-ray analysis, Appendix 4.

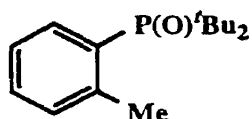


Optimization studies for metalation of 1.170: To a solution of di-*tert*-butylphenylphosphine oxide (**1.170**, 60 mg, 0.25 mmol) in anhydrous THF (2.5 mL) at -78 °C was added a solution of *n*-BuLi, *s*-BuLi, or *t*-BuLi (0.50 mmol) according to Scheme 1.60. After the specified length of time (Scheme 1.60), an excess of TMSCl (0.10 mL, 0.75 mmol) was added and the reaction mixture was allowed to warm to room temperature. Undecane (60 μL) was added followed by H₂O (5 mL). After thorough mixing, a micro-workup was performed by removing a small amount of the organic layer (0.2 mL) and diluting with EtOAc (1.8 mL). The resulting solution was passed through a micro column of silica gel (3 mm diameter x 5 mm length) and analyzed by GC providing **1.171a** as outlined in Scheme 1.60.



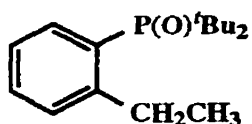
2-(Trimethylsilyl)phenyldi-*tert*-butylphosphine oxide (1.171a): According to General Procedure D, *t*-BuLi (1.36 mL, 2.0 mmol, 1.47 M in pentane) was added to a stirred solution of **1.170** (238 mg, 1.0 mmol) in THF (10 mL) at -78 °C. After addition of TMSCl (0.13 mL, 1.0

mmol) the mixture was worked up and purified by flash chromatography (98/2 CH₂Cl₂/MeOH) to afford **1.171a** as a white solid (482 mg, 76%): m.p. 134-136.5 °C (hexane); ¹H-NMR (250 MHz, CDCl₃) δ 0.43 (s, 9H), 1.27 (d, J = 13.2 Hz, 18H), 7.3-7.5 (m, 2H), 7.61 (bt, J = 9.0 Hz, 1H), 7.87 (bd, J = 7.7 Hz, 1H); ¹³C-NMR (62.5 MHz, CDCl₃) δ 2.9, 27.7, 36.7 (d, J = 57.1 Hz), 126.8 (d, J = 11.7 Hz), 129.9 (d, J = 2.6 Hz), 130.8 (d, J = 14.3 Hz), 136.8 (d, J = 83.1 Hz), 137.0 (d, J = 13.0 Hz), 147.1 (d, J = 11.7 Hz); ³¹P-NMR (81.0 MHz, CDCl₃) δ 56.0; IR (KBr) ν_{max} 2951, 2900, 1477, 1236, 1160, 1111, 844, 749, 645 cm⁻¹; MS CI *m/z* (rel. intensity): 311 (M⁺+1, 20), 296 (52), 295 (100), 255 (20), 239 (12), 197 (7), 182 (17), 119 (10), 107 (30), 105 (9), 87 (16), 85 (28), 57 (23); HRMS calcd for C₁₇H₃₂OPSi: 311.1975; found 311.1960. Anal. calcd for C₁₇H₃₁OPSi: C, 65.76; H, 10.06. found: C, 65.88; H, 9.86.



2-Methylphenyldi-*tert*-butylphosphine oxide (1.171b):

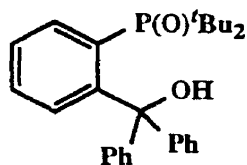
According to General Procedure D, *t*-BuLi (0.63 mL, 1.0 mmol, 1.59 M in pentane) was added to a stirred solution of **1.170** (119 mg, 0.5 mmol) in THF (10 mL) at -78 °C. After addition of CH₃I (0.06 mL, 1.0 mmol) the mixture was worked up and purified by flash chromatography (97/3 CH₂Cl₂/MeOH) to afford **1.171b** as a white solid (148 mg, 82%): m.p. 117-119 °C (hexane); ¹H-NMR (200 MHz, CDCl₃) δ 1.30 (d, J = 13.2 Hz, 18H), 2.78 (s, 3H), 7.11-7.26 (m, 2H), 7.28-7.40 (m, 1H), 7.41-7.56 (m, 1H); ¹³C-NMR (50.3 MHz, CDCl₃) δ 22.0, 27.4, 37.3 (d, J = 59.1 Hz), 123.7 (d, J = 11.8 Hz), 128.4 (d, J = 77.8 Hz), 130.5 (d, J = 3.0 Hz), 131.4 (d, J = 11.8 Hz), 133.0 (D, J = 9.8 Hz), 146.07; ³¹P-NMR (81.0 MHz, CDCl₃) δ 57.4; IR (KBr) ν_{max} 2976, 2949, 1476, 1388, 1156, 1125, 813, 758, 646 cm⁻¹. Anal. calcd for C₁₅H₂₅OP: C, 71.40; H, 9.99. found: C, 71.18; H, 10.04.



2-Ethylphenyldi-*tert*-butylphosphine oxide (1.171c):

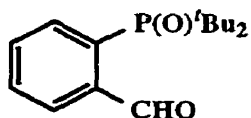
According to General Procedure D, *t*-BuLi (1.9 mL, 3.23 mmol, 1.70

M in pentane) was added to a stirred solution of **1.170** (695 mg, 2.91 mmol) in THF (30 mL) at -78 °C. After addition of iodoethane (0.28 mL, 3.50 mmol) over 2 min. the mixture was allowed to slowly warm to room temperature (2 h). Stirring was continued at room temperature overnight (12 h) and an additional portion of iodoethane (0.12 mL, 1.47 mmol) was added to the yellow solution. Workup and purification by flash chromatography (3/1 EtOAc/hexane, followed by EtOAc and then 95/5 EtOAc/MeOH) afforded **1.171c** as a white solid (303 mg, 39%): ¹H-NMR (250 MHz, CDCl₃) δ 1.26 (t, J = 7.4 Hz, 3H), 1.30 (d, J = 13.2 Hz, 18H), 3.27 (q, 2H, J = 7.4 Hz), 7.13-7.52 (m, 4H); ¹³C-NMR (62.5 MHz, CDCl₃) δ 17.4, 27.1, 27.4, 36.6, 37.5, 123.4, 123.6, 127.1, 128.3, 130.6, 131.1, 131.3, 131.6, 131.8, 152.6 (x2); ³¹P-NMR (81.0 MHz, CDCl₃) δ 57.9; IR (KBr) ν_{max} 3048, 2991, 2961, 2869, 1468, 1154 cm⁻¹; MS (EI) *m/z* (rel intensity) 266 (M⁺, 5), 210 (41), 154 (100), 133 (16), 107 (27); HRMS calcd for C₁₆H₂₇OP: 268.1799; found 266.1789.



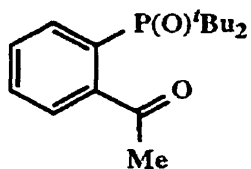
2-(Diphenylhydroxymethyl)phenyldi-*tert*-butylphosphine

oxide (1.171d): According to General Procedure D, *t*-BuLi (0.65 mL, 1.0 mmol, 1.53 M in pentane) was added to a stirred solution of **1.170** (119 mg, 0.5 mmol) in THF (10 mL) at -78 °C. After addition of benzophenone (182 mg, 1.0 mmol) the mixture was worked up and crystallized from hexane to afford **1.171d** as a white solid (154 mg, 75%): m.p. 212-213 °C; ¹H-NMR (200 MHz, CDCl₃) δ 1.18 (d, J = 13.8 Hz, 18H), 6.80-7.00 (m, 1H), 7.10-7.40 (m, 12H), 7.50-7.75 (m, 1H), 9.58 (s, 1H); ¹³C-NMR (50 MHz, CDCl₃) δ 27.6, 38.0 (d, J = 57.5 Hz), 83.0 (d, J = 2.6 Hz), 124.5 (d, J = 12.3 Hz), 126.6, 127.4, 128.3, 128.7 (d, J = 73.7 Hz), 129.6 (d, J = 2.7 Hz), 132.3 (d, J = 13.3 Hz), 133.2 (d, J = 8.6 Hz), 148.1, 155.7 (d, J = 2.9 Hz); ³¹P-NMR (81 MHz, CDCl₃) δ 62.1; IR (KBr) ν_{max} 3456, 3059, 2990, 2965, 2814, 1468, 1448, 1431, 1138, 1113, 702 cm⁻¹; EI MS (rel. intensity) 420 (M⁺, 35), 343 (32), 327 (100), 295 (25), 287 (11), 271 (19), 241 (17), 239 (18), 213 (29), 182 (52), 126 (29), 105 (12), 57 (45); HRMS calcd for C₂₇H₃₂O₂P: 420.2218; found: 420.2209.



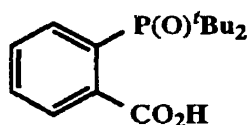
2-(Di-*tert*-butylphosphinyl)benzaldehyde (1.171e):

According to General Procedure D, *t*-BuLi (1.67 mL, 2.0 mmol, 1.20 M in pentane) was added to a stirred solution of **1.170** (238 mg, 1.0 mmol) in THF (10 mL) at -78 °C. The bright yellow anion was quenched with DMF (0.15 mL, 2.0 mmol) and stirring was continued at -78 °C for 3 h, after which time all of the colour had been discharged from the solution. A small portion of MeOH (0.5 mL) was added at low temperature and the mixture was allowed to warm up to room temperature. Standard workup provided a light yellow waxy solid which was crystallized from hexane to afford **1.171e** as a white solid (197 mg, 74%): m.p. 145-147 °C; ¹H-NMR (200 MHz, CDCl₃) δ 1.34 (d, J = 13.8 Hz, 18H), 7.5-7.7 (m, 3H), 7.9-8.1 (m, 1H), 9.36 (s, 1H); ¹³C-NMR (62.9 MHz, CDCl₃) δ 27.1, 36.8 (d, J = 58.1 Hz), 128.9 (d, J = 8.1 Hz), 130.4 (d, J = 10.6 Hz), 131.0 (d, J = 10.8 Hz), 131.3 (d, J = 2.5 Hz), 132.3 (d, J = 72.9 Hz), 144.3 (d, J = 4.3 Hz), 195.2; ³¹P-NMR (81 MHz, CDCl₃) δ 59.5; IR (KBr) ν_{max} 2966, 2906, 2868, 1692, 1586, 1474, 1396, 1369, 1197, 1148, 1118, 814, 772, 651 cm⁻¹; EI MS m/z (rel. intensity) 267 (M+1, 15), 238 (7), 210 (31), 182 (98), 153 (78), 126 (100), 105 (24), 79 (69); HRMS calcd for C₁₅H₂₄O₂P: 267.1514; found 267.1511.



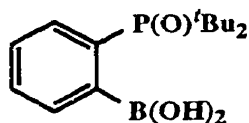
2-(Di-*tert*-butylphosphinyl)acetophenone (1.171f):

According to General Procedure D, *t*-BuLi (1.18 mL, 2.0 mmol, 1.70 M in pentane) was added to a stirred solution of **1.170** (238 mg, 1.0 mmol) in THF (10 mL) at -78 °C. After addition of *N*-methoxy-*N*-methyl acetamide, the solution was warmed to room temperature. TLC analysis of the mixture revealed only starting material and standard workup provided **1.170** (90% recovery).



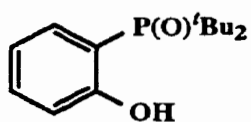
2-Di-*tert*-butylphosphinylbenzoic acid (1.171g): According to General Procedure D, *t*-BuLi (0.83 mL, 1.3 mmol, 1.59 M in pentane)

was added to a stirred solution of **1.170** (286 mg, 1.2 mmol) in THF (12 mL) at -78 °C. Excess anhydrous gaseous CO₂ (passed through a CaCl₂ drying tube) was bubbled through the yellow suspension for a several minutes. The internal temperature rose to -55 °C and the yellow colour was quickly dissipated. After 10 min the bath was removed and the mixture was allowed to warm to 10 °C. Acidification (1M HCl) and extraction with EtOAc followed by drying (MgSO₄) and evaporation provided **1.171g** as a white crystalline solid (144 mg, 42 %): m.p. 272-273.5 °C (dec.); ¹H-NMR (250 MHz, DMSO-d₆) δ 1.26 (d, J = 13.8 Hz, 18H), 7.5-7.8 (m, 4H), 11.6 (bs, 1H); ¹³C-NMR (50.3 MHz, CDCl₃) δ 27.1, 37.6 (d, J = 58.0 Hz), 127.4 (d, J = 71.7 Hz), 129.4 (d, J = 12.2 Hz), 131.2 (d, J = 12.2 Hz), 132.0, 136.5, 139.5, 167.6; ³¹P-NMR (81.0 MHz, CDCl₃) δ 60.2; IR (KBr) ν_{max} 1714, 1469, 1120 cm⁻¹; CI (CH₄) MS *m/z* (rel intensity) 283 ((M-H)⁺, 73), 265 (27), 225 (43), 209 (49), 182 (100), 169 (98), 126 (68); HRMS calcd for (M-H)⁺ 283.1463, found 283.1449; Anal. calcd for C₁₅H₂₃O₃P: C, 63.82; H, 8.21; P, 10.97; found: C, 63.69; H, 8.07; P, 11.21.

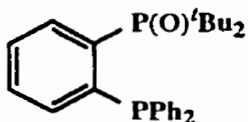


2-(Di-*tert*-butylphosphinyl)phenylboronic acid (1.171h):

According to General Procedure D, *t*-BuLi (0.65 mL, 1.0 mmol, 1.53 M in pentane) was added to a stirred solution of **1.170** (119 mg, 0.5 mmol) in THF (10 mL) at -78 °C. After quench with B(OMe)₃ (0.25 mL, 1.1 mmol) in one portion, the reaction mixture was warmed to room temperature and acidified with HCl (10% solution) until a pH < 3 was obtained. The mixture was poured into H₂O and extracted with CH₂Cl₂ (3 x 20 mL). The combined organic layers were dried (Na₂SO₄) and evaporated to yield a white solid which was used without further purification: m.p. > 260 °C; ¹H-NMR (250 MHz, CDCl₃) δ 1.36 (d, J = 15.0 Hz, 18H), 7.3-7.9 (m, 4H); ³¹P-NMR (81.0 MHz, CDCl₃) δ 86.6; IR ν_{max}(KBr) 3392, 2970, 1474, 1429, 1384, 1299, 1194, 1027, 996, 767, 746 cm⁻¹; MS CI *m/z* (rel intensity): 267 (M+1, 14), 240 (16), 239 (100), 183 (15), 182 (28), 161 (11), 126 (19), 57 (47); HRMS calcd for C₁₄H₂₅BO₂P: 267.1685; found 267.1698.

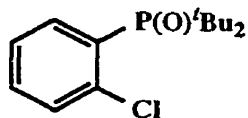


2-(Di-*tert*-butylphosphinyl)phenol (1.171i): According to General Procedure D, *t*-BuLi (0.63 mL, 1.0 mmol, 1.59 M in pentane) was added to a stirred solution of **1.170** (119 mg, 0.5 mmol) in THF (10 mL) at -78 °C. After addition of B(OMe)₃ (0.25 mL, 1.1 mmol), the mixture was warmed to room temperature and oxidized with H₂O₂ (1.2 mL of 30%) and NaOH (3.0 mL, 6.0 mmol, 2.0 M). The reaction mixture was stirred for 6 h at room temperature before addition of Na₂S₂O₃ (3.0 mL, 6.0 mmol, 2.0 M) and HCl (10 % solution, 15 mL). Extraction of the mixture with CH₂Cl₂ (3 x 30 mL) followed by drying (Na₂SO₄) and evaporation provided **1.171i** as a white solid (170 mg, 67%): m.p. 98-102 °C; ¹H-NMR (200 MHz, CDCl₃) δ 1.34 (d, J = 13.9 Hz, 18H), 6.7-6.9 (m, 2H), 7.2-7.5 (m, 2H); ³¹P-NMR (81.0 MHz, CDCl₃) δ 68.8; IR ν_{max}(KBr) 3433, 2971, 2663, 1591, 1495, 1490, 1299, 1115, 1099, 794; MS EI *m/z* (rel. intensity): 254 (M⁺, 59), 198 (60), 182 (12), 172 (17), 142 (100), 141 (50), 124 (20), 95 (55), 77 (42); HRMS calcd for C₁₄H₂₃O₂P: 254.1436; found 254.1431.



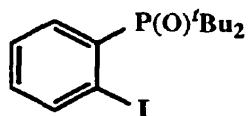
2-(Diphenylphosphino)phenyldi-*tert*-butylphosphine oxide (1.171j): According to General Procedure D, *t*-BuLi (1.67 mL, 2.0 mmol, 1.20 M in pentane) was added to a stirred solution of **1.170** (238 mg, 1.0 mmol) in THF (10 mL) at -78 °C. After addition of chlorodiphenylphosphine (0.36 mL, 442 mg, 2.0 mmol) the mixture was worked up and crystallized from hexane to afford **1.171j** as a white solid (266 mg, 63%): m.p. 250-252 °C; ¹H-NMR (250 MHz, CDCl₃) δ 1.13 (d, J = 13.5 Hz, 18H), 7.3-7.6 (m, 9H), 7.6-7.8 (m, 4H), 7.8-8.0 (m, 1H); ¹³C-NMR (125.8 MHz, CDCl₃) δ 27.7, 37.3 (d, J = 57.4 Hz), 127.8 (d, J = 12.9 Hz), 129.3 (d, J = 10.0 Hz), 130.2 (d, J = 11.4 Hz), 130.4 (d, J = 2.6 Hz), 131.8 (d, J = 9.7 Hz), 132.4 (t, J = 11.2 Hz), 135.7 (d, J = 109.6 Hz), 136.6 (dd, J = 75.0 and 8.6 Hz), 137.2 (dd, J = 11.8 and 7.5 Hz), 139.0 (dd, J = 96.9 and 7.0 Hz); ³¹P-NMR (81 MHz, CDCl₃) δ 54.9 (d, J = 5.0 Hz), 30.9 (d, J = 5.0 Hz); IR ν_{max}(KBr) 2962, 2900, 1475, 1438, 1201, 1178, 1170, 1115 cm⁻¹; MS CI (isobutane) *m/z* 423 (M+1, 47), 365 (100), 309 (1), 262 (1). Anal. calcd

for C₂₆H₃₂OP₂: C, 73.92; H, 7.63; found: C, 73.41; H, 7.32; CI MS (air-oxidized phosphine) *m/z* (rel intensity) 439 (M⁺+1, 13), 247 (14), 219 (100), 201 (20), 141 (40), 107 (4), 79 (9), 57 (5).



2-Chlorophenyldi-*tert*-butylphosphine oxide (1.171k):

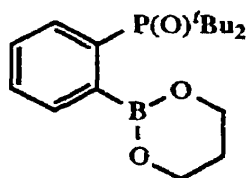
According to General Procedure D, *t*-BuLi (1.30 mL, 2.0 mmol, 1.53 M in pentane) was added to a stirred solution of **1.170** (238 mg, 1.0 mmol) in THF (10 mL) at -78 °C. After addition of hexachloroethane (473 mg, 2.0 mmol) the mixture was worked up and crystallized from hexane to afford **1.171k** as a white solid (145 mg, 53%): m.p. 81-82 °C; ¹H-NMR (250 MHz, CDCl₃) δ 1.35 (d, *J* = 14.5 Hz, 18H), 7.42 (bs, 4H); ¹³C-NMR (50.3 MHz, CDCl₃) δ 27.1, 37.1 (d, *J* = 59.1 Hz), 126.4 (d, *J* = 8.3 Hz), 130.5 (d, *J* = 6.5 Hz), 132.0 (d, *J* = 69.7 Hz), 132.2, 134.1 (d, *J* = 4.7 Hz), 138.6 (d, *J* = 4.3 Hz); ³¹P-NMR (81 MHz, CDCl₃) δ 60.8; IR (KBr) ν_{max} 2967, 2902, 1578, 1478, 1455, 1422, 1365, 1139, 1033, 813, 741, 648 cm⁻¹; MS EI *m/z* (rel intensity): 273 (4), 257 (1), 218 (35), 216 (75), 199 (9), 181 (10), 162 (41), 160 (91), 125 (20), 123 (17), 113 (23), 107 (14), 95 (11), 77 (31), 57 (100); HRMS calcd for : 272.1097, found: 272.1103.



2-Iodophenyldi-*tert*-butylphosphine oxide (1.171m):

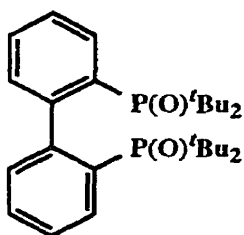
According to General Procedure D, *t*-BuLi (3.10 mL, 4.0 mmol, 1.29 M in pentane) was added to a stirred solution of **1.170** (476 mg, 2.0 mmol) in THF (20 mL) at -78 °C. Iodine (1.015 g, 4.0 mmol) was added to the reaction mixture either directly or as a solution in anhydrous THF (15 mL). After warming to room temperature over several hours, the resulting dark orange/red solution was poured into a mixture of H₂O (20 mL), CH₂Cl₂ (50 mL), and Na₂S₂O₃ (20 mL, 2 M aqueous solution) discharging most of the colour. The organic layer was separated and the aqueous layer was extracted with CH₂Cl₂ (3 x 50 mL). The combined organic extracts were dried (Na₂SO₄) and evaporated to yield a light yellow solid. Purification by flash chromatography (3%

MeOH/CH₂Cl₂) afforded **1.171m** as a white solid (549 mg, 76%): m.p. 164.5-165.0 °C (Et₂O / CH₂Cl₂); ¹H-NMR (250 MHz, CDCl₃) δ 1.33 (d, J = 13.6 Hz, 18H), 7.09 (dddd, J = 1.5, 3.0, 7.6 and 7.7 Hz, 1H), 7.37 (dddd, J = 1.4, 2.2, 7.5 and 7.7 Hz, 1H), 7.54 (ddd, J = 1.5, 7.8 and 9.7 Hz, 1H), 8.15 (ddd, J = 1.3, 2.1 and 8.0 Hz, 1H); ¹³C-NMR (63 MHz, CDCl₃) δ 27.5, 37.2 (d, J = 59.1 Hz), 98.7, 125.8 (d, J = 10.0 Hz), 131.3 (d, J = 76.5 Hz), 131.7, 144.4 (d, J = 8.0 Hz); ³¹P-NMR (81 MHz, CDCl₃) δ 53.3; IR (KBr) ν_{max} 3091, 3057, 2976, 2951, 2895, 1574, 1556, 1469, 1445, 1407, 1164 cm⁻¹; MS EI *m/z* (rel intensity) 364 (M⁺, 49%), 252 (100%), 125 (76%), 57 (44%); Anal. calcd for C₁₄H₂₂IOP: C, 46.17; H, 6.09, P, 8.50; found: C, 45.95; H, 5.89; P, 8.69.

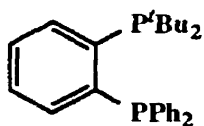


2-(Di-tert-butylphosphinyl)phenylboronic acid 1,3-propanediol ester (1.171n): A solution of crude boronic acid **1.171h**, used without further purification, was dissolved in anhydrous CH₂Cl₂ (10 mL) and a solution of 1,3-propanediol (40 mg, 0.52 mmol)

in anhydrous CH₂Cl₂ was added. A small portion (50 mg) of MgSO₄ was added to absorb the water that was produced and the mixture was stirred under nitrogen for 24 h. The mixture was filtered and the filtrate was evaporated to give a white solid. Recrystallization from hexane provided **1.171n** as a white solid (105 mg, 65% from **1.170**): m.p. 194-197 °C (hexane); ¹H-NMR (200 MHz, CDCl₃) δ 1.32 (d, J = 14.8 Hz, 18H), 1.79 (bs, 2H), 4.01 (bs, 4H), 7.28-7.35 (m, 1H), 7.42-7.54 (m, 2H), 7.73 (dd, J = 7.4 and 0.8 Hz, 1H); ³¹P-NMR (81 MHz, CDCl₃) δ 79.5; IR (KBr) ν_{max} 2965, 1476, 1438, 1383, 1299, 1194, 1108, 1069, 1024, 816, 652 cm⁻¹; MS CI *m/z* (rel intensity): 323 (M+1, 6), 283 (28), 255 (100), 239 (99), 198 (23), 182 (50), 161 (21), 142 (29), 126 (34), 57 (62); Anal. calcd for C₁₇H₂₈BO₃P: C, 63.37; H, 8.76; found: C, 63.42; H, 8.85. X-ray analysis, Appendix 5.

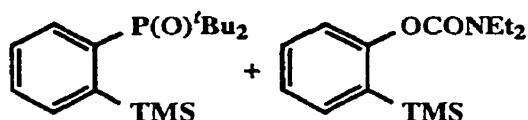


2,2'-Bis(di-*tert*-butylphosphinyl)biphenyl (1.176): To a solution of 2-iododi-*tert*-butylphenylphosphine oxide (**1.171m**, 163 mg, 0.45 mmol) in DMF (10 mL) was added copper powder (570 mg, 9.00 mmol), and the mixture was heated at 160 °C for 12 h. The mixture was cooled and filtered through glass wool and the residue was washed with CH₂Cl₂ (5 mL). The filtrate was washed with HCl (2 M, 2 x 10 mL) then water (1 x 10 mL). The combined aqueous layers were extracted with CH₂Cl₂ (1 x 10 mL) and the combined organic extracts were dried (Na₂SO₄) and evaporated affording a pale yellow solid. Recrystallization (hexane) provided **1.176** as a white crystalline solid (96%): m.p. 247-250 °C; ¹H-NMR (200 MHz, CDCl₃) δ 1.25 (d, J = 13.2 Hz, 18H), 1.37 (d, J = 13.5 Hz, 18H), 7.23-7.40 (m, 6H), 7.44-7.58 (m, 2H); ¹³C-NMR (63 MHz, CDCl₃) δ 27.4, 29.2, 36.6 (d, J = 8.8 Hz), 124.9 (d, J = 11.8 Hz), 128.2, 128.4 (d, J = 79.6 Hz), 130.8 (d, J = 11.7 Hz), 132.9 (d, J = 9.4 Hz), 148.8; ³¹P-NMR (81.0 MHz, CDCl₃) δ 54.2; IR (KBr) ν_{max} 3059, 2988, 2963, 1644, 1590, 1561, 1470, 1425, 1170 cm⁻¹; CI MS (CH₄) *m/z* (rel intensity) 475 (M+1, 100), 417 (33), 313 (84), 183 (30); Anal. calcd for C₂₈H₄₄O₂P₂; C, 70.86; H, 9.34; P, 13.05; found: C, 71.06; H, 9.24; P, 12.79. X-ray analysis, Appendix 6.



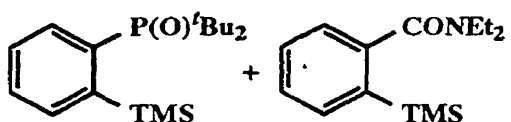
2-(Di-*tert*-butylphosphino)triphenylphosphine (1.177): A solution of 2-di-*tert*-butylphosphinyltriphenylphosphine (210 mg, 0.5 mmol) in anhydrous toluene (30 mL) and triethylamine (0.69 mL, 5.0 mmol), was treated with HSiCl₃ (0.5 mL, 5.0 mmol). The reaction mixture was stirred for 1 h during which a white precipitate was formed. The reaction mixture was then heated to reflux for 3 hours, cooled on an ice bath and treated slowly with aqueous NaOH (10 mL, 2 M). The organic phase was separated, washed with water, dried (MgSO₄), and evaporated to provide a white solid. Purification by flash chromatography (EtOAc, followed by 3% MeOH/EtOAc) afforded **1.177** as a white solid (159 mg, 78%): m.p. 248 °C (dec.); ¹H-NMR (250 MHz, CDCl₃) δ 1.24 (d, J = 13.5 Hz, 18H), 7.00-7.15 (m, 1H), 7.20-7.45 (m, 12H), 7.55-7.70

(m, 1H); ^{13}C -NMR (62.5 MHz, CDCl_3) δ 27.3, 37.1 (d, $J = 57.2$ Hz), 125.9 (d, $J = 10.3$ Hz), 127.6, 127.8, 127.9, 130.2, 131.2-131.8 (m), 133.9, 134.2, 135.1 (dd, $J = 77.0$ and 21.4 Hz), 135.9, 136.1, 139.9 (d, $J = 18.2$ Hz), 146.6 (dd, $J = 34.2$ and 7.5 Hz); ^{31}P -NMR (81.0 MHz, CDCl_3) δ 57.8, -5.5. Anal. calcd for $\text{C}_{26}\text{H}_{32}\text{P}_2$: C, 76.83; H, 7.93. found: C, 76.63; H, 7.77.



Competitive formation of *N,N*-Diethyl (2-trimethylsilyl)phenyl-*O*-carbamate (1.179a) and 2-(trimethylsilyl)phenyldi-*tert*-butylphosphine oxide (1.171a):

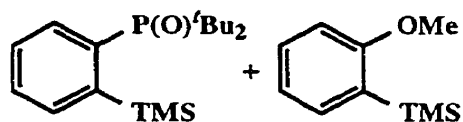
According to General Procedure E, a solution of **1.170** (83 mg, 0.35 mmol) and **1.178a** (68 mg, 0.35 mmol, prepared according to General Procedure F) in anhydrous THF (5 mL) was treated with *t*-BuLi (0.21 mL, 0.35 mmol, 1.69 M). After stirring for a period of 5 min, TMSCl (0.07 mL, 0.53 mmol) was added and the mixture was worked up and analyzed by GC to give a product mixture consisting of **1.170** (94% of original), **1.178a** (30% of original), and **1.179a** (66% yield). There was no detectable amount of **1.171a** in the reaction mixture. A metalation period of 1 h gave a similar product ratio (92%, 35%, 65%, and 0% of **1.170**, **1.178a**, **1.79a**, and **1.171a**, respectively).



Competitive formation of *N,N*-Diethyl 2-(trimethylsilyl)benzamide (1.179b) and 2-(trimethylsilyl)phenyldi-*tert*-butylphosphine oxide (1.171a):

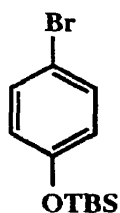
According to General Procedure E, a solution of **1.170** (95 mg, 0.40 mmol) and **1.178b** (71 mg, 0.40 mmol, prepared according to General Procedure G) in anhydrous THF (5 mL) was treated with *t*-BuLi (0.24 mL, 0.40 mmol, 1.69 M). After stirring for a period of 5 min, TMSCl (0.08 mL, 0.57 mmol) was added and the mixture was worked up and analyzed by GC to give a product mixture consisting of **1.170** (82% of original), **1.171a** (15% yield), **1.178b** (35% of original), and **1.179b** (61% yield). A metalation

period of 1 h gave a similar product ratio but slightly higher yield of products (70%, 21%, 15%, and 82% of **1.170**, **1.171a**, **1.178b**, and **1.179b**, respectively). In a related experiment contributed by another researcher, the same two substrates were allowed to compete for a molar equivalent of *t*-BuLi and then quenched with CH₃I. The ratio of products was 4:1 as determined by integration of the CH₃ peaks in the ¹H-NMR spectrum.²⁷⁵



Competitive formation of 2-Trimethylsilylanisole (1.179c) and 2-(trimethylsilyl)phenyldi-*tert*-butylphosphine oxide (1.171a):

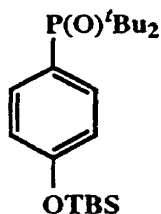
(**1.171a**): According to General Procedure E, a solution of **1.170** (83 mg, 0.35 mmol) and **1.178c** (38 mg, 0.35 mmol, distilled from CaH₂) in anhydrous THF (5 mL) was treated with *t*-BuLi (0.21 mL, 0.35 mmol, 1.69 M). After stirring for a period of 5 min. TMSCl (0.07 mL, 0.53 mmol) was added and the mixture was worked up and analyzed by GC to give a product mixture consisting of **1.170** (73% of original), **1.178a** (100% of original), and **1.171a** (13% yield). There was no detectable amount of **1.179c** in the reaction mixture. A metalation period of 1 h gave a greater yield of product while maintaining a similar product ratio (45%, 100%, 46%, and 0% of **1.170**, **1.178a**, **1.171a**, and **1.179c**, respectively).



4-(*tert*-Butyldimethylsilyloxy)bromobenzene (1.180): To a solution of *p*-bromophenol (8.65 g, 50 mmol) in DMF (100 mL) was added imidazole (3.40 g, 50 mmol) and TBSCl (7.54 g, 50 mmol). The reaction mixture was stirred at room temperature for 3 h, after which there was no

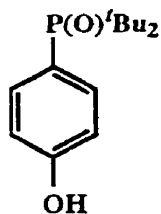
starting material evident by TLC. The solution was poured into H₂O (100 mL) and Et₂O (100 mL) was added. The layers were separated and the Et₂O layer was extracted successively with H₂O (6 x 100 mL), NaOH (10%, 1 x 50 mL), HCl (10%, 1 x 50 mL), and finally H₂O (1 x 100 mL). The Et₂O layer was dried (Na₂SO₄) and evaporated to yield a colourless oil. Purification by flash chromatography (hexane) provided a colourless oil with data matching

that reported for **1.180** (12.95 g, 94%): $^1\text{H-NMR}$ (200 MHz, CDCl_3) δ 7.31 (d, $J = 8.8$ Hz, 2H), 6.71 (d, $J = 8.8$ Hz, 2H), 0.97 (s, 9H), 0.18 (s, 6H); $^{13}\text{C-NMR}$ (50.3 MHz, CDCl_3) δ 154.8, 132.3, 121.9, 113.6, 25.6, 18.2, -4.5.



(4-*tert*-Butyldimethylsilyloxyphenyl)di-*tert*-butylphosphine

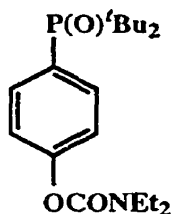
oxide: According to General Procedure C, a solution of **1.180** (3.02 g, 10.5 mmol) in anhydrous Et_2O (20 mL) at -78 °C was treated with $t\text{-BuLi}$ (14.3 mL, 22.0 mmol, 1.54 M solution). The newly-formed aryllithium was transferred to a solution of chloro-di-*tert*-butylphosphine (1.90 g, 10.5 mmol) in Et_2O (20 mL) and heated to reflux for a period of 6 h. Workup and oxidation of the crude phosphine with H_2O_2 in MeOH allowed isolation of an off-white solid. Upon analysis of the $^1\text{H-NMR}$ spectrum of the crude product, it was determined that partial cleavage of the silyl ether had occurred and thus the entire mixture was subjected to hydrolysis conditions.



4-(Di-*tert*-butylphosphinyl)phenol (1.182): The crude product from the formation of **1.181** was dissolved in a mixture of THF (100 mL) and DMF (40 mL) and to it was added H_2O (1 mL) and CsF (1.91 g, 12.6 mmol). After stirring for 12 h at room temperature, the brown solution was

poured into water (100 mL) and extracted with CH_2Cl_2 (1 x 50 mL). The aqueous layer was acidified (10% HCl) and extracted with CH_2Cl_2 (3 x 50 mL). The combined organic layers were dried and evaporated to give an oily mixture. The remaining DMF was removed under high vacuum providing a slightly yellow solid. Trituration with hot hexane followed by filtration provided **1.182** as a white solid (1.807 g, 68% from **1.180**): m.p. 269-272 °C; $^1\text{H-NMR}$ (250 MHz, CDCl_3) δ 1.29 (d, $J = 13.9$ Hz, 18H), 7.20 (bs, 2H), 7.75 (bs, 2H); $^{13}\text{C-NMR}$ (50.3 MHz, CDCl_3) δ 27.0, 35.9 (d, $J = 60.5$ Hz), 115.7 (d, $J = 11.3$ Hz), 117.6 (d, $J = 89.3$ Hz), 133.8, 161.5 (d, $J = 2.8$ Hz); $^{31}\text{P-NMR}$ (81.0 MHz, CDCl_3) δ 56.4; IR ν_{max} (KBr) 3428, 2970, 2491, 1599, 1579, 1505, 1295, 1125, 1096, 837, 814 cm^{-1} ; EI MS

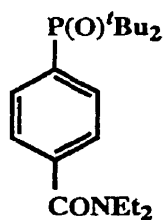
m/z (rel. intensity) 254 (M^+ , 8), 209 (28), 198 (81), 162 (14), 157 (12), 153 (13), 151 (47), 142 (100), 124 (14), 106 (18), 95 (54), 77 (55), 65 (22), 57 (91); HRMS calcd for $C_{14}H_{23}O_2P$: 254.1436; found: 254.1433; Anal. calcd for $C_{14}H_{23}O_2P$: C, 66.12; H, 9.12. found: C, 65.42; H, 9.24.



***N,N*-Diethyl-*O*-(4-di-*tert*-butylphosphinyl)phenyl carbamate**

(1.183a): According to General Procedure F, a solution of phenol **1.182** (508 mg, 2.0 mmol) in CH_3CN (25 mL) was treated with K_2CO_3 (332 mg, 2.4 mmol) and *N,N*-diethyl carbamoyl chloride (0.38 mL, 3.0 mmol). After

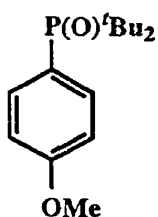
heating at reflux for a period of 30 h, TLC showed no remaining starting material. The cooled reaction mixture was poured into H_2O (150 mL) and extracted with CH_2Cl_2 (3 x 50 mL). The combined organic layers were dried (Na_2SO_4) and evaporated to yield a waxy brown solid. Purification by flash chromatography (4% MeOH/ CH_2Cl_2) afforded **1.183a** as a white solid: m.p. 99.5-101 °C; 1H -NMR (250 MHz, $CDCl_3$) δ 1.27 (d, $J = 13.5$ Hz, 18H), 1.1-1.4 (m, 6H), 3.3-3.5 (m, 4H), 7.25 (d, $J = 8.0$ Hz, 2H), 7.86 (bs, 2H); ^{13}C -NMR (62.9 MHz, $CDCl_3$) δ 13.2, 14.1, 26.9, 35.7 (d, $J = 60.3$ Hz), 41.9, 42.3, 121.0 (d, $J = 11.0$ Hz), 127.5 (d, $J = 79.8$ Hz), 133.5, 153.4, 153.7 (d, $J = 3.1$ Hz); ^{31}P -NMR (81.0 MHz, $CDCl_3$) δ 52.0; IR ν_{max} (KBr) 2978, 1717, 1473, 1422, 1276, 1213, 1180, 1152, 1098 cm^{-1} ; EI MS m/z (rel. intensity) 354 (10), 296 (9), 241 (100), 194 (14), 141 (4), 100 (20), 72 (27); Anal. calcd for $C_{19}H_{32}NO_3P$: C, 64.56; H, 9.13; N, 3.96. found: C, 64.62; H, 8.95; N, 4.08.



***N,N*-Diethyl 4-di-*tert*-butylphosphinylbenzamide** (**1.183b**):

According to a literature procedure,²⁶⁸ a solution of phosphine oxide **1.185** (567 mg, 4.0 mmol) in pyridine/ H_2O (4.5 mL, 2.0 mL) was treated with $KMnO_4$ (1.066 g, 6.7 mmol) and heated to reflux for 3 h. The solution was cooled to room temperature, acidified with several drops of conc. HCl, and finally treated with $NaNO_2$ (sat. sol'n, 0.5 mL) resulting in a colourless solution with a white precipitate. The

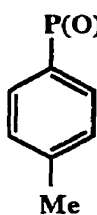
solution was extracted with CH₂Cl₂ (3 x 20 mL), and the combined organics were dried (Na₂SO₄) and evaporated yielding benzoic acid **1.186** as a white solid. According to General Procedure G, **1.186** was dissolved in excess SOCl₂ (15 mL) and a few drops of DMF were added. When evolution of gas was no longer evident, SOCl₂ was removed by azeotroping with toluene (3 x 50 mL). The residue was dissolved in THF (30 mL) and cooled to 0 °C and HNEt₂ (0.88 mL, 8.5 mmol) was added. After stirring for 1-2 h, extraction with CH₂Cl₂ (3 x 20 mL) followed by drying (Na₂SO₄) and evaporation provided a colourless oil. Purification by column chromatography (EtOAc, then 3% MeOH/EtOAc) provided **1.183b** as a white solid (732 mg, 51% from 4-bromotoluene): m.p. 157-157.5 °C; ¹H-NMR (250 MHz, CDCl₃) δ 1.0–1.4 (m, 6H), 1.28 (d, J = 13.7 Hz, 18H), 3.2-3.4 (m, 2H), 3.5-3.7 (m, 2H), 7.47 (dd, J = 8.2, 1.8 Hz, 2H), 7.92 (bs, 2H); ¹³C-NMR (62.9 MHz, CDCl₃) δ 12.7, 14.0, 26.8, 35.6 (d, J = 60.5 Hz), 39.1, 43.1, 125.5 (d, J = 10.1 Hz), 132.3, 132.3 (d, J = 76.5 Hz), 139.4, 170.2; ³¹P-NMR (81.0 MHz, CDCl₃) δ 52.3; IR ν_{max}(KBr) 2970, 2904, 2871, 1624, 1475, 1429, 1158, 846, 815, 652 cm⁻¹; EI MS *m/z* (rel intensity) 338 (M⁺, 100), 281 (15), 265 (12), 225 (70), 152 (38), 151 (28), 124 (27); Anal. calcd for C₁₉H₃₂NO₂P: C, 67.63; H, 9.56; N, 4.15. found: C, 67.61; H, 9.31; N, 4.09.



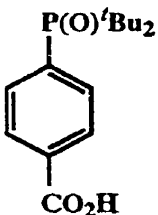
4-(Di-tert-butylphosphinyl)anisole (1.183c): To a solution of phenol **1.182** (508 mg, 2.0 mmol) in CH₃CN (25 mL) at room temperature was added K₂CO₃ (332 mg, 2.4 mmol) and CH₃I (0.19 mL, 3.0 mmol). The mixture was heated to reflux and stirred for 6 h after which TLC analysis

indicated no remaining starting material. The solution was cooled to room temperature, poured into H₂O (150 mL) and extracted with CH₂Cl₂ (3 x 50 mL). The combined organic layers were dried (Na₂SO₄) and evaporated to give a light yellow solid. Purification by flash chromatography (3% MeOH/CH₂Cl₂) afforded **1.183c** as a white solid (494 mg, 92%): m.p. 104-106 °C; ¹H-NMR (200 MHz, CDCl₃) δ 1.26 (d, J = 13.5 Hz, 18H), 3.85 (s, 3H), 6.97 (dd, J = 8.9, 1.9 Hz, 2H), 7.79 (t, J = 7.9 Hz, 2H); ¹³C-NMR (50.3 MHz, CDCl₃) δ 26.9,

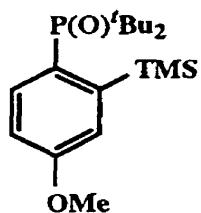
35.6 (d, $J = 61.0$ Hz), 55.0, 113.2 (d, $J = 10.7$ Hz), 122.2 (d, $J = 83.0$ Hz), 133.8, 161.5 (d, $J = 3.2$ Hz); ^{31}P -NMR (81.0 MHz, CDCl_3) δ 51.9; IR (KBr) ν_{max} 3060, 2961, 2901, 2869, 2838, 1596, 1569, 1493, 1474, 1462, 1285, 1252, 1180, 1151, 1100 cm^{-1} ; MS CI m/z (rel intensity): 269 ($M+1$, 96), 213 (16), 212 (99), 211 (25), 161 (14), 156 (53), 155 (100), 109 (18), 77 (14), 57 (29); HRMS calcd for $\text{C}_{15}\text{H}_{26}\text{O}_2\text{P}$: 269.1670; found 267.1668.



Di-tert-butyl-*p*-tolylphosphine oxide (1.185): According to General Procedure C, a solution of freshly distilled *p*-bromotoluene (**1.184**, 730 mg, 4.3 mmol) in anhydrous Et_2O (20 mL) at -78 °C was treated with *t*-BuLi (5.0 mL, 8.6 mmol, 1.71 M solution). An excess of the newly-formed aryllithium was added to a solution of chloro-di-*tert*-butylphosphine (432 mg, 2.4 mmol) in Et_2O (20 mL) and heated to reflux for a period of 2 h. The reaction mixture was cooled and quenched by addition of MeOH (2 mL). After removal of the solvent under reduced pressure, the residue was suspended in MeOH (10 mL) and cooled to 0 °C before H_2O_2 (1.0 mL of a 30% solution, approx. 9 mmol) was added dropwise. Workup with excess Na_2SO_3 (10 mL, 2 M solution) and HCl (10 mL, 10% solution) followed by removal of MeOH, extraction with CH_2Cl_2 (3 x 20 mL), drying with Na_2SO_4 , and evaporation of solvent allowed isolation of a colourless oil. Upon analysis of the ^1H -NMR spectrum of the crude product, it was used without further purification: ^1H -NMR (250 MHz, CDCl_3) δ 1.25 (d, $J = 12.4$ Hz, 18H), 2.40 (s, 3H), 7.32-7.40 (m, 2H), 7.65-7.90 (m, 2H).



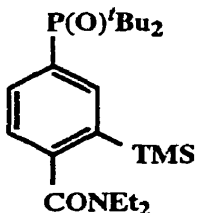
4-Di-tert-butylphosphinylbenzoic acid (1.186): Benzoic acid **1.186** was prepared and used without purification as described in the procedure for preparation of benzamide **1.183b** above.



Di-tert-butyl-(4-methoxy-2-trimethylsilylphenyl)phosphine

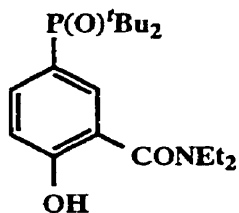
oxide (1.187c): According to General Procedure H, a solution of anisole **1.183c** (94 mg, 0.35 mmol) in anhydrous THF (5 mL) at $-78\text{ }^{\circ}\text{C}$ was treated with *t*-BuLi (0.25 mL, 0.42 mmol, 1.69 M). The resulting yellow solution

was stirred for 2-3 min at $-78\text{ }^{\circ}\text{C}$ before excess TMSCl (0.070 mL, 0.53 mmol) was added causing an immediate discharge of the yellow colour. After slowly warming the solution to room temperature, TLC analysis indicated one new compound and some remaining starting material. The mixture was quenched with saturated NH_4Cl solution, poured into H_2O (20 mL) and extracted with CH_2Cl_2 (3 x 20 mL). The combined organic extracts were dried (Na_2SO_4) and evaporated providing a colourless oil. Flash chromatography (1% MeOH/ CH_2Cl_2) of the mixture allowed isolation of starting material (11 mg, 12%) and **1.187c** (76 mg, 64%). Extending the metalation time to 1 h increased the yield of **1.187c** to 73%. A small amount of starting material was present by TLC but was not isolated. m.p. $177\text{-}179\text{ }^{\circ}\text{C}$; $^1\text{H-NMR}$ (250 MHz, CDCl_3) δ 0.43 (s, 9H), 1.26 (d, $J = 13.2\text{ Hz}$, 18H), 3.86 (s, 3H), 6.89 (dt, $J = 8.5, 2.4\text{ Hz}$, 1H), 7.41 (t, $J = 2.1\text{ Hz}$, 1H), 7.54 (dd, $J = 9.7, 8.7\text{ Hz}$, 1H); $^{13}\text{C-NMR}$ (62.9 MHz, CDCl_3) δ 2.80, 27.6, 36.7 (d, $J = 58.2\text{ Hz}$), 54.9, 111.6 (d, $J = 13.2\text{ Hz}$), 123.2 (d, $J = 13.9\text{ Hz}$), 127.7 (d, $J = 88.8\text{ Hz}$), 132.3 (d, $J = 16.0\text{ Hz}$), 149.6 (d, $J = 11.8\text{ Hz}$), 160.4 (d, $J = 2.8\text{ Hz}$); $^{31}\text{P-NMR}$ (81.0 MHz, CDCl_3) δ 56.0; IR (KBr) ν_{max} 2945, 2900, 1585, 1564, 1476, 1388, 1285, 1226, 1157, 1148, 1118, 1052, 1032, 870 cm^{-1} ; CI MS m/z (rel. intensity) 341 ($\text{M}+1$, 31), 340 (M^+ , 2), 327 (26), 325 (100), 309 (15), 285 (14), 283 (30), 269 (26), 227 (32), 213 (17), 211 (25), 57 (33); HRMS calcd for $\text{C}_{18}\text{H}_{34}\text{O}_2\text{PSi}$: 341.2058; found 341.2066.



***N,N*-Diethyl 4-di-tert-butylphosphinyl-2-trimethylsilylbenzamide (1.188b):** According to General Procedure H, a solution of benzamide **1.183b** (97 mg, 0.29 mmol) in anhydrous THF (5 mL) at $-78\text{ }^{\circ}\text{C}$ was treated with *t*-BuLi (0.22 mL, 0.35 mmol, 1.62 M). The resulting

yellow solution was stirred for 60 min at $-78\text{ }^{\circ}\text{C}$ before excess TMSCl (0.10 mL, 0.78 mmol) was added causing an immediate discharge of the yellow colour. After slowly warming the solution to room temperature, MeOH (5 mL) was added and the mixture was poured into H_2O (20 mL) and extracted with CH_2Cl_2 (3 x 20 mL). The combined organic extracts were dried (Na_2SO_4) and evaporated providing a colourless oil. Purification by column chromatography (EtOAc) provided **1.188b** as a colourless oil (68 mg, 57%). Enhancement (11%) of the TMS signal in the $^1\text{H-NMR}$ spectrum upon irradiation of the amide methylene signal confirmed the regioselectivity of silylation: $^1\text{H-NMR}$ (250 MHz, CDCl_3) δ 0.30 (s, 9H), 1.1-1.4 (m, 6H), 1.28 (d, $J = 13.6$ Hz, 18H), 3.15 (q, $J = 7.1$ Hz, 2H), 3.57 (q, $J = 7.1$ Hz, 2H), 7.30 (dd, $J = 8.1, 2.1$ Hz, 1H), 7.89 (d, $J = 8.1$ Hz, 1H), 8.02 (d, $J = 8.1$ Hz, 1H); $^{13}\text{C-NMR}$ (50.3 MHz, CDCl_3) δ 6.4, 11.9, 15.2, 26.6, 36.0 (d, $J = 60.1$ Hz), 42.9, 44.1, 116.1 (d, $J = 8.9$ Hz), 125.5 (d, $J = 10.6$ Hz), 131.0 (d, $J = 11.0$ Hz), 132.2 (d, $J = 75.9$ Hz), 134.1 (d, $J = 15.7$ Hz), 135.2, 168.9; $^{31}\text{P-NMR}$ (81.0 MHz, CDCl_3) δ 52.4; Anal. calcd for $\text{C}_{22}\text{H}_{40}\text{NO}_2\text{PSi}$: C, 64.51; H, 9.84; N, 3.42. found: C, 64.55; H, 9.69; N, 3.50.

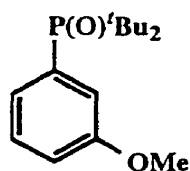


***N,N*-Diethyl 5-(di-*tert*-butylphosphinyl)salicylamide**

(1.189): According to General Procedure H, a solution of **1.183a** (120 mg, 0.34 mmol) in anhydrous THF (10 mL) at $-78\text{ }^{\circ}\text{C}$ was treated with *t*-BuLi (0.34 mmol, 0.21 mL of a 1.62 M solution in pentane).

The solution turned yellow upon addition of the *t*-BuLi, however, after only 2-3 minutes, the colour dissipated. Stirring was continued for 1.5 h at $-78\text{ }^{\circ}\text{C}$ before TMSCl (44.3 mg, 0.41 mmol, 0.05 mL) was added. After slowly warming to room temperature, NH_4Cl (sat'd aqueous) was added and the mixture was worked up and extracted with CH_2Cl_2 . The combined organics were dried (Na_2SO_4) and evaporated providing a colourless oil. Purification by flash chromatography (4% MeOH/ CH_2Cl_2) provided **1.189** as a white solid (42 mg, 35%). Shortening the metalation period had no appreciable effect on product distribution: m.p. $194\text{-}197\text{ }^{\circ}\text{C}$; $^1\text{H-NMR}$ (200 MHz, $50\text{ }^{\circ}\text{C}$, CDCl_3) δ 1.27 (t, $J = 7.1$ Hz,

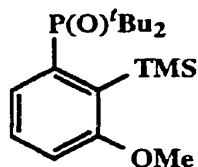
6H), 1.27 (d, $J = 13.9$ Hz, 18H), 3.49 (q, $J = 7.1$ Hz, 4H), 7.09 (d, $J = 8.4$ Hz, 1H), 7.66 (s, 1H), 7.95 (d, $J = 9.5$ Hz, 1H), 10.71 (s, 1H exch.); ^{13}C -NMR (50.3 MHz, CDCl_3) δ 12.6, 15.2, 27.0, 35.6 (d, $J = 59.9$ Hz), 36.2, 44.2, 120.9 (d, $J = 13.0$ Hz), 124.6 (d, $J = 11.1$ Hz), 130.1 (d, $J = 71.0$ Hz), 132.5, 139.0 (d, $J = 11.9$ Hz), 158.7, 165.4; ^{31}P -NMR (81.0 MHz, CDCl_3 , room temp) δ 53.3, 55.1; ^{31}P -NMR (81.0 MHz, CDCl_3 , 50 °C) δ 52.8, 54.5; MS EI m/z (rel intensity): 353 (M^+ , 31), 325 (7), 296 (24), 282 (9), 254 (12), 240 (100), 198 (14), 167 (53), 149 (11), 142 (18), 95 (18), 74 (37), 57 (83); HRMS calcd for $\text{C}_{19}\text{H}_{32}\text{NO}_3\text{P}$ 353.2120; found 353.2114.



Di-*tert*-butyl-(3-methoxyphenyl)phosphine oxide (1.190a):

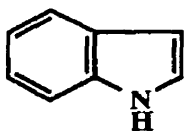
According to General Procedure C, a solution of freshly distilled 3-bromoanisole (846 mg, 4.52 mmol) in anhydrous Et_2O (20 mL) at -78 °C was treated with *t*-BuLi (5.3 mL, 9.06 mmol, 1.71 M solution). The newly-formed phenyllithium was added to a solution of chloro-di-*tert*-butylphosphine (816 mg, 4.52 mmol) in Et_2O (20 mL) at -78 °C and the mixture was stirred for 1 h. The cooling bath was removed and replaced with an ice bath and the reaction mixture was allowed to stir and slowly warm to room temperature. The reaction mixture was cooled and quenched by addition of MeOH (2 mL). After removal of the solvent under reduced pressure, the residue was suspended in MeOH (20 mL) and cooled to 0 °C before H_2O_2 (1.0 mL of a 30% solution, approx. 9 mmol) was added dropwise. Workup with excess Na_2SO_3 (20 mL, 2 M solution) and HCl (20 mL, 10% solution) followed by removal of MeOH, extraction with CH_2Cl_2 (3 x 50 mL), drying with Na_2SO_4 , and evaporation of solvent allowed isolation of a white solid. Purification by flash chromatography (3% MeOH/EtOAc) provided **1.190a** as a white waxy solid (703 mg, 58%): ^1H -NMR (250 MHz, CDCl_3) δ 1.28 (d, $J = 13.6$ Hz, 18H), 3.86 (s, 3H), 7.02 (s, 1H), 7.2-7.7 (m, 3H); ^{13}C -NMR (62.9 MHz, CDCl_3) δ 26.9, 35.7 (d, $J = 61.1$ Hz), 55.2, 116.6, 117.4, 117.8, 128.6 (d, $J = 11.9$ Hz), 132.7 (d, $J = 78.0$ Hz), 159.1; ^{31}P -NMR (81.0 MHz, CDCl_3) δ 52.1; IR (KBr) ν_{max} 2960, 2913, 1599, 1558, 1490, 1472, 1460,

1315, 1280, 1251 cm^{-1} . Anal. calcd for $\text{C}_{15}\text{H}_{25}\text{O}_2\text{P}$: C, 67.14; H, 9.39. found: C, 66.97; H, 9.15.



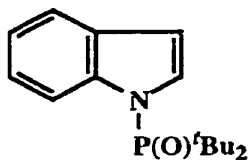
Di-*tert*-butyl-(3-methoxy-2-trimethylsilylphenyl)phosphine

oxide (1.191a): To a solution of phosphinyl anisole **1.190a** (268 mg, 1.0 mmol) in anhydrous THF (10 mL) at $-78\text{ }^\circ\text{C}$ was added *t*-BuLi (1.17 mL, 2.0 mmol, 1.71 M solution) dropwise over 5 min. The solution was stirred and maintained at $-78\text{ }^\circ\text{C}$ for a period of 2 h before TMSCl (0.31 mL, 2.5 mmol) was added. The solution was allowed to slowly warm to room temperature over several hours, and NH_4Cl (2 mL, sat'd aqueous solution) was added. The mixture was transferred to a separatory funnel containing H_2O (20 mL) and extracted with CH_2Cl_2 (3 x 25 mL). The combined organic layers were washed with H_2O (1 x 20 mL) and brine (1 x 20 mL), dried (Na_2SO_4) and evaporated to yield a colourless oil. Purification by flash chromatography (EtOAc) allowed isolation of **1.191a** as an oily solid: $^1\text{H-NMR}$ (250 MHz, CDCl_3) δ 0.28 (s, 9H), 1.28 (d, $J = 13.6\text{ Hz}$, 18H), 3.86 (s, 3H), 7.2-7.5 (m, 3H); $^{31}\text{P-NMR}$ (81.0 MHz, CDCl_3) δ 52.3; EI MS (rel. intensity) 340 (M^+ , 33), 325 (20), 295 (15), 284 (68), 268 (26), 228 (51), 212 (68), 181 (34), 156 (82), 149 (14), 120 (20), 109 (41), 77 (38), 57 (100); HRMS calcd for $\text{C}_{18}\text{H}_{33}\text{O}_2\text{PSi}$: 340.1988; found: 340.1983.



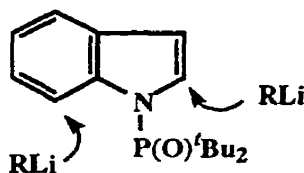
Indole (2.1): To a solution of phosphinylindole **2.83** (139 mg, 0.50 mmol) in anhydrous toluene (15 mL) was added a large excess of LAH (76 mg, 2.0 mmol). The mixture was heated to reflux and reaction progress was monitored by GC over several hours. After 1, 3, and 4 h, decreasing amounts of starting material were present and after 7 h no starting material remained by GC. The reaction mixture was cooled to room temperature and then to $0\text{ }^\circ\text{C}$ in an ice bath. Excess LAH was quenched by the careful addition of H_2O (5 mL) over several minutes (exothermic). When all effervescence had ceased, the mixture was transferred to a separatory funnel containing H_2O

(50 mL) and extracted with EtOAc (3 x 40 mL). The combined organics were dried (Na₂SO₄) and evaporated to provide a light yellow solid. Purification by flash column (5% EtOAc/hexane) provided **2.1** as a light yellow solid (57 mg, 98%): m.p. 49-52 °C; ¹H-NMR (200 MHz, CDCl₃) δ 6.52 (d, J = 3.0 Hz, 1H), 7.05 (d, J = 3.0 Hz, 1H), 7.1-7.3 (m, 3H), 7.64 (dd, J = 7.8 Hz and unresolved J, 1H), 7.83 (s, 1H).

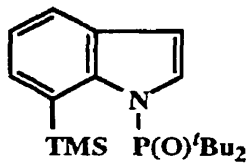


***N*-Di-*tert*-butylphosphinylindole (2.83)**: To a solution of indole (586 mg, 5.0 mmol) in anhydrous THF (10 mL) at 0 °C was added a solution of *n*-BuLi (3.0 mL, 6.0 mmol, 2.00 M solution) dropwise. After stirring for 15 min, chloro-di-*tert*-butylphosphine (1.14 mL, 6.0 mmol) was added dropwise. The mixture was allowed to stir and warm to room temperature over several hours. After addition of MeOH (2 mL), most of the solvent was removed under reduced pressure and the residue was suspended in MeOH (30 mL) and cooled to 0°C. Slow addition of excess H₂O₂ (1 mL of 30%, approx. 8 mmol) caused the suspended material to dissolve over a 30 min period resulting in a light yellow solution. After adding Na₂SO₃ (8 mL, 2 M solution) dropwise, the solution was stirred for 2 h, allowed to warm to room temperature, treated with HCl (12 mL, 10% solution), and stirred for another hour. Most of the MeOH was removed under reduced pressure, and the remaining residue was poured into H₂O (40 mL) and extracted with CH₂Cl₂ (3 x 50 mL). The combined organics were dried (Na₂SO₄) and evaporated to give an orange solid. Purification by flash chromatography (1% MeOH/CH₂Cl₂) provided **2.83** as a white solid (1.076 g, 78%): m.p. 166-167 °C; ¹H-NMR (200 MHz, CDCl₃) δ 1.31 (d, J = 14.7 Hz, 18H), 6.67 (t, J = 2.4 Hz, 1H), 7.57 (d, J = 7.4 Hz, 1H), 7.1-7.3 (m, 3H), 8.53 (d, J = 7.8 Hz, 1H); ¹³C-NMR (50.3 MHz, CDCl₃) δ 26.5, 38.4 (d, J = 69.2 Hz), 106.9 (d, J = 4.9 Hz), 116.1, 120.0, 121.3, 123.2, 126.2 (d, J = 4.8 Hz), 129.0 (d, J = 5.4 Hz), 141.4; ³¹P-NMR (81.0 MHz, CDCl₃) δ 63.0; IR ν_{max}(KBr) 2973, 1475, 1445, 1266, 1175, 1133, 994, 749, 657 cm⁻¹; CI MS *m/z* (rel intensity): 279 (M+2, 14), 278 (M+1, 49), 277 (M⁺, 57), 165 (18), 164 (18), 117 (11), 116 (10), 89 (12), 57 (100); HRMS calcd for:

277.1596, found: 277.1577. Anal. calcd for C₁₆H₂₄NOP: C, 69.29; H, 8.72; N, 5.05.
found: C, 69.41; H, 8.77; N, 5.08.

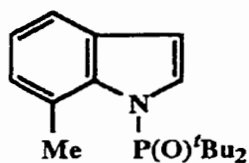


Optimization studies for metalation of 2.83: To a solution of *N*-di-*tert*-butylphenylphosphinylindole (**2.83**, 50 mg, 0.18 mmol) in anhydrous THF (4 mL) at -78 °C was added a solution of *n*-BuLi or LDA (0.40 mmol) according to Scheme 2.23. After the specified length of time (Scheme 2.23), an excess of TMSCl (0.06 mL, 0.45 mmol) was added and the reaction mixture was allowed to warm to room temperature. After addition of H₂O (5 mL) and thorough mixing, a micro-workup was performed by removing a small amount of the organic layer (0.2 mL) and diluting with EtOAc (1.8 mL). The resulting solution was passed through a micro column of silica gel (3 mm diameter x 5 mm length) and analyzed by GC providing **2.84a** and **2.85** as outlined in Scheme 2.23.



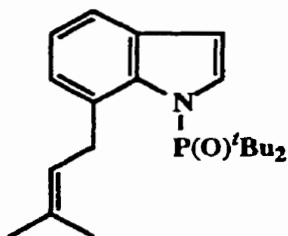
***N*-Di-*tert*-butylphosphinyl-7-trimethylsilylindole (2.84a):**
According to General Procedure I, a solution of phosphinylindole **2.83** (100 mg, 0.36 mmol) in anhydrous THF (10 mL) at -40 °C was treated with *n*-BuLi (0.44 mL, 0.79 mmol, 1.80 M solution). After 2 h, TMSCl (0.11 mL, 0.90 mmol) was added and the solution was allowed to warm to room temperature. Aqueous NH₄Cl (10 mL, saturated solution) was added and the mixture was extracted with CH₂Cl₂ (3 x 20 mL). The combined organics were dried (Na₂SO₄) and evaporated to provide a white solid. Purification by column chromatography (CH₂Cl₂) provided **2.84a** as a white solid (91 mg, 72%): m.p. 127-128 °C; ¹H-NMR (500 MHz, {³¹P}, CDCl₃) δ 0.47 (s, 9H), 1.25 (s, 18H), 6.72 (d, *J* = 3.6 Hz, 1H), 7.18 (t, *J* = 7.5 Hz, 1H), 7.28 (d, *J* = 3.6 Hz, 1H), 7.59 (dd, *J* = 7.6, 1.4 Hz, 1H), 7.64 (dd, *J* = 7.3, 1.3 Hz, 1H); ¹³C-NMR (50.3 MHz, CDCl₃) δ 4.3, 27.8, 39.5 (d, *J* = 6.7 Hz), 108.5 (d, *J* = 5.8 Hz), 121.5, 121.8, 127.3 (d, *J* = 5.7 Hz),

128.2, 130.3 (d, $J = 5.2$ Hz), 133.5, 145.7; ^{31}P -NMR (202.5 MHz, CDCl_3) δ 61.8; IR (KBr) ν_{max} 2953, 2901, 1477, 1392, 1259, 1235, 1183, 1144, 1128, 841, 727, 658 cm^{-1} ; EI MS m/z (rel intensity): 349 (0.6 (M^+)), 334 (100), 278 (46), 236 (26), 222 (41), 220 (47), 190 (21), 174 (12); HRMS calcd for: 349.1991, found: 349.1988.



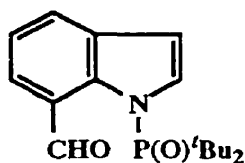
***N*-Di-*tert*-butylphosphinyl-7-methylindole (2.84b):**

According to General Procedure I, a solution of phosphinylindole **2.83** (140 mg, 0.50 mmol) in anhydrous THF (10 mL) at -40 °C was treated with *n*-BuLi (0.65 mL, 1.1 mmol, 1.72 M solution). After 2 h, MeI (0.07 mL, 1.1 mmol) was added and the solution was allowed to warm to room temperature. Aqueous NH_4Cl (10 mL, saturated solution) was added and the mixture was extracted with CH_2Cl_2 (3 x 20 mL). The combined organics were dried (Na_2SO_4) and evaporated to provide a white solid. Purification by column chromatography (1% MeOH/ CH_2Cl_2) provided **2.84b** as a white solid (135 mg, 93%): m.p. 52-53 °C; ^1H -NMR (200 MHz, CDCl_3) δ 1.33 (d, $J = 14.7$ Hz, 18H), 2.88 (s, 3H), 6.70 (dd, $J = 3.5, 1.5$ Hz, 1H), 7.08-7.14 (m, 2H), 7.33 (t, $J = 3.2$ Hz, 1H), 7.37-7.48 (m, 1H); ^{13}C -NMR (75.5 MHz, CDCl_3) δ 23.9, 27.2, 39.6 (d, $J = 69.5$ Hz), 107.8 (d, $J = 6.3$ Hz), 118.2, 121.9, 126.4, 127.5, 127.8 (d, $J = 6.3$ Hz), 131.3 (d, $J = 5.3$ Hz), 140.4; ^{31}P -NMR (81.0 MHz, CDCl_3) δ 62.1; IR (KBr) ν_{max} 2964, 1477, 1448, 1402, 1262, 1232, 1205, 1125, 1092, 985, 815, 788, 680, 657 cm^{-1} ; EI MS (rel. intensity) 291 (M^+ , 42), 235 (17), 179 (55), 178 (77), 130 (39), 105 (21), 77 (13), 57 (100); HRMS calcd for $\text{C}_{17}\text{H}_{26}\text{NOP}$: 291.1752; found: 291.1757.



***N*-Di-*tert*-butylphosphinyl-7-prenylindole (2.84c):** According to General Procedure I, a solution of phosphinylindole **2.83** (277 mg, 1.0 mmol) in anhydrous THF (10 mL) at -40 °C was treated with *n*-BuLi (1.26 mL, 2.1 mmol, 1.67 M solution). After 2 h, 1-bromo-3-methylbut-2-ene (0.24 mL, 2.1 mmol) was added and the solution was

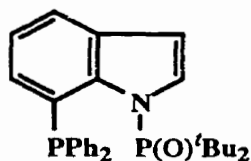
allowed to warm to room temperature. Aqueous NH_4Cl (10 mL, saturated solution) was added and the mixture was extracted with CH_2Cl_2 (3 x 20 mL). The combined organics were dried (Na_2SO_4) and evaporated to provide a white solid. Purification by column chromatography (CH_2Cl_2) provided **2.84c** as a white crystalline solid (299 mg, 87%): m.p. 98.5-99 °C; $^1\text{H-NMR}$ (200 MHz, CDCl_3) δ 1.32 (d, $J = 15.0$ Hz, 18H), 1.78 (s, 6H), 4.19 (d, $J = 10.1$ Hz, 2H), 5.38 (tsp, $J = 10.0$ Hz and unresolved J , 1H), 6.73 (dd, $J = 4.8$ and 2.0 Hz, 1H), 7.1-7.2 (m, 2H), 7.35 (t, $J = 3.4$ Hz, 1H), 7.43 (dt, $J = 4.6$ Hz and unresolved J , 1H); $^{13}\text{C-NMR}$ (50.3 MHz, CDCl_3) δ 17.9, 25.8, 27.1, 33.2, 39.7 (d, $J = 6.8$ Hz), 108.0 (d, $J = 6.0$ Hz), 118.2, 122.1, 125.0, 126.0, 128.0 (d, $J = 5.8$ Hz), 130.2, 130.7, 131.4 (d, $J = 4.2$ Hz), 140.0; $^{31}\text{P-NMR}$ (81.0 MHz, CDCl_3) δ 62.5; IR (KBr) ν_{max} 2968, 2908, 2869, 1477, 1448, 1408, 1369, 1259, 1225, 1203, 1178, 1127, 1089, 983 cm^{-1} ; CI MS m/z (rel intensity): 346 (8 (M+1)), 345 (8 (M+)), 232 (12), 184 (17), 176 (14), 168 (14), 105 (10), 63 (10), 57 (100); HRMS calcd for : 345.2222, found: 345.2207. X-ray analysis, Appendix 7.



***N*-Di-*tert*-butylphosphinyl-7-formylindole (2.84e):**

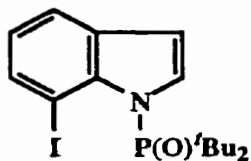
According to General Procedure I, a solution of phosphinylindole **2.83** (140 mg, 0.5 mmol) in anhydrous THF (10 mL) at -40 °C was treated with *n*-BuLi (0.65 mL, 1.1 mmol, 1.72 M solution). After 2 h, anhydrous DMF (0.09 mL, 1.1 mmol) was added. The solution was maintained at -78 °C for 1 h, and MeOH (0.5 mL) was added before the solution was allowed to warm to room temperature. Aqueous NH_4Cl (10 mL, saturated solution) was added and the mixture was extracted with CH_2Cl_2 (3 x 20 mL). The combined organics were dried (Na_2SO_4) and evaporated to provide a white solid. Purification by column chromatography (2% MeOH/ CH_2Cl_2) provided **2.84e** as a white solid (82 mg, 53%): m.p. 105-107 °C; $^1\text{H-NMR}$ (250 MHz, CDCl_3) δ 1.30 (d, $J = 14.9$ Hz, 18H), 6.90 (d, $J = 3.4$ Hz, 1H), 7.31 (t, $J = 7.5$ Hz, 1H), 7.40 (dd, $J = 3.2, 1.9$ Hz, 1H), 7.75 (d, $J = 7.3$ Hz, 1H), 7.80 (d, $J = 7.7$ Hz, 1H), 10.56 (s, 1H); $^{31}\text{P-NMR}$ (81.0 MHz, CDCl_3) δ 63.3; IR (KBr) ν_{max} 2969, 2902, 2872, 1683, 1478, 1415, 1400, 1263, 1248, 1167, 1129,

1094, 663 cm^{-1} ; CI MS m/z (rel intensity): 306 ($\text{M}^{+}+1$, 100), 277 (85), 221 (30), 165 (59), 161 (11), 117 (14), 57 (37).



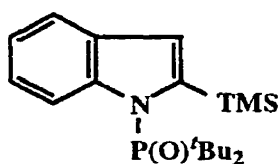
***N*-Di-*tert*-butylphosphinyl-7-diphenylphosphinoindole**

(2.84f): According to General Procedure I, a solution of phosphinylindole **2.83** (140 mg, 0.50 mmol) in anhydrous THF (10 mL) at $-40\text{ }^{\circ}\text{C}$ was treated with *n*-BuLi (0.65 mL, 1.1 mmol, 1.72 M solution). After 2 h, chlorodiphenylphosphine (0.20 mL, 1.1 mmol) was added and the solution was allowed to warm to room temperature. Aqueous NH_4Cl (10 mL, saturated solution) was added and the mixture was extracted with CH_2Cl_2 (3 x 20 mL). The combined organics were dried (Na_2SO_4) and evaporated to provide a slightly yellow solid. Purification by column chromatography (CH_2Cl_2) provided **2.84f** as a white solid (101 mg, 44%): m.p. $161\text{-}165\text{ }^{\circ}\text{C}$; $^1\text{H-NMR}$ (250 MHz, CDCl_3) δ 1.19 (d, $J = 14.6\text{ Hz}$, 18H), 6.9-7.1 (m, 2H), 7.2-7.4 (m, 11H), 7.54 (d, $J = 7.3\text{ Hz}$, 1H), 7.75 (d, $J = 3.7\text{ Hz}$, 1H); $^{13}\text{C-NMR}$ (62.9 MHz, CDCl_3) δ 27.2, 39.5 (d, $J = 66.8\text{ Hz}$), 108.2 (d, $J = 5.7\text{ Hz}$), 121.6 (d, $J = 51.5\text{ Hz}$), 125.8 (d, $J = 30.5\text{ Hz}$), 127.3, 127.8 (d, $J = 7.6\text{ Hz}$), 128.3 (d, $J = 3.8\text{ Hz}$), 131.0-131.5 (m, 2C), 133.3, 133.8 (d, $J = 21.0\text{ Hz}$), 141.9 (d, $J = 17.2\text{ Hz}$), 144.4 (d, $J = 24.8\text{ Hz}$); $^{31}\text{P-NMR}$ (81.0 MHz, CDCl_3) δ (25 $^{\circ}\text{C}$) 62.2 (d, $J = 8.7\text{ Hz}$), -4.8 (d, $J = 8.3\text{ Hz}$), δ (48 $^{\circ}\text{C}$), 62.0 (d, $J = 8.7\text{ Hz}$), -4.6 (d, $J = 8.7\text{ Hz}$); IR (KBr) ν_{max} 2964, 1477, 1435, 1255, 1235, 1208, 1180, 1119, 1075, 693 cm^{-1} ; EI MS m/z (rel intensity): 461 (M^{+} , 6), 420 (21), 404 (100), 364 (18), 347 (69), 258 (15), 222 (85), 183 (33), 154 (16), 107 (22), 77 (30), 57 (56); HRMS calcd for $\text{C}_{28}\text{H}_{33}\text{NOP}_2$: 461.2037; found: 461.2030.



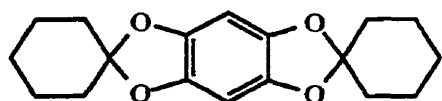
***N*-Di-*tert*-butylphosphinyl-7-iodoindole (2.84g)**: According to General Procedure I, a solution of phosphinylindole **2.83** (140 mg, 0.50 mmol) in anhydrous THF (10 mL) at $-40\text{ }^{\circ}\text{C}$ was treated with *n*-BuLi (0.65 mL, 1.1 mmol, 1.72 M solution). After 2 h, a solution of I_2 (279 mg, 1.1 mmol)

in anhydrous THF (4 mL) was added and the solution was allowed to warm to room temperature. Aqueous Na₂S₂O₃ (25 mL, 2 M solution) was added and the mixture was extracted with CH₂Cl₂ (3 x 20 mL). The combined organics were dried (Na₂SO₄) and evaporated to provide a light yellow oil. Purification by column chromatography (1 % MeOH/CH₂Cl₂) provided **2.84f** as a colourless oil which crystallized on standing (157 mg, 78%): m.p. 122-123 °C; ¹H-NMR (300 MHz, CDCl₃) δ 1.34 (d, J = 14.7 Hz, 18H), 6.70 (d, J = 3.6 Hz, 1H), 6.85 (t, J = 7.6 Hz, 1H), 7.35 (t, J = 3.1 Hz, 1H), 7.55 (d, J = 7.6 Hz, 1H), 7.98 (dd, J = 7.5, 0.7 Hz, 1H); ¹³C-NMR (50.3 MHz, CDCl₃) δ 27.2, 40.3 (d, J = 65.6 Hz), 77.2, 109.0 (d, J = 6.1 Hz), 120.7, 123.6, 129.0, 133.3 (d, J = 3.1 Hz), 139.2, 143.6; ³¹P-NMR (81.0 MHz, CDCl₃) δ 66.6; IR (KBr) ν_{max} 2990, 2970, 1476, 1393, 1360, 1255, 1234, 1180, 1124, 973, 798, 657 cm⁻¹; EI MS *m/z* (rel intensity) 403 (M⁺, 62), 291 (33), 276 (84), 243 (15), 220 (31), 164 (90), 163 (90), 128 (12), 116 (42), 105 (49), 89 (22), 57 (100); HRMS calcd for C₁₆H₂₃INOP: 403.0562; found: 403.0559.



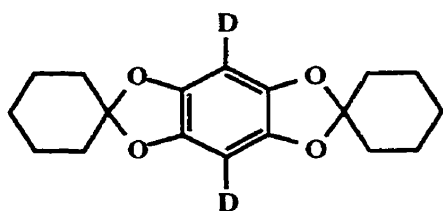
***N*-Di-*tert*-butylphosphinyllindole (2.85):** To a solution of phosphinyllindole **2.83** (277 mg, 1.0 mmol) in anhydrous THF (20 mL) at 0 °C was added freshly prepared LDA (2.1 mL, 2.1 mmol, 1.0 M solution prepared by adding *n*-BuLi to a cooled solution of freshly distilled diisopropylamine in anhydrous THF). After stirring for 15 min while maintaining the temperature at 0 °C, TMSCl (0.32 mL, 2.5 mmol) was added and the solution was gradually warmed to room temperature. Aqueous NH₄Cl (10 mL, saturated solution) was added and the mixture was extracted with CH₂Cl₂ (3 x 30 mL). The combined organics were dried (Na₂SO₄) and evaporated to provide a slightly yellow solid. Purification by column chromatography (CH₂Cl₂) provided **2.85** as a white solid (286 mg, 82%): m.p. 208-210 °C; ¹H-NMR (500 MHz, CDCl₃) δ 0.36 (s, 9H), 1.30 (d, J = 15.0 Hz, 18H), 7.01 (s, 1H), 7.13 (t, J = 7.2 Hz, 1H), 7.17 (t, J = 7.6 Hz, 1H), 7.57 (d, J = 7.3 Hz, 1H), 7.67 (d, J = 8.3 Hz, 1H); ¹³C-NMR (62.9 MHz, CDCl₃) δ 2.6, 27.6, 39.8 (d, J = 65.5 Hz), 119.8 (d, J = 6.7

Hz), 120.9, 121.0, 122.2, 132.2 (d, $J = 5.8$ Hz), 139.5 (d, $J = 5.4$ Hz), 148.2 (d, $J = 5.9$ Hz); ^{31}P -NMR (81.0 MHz, CDCl_3) δ 67.0; IR (KBr) ν_{max} 2990, 2958, 2897, 1479, 1467, 1239, 1222, 1199, 1171, 1132, 1096, 1028, 843 cm^{-1} ; EI MS m/z (rel intensity): 349 (M^+ , 3), 334 (100), 278 (49), 236 (35), 222 (40), 220 (56), 190 (12), 174 (13), 146 (14); HRMS calcd for $\text{C}_{19}\text{H}_{32}\text{NOPSi}$: 349.1991, found: 349.1994; Anal. calcd for $\text{C}_{19}\text{H}_{32}\text{NOPSi}$: C, 65.29; H, 9.23; N, 4.01. found: C, 65.09; H, 9.26; N, 3.94.



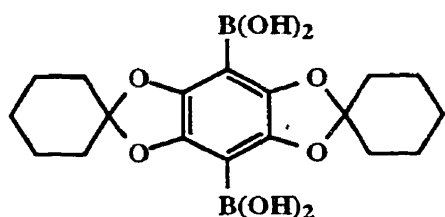
1,2,4,5-Tetrahydroxybenzene bis(cyclohexylidene) ketal (2.104). According to a literature procedure,^{361,362} 2,5-dihydroxybenzo-

quinone (5.60 g, 40 mmol) was dissolved in conc. HCl (120 mL) and to the orange slurry was slowly added tin powder (5.70 g, 48 mmol). The mixture was heated to reflux for a period of 1.5 h, after which the solution was clear and colourless. The hot mixture was filtered through CeliteTM and gradually cooled to room temperature, and then to 0 °C in an ice bath causing precipitation of a white solid. The crystalline 1,2,4,5-tetrahydroxybenzene was filtered by suction and recrystallized from THF. A portion of the freshly prepared tetrahydroxybenzene (284 mg, 2.0 mmol) was dissolved in anhydrous CH_2Cl_2 (15 mL) and to it was added cyclohexanone (589 mg, 6.0 mmol), a catalytic amount of TsOH (40 mg, 0.2 mmol) and excess MgSO_4 (1.20 g, 10 mmol). The mixture was heated to reflux for a period of 2 days before being cooled, filtered through CeliteTM, and rinsed with CH_2Cl_2 (20 mL). The combined organic layers were washed with NaHCO_3 (saturated, 10 mL), dried (Na_2SO_4), and evaporated to provide a brown oily solid. Recrystallization from toluene provided **2.104** as a white solid with spectral data matching that provided in the literature (157 mg, 26%): m.p. 188-190 °C (lit.³⁶¹ 190-191 °C); ^1H -NMR (200 MHz, CDCl_3) δ 1.4-1.6 (m, 4H), 1.6-1.8 (m, 8H), 1.8-1.9 (m, 8H), 6.33 (s, 2H); ^{13}C -NMR (50.3 MHz, CDCl_3) δ 23.2, 24.6, 34.9, 92.8, 118.5, 140.3.



3,6-Dideutero-1,2,4,5-tetrahydroxybenzene bis(cyclohexylidene) ketal (2.107a):

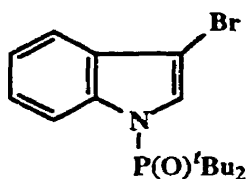
Conditions for metalation of bisketal **2.104** are as described in Scheme 2.34. The optimal conditions (Scheme 2.34, entry 3) were as follows: To a solution of bisketal **2.104** (302 mg, 1.0 mmol) in anhydrous Et₂O (10 mL) at -78 °C was added *t*-BuLi (1.83 mL, 3.0 mmol, 1.64 M solution) resulting in a white suspension. After 30 min at -78 °C, the suspension was allowed to warm to room temperature and was allowed to continue stirring at room temperature for 18 h. A large excess of MeOD (0.5 mL) was added and the resulting solution was poured into H₂O (50 mL) and extracted with CH₂Cl₂ (3 x 50 mL). The combined organics were dried (Na₂SO₄) and evaporated to provide a light yellow solid: m.p. 185-189 °C; ¹H-NMR (250 MHz, CDCl₃) δ 1.3-1.6 (m, 4H), 1.6-1.8 (m, 8H), 1.8-2.0 (m, 8H). See Appendix 8 for ¹H-NMR spectra.



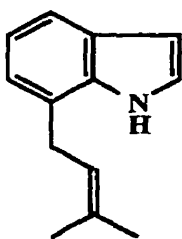
1,2,4,5-Tetrahydroxybenzene bis(cyclohexylidene) ketal, 3,6-bisboronic acid (2.107b):

According to the optimal conditions for preparation of **2.107a**, a solution of bisketal **2.104** (302 mg, 1.0 mmol) in anhydrous Et₂O (10 mL) at -78 °C was treated with *t*-BuLi (1.83 mL, 3.0 mmol, 1.64 M solution). Over a period of 30 min at -78 °C, a white suspension was formed. The mixture was then allowed to warm to room temperature and was stirred at room temperature for a period of 22 h. An ice bath was used to lower the temperature of the mixture to 0 °C before excess B(OMe)₃ (0.51 mL, 4.5 mmol) was added resulting in the formation of a thick white precipitate. Water (20 mL) was added followed by NH₄Cl (30 mL, saturated), and the entire mixture was extracted with CH₂Cl₂ (3 x 30 mL). The combined organics were dried (MgSO₄) and evaporated to provide a light yellow foamy solid that was used without further

purification (244 mg, 68%): $^1\text{H-NMR}$ (250 MHz, CDCl_3) δ 1.4-1.6 (m, 4H), 1.6-1.8 (m, 8H), 1.8-2.0 (m, 8H), 5.55 (s, 4H, exch).

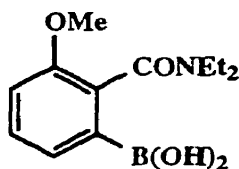


3-Bromo-*N*-di-*tert*-butylphosphinylindole (2.109a): Method 1: To a solution of phosphinylindole **2.83** (139 mg, 0.5 mmol) in DMF (10 mL) at room temperature was added NBS (89 mg, 0.5 mmol). The mixture was stirred at room temperature for 12 h and then was poured into H_2O (100 mL) and extracted with Et_2O (8 x 20 mL). The combined organic layers were dried (Na_2SO_4) and evaporated to provide a beige solid. Purification by trituration in warm hexane, and filtration provided **2.109a** as a white solid (170 mg, 95%); *or* Method 2: To a solution of phosphinylindole **2.83** (1.387g, 5.0 mmol) in cyclohexane (250 mL) at room temperature was added NBS (890 mg, 5.0 mmol). The mixture was stirred at room temperature for 12 h and then filtered through coarse filter paper. Evaporation of the filtrate under reduced pressure provided a white solid. Purification by trituration in warm hexane provided **2.109a** as a white solid (1.683 g, 94%): m.p. 170-171 $^\circ\text{C}$; $^1\text{H-NMR}$ (300 MHz, CDCl_3) δ 1.35 (d, $J = 14.9$ Hz, 18H), 7.2-7.3 (m, 3H), 7.5-7.6 (m, 1H), 8.5-8.6 (m, 1H); $^{31}\text{P-NMR}$ (81.0 MHz, CDCl_3) δ 64.6; IR (KBr) ν_{max} 2984, 2962, 1477, 1435, 1275, 1195, 1179, 1108, 1028, 1016, 814, 756 cm^{-1} ; EI MS m/z (rel intensity): 357 ($M+2$, 35), 355 (35), 301 (19), 299 (20), 245 (35), 244 (24), 243 (47), 242 (22), 196 (15), 194 (15), 116 (32), 105 (23), 57 (100); HRMS calcd for $\text{C}_{16}\text{H}_{23}\text{BrNOP}$: 355.0701; found: 355.0696.



7-Prenylindole (2.110): To a solution of phosphinylindole **2.84c** (250 mg, 0.70 mmol) in anhydrous toluene (15 mL) was added a large excess of LAH (133 mg, 3.5 mmol). The mixture was heated to reflux and reaction progress was monitored by GC over several hours. After 1 h the reaction was incomplete, and after 3 h no further progress had been noted so a second portion of LAH (95 mg, 2.5 mmol) was added. After another 2h,

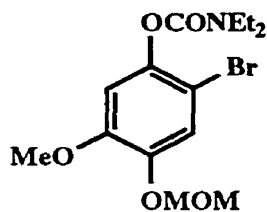
minimal starting material remained, decreasing amounts of starting material were present and after 7 h no starting material remained by GC. The reaction mixture was cooled to room temperature and then to 0 °C in an ice bath. Excess LAH was quenched by the careful addition of H₂O (5 mL) over several minutes (exothermic). When all effervescence had ceased, the mixture was transferred to a separatory funnel containing H₂O (50 mL) and extracted with EtOAc (3 x 40 mL). The combined organics were dried (Na₂SO₄) and evaporated to provide a light yellow solid. Purification by flash column (5% EtOAc/hexane) provided **2.110** as a light yellow solid (57 mg, 98%): m.p. 35-38 °C (lit.³³² 43-44 °C); ¹H-NMR (250 MHz, CDCl₃) δ 1.80 (s, 6H), 3.53 (d, J = 7.2 Hz), 5.40 (ts, J = 7.2 Hz and unresolved J, 1H), 6.56 (dd, J = 3.2 Hz and 2.2 Hz, 1H), 7.0-7.1 (m, 2H), 7.18 (dd, J = 3.2 Hz and 2.5 Hz, 1H), 7.4-7.5 (m, 1H), 8.11 (s, 1H).



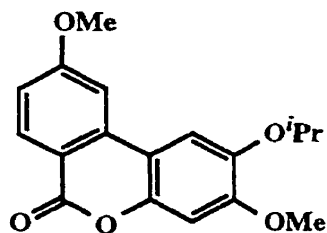
2-(*N,N*-Diethylcarbamyl)-3-methoxyphenylboronic acid

(3.61): To a solution of TMEDA (8.7 mL, 57 mmol) in anhydrous THF (200 mL) at -78 °C was added *s*-BuLi (48 mL, 57 mmol, 1.20 M

solution) dropwise resulting in a yellow solution. After 15 min of stirring at low temperature, benzamide **3.76** (10.00 g, 48.2 mmol) was added dropwise *via* cannula as a solution in anhydrous THF (50 mL). After stirring for 1 h at -78 °C, B(OMe)₃ (6.0 mL, 53 mmol) was added quickly in one portion with rapid stirring causing a rise in temperature. Stirring was continued and the solution was allowed to warm slowly to room temperature. The reaction mixture was quenched by slow addition of HCl (10%) until a pH of 1-2 was achieved. The solution was then transferred to a separatory funnel containing H₂O (100 mL), and extracted with CH₂Cl₂ (3 x 100 mL). The combined organic layers were dried (Na₂SO₄) and evaporated to give a light yellow oil. Further drying the oil under reduced pressure resulted in formation of a white foamy solid that was used without further purification.

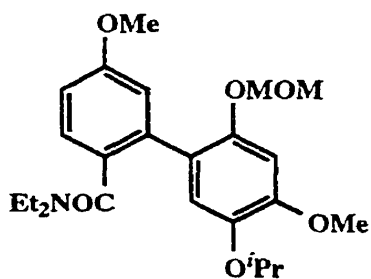


***N,N*-Diethyl *O*-[2-bromo-5-methoxy-4-(methoxymethoxy)phenyl]carbamate (3.62):** Method 1: To a solution of crude bromophenol **3.93** (1.052 g, 4.0 mmol) in CH₃CN (100 mL) at room temperature was added K₂CO₃ (1.105 g, 8.0 mmol) and the mixture was stirred for 15 min before ClCONEt₂ (1.02 mL, 8.0 mmol) was added. The mixture was heated to reflux and stirred for 16 h and then was cooled to room temperature, poured into H₂O (50 mL), and extracted with Et₂O (3 x 50 mL). The combined organic extracts were washed with brine (20 mL), dried (Na₂SO₄) and evaporated to give a brown oil. Purification by flash chromatography (25% Et₂O/hexane) provided **3.62** as a white solid (807 mg, 41% from phenol **3.83**); *or* Method 2: To a solution of carbamate **3.84** (566 mg, 2.0 mmol) in DMF (20 mL) at room temperature was added a solution of NBS (356 mg, 2.0 mmol) in DMF (20 mL). The solution was stirred at room temperature for 24 h and was then poured into H₂O (50 mL) and extracted with Et₂O (100 mL). The Et₂O extract was washed with H₂O (8 x 50 mL), dried (Na₂SO₄) and evaporated to give a red oil. Purification as described above provided **3.62** as a white solid (623 mg, 86%): m.p. 76.5-77 °C (hexane); ¹H-NMR (250 MHz, CDCl₃) δ 1.22 (t, J = 7.0 Hz, 3H), 1.30 (t, J = 7.0 Hz, 3H), 3.39 (q, J = 7.0 Hz, 2H), 3.48 (q, J = 7.0 Hz, 2H), 3.50 (s, 3H), 3.85 (s, 3H), 5.18 (s, 2H), 6.79 (s, 1H), 7.34 (s, 1H); ¹³C-NMR (62.9 MHz, CDCl₃) δ 13.4, 14.3, 42.1, 42.5, 56.3, 56.4, 96.0, 96.2, 106.1, 108.1, 120.2, 143.3, 144.6, 154.9; EI MS *m/z* (rel intensity): 363 (5), 361 (5), 282 (8), 100 (100), 72 (34); HRMS calcd for : 361.0525, found: 361.0576; Anal. calcd for C₁₄H₂₀BrNO₅: C, 46.42; H, 5.57; N, 3.87; found: C, 46.35; H, 5.69; N, 3.86.



2,6-Dimethoxy-3-isopropoxydibenzo[*b,d*]pyran-6-one (3.65): A solution of biaryl **3.66** (259 mg, 0.6 mmol) in glacial acetic acid (30 mL) was heated to reflux with stirring for a period of 1 h. The solvent was removed under reduced pressure to give a light yellow solid. Recrystallization (EtOH) provided **3.65** as a white

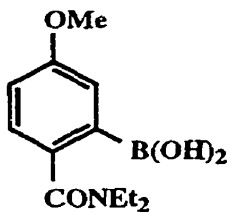
crystalline solid (175 mg, 93%): m.p. 174.5-175 °C; ¹H-NMR (250 MHz, CDCl₃) δ 1.41 (d, J = 6.1 Hz, 6H), 3.92 (s, 3H), 3.98 (s, 3H), 4.58 (sp, J = 6.1 Hz, 1H), 6.85 (s, 1H), 7.03 (dd, J = 8.8 and 2.2 Hz, 1H), 7.28 (d, J = 2.2 Hz, 1H), 7.41 (s, 1H), 8.29 (d, J = 8.8 Hz, 1H); ¹³C-NMR (62.9 MHz, CDCl₃) δ 22.2, 55.8, 56.2, 73.3, 101.3, 104.7, 110.2, 111.0, 113.4, 114.8, 132.9, 137.3, 144.3, 147.6, 153.6, 161.4, 164.8; EI MS *m/z* (rel intensity): 314 (M⁺, 17), 272 (100), 257 (32), 229 (6), 201 (22), 187 (8), 159 (24); Anal. calcd for C₁₈H₁₈O₅: C, 68.78; H, 5.77; found: C, 68.50; H, 5.59.



2'-(*N,N*-Diethylcarbamyl)-4,5'-dimethoxy-5-isopropoxy-2-(methoxymethoxy)biphenyl (3.66).

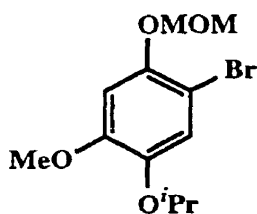
To a solution of bromoarene **3.68** (275 mg, 0.9 mmol) in DME (5 mL) under an inert atmosphere at room temperature was added Pd(PPh₃)₄ (58 mg, 0.05 mmol) and the mixture was stirred for 20 min. A solution of boronic acid **3.67** (375 mg, 1.5 mmol) in DME (5 mL) was added to the first solution, followed by Na₂CO₃ (2 mL, 2 M solution). The mixture was heated to reflux, and after 1 h had turned black. After 12 h at reflux, the mixture was cooled to room temperature and NH₄Cl (5 mL, saturated solution) was added. The entire mixture was filtered through Celite™ and the solvent was removed under reduced pressure. The residue was poured into H₂O (50 mL) and extracted with CH₂Cl₂ (3 x 50 mL). The combined organic extracts were dried (Na₂SO₄) and evaporated to give a brown oil. Purification by column chromatography provided **3.66** as a colourless oil (259 mg, 68%): ¹H-NMR (200 MHz, CDCl₃) δ 0.85 (q, J = 7.1 Hz, 6H), 1.32 (d, J = 6.1 Hz, 6H), 2.6-3.9 (m, 4H), 3.41 (s, 3H), 3.83 (s, 3H), 3.86 (s, 3H), 4.41 (sp, J = 6.1 Hz, 1H), 5.07 (s, 2H), 6.8-6.9 (m, 4H), 7.2-7.3 (m, 1H); ¹³C-NMR (50.3 MHz, CDCl₃) δ 12.1, 13.6, 22.0, 38.0, 42.1, 55.1, 55.8, 56.0, 71.9, 95.6, 101.0, 112.6, 116.3, 118.9, 120.9, 128.0, 129.8, 136.4, 141.7, 148.7, 150.6, 158.9, 170.4; EI MS *m/z* (rel. intensity): 431 (M⁺, 4), 416 (2), 389 (30), 374 (11),

359 (100), 287 (21), 191 (15), 105 (24); Anal. calcd for C₂₄H₃₃NO₆: C, 66.80; H, 7.71; N, 3.25; found: C, 66.61; H, 7.75; N, 3.35.



2-(*N,N*-Diethylcarbamyl)-5-methoxyphenylboronic acid

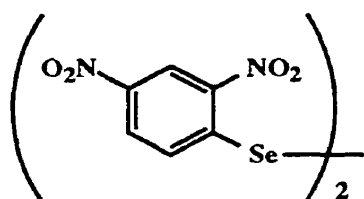
(3.67): To a solution of TMEDA (3.1 mL, 20.5 mmol) in anhydrous THF (100 mL) at -78 °C was added *s*-BuLi (16.7 mL, 20.5 mmol, 1.23 M solution) dropwise resulting in a yellow solution. After 15 min of stirring at low temperature, benzamide **3.72** (3.533 g, 17.0 mmol) was added dropwise *via* cannula as a solution in anhydrous THF (50 mL). After stirring for 1 h at -78 °C, B(OMe)₃ (4.8 mL, 42 mmol) was added quickly in one portion with rapid stirring causing a rise in temperature. Stirring was continued and the solution was allowed to warm slowly to room temperature. The reaction mixture was quenched by slow addition of HCl (10%) until a pH of 1-2 was achieved. The solution was then transferred to a separatory funnel containing H₂O (100 mL), and extracted with CH₂Cl₂ (3 x 100 mL). The combined organic layers were dried (Na₂SO₄) and evaporated to give a light yellow oil. Further drying the oil under reduced pressure resulted in formation of a white foamy solid that was used without further purification.



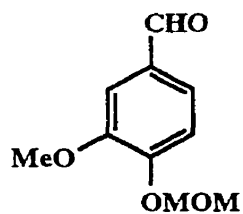
6-Bromo-4-isopropoxy-3-methoxyphenol, methoxymethyl

ether (3.68): To a solution of protected phenol **3.95** (1.561 g, 6.9 mmol) in DMF (20 mL) at room temperature was added a solution of NBS (1.228 g, 6.9 mmol) in DMF (20 mL). The solution was stirred at room temperature for 24 h and was then poured into H₂O (50 mL) and extracted with Et₂O (100 mL). The Et₂O extract was washed with H₂O (8 x 50 mL), dried (Na₂SO₄) and evaporated to give a light orange oil. Purification by vacuum distillation provided **3.68** as a colourless oil (1.791 g, 85%): b.p. 128-130 °C (0.1 mm Hg); ¹H-NMR (250 MHz, CDCl₃) δ 1.33 (d, J = 6.1 Hz, 6H), 3.54 (s, 3H), 3.82 (s, 3H), 4.40 (sp, J = 6.1 Hz, 1H), 5.17 (s,

2H), 6.78 (s, 1H), 7.06 (s, 1H); ^{13}C -NMR (50.3 MHz, CDCl_3) δ 21.7, 55.9, 56.1, 72.4, 95.9, 102.1, 102.5, 121.0, 142.7, 148.3, 150.5; EI MS m/z (rel intensity): 306 ($M+2$, 50), 304 (M^+ , 49), 264 (41), 262 (41), 234 (100), 232 (98), 219 (43), 217 (44), 191 (18), 189 (19), 183 (35), 152 (18), 140 (13); Anal. calcd for $\text{C}_{12}\text{H}_{17}\text{BrO}_4$: C, 47.23; H, 5.61; found: C, 47.39; H, 5.67.

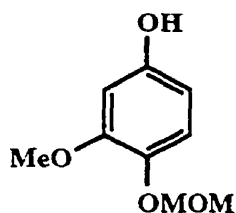


Bis(2,4-dinitrophenyl) diselenide (3.79): According to a literature procedure,⁴⁵⁹ to a solution of diphenylacetylene (232 mg, 1.3 mmol) in anhydrous THF (25 mL) was added freshly sliced lithium solid (349 mg, 50.3 mmol). The mixture was stirred vigorously for 1 h before selenium (3.720 g, 46.5 mmol) was added in one portion and the entire mixture was stirred at room temperature for 24 h. The resulting red-brown solution was transferred dropwise over 30 min to a stirred solution of 2,4-dinitrochlorobenzene (10.958 g, 54.1 mmol) in anhydrous THF (50 mL) at 0 °C. Stirring was continued for another 24 h, after which the precipitate was filtered by suction and washed with THF (20 mL), H_2O (20 mL), and MeOH (20 mL) and dried in air giving **3.79** as a red-brown solid (6.664 g, 58%) that was used without further purification: m.p. 248 °C dec. (lit.⁴⁵⁹ 263 °C dec., and⁴⁶⁵ 264-265 °C).



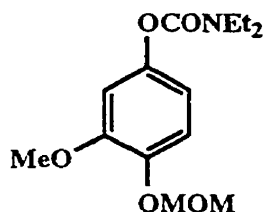
3-Methoxy-4-(methoxymethoxy)benzaldehyde (3.81).
 Method 1: According to a literature procedure,⁴⁶⁰ to a solution of vanillin (7.61 g, 50.0 mmol) in THF (70 mL) at room temperature was added a catalytic amount of tetrabutylammonium bromide (966 mg, 3.0 mmol) and freshly powdered NaOH (12 g). The mixture was stirred and cooled to 0 °C and to it was added a large excess of MOMCl (12.0 mL, 160 mmol) dropwise as a solution in THF (30 mL). The mixture was stirred for 2 h and then poured into H_2O (100 mL) and extracted with EtOAc (3 x 50 mL). The combined organic extracts were dried (MgSO_4) and evaporated

to give a yellow oil. Purification by vacuum distillation provided **3.81** as a colourless oil (6.47 g, 66%); *or* Method 2: To a solution of NaH (288 mg, 6.0 mmol) in THF (50 mL) at 0 °C was added MOMCl (0.45 mL, 6.0 mmol) followed by dropwise addition of vanillin (761 mg, 5.0 mmol) as a solution in THF (25 mL) over 30 min. When all of the vanillin solution had been added, the mixture was stirred for an additional 2 h as it slowly warmed to room temperature. The reaction mixture was poured into H₂O (100 mL) and extracted with EtOAc (3 x 50 mL). The combined organic extracts were dried (Na₂SO₄) and evaporated to give a light yellow oil. Purification by vacuum distillation provided **3.81** as a colourless oil (768 mg, 80%): m.p. 34.5-36 °C; b.p. 122-124 °C (0.4 mm Hg); ¹H-NMR (250 MHz, CDCl₃) δ 3.53 (s, 3H), 3.95 (s, 3H), 5.33 (s, 2H), 7.29 (d, unresolved J, 1H), 7.4-7.5 (m, 2H), 9.87 (s, 1H); EI MS *m/z* (rel intensity): 196 (M⁺, 100), 166 (37), 150 (13), 137 (6), 119 (16).



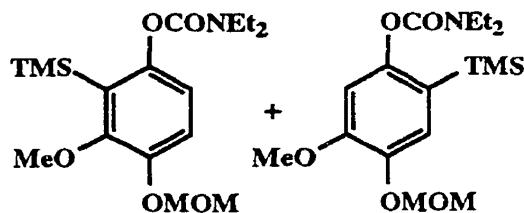
3-Methoxy-4-(methoxymethoxy)phenol (3.83). According to a literature procedure,⁴⁵⁸ to a solution of aldehyde **3.81** (2.943 g, 15.0 mmol) in CH₂Cl₂ (50 mL) at room temperature was added selenium catalyst **3.79** (310 mg, 0.6 mmol) and H₂O₂ (3.9 mL, 30% solution, approximately 30 mmol), and the mixture was stirred vigorously for 48 h. The yellow mixture was filtered to remove the insoluble catalyst, and the filtrate was poured into H₂O (30 mL) and extracted with CH₂Cl₂ (3 x 50 mL). The combined organic layers were washed successively with NaHSO₃ (50 mL, 10% solution), Na₂CO₃ (50 mL, 10% solution), and H₂O (50 mL). Drying (Na₂SO₄) and evaporating led to isolation the crude formate ester, which was dissolved in CH₃OH (50 mL) and cooled to 0 °C. To this was added powdered KOH (3.0 g, 53.5 mmol) in several portions. After stirring for 1 h, H₂O (100 mL) was added and the mixture was extracted with Et₂O (2 x 50 mL). The aqueous layer was acidified (10% HCl) and extracted with CHCl₃ (3 x 50 mL). The combined organic extracts were dried (Na₂SO₄) and evaporated to provide a brown residue. The oily mixture was passed through a short silica gel column (20% hexane/Et₂O) and the resulting solid was recrystallized (Et₂O/hexane) to provide

3.83 as a white solid (2.041 g, 74%): m.p. 69.5-70.5 °C (ether / hexane) (lit.^{458,460} 74 °C); ¹H-NMR (250 MHz, CDCl₃) δ 3.53 (s, 3H), 3.79 (s, 3H), 5.12 (s, 2H), 5.63 (s, 1H, exch.), 6.28 (dd, J = 8.6 and 2.8 Hz, 1H), 6.44 (d, J = 2.8 Hz, 1H), 6.95 (d, J = 8.6 Hz, 1H); IR (CHCl₃) ν_{max} 3398, 3017, 1608, 1511, 1195, 1155, 755 cm⁻¹; EI MS *m/z* (rel intensity): 184 (M⁺, 90), 154 (100), 139 (87), 138 (39), 111 (35), 93 (25).



***N,N*-Diethyl *O*-[3-methoxy-4-(methoxymethoxy)phenyl]-carbamate (3.84)**: According to General Procedure F, to a solution of phenol **3.83** (2.763 g, 15.0 mmol) in CH₃CN (50 mL) at room temperature was added K₂CO₃ (2.488 g, 18.0 mmol) and ClCONEt₂

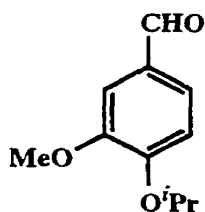
(3.80 mL, 30.0 mmol). The mixture was stirred vigorously and heated to reflux. After 8 h, the mixture was cooled to room temperature, poured into H₂O (100 mL), and extracted with EtOAc (3 x 50 mL). The combined organic extracts were dried (Na₂SO₄) and evaporated to give a straw coloured oil. Purification by vacuum distillation provided **3.84** as a colourless oil (3.741 g, 88%): b.p. 192-194 °C (0.2 mm Hg); ¹H-NMR (250 MHz, CDCl₃) δ 1.1-1.3 (m, 6H), 3.40 (t, J = 7.8 Hz, 4H), 3.50 (s, 3H), 3.85 (s, 3H), 5.18 (s, 2H), 6.72 (d, J = 2.7 Hz, 1H), 6.63 (dd, J = 8.7 and 2.7 Hz, 1H), 7.11 (d, J = 8.7 Hz, 1H); ¹³C-NMR (50.3 MHz, CDCl₃) δ 13.2, 14.1, 41.7, 42.0, 55.7, 55.9, 95.7, 106.3, 113.1, 116.6, 143.6, 146.4, 150.0, 154.2; IR (neat) ν_{max} 3552, 3504, 3403, 2360, 1728, 1600, 920, 853 cm⁻¹; EI MS *m/z* (rel intensity): 283 (M⁺, 15), 100 (100), 72 (39); Anal. calcd for C₁₄H₂₁NO₅: C, 59.35; H, 7.47; N, 4.94; found: C, 59.15; H, 7.45; N, 5.01.



***N,N*-Diethyl *O*-[3-methoxy-4-(methoxymethoxy)-2-trimethylsilylphenyl]carbamate (3.85)** and ***N,N*-Diethyl *O*-[5-methoxy-4-(methoxymethoxy)-2-trimethylsilylphenyl]-**

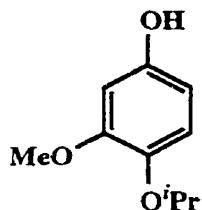
carbamate (3.87): To a solution of TMEDA (0.33 mL, 2.2 mmol) in anhydrous THF (20

mL) at $-78\text{ }^{\circ}\text{C}$ was added *s*-BuLi (1.65 mL, 2.2 mmol, 1.33 M solution). After stirring for 15 min, a solution of carbamate **3.84** (567 mg, 2.0 mmol) in anhydrous THF (15 mL) was added dropwise. After stirring at $-78\text{ }^{\circ}\text{C}$ for 1 h, NH_4Cl (2 mL, saturated) was added and the solution was warmed to room temperature. Most of the solvent was removed under reduced pressure and the residue was partitioned between H_2O (100 mL) and CH_2Cl_2 (100 mL). The organic layer was dried (Na_2SO_4) and evaporated to give a light brown oil. Purification by flash chromatography (40% hexane/ Et_2O) provided **3.85** (230 mg, 32%) as a colourless oil along with **3.87** (est. 10-15%) and starting material that were inseparable by flash chromatography. The experiment was repeated at $-100\text{ }^{\circ}\text{C}$ providing 18% of **3.85**, and with direct addition of *t*-BuLi at $-78\text{ }^{\circ}\text{C}$ providing 16% of **3.85**. Data for **3.85**: $^1\text{H-NMR}$ (200 MHz, CDCl_3) δ 0.31 (s, 9H), 1.18 (t, $J = 7.1\text{ Hz}$, 3H), 1.23 (t, $J = 7.1\text{ Hz}$, 3H), 3.38 (q, $J = 7.1\text{ Hz}$, 2H), 3.43 (q, $J = 7.1\text{ Hz}$, 2H), 3.50 (s, 3H), 3.84 (s, 3H), 5.17 (s, 2H), 6.66 (d, $J = 8.8\text{ Hz}$, 1H), 7.14 (d, $J = 8.8\text{ Hz}$, 1H); $^{13}\text{C-NMR}$ (50.3 MHz, CDCl_3) δ 1.1, 13.3, 14.2, 41.6, 41.9, 56.2, 61.0, 95.5, 118.3, 118.6, 126.0, 147.3, 150.5, 154.1, 154.8; IR (neat) ν_{max} 2976, 2072, 1993, 1926, 1747, 1583, 922 cm^{-1} ; EI MS m/z (rel intensity): 355 (M^+ , 6), 340 (33), 100 (100), 72 (28); HRMS calcd for $\text{C}_{17}\text{H}_{29}\text{NO}_5\text{Si}$: 355.1815; found: 355.1810. Data for **3.87**: $^1\text{H-NMR}$ (250 MHz, CDCl_3) δ 0.25 (s, 9H), 1.20 (t, $J = 7.1\text{ Hz}$, 3H), 1.26 (t, $J = 7.1\text{ Hz}$, 3H), 3.39 (q, $J = 7.1\text{ Hz}$, 2H), 3.48 (q, $J = 7.1\text{ Hz}$, 2H), 3.52 (s, 3H), 3.86 (s, 3H), 5.18 (s, 2H), 6.61 (s, 1H), 7.15 (s, 1H).



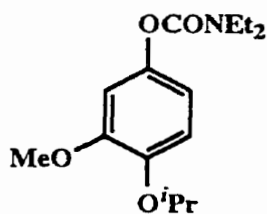
4-Isopropoxy-3-methoxybenzaldehyde (3.90): To a solution of vanillin (1.521 g, 10.0 mmol) in CH_3CN (100 mL) at room temperature was added K_2CO_3 (2.761 g, 20.0 mmol) and 2-iodopropane (1.20 mL, 12.0 mmol). The mixture was stirred vigorously and heated to reflux. After 12 h at reflux, the mixture was cooled to room temperature and most of the solvent was removed under reduced pressure. The residue was partitioned between H_2O (100 mL) and CH_2Cl_2 (100 mL), and the organic layer was washed

with NaOH (50 mL, 1 M solution), dried (Na₂SO₄) and evaporated to give a colourless oil. Purification by vacuum distillation provided **3.90** as a colourless oil (1.729 g, 89%): b.p. 108-112 °C (6.5 mm Hg) [lit. 117-120 °C (3 mm Hg)⁴⁶⁶ and 150-152 °C (13 mm Hg)⁴⁶⁷]; ¹H-NMR (250 MHz, CDCl₃) δ 1.43 (d, J = 6.1 Hz, 6H), 3.91 (s, 3H), 4.69 (sp, J = 6.1 Hz, 1H), 6.98 (d, J = 8.1 Hz, 1H), 7.4-7.5 (m, 2H), 9.84 (s, 1H); ¹³C-NMR (50.3 MHz, CDCl₃) δ 21.5, 55.6, 70.9, 109.3, 112.6, 126.2, 129.4, 150.0, 152.7, 190.4.



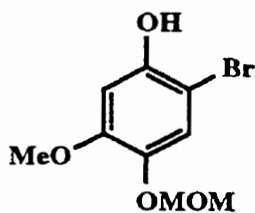
4-Isopropoxy-3-methoxyphenol (3.91): Method 1: To a solution of aldehyde **3.90** (4.866 g, 25.0 mmol) in CH₂Cl₂ (50 mL) at room temperature was added selenium catalyst **3.79** (492 mg, 1.0 mmol) and H₂O₂ (6.5 mL, 30% solution, approximately 50 mmol), and the mixture was stirred vigorously for 48 h. The yellow mixture was filtered to remove the insoluble catalyst, and the filtrate was poured into H₂O (50 mL) and extracted with CH₂Cl₂ (3 x 50 mL). The combined organic layers were washed successively with NaHSO₃ (50 mL, 10% solution), Na₂CO₃ (50 mL, 10% solution), and H₂O (50 mL). Drying (Na₂SO₄) and evaporating led to isolation the crude formate ester, which was dissolved in CH₃OH (50 mL) and cooled to 0 °C. To this was added powdered KOH (5.0 g, 89 mmol) in several portions. After stirring for 1 h, H₂O (100 mL) was added and the mixture was extracted with Et₂O (2 x 50 mL). The aqueous layer was acidified (10% HCl) and extracted with CHCl₃ (3 x 50 mL). The combined organic extracts were dried (Na₂SO₄) and evaporated to provide a dark brown residue. The oily mixture was passed through a short silica gel column (50% hexane/Et₂O) and the resulting solid was recrystallized (Et₂O/hexane) to provide **3.91** as a white solid (2.957 g, 65%); *or* Method 2: According to a literature procedure,⁴⁶¹ to a solution of aldehyde **3.90** (1.123 g, 5.8 mmol) in MeOH (10 mL) at room temperature was added H₂O₂ (2 mL, 30% solution, approximately 15 mmol) and conc. H₂SO₄ (0.25 mL). The solution was stirred at room temperature for 8 h during which time a red colour developed. The solution was cooled to 0 °C and NaHCO₃ (3 mL, 2 M solution) was added dropwise followed by Na₂SO₃

(20 mL, 2 M solution). After warming to room temperature, the volatile solvent was removed under reduced pressure and the residue was poured into H₂O (50 mL) and extracted with EtOAc (3 x 50 mL). The combined organic extracts were dried (Na₂SO₄) and evaporated to provide a waxy brown solid. Purification as above provided **3.91** as a white solid (928 mg, 88%): m.p. 41.5-42.5 °C (lit.⁴⁶⁸ 38-44 °C); ¹H-NMR (250 MHz, CDCl₃) δ 1.30 (d, J = 6.1 Hz, 6H), 3.75 (s, 3H), 4.34 (sp, J = 6.1 Hz, 1H), 5.3 (bs, 1H, exch.), 6.30 (dd, J = 8.5 Hz and 2.7 Hz, 1H), 6.43 (d, J = 2.7 Hz, 1H), 6.77 (d, J = 8.5 Hz, 1H); ¹³C-NMR (50.3 MHz, CDCl₃) δ 22.1, 55.7, 73.1, 100.8, 106.1, 119.0, 140.6, 151.1, 151.8.



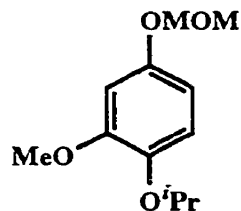
***N,N*-Diethyl *O*-(4-isopropoxy-3-methoxyphenyl)carbamate**

(3.92): According to General Procedure F, to a solution of phenol **3.91** (364 mg, 2.0 mmol) in CH₃CN (20 mL) at room temperature was added K₂CO₃ (304 mg, 2.2 mmol) and ClCONEt₂ (0.28 mL, 2.2 mmol). The mixture was stirred vigorously and heated to reflux. After 5 h, the mixture was cooled to room temperature, poured into H₂O (100 mL), and extracted with CH₂Cl₂ (3 x 20 mL). The combined organic extracts were dried (Na₂SO₄) and evaporated to give a yellow oil. Purification by flash chromatography (40% Et₂O/hexane) provided **3.92** as a colourless oil (472 mg, 84%): ¹H-NMR (200 MHz, CDCl₃) δ 1.23 (d, J = 6.2 Hz, 6H), 1.34 (d, J = 6.1 Hz, 6H), 3.41 (bs, 4H), 3.83 (s, 3H), 4.44 (sp, J = 6.1 Hz, 1H), 6.62 (dd, J = 8.6 Hz and 2.7 Hz, 1H), 6.69 (d, J = 2.7 Hz, 1H), 6.86 (d, J = 8.6 Hz, 1H).



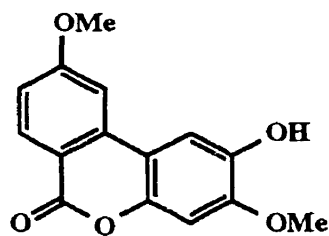
2-Bromo-4-isopropoxy-3-methoxyphenol (3.93): To a solution of phenol **3.83** (184 mg, 1.0 mmol) in DMF (10 mL) at room temperature was added a solution of NBS (178 mg, 1.0 mmol) in DMF (10 mL). The solution was stirred at room temperature for 24 h and

was then poured into H₂O (20 mL) and extracted with Et₂O (50 mL). The Et₂O extract was washed with H₂O (8 x 20 mL), dried (Na₂SO₄) and evaporated to give a brown oil that was immediately protected as the corresponding carbamate (see Procedure 3.62).



4-Isopropoxy-3-methoxyphenol, methoxymethyl ether

(3.95): To a solution of NaH (250 mg, 5.2 mmol) in THF (50 mL) at 0 °C was added MOMCl (0.39 mL, 5.2 mmol) followed by dropwise addition of phenol **3.91** (783 mg, 4.3 mmol) as a solution in THF (10 mL) over 30 min. When all of the phenol solution had been added, the mixture was stirred for an additional 2 h as it slowly warmed to room temperature. The reaction mixture was poured into H₂O (50 mL) and extracted with EtOAc (3 x 50 mL). The combined organic extracts were dried (Na₂SO₄) and evaporated to give a yellow oil. Purification by flash chromatography (50% Et₂O/hexane) provided **3.95** as a colourless oil (722 mg, 74%): ¹H-NMR (250 MHz, CDCl₃) δ 1.32 (d, J = 6.1 Hz, 6H), 3.48 (s, 3H), 3.82 (s, 3H), 4.37 (sp, J = 6.1 Hz, 1H), 5.11 (s, 2H), 6.55 (dd, J = 8.7 Hz and 2.8 Hz, 1H), 6.62 (d, J = 2.8 Hz, 1H), 6.81 (d, J = 8.7 Hz, 1H); ¹³C-NMR (62.9 MHz, CDCl₃) δ 22.0, 55.6, 72.4, 95.0, 102.4, 107.0, 118.3, 142.2, 151.6, 152.5; IR (neat) ν_{max} 3385, 2974, 2934, 2827, 1608, 1595, 1507 cm⁻¹; EI MS *m/z* (rel intensity): 226 (M⁺, 47), 184 (53), 154 (100), 139 (41), 123 (7), 111 (11). Anal. calcd for C₁₂H₁₈O₄: C, 63.70; H, 8.01; found: C, 63.89; H, 7.98.



2,6-Dimethoxy-3-hydroxydibenzo[*b,d*]pyran-6-one

(3.97): To a solution of pyranone **3.65** (10.4 mg, 0.033 mmol) and oxalyl chloride (1.03 mL of a 0.057 M solution in CH₃NO₂) in CH₃NO₂ (1 mL) at room temperature was added excess TiCl₄ (1 drop, approximately 0.5 mmol). The flask was warmed to slightly above room temperature and the solution quickly turned dark orange, then black. After 10 min, the solution was cooled to room temperature and NaHCO₃ (2 mL, 2 M solution) was added

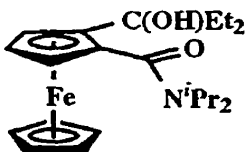
changing the colour immediately to light orange. The mixture was partitioned between H₂O (50 mL) and CHCl₃ (50 mL) and sodium potassium tartrate (1 g) was added. After separation of the layers, the H₂O layer was washed with CHCl₃ (25 mL) and the combined organic layers were dried (Na₂SO₄) and evaporated to provide **3.97** as an off-white solid (6.4 mg, 71%): ¹H-NMR (200 MHz, CDCl₃) δ 3.88 (s, 3H), 3.97 (s, 3H), 7.01 (s, 1H), 7.12 (dd, J = 8.7 Hz and 2.1 Hz, 1H), 7.54 (d, J = 2.1 Hz, 1H), 7.65 (s, 1H), 8.11 (d, J = 8.7 Hz, 1H), 9.20 (bs, 1H, exch.).

5.0 Appendices

- 5.1 X-ray analysis of **1.159d**
- 5.2 X-ray analysis of **1.161**
- 5.3 ¹H-NMR spectrum of **1.169a**
- 5.4 X-ray analysis of **1.170**
- 5.5 X-ray analysis of **1.171n**
- 5.6 X-ray analysis of **1.176**
- 5.7 X-ray analysis of **2.84c**
- 5.8 ¹H-NMR spectra of **2.101a**

5.1 Appendix 1 - X-ray analysis of 1.159d

The following 8 pages contain a structure determination summary as well as bond length and bond angle tables for single crystal X-ray diffraction analysis of **1.159d**.



STRUCTURE DETERMINATION SUMMARY

Crystal Data

Empirical Formula	$C_{22}H_{33}FeNO_2$
Color; Habit	Orange Pseudo-octagonal Needle Prism Fragment
Crystal Size (mm)	0.38{100}x0.36{010}x0.38{001}x0.34{012}
Crystal System	Orthorhombic
Space Group	$P2_1^2 2_1^2$
Unit Cell Dimensions	$a = 7.4383(7) \text{ \AA}$ $b = 9.8099(8) \text{ \AA}$ $c = 28.763(2) \text{ \AA}$
Volume	$2098.8(3) \text{ \AA}^3$
Z	4
Formula Weight	399.3
Density(calc.)	1.264 g/cm^3
Absorption Coefficient	7.33 cm^{-1}
F(000)	856

Data Collection

Diffractometer Used	Siemens P4
Radiation	MoK α ($\lambda = 0.71073 \text{ \AA}$)
Temperature (K)	200
Monochromator	Highly oriented graphite crystal
2θ Range	4.0 to 60.0 $^{\circ}$
Scan Type	ω
Scan Speed	Variable; 3.00 to 30.00 $^{\circ}$ /min. in ω
Scan Range (ω)	1.20 $^{\circ}$
Background Measurement	Stationary crystal and stationary counter at beginning and end of scan, each for 0.5% of total scan time
Standard Reflections	3 measured every 100 reflections
Index Ranges	$0 \leq h \leq 10, 0 \leq k \leq 13$ $-40 \leq l \leq 40$
Reflections Collected	6866
Independent Reflections	6130 ($R_{\text{int}} = 1.43\%$)*
Observed Reflections	5006 ($F > 6.0\sigma(F)$)
Absorption Correction	Face-indexed numerical
Min./Max. Transmission	0.7950 / 0.8155
* Unmerged Friedels	

Solution and Refinement

System Used	Siemens SHELXTL IRIS
Solution	Patterson and Fourier
Refinement Method	Full-Matrix Least-Squares
Quantity Minimized	$\sum w(F_o - F_c)^2$
Absolute Structure	*
Extinction Correction	$\chi = 0.00264(4)$, where $F^* = F [1 + 0.002\chi F^2 / \sin(2\theta)]^{-1/4}$
Hydrogen Atoms	Riding model, refined isotropic U
Weighting Scheme	$w^{-1} = \sigma^2(F)$
Number of Parameters Refined	269
Final R Indices (obs. data)	R = 2.83 %, wR = 2.98 %
(R Indices (all data)	R = 3.47 %, wR = 3.05 %)
Goodness-of-Fit	1.59
Largest and Mean Δ/σ	0.005, 0.001
Data-to-Parameter Ratio	18.6:1
Largest Difference Peak	0.47 eÅ ⁻³
Largest Difference Hole	-0.44 eÅ ⁻³

* The alternative enantiomer gave R, wR, and GoF values of 4.30, 4.67, and 2.489 respectively.

Table 1. Atomic coordinates ($\times 10^4$) and equivalent isotropic displacement coefficients ($\text{\AA}^2 \times 10^4$)

	x	y	z	U(eq)
Fe(1)	1314.8(3)	279.5(3)	453.4(1)	225.6(6)
C(1)	2642(2)	52(2)	1067.7(6)	207(5)
C(2)	2020(2)	-1252(2)	896.1(6)	207(5)
C(3)	2853(2)	-1437(2)	454.4(6)	248(5)
C(4)	3919(2)	-282(2)	346.2(5)	253(5)
C(5)	3789(3)	644(2)	724.2(5)	245(5)
C(1')	-886(4)	1425(4)	564.3(9)	755(13)
C(2')	-1365(3)	182(4)	345(1)	718(11)
C(3')	-490(3)	117(3)	-76.2(9)	526(9)
C(4')	510(3)	1295(3)	-126.5(8)	451(8)
C(5')	300(4)	2111(3)	259.0(9)	541(9)
C(6)	2082(3)	695(2)	1518.4(6)	226(5)
O(7)	481(2)	656(2)	1641.5(5)	324(4)
N(8)	3324(2)	1308(2)	1786.3(5)	214(4)
C(9)	5288(2)	1213(2)	1711.2(6)	284(6)
C(10)	6208(3)	474(3)	2110.6(7)	526(9)
C(11)	6102(3)	2611(3)	1621.6(8)	487(8)
C(12)	2723(3)	2028(2)	2213.7(7)	296(6)
C(13)	1481(3)	3214(2)	2106.0(9)	494(8)
C(14)	1956(3)	1070(3)	2581.9(7)	479(8)
C(15)	904(2)	-2309(2)	1157.2(6)	243(5)
O(16)	-746(2)	-1755(1)	1325.6(5)	312(4)
C(17)	343(3)	-3464(2)	830.0(7)	309(6)
C(18)	-927(3)	-4502(2)	1050.2(8)	455(8)
C(19)	2016(3)	-2821(2)	1572.4(6)	322(6)
C(20)	3840(3)	-3425(3)	1451.4(9)	533(8)

* Equivalent isotropic U defined as one third of the trace of the orthogonalized U_{ij} tensor

Table 2. Bond lengths (Å)

Fe(1)-C(1)	2.036(2)	Fe(1)-C(2)	2.038(2)
Fe(1)-C(3)	2.036(2)	Fe(1)-C(4)	2.037(2)
Fe(1)-C(5)	2.030(2)	Fe(1)-C(1')	2.011(3)
Fe(1)-C(2')	2.019(2)	Fe(1)-C(3')	2.037(3)
Fe(1)-C(4')	2.033(2)	Fe(1)-C(5')	2.028(3)
C(1)-C(2)	1.447(2)	C(1)-C(5)	1.428(2)
C(1)-C(6)	1.501(2)	C(2)-C(3)	1.425(2)
C(2)-C(15)	1.525(3)	C(3)-C(4)	1.417(3)
C(4)-C(5)	1.420(2)	C(1')-C(2')	1.418(5)
C(1')-C(5')	1.415(4)	C(2')-C(3')	1.377(4)
C(3')-C(4')	1.382(4)	C(4')-C(5')	1.376(4)
C(6)-O(7)	1.242(2)	C(6)-N(8)	1.345(2)
N(8)-C(9)	1.479(2)	N(8)-C(12)	1.486(2)
C(9)-C(10)	1.521(3)	C(9)-C(11)	1.522(3)
C(12)-C(13)	1.518(3)	C(12)-C(14)	1.526(3)
C(15)-O(16)	1.427(2)	C(15)-C(17)	1.531(3)
C(15)-C(19)	1.537(3)	C(17)-C(18)	1.526(3)
C(19)-C(20)	1.521(3)	Fe(1)-cent(1)	1.634
Fe(1)-cent(1')	1.642		

Table 3. Bond angles ($^{\circ}$)

C(1)-Fe(1)-C(2)	41.6(1)	C(1)-Fe(1)-C(3)	68.6(1)
C(2)-Fe(1)-C(3)	41.0(1)	C(1)-Fe(1)-C(4)	68.9(1)
C(2)-Fe(1)-C(4)	69.6(1)	C(3)-Fe(1)-C(4)	40.7(1)
C(1)-Fe(1)-C(5)	41.1(1)	C(2)-Fe(1)-C(5)	69.9(1)
C(3)-Fe(1)-C(5)	68.6(1)	C(4)-Fe(1)-C(5)	40.9(1)
C(1)-Fe(1)-C(1')	108.6(1)	C(2)-Fe(1)-C(1')	121.5(1)
C(3)-Fe(1)-C(1')	156.8(1)	C(4)-Fe(1)-C(1')	161.6(1)
C(5)-Fe(1)-C(1')	125.4(1)	C(1)-Fe(1)-C(2')	127.4(1)
C(2)-Fe(1)-C(2')	108.4(1)	C(3)-Fe(1)-C(2')	121.0(1)
C(4)-Fe(1)-C(2')	154.5(1)	C(5)-Fe(1)-C(2')	164.2(1)
C(1')-Fe(1)-C(2')	41.2(1)	C(1)-Fe(1)-C(3')	163.7(1)
C(2)-Fe(1)-C(3')	125.4(1)	C(3)-Fe(1)-C(3')	107.9(1)
C(4)-Fe(1)-C(3')	119.5(1)	C(5)-Fe(1)-C(3')	153.9(1)
C(1')-Fe(1)-C(3')	68.0(1)	C(2')-Fe(1)-C(3')	39.7(1)
C(1)-Fe(1)-C(4')	155.3(1)	C(2)-Fe(1)-C(4')	161.7(1)
C(3)-Fe(1)-C(4')	124.9(1)	C(4)-Fe(1)-C(4')	106.8(1)
C(5)-Fe(1)-C(4')	119.7(1)	C(1')-Fe(1)-C(4')	67.5(1)
C(2')-Fe(1)-C(4')	66.8(1)	C(3')-Fe(1)-C(4')	39.7(1)
C(1)-Fe(1)-C(5')	121.1(1)	C(2)-Fe(1)-C(5')	157.1(1)
C(3)-Fe(1)-C(5')	160.5(1)	C(4)-Fe(1)-C(5')	123.5(1)
C(5)-Fe(1)-C(5')	106.7(1)	C(1')-Fe(1)-C(5')	41.0(1)
C(2')-Fe(1)-C(5')	68.4(1)	C(3')-Fe(1)-C(5')	67.5(1)
C(4')-Fe(1)-C(5')	39.6(1)	Fe(1)-C(1)-C(2)	69.3(1)
Fe(1)-C(1)-C(5)	69.2(1)	C(2)-C(1)-C(5)	108.3(1)
Fe(1)-C(1)-C(6)	124.7(1)	C(2)-C(1)-C(6)	125.3(1)
C(5)-C(1)-C(6)	126.3(2)	Fe(1)-C(2)-C(1)	69.1(1)
Fe(1)-C(2)-C(3)	69.5(1)	C(1)-C(2)-C(3)	106.1(1)
Fe(1)-C(2)-C(15)	132.0(1)	C(1)-C(2)-C(15)	127.4(1)
C(3)-C(2)-C(15)	126.1(2)	Fe(1)-C(3)-C(2)	69.6(1)
Fe(1)-C(3)-C(4)	69.7(1)	C(2)-C(3)-C(4)	109.7(2)
Fe(1)-C(4)-C(3)	69.6(1)	Fe(1)-C(4)-C(5)	69.3(1)
C(3)-C(4)-C(5)	107.8(1)	Fe(1)-C(5)-C(1)	69.7(1)
Fe(1)-C(5)-C(4)	69.8(1)	C(1)-C(5)-C(4)	108.1(2)
Fe(1)-C(1')-C(2')	69.7(2)	Fe(1)-C(1')-C(5')	70.1(2)
C(2')-C(1')-C(5')	106.9(2)	Fe(1)-C(2')-C(1')	69.1(2)
Fe(1)-C(2')-C(3')	70.8(1)	C(1')-C(2')-C(3')	108.2(3)
Fe(1)-C(3')-C(2')	69.5(2)	Fe(1)-C(3')-C(4')	70.0(1)
C(2')-C(3')-C(4')	107.9(2)	Fe(1)-C(4')-C(3')	70.3(1)
Fe(1)-C(4')-C(5')	70.0(1)	C(3')-C(4')-C(5')	109.9(2)
Fe(1)-C(5')-C(1')	68.9(2)	Fe(1)-C(5')-C(4')	70.4(1)
C(1')-C(5')-C(4')	107.1(2)	C(1)-C(6)-O(7)	119.9(2)
C(1)-C(6)-N(8)	119.5(2)	O(7)-C(6)-N(8)	120.6(2)
C(6)-N(8)-C(9)	124.5(1)	C(6)-N(8)-C(12)	118.7(1)
C(9)-N(8)-C(12)	116.6(1)	N(8)-C(9)-C(10)	111.4(2)
N(8)-C(9)-C(11)	111.1(2)	C(10)-C(9)-C(11)	112.2(2)
N(8)-C(12)-C(13)	112.2(2)	N(8)-C(12)-C(14)	113.2(2)
C(13)-C(12)-C(14)	112.7(2)	C(2)-C(15)-O(16)	112.1(1)
C(2)-C(15)-C(17)	110.4(1)	O(16)-C(15)-C(17)	104.8(1)
C(2)-C(15)-C(19)	108.2(1)	O(16)-C(15)-C(19)	108.9(1)
C(17)-C(15)-C(19)	112.5(2)	C(15)-C(17)-C(18)	114.0(2)
C(15)-C(19)-C(20)	115.4(2)		

Table 4. Anisotropic displacement coefficients ($\text{\AA}^2 \times 10^4$)

	U_{11}	U_{22}	U_{33}	U_{12}	U_{13}	U_{23}
Fe(1)	192(1)	248(1)	237(1)	10(1)	-20(1)	28(1)
C(1)	155(7)	240(10)	226(8)	-7(6)	7(6)	-15(6)
C(2)	192(8)	227(9)	202(8)	25(7)	12(7)	-12(7)
C(3)	272(9)	261(9)	211(8)	52(7)	25(8)	-8(9)
C(4)	216(8)	356(9)	188(7)	31(10)	31(6)	13(8)
C(5)	209(8)	307(10)	218(8)	-46(9)	-1(8)	7(6)
C(1')	623(20)	1213(29)	428(15)	704(21)	43(13)	54(16)
C(2')	201(9)	988(24)	965(22)	17(17)	-96(13)	549(20)
C(3')	455(13)	547(17)	577(15)	-40(12)	-305(12)	100(13)
C(4')	410(13)	553(15)	389(12)	127(12)	-69(10)	189(11)
C(5')	562(16)	345(13)	717(18)	159(13)	-207(14)	26(13)
C(6)	223(9)	236(9)	219(8)	-31(7)	8(7)	-19(7)
O(7)	198(6)	435(9)	340(7)	-74(6)	66(6)	-158(6)
N(8)	174(8)	257(8)	212(7)	-1(6)	0(5)	-31(6)
C(9)	183(9)	450(12)	220(9)	-2(9)	10(7)	-45(9)
C(10)	303(11)	955(22)	319(10)	211(17)	-26(10)	41(13)
C(11)	355(13)	644(16)	462(13)	-254(13)	51(11)	-97(12)
C(12)	248(10)	357(11)	283(9)	-17(9)	-8(8)	-134(8)
C(13)	404(14)	401(13)	679(16)	97(12)	-74(14)	-234(12)
C(14)	431(13)	736(18)	270(11)	-26(14)	98(10)	-45(11)
C(15)	255(10)	236(9)	238(8)	-7(7)	41(7)	-32(7)
O(16)	251(7)	305(8)	380(8)	-58(6)	95(6)	-65(6)
C(17)	383(11)	267(10)	277(10)	-44(9)	47(8)	-29(8)
C(18)	573(16)	342(13)	450(12)	-175(12)	67(11)	-80(10)
C(19)	387(11)	332(11)	246(9)	-26(10)	36(9)	49(9)
C(20)	462(14)	659(17)	477(13)	189(15)	-8(13)	208(13)

The anisotropic displacement factor exponent takes the form:

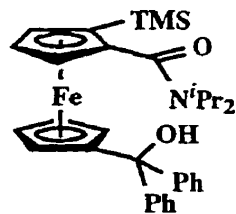
$$-2\pi^2 (h^2 a^2 U_{11} + \dots + 2klb^*c^*U_{23})$$

Table 5. H-Atom coordinates ($\times 10^4$) and isotropic displacement coefficients ($\text{\AA}^2 \times 10^3$)

	x	y	z	U
H(3)	2676	-2200	250	29(6)
H(4)	4575	-138	63	33(6)
H(5)	4368	1516	745	14(5)
H(1')	-1315	1758	858	78(9)
H(2')	-2159	-500	468	85(10)
H(3')	-542	-618	-296	133(16)
H(4')	1281	1497	-385	84(10)
H(5')	861	2981	307	72(9)
H(9)	5476	670	1438	24(5)
H(10x)	5597	-372	2168	73(10)
H(10y)	6160	1030	2385	61(8)
H(10z)	7446	294	2039	79(9)
H(11x)	5559	2981	1346	60(9)
H(11y)	7380	2553	1579	68(9)
H(11z)	5868	3203	1880	58(8)
H(12)	3786	2417	2349	28(5)
H(13x)	315	2885	2018	63(9)
H(13y)	2017	3724	1857	65(9)
H(13z)	1395	3807	2370	91(10)
H(14x)	2728	294	2618	80(10)
H(14y)	783	784	2483	48(7)
H(14z)	1825	1537	2873	72(9)
H(17x)	1405	-3930	726	42(6)
H(17y)	-233	-3077	562	36(6)
H(18x)	-1280	-5182	828	60(7)
H(18y)	-1966	-4031	1166	73(10)
H(18z)	-332	-4921	1310	99(12)
H(19x)	1339	-3507	1733	48(6)
H(19y)	2197	-2075	1783	35(6)
H(20x)	3697	-4200	1251	73(9)
H(20y)	4463	-3680	1730	49(7)
H(20z)	4534	-2730	1300	70(10)
H(16)	-458	-975	1419	47(7)

5.2 Appendix 2 - X-ray analysis of 1.161

The following 9 pages contain a structure determination summary as well as bond length and bond angle tables for single crystal X-ray diffraction analysis of **1.161**.



STRUCTURE DETERMINATION SUMMARY

Crystal Data

Empirical Formula	$C_{33}H_{41}FeNO_2Si$
Color; Habit	Orange Pseudo-hexagonal Needle Prism Fragment
Crystal Size (mm)	0.54{100}x0.42{011}
Crystal System	Orthorhombic
Space Group	$P2_1^2 2_1$
Unit Cell Dimensions	$\underline{a} = 8.353(1) \text{ \AA}$ $\underline{b} = 18.301(2) \text{ \AA}$ $\underline{c} = 19.694(2) \text{ \AA}$
Volume	$3010.6(6) \text{ \AA}^3$
Z	4
Formula Weight	567.6
Density(calc.)	1.252 g/cm^3
Absorption Coefficient	5.70 cm^{-1}
F(000)	1208

Data Collection

Diffractometer Used	Siemens P4
Radiation	MoK α ($\lambda = 0.71073 \text{ \AA}$)
Temperature (K)	200
Monochromator	Highly oriented graphite crystal
2θ Range	4.0 to 56.0 $^\circ$
Scan Type	ω
Scan Speed	Variable; 3.00 to 30.00 $^\circ$ /min. in ω
Scan Range (ω)	1.20 $^\circ$
Background Measurement	Stationary crystal and stationary counter at beginning and end of scan, each for 25.0% of total scan time
Standard Reflections	3 measured every 100 reflections
Index Ranges	$0 \leq h \leq 11, 0 \leq k \leq 24$ $-26 \leq l \leq 26$
Reflections Collected	7948
Independent Reflections	7259 ($R_{\text{int}} = 5.96\%$)*
Observed Reflections	6289 ($F > 6.0\sigma(F)$)
Absorption Correction	Face-indexed numerical
Min./Max. Transmission	0.7822 / 0.8161
* Unmerged Friedels	

Solution and Refinement

System Used	Siemens SHELXTL IRIS
Solution	Patterson and Fourier
Refinement Method	Full-Matrix Least-Squares
Quantity Minimized	$\sum w(F_o - F_c)^2$
Absolute Structure	*
Extinction Correction	$\chi = 0.00033(2)$, where $F^* = F [1 + 0.002\chi F^2 / \sin(2\theta)]^{-1/4}$
Hydrogen Atoms	Riding model, refined isotropic U
Weighting Scheme	$w^{-1} = \sigma^2(F)$
Number of Parameters Refined	385
Final R Indices (obs. data)	R = 2.79 %, wR = 2.91 %
(R Indices (all data))	R = 3.24 %, wR = 2.94 %
Goodness-of-Fit	1.82
Largest and Mean Δ/σ	0.006, 0.001
Data-to-Parameter Ratio	16.3:1
Largest Difference Peak	0.50 eÅ ⁻³
Largest Difference Hole	-0.44 eÅ ⁻³

* The alternative enantiomer gave R, wR, and GoF values of 4.35, 4.72 and 2.95 respectively.

Table 1. Atomic coordinates ($\times 10^4$) and equivalent isotropic displacement coefficients ($\text{\AA}^2 \times 10^4$)

	x	y	z	U(eq)
Fe(1)	7992.8(3)	4503.6(1)	3494.9(1)	239.7(7)
C(1)	7466(2)	3463.3(9)	3189(1)	252(5)
C(2)	8794(2)	3745(1)	2804(1)	304(6)
C(3)	10013(2)	3919(1)	3293(1)	331(6)
C(4)	9460(3)	3753(1)	3951(1)	341(6)
C(5)	7882(3)	3470.7(9)	3896(1)	298(6)
C(6)	5903(2)	3196(1)	2903(1)	248(5)
O(7)	4829(2)	3625.6(7)	2743.0(7)	298(4)
N(8)	5736(2)	2468.6(8)	2816.6(9)	307(5)
C(9)	4230(3)	2180(1)	2513(1)	341(6)
C(10)	3996(3)	2443(1)	1789(1)	444(8)
C(11)	2770(3)	2321(1)	2958(1)	406(7)
C(12)	6941(3)	1925(1)	3046(1)	433(7)
C(13)	6303(4)	1479(1)	3640(1)	617(10)
C(14)	7513(3)	1432(1)	2475(2)	600(10)
Si(15)	9031.9(8)	3885.6(4)	1868.9(3)	417(2)
C(16)	7252(3)	4352(2)	1497(1)	664(11)
C(17)	9260(5)	2977(2)	1435(2)	828(13)
C(18)	10887(3)	4427(2)	1730(1)	545(9)
C(1')	6119(2)	5125(1)	3840(1)	271(6)
C(2')	6371(3)	5252(1)	3134(1)	303(6)
C(3')	7966(3)	5511(1)	3042(1)	354(6)
C(4')	8702(3)	5555(1)	3690(1)	371(6)
C(5')	7572(2)	5316(1)	4176(1)	326(6)
C(19)	4502(2)	4885(1)	4131(1)	273(6)
O(20)	3485(2)	4671.2(7)	3586.1(7)	330(4)
C(21)	4705(2)	4251(1)	4640(1)	282(6)
C(22)	5523(3)	4362(1)	5248(1)	351(6)
C(23)	5760(3)	3793(1)	5696(1)	412(7)
C(24)	5160(3)	3104(1)	5555(1)	423(7)
C(25)	4290(3)	2998(1)	4974(1)	425(7)
C(26)	4063(3)	3571(1)	4515(1)	355(6)
C(27)	3629(2)	5512(1)	4485.5(9)	303(5)
C(28)	2196(3)	5370(1)	4815(1)	499(8)
C(29)	1349(3)	5922(2)	5136(1)	593(10)
C(30)	1922(3)	6629(1)	5122(1)	509(8)
C(31)	3316(3)	6774(1)	4802(1)	545(9)
C(32)	4186(3)	6222(1)	4484(1)	437(7)

* Equivalent isotropic U defined as one third of the trace of the orthogonalized U_{ij} tensor

Table 2. Bond lengths (Å)

Fe(1)-C(1)	2.045(2)	Fe(1)-C(2)	2.057(2)
Fe(1)-C(3)	2.038(2)	Fe(1)-C(4)	2.048(2)
Fe(1)-C(5)	2.051(2)	Fe(1)-C(1')	2.051(2)
Fe(1)-C(2')	2.053(2)	Fe(1)-C(3')	2.047(2)
Fe(1)-C(4')	2.050(2)	Fe(1)-C(5')	2.034(2)
C(1)-C(2)	1.440(3)	C(1)-C(5)	1.435(3)
C(1)-C(6)	1.504(3)	C(2)-C(3)	1.438(3)
C(2)-Si(15)	1.869(2)	C(3)-C(4)	1.408(3)
C(4)-C(5)	1.420(3)	C(6)-O(7)	1.233(2)
C(6)-N(8)	1.350(2)	N(8)-C(9)	1.489(3)
N(8)-C(12)	1.485(3)	C(9)-C(10)	1.519(3)
C(9)-C(11)	1.523(3)	C(12)-C(13)	1.523(4)
C(12)-C(14)	1.519(4)	Si(15)-C(16)	1.864(3)
Si(15)-C(17)	1.880(3)	Si(15)-C(18)	1.859(3)
C(1')-C(2')	1.423(3)	C(1')-C(5')	1.427(3)
C(1')-C(19)	1.533(3)	C(2')-C(3')	1.425(3)
C(3')-C(4')	1.419(3)	C(4')-C(5')	1.414(3)
C(19)-O(20)	1.423(2)	C(19)-C(21)	1.541(3)
C(19)-C(27)	1.529(3)	C(21)-C(22)	1.393(3)
C(21)-C(26)	1.378(3)	C(22)-C(23)	1.380(3)
C(23)-C(24)	1.384(3)	C(24)-C(25)	1.370(3)
C(25)-C(26)	1.398(3)	C(27)-C(28)	1.386(3)
C(27)-C(32)	1.381(3)	C(28)-C(29)	1.386(4)
C(29)-C(30)	1.381(4)	C(30)-C(31)	1.350(4)
C(31)-C(32)	1.393(3)	.	.
Hydrogen Bond		H(20)...O(7)	1.91
O(20)-H(20)	0.89		
O(20)...O(7)	2.771(2)		

Table 3. Bond Angles (°)

C(1)-Fe(1)-C(2)	41.1(1)	C(1)-Fe(1)-C(3)	68.4(1)
C(2)-Fe(1)-C(3)	41.1(1)	C(1)-Fe(1)-C(4)	68.5(1)
C(2)-Fe(1)-C(4)	69.1(1)	C(3)-Fe(1)-C(4)	40.3(1)
C(1)-Fe(1)-C(5)	41.0(1)	C(2)-Fe(1)-C(5)	69.4(1)
C(3)-Fe(1)-C(5)	68.2(1)	C(4)-Fe(1)-C(5)	40.5(1)
C(1)-Fe(1)-C(1')	116.8(1)	C(2)-Fe(1)-C(1')	147.4(1)
C(3)-Fe(1)-C(1')	171.2(1)	C(4)-Fe(1)-C(1')	133.1(1)
C(5)-Fe(1)-C(1')	110.5(1)	C(1)-Fe(1)-C(2')	112.2(1)
C(2)-Fe(1)-C(1')	115.9(1)	C(3)-Fe(1)-C(2')	146.0(1)
C(4)-Fe(1)-C(1')	173.6(1)	C(5)-Fe(1)-C(2')	135.9(1)
C(1')-Fe(1)-C(2')	40.6(1)	C(1)-Fe(1)-C(3')	135.0(1)
C(2)-Fe(1)-C(3')	108.8(1)	C(3)-Fe(1)-C(3')	113.4(1)
C(4)-Fe(1)-C(3')	143.3(1)	C(5)-Fe(1)-C(3')	175.5(1)
C(1')-Fe(1)-C(3')	68.7(1)	C(2')-Fe(1)-C(3')	40.7(1)
C(1)-Fe(1)-C(4')	172.5(1)	C(2)-Fe(1)-C(4')	131.6(1)
C(3)-Fe(1)-C(4')	106.9(1)	C(4)-Fe(1)-C(4')	112.0(1)
C(5)-Fe(1)-C(4')	143.7(1)	C(1')-Fe(1)-C(4')	68.8(1)
C(2')-Fe(1)-C(4')	68.2(1)	C(3')-Fe(1)-C(4')	40.5(1)
C(1)-Fe(1)-C(5')	146.9(1)	C(2)-Fe(1)-C(5')	170.7(1)
C(3)-Fe(1)-C(5')	131.0(1)	C(4)-Fe(1)-C(5')	107.7(1)
C(5)-Fe(1)-C(5')	114.3(1)	C(1')-Fe(1)-C(5')	40.9(1)
C(2')-Fe(1)-C(5')	68.1(1)	C(3')-Fe(1)-C(5')	68.1(1)
C(4')-Fe(1)-C(5')	40.5(1)	Fe(1)-C(1)-C(2)	69.9(1)
Fe(1)-C(1)-C(5)	69.7(1)	C(2)-C(1)-C(5)	108.8(2)
Fe(1)-C(1)-C(6)	126.8(1)	C(2)-C(1)-C(6)	126.0(2)
C(5)-C(1)-C(6)	125.2(2)	Fe(1)-C(2)-C(1)	69.0(1)
Fe(1)-C(2)-C(3)	68.7(1)	C(1)-C(2)-C(3)	105.7(2)
Fe(1)-C(2)-Si(15)	126.4(1)	C(1)-C(2)-Si(15)	130.6(2)
C(3)-C(2)-Si(15)	123.7(1)	Fe(1)-C(3)-C(2)	70.2(1)
Fe(1)-C(3)-C(4)	70.2(1)	C(2)-C(3)-C(4)	109.7(2)
Fe(1)-C(2)-Si(15)	69.4(1)	Fe(1)-C(4)-C(5)	69.8(1)
C(3)-C(4)-C(5)	108.3(2)	Fe(1)-C(5)-C(1)	69.3(1)
Fe(1)-C(5)-C(4)	69.6(1)	C(1)-C(5)-C(4)	107.5(2)
C(1)-C(6)-O(7)	121.4(2)	C(1)-C(6)-N(8)	117.2(2)
O(7)-C(6)-N(8)	121.4(2)	C(6)-N(8)-C(9)	119.2(2)
C(6)-N(8)-C(12)	123.5(2)	C(9)-N(8)-C(12)	117.2(2)
N(8)-C(9)-C(10)	111.9(2)	N(8)-C(9)-C(11)	112.6(2)
C(10)-C(9)-C(11)	112.5(2)	N(8)-C(12)-C(13)	110.8(2)
N(8)-C(12)-C(14)	112.7(2)	C(13)-C(12)-C(14)	111.1(2)
C(2)-Si(15)-C(16)	111.4(1)	C(2)-Si(15)-C(17)	109.7(1)
C(16)-Si(15)-C(17)	107.9(2)	C(2)-Si(15)-C(18)	107.9(1)
C(16)-Si(15)-C(18)	111.3(1)	C(17)-Si(15)-C(18)	108.7(2)
Fe(1)-C(1')-C(2')	69.8(1)	Fe(1)-C(1')-C(5')	68.9(1)
C(2')-C(1')-C(5')	106.7(2)	Fe(1)-C(1')-C(19)	129.6(1)
C(2')-C(1')-C(19)	122.9(2)	C(5')-C(1')-C(19)	130.3(2)
Fe(1)-C(2')-C(1')	69.6(1)	Fe(1)-C(2')-C(3')	69.5(1)
C(1')-C(2')-C(3')	108.5(2)	Fe(1)-C(3')-C(2')	69.9(1)
Fe(1)-C(3')-C(4')	69.8(1)	C(2')-C(3')-C(4')	108.0(2)
Fe(1)-C(4')-C(3')	69.6(1)	Fe(1)-C(4')-C(5')	69.1(1)
C(3')-C(4')-C(5')	107.6(2)	Fe(1)-C(5')-C(1')	70.2(1)
Fe(1)-C(5')-C(4')	70.4(1)	C(1')-C(5')-C(4')	109.2(2)
C(1')-C(19)-O(20)	108.8(1)	C(1')-C(19)-C(21)	111.3(2)

Table 3. Bond Angles (°) continued

O(20)-C(19)-C(21)	110.5(1)	C(1')-C(19)-C(27)	112.0(2)
O(20)-C(19)-C(27)	105.4(1)	C(21)-C(19)-C(27)	108.7(1)
C(19)-C(21)-C(22)	120.2(2)	C(19)-C(21)-C(26)	121.4(2)
C(22)-C(21)-C(26)	118.4(2)	C(21)-C(22)-C(23)	120.7(2)
C(22)-C(23)-C(24)	120.5(2)	C(23)-C(24)-C(25)	119.2(2)
C(24)-C(25)-C(26)	120.4(2)	C(21)-C(26)-C(25)	120.7(2)
C(19)-C(27)-C(28)	119.0(2)	C(19)-C(27)-C(32)	123.1(2)
C(28)-C(27)-C(32)	117.9(2)	C(27)-C(28)-C(29)	121.2(2)
C(28)-C(29)-C(30)	119.8(2)	C(29)-C(30)-C(31)	119.5(2)
C(30)-C(31)-C(32)	121.2(2)	C(27)-C(32)-C(31)	120.4(2)

Table 4. Anisotropic displacement coefficients ($\text{\AA}^2 \times 10^4$)

	U_{11}	U_{22}	U_{33}	U_{12}	U_{13}	U_{23}
Fe(1)	213(1)	187(1)	319(1)	-6(1)	-41(1)	24(1)
C(1)	249(9)	174(8)	333(10)	14(7)	-33(8)	-2(8)
C(2)	250(10)	234(10)	429(11)	-1(8)	-23(9)	-33(9)
C(3)	205(9)	258(9)	531(13)	24(8)	-47(9)	-14(9)
C(4)	319(11)	248(10)	457(12)	39(9)	-161(10)	12(9)
C(5)	323(10)	194(8)	378(11)	2(9)	-83(10)	49(8)
C(6)	230(9)	242(9)	271(9)	-27(8)	19(8)	3(7)
O(7)	289(7)	229(7)	375(8)	-6(6)	-79(6)	-5(6)
N(8)	265(8)	209(8)	448(10)	-1(7)	-49(8)	-23(7)
C(9)	311(11)	241(10)	472(12)	-56(9)	-46(10)	-83(9)
C(10)	441(14)	484(14)	407(12)	-34(12)	-20(11)	-130(11)
C(11)	302(12)	408(12)	507(13)	-129(10)	12(10)	-25(10)
C(12)	361(12)	226(9)	713(16)	20(10)	-153(13)	-5(10)
C(13)	726(19)	422(14)	702(18)	49(14)	-168(16)	122(14)
C(14)	472(15)	328(12)	999(21)	120(11)	19(15)	-57(14)
Si(15)	359(3)	509(4)	385(3)	-116(3)	79(3)	-34(3)
C(16)	457(15)	1119(27)	416(13)	-171(16)	-28(13)	232(16)
C(17)	1058(28)	825(21)	602(18)	-370(23)	335(22)	-327(17)
C(18)	406(13)	603(18)	625(16)	-127(14)	149(12)	41(13)
C(1')	254(10)	175(9)	385(10)	15(8)	-6(9)	-12(8)
C(2')	321(10)	220(9)	368(11)	61(8)	-33(9)	78(8)
C(3')	372(10)	224(8)	465(11)	20(11)	48(10)	104(10)
C(4')	308(10)	200(9)	604(14)	-41(9)	-3(9)	-26(10)
C(5')	333(11)	241(10)	404(11)	-15(8)	-58(9)	-48(8)
C(19)	243(10)	282(10)	296(10)	12(8)	-43(8)	-3(8)
O(20)	251(6)	403(8)	334(7)	3(6)	-66(6)	-42(6)
C(21)	255(10)	276(9)	314(10)	-9(8)	25(8)	10(8)
C(22)	389(12)	285(11)	378(11)	-42(9)	-41(9)	-9(9)
C(23)	476(13)	406(12)	354(11)	-27(11)	-83(11)	62(10)
C(24)	489(14)	345(11)	436(13)	-49(11)	21(11)	122(10)
C(25)	460(13)	326(11)	490(13)	-142(11)	76(12)	21(10)
C(26)	343(11)	376(11)	346(11)	-85(10)	20(10)	-7(9)
C(27)	287(9)	355(10)	267(9)	87(10)	-55(8)	-1(9)
C(28)	324(12)	530(15)	642(15)	-13(12)	39(11)	-168(12)
C(29)	342(13)	845(21)	592(16)	94(14)	73(13)	-175(15)
C(30)	513(15)	569(15)	444(13)	241(15)	-74(13)	-131(11)
C(31)	643(19)	368(13)	623(16)	113(13)	88(14)	-32(11)
C(32)	481(13)	347(12)	484(13)	77(11)	110(12)	47(10)

The anisotropic displacement factor exponent takes the form:

$$-2\pi^2(h^2 a^2 U_{11} + \dots + 2klb^*c^*U_{23})$$

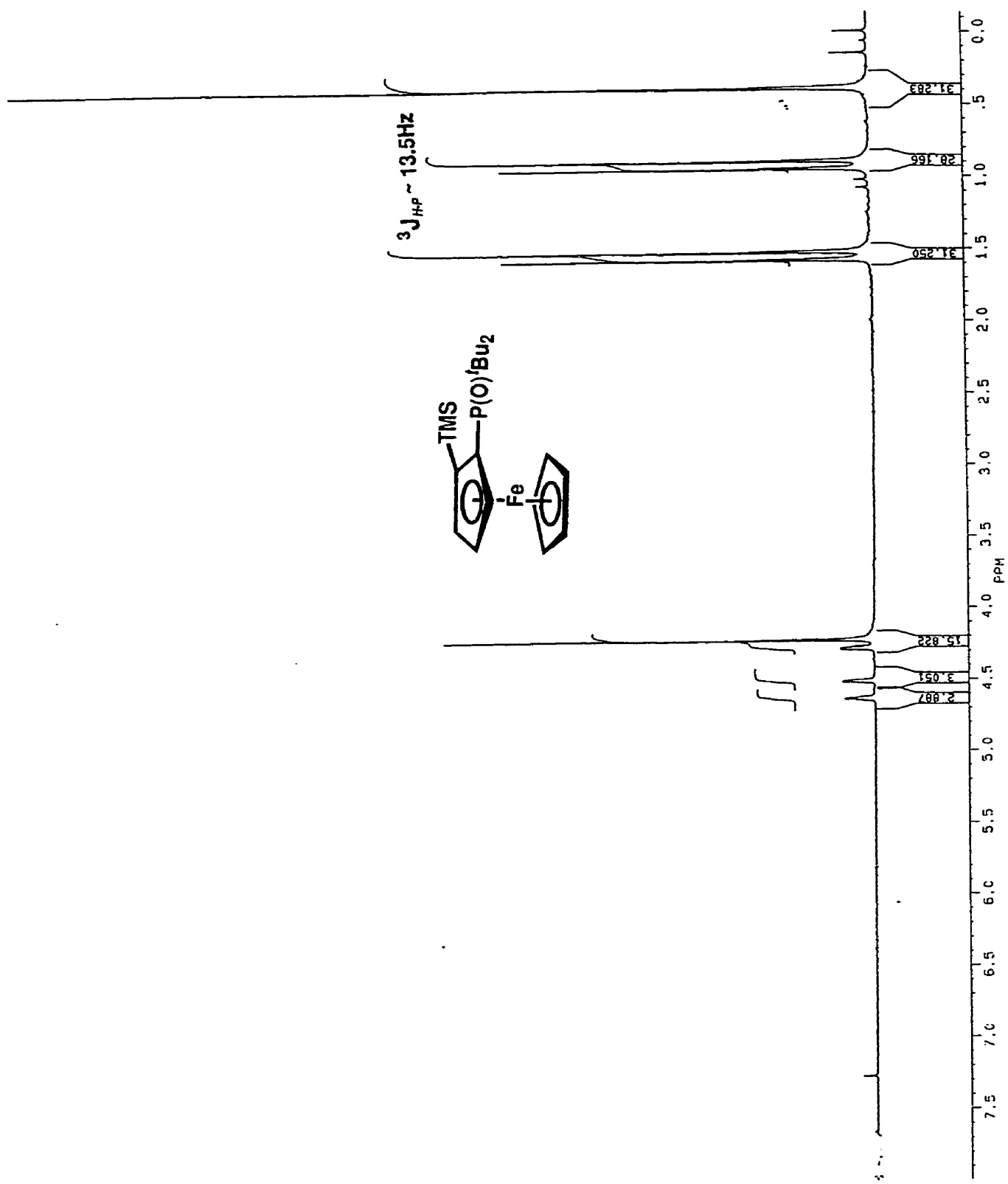
Table 5. H-Atom coordinates ($\times 10^4$) and isotropic displacement coefficients ($\text{\AA}^2 \times 10^3$)

	x	y	z	U
H(3)	11041	4124	3188	37(6)
H(4)	10039	3826	4366	41(6)
H(5)	7212	3316	4265	42(6)
H(9)	4358	1659	2486	36(6)
H(10x)	3242	2136	1557	39(6)
H(10y)	3604	2936	1798	69(9)
H(10z)	4998	2440	1550	71(9)
H(11x)	1871	2048	2792	38(6)
H(11y)	3005	2181	3417	68(8)
H(11z)	2526	2834	2955	57(8)
H(12)	7853	2192	3210	45(6)
H(13x)	7153	1264	3900	118(13)
H(13y)	5645	1785	3920	96(12)
H(13z)	5624	1109	3448	67(8)
H(14x)	7985	1739	2134	85(10)
H(14y)	8317	1088	2614	67(8)
H(14z)	6633	1180	2266	137(16)
H(16x)	6292	4183	1714	66(9)
H(16y)	7368	4869	1560	101(12)
H(16z)	7204	4259	1018	76(9)
H(17x)	10154	2724	1631	146(21)
H(17y)	8297	2698	1495	130(15)
H(17z)	9422	3043	956	132(15)
H(18x)	11372	4308	1302	98(11)
H(18y)	10616	4936	1753	125(14)
H(18z)	11602	4327	2100	112(13)
H(2')	5603	5165	2781	31(6)
H(3')	8462	5630	2617	45(7)
H(4')	9777	5710	3785	36(6)
H(5')	7749	5282	4657	32(6)
H(22)	5945	4837	5349	37(6)
H(23)	6306	3880	6118	44(7)
H(24)	5377	2703	5856	61(8)
H(25)	3820	2530	4882	50(7)
H(26)	3460	3497	4106	23(5)
H(28)	1782	4881	4818	64(8)
H(29)	363	5812	5365	87(11)
H(30)	1328	7015	5336	56(7)
H(31)	3734	7263	4803	75(10)
H(32)	5169	6336	4254	57(8)
H(20)*	4103	4385	3331	101(12)

* OH proton fixed in found position.

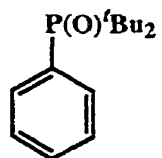
5.3 Appendix 3 - ^1H -NMR spectrum of 1.169a

The following is an ^1H -NMR spectrum of ferrocene derivative 1.169a, demonstrating the magnetic inequivalence of the two *tert*-butyl substituents.



5.4 Appendix 4 - X-ray analysis of 1.170

The following 8 pages contain a structure determination summary as well as bond length and bond angle tables for single crystal X-ray diffraction analysis of 1.170.



STRUCTURE DETERMINATION SUMMARY

Crystal Data

Empirical Formula	$C_{14}H_{23}OP$
Color; Habit	Colourless prism fragment
Crystal Size (mm)	0.41{100}x0.40{010}x0.24{10 $\bar{2}$ }
	Distances from common centre
Crystal System	Monoclinic
Space Group	$P2_1/c$
Unit Cell Dimensions	$a = 12.742(1) \text{ \AA}$ $b = 14.688(1) \text{ \AA}$ $c = 15.820(1) \text{ \AA}$ $\beta = 109.469(4)^\circ$
Volume	$2791.6(5) \text{ \AA}^3$
Z	8
Formula Weight	238.3
Density(calc.)	1.134 g/cm^3
Absorption Coefficient	1.77 cm^{-1}
F(000)	1040

Data Collection

Diffractometer Used	Siemens P4
Radiation	MoK α ($\lambda = 0.71073 \text{ \AA}$)
Temperature (K)	160
Monochromator	Highly oriented graphite crystal
2θ Range	4.0 to 52.0 $^{\circ}$
Scan Type	ω
Scan Speed	Variable; 3.00 to 30.00 $^{\circ}$ /min. in ω
Scan Range (ω)	1.20 $^{\circ}$
Background Measurement	Stationary crystal and stationary counter at beginning and end of scan, each for 25.0% of total scan time
Standard Reflections	3 measured every 100 reflections
Index Ranges	$0 \leq h \leq 15$, $0 \leq k \leq 18$ $-19 \leq l \leq 18$
Reflections Collected	5710
Independent Reflections	5460 ($R_{\text{int}} = 1.25\%$)
Observed Reflections	4619 ($F > 6.0\sigma(F)$)
Absorption Correction	Face-indexed numerical
Min./Max. Transmission	0.8745 / 0.9226

Solution and Refinement

System Used	Siemens SHELXTL IRIS
Solution	Direct Methods
Refinement Method	Full-Matrix Least-Squares
Quantity Minimized	$\sum w(F_o - F_c)^2$
Extinction Correction	$\chi = 0.00064(5)$, where $F^* = F [1 + 0.002\chi F^2 / \sin(2\theta)]^{-1/4}$
Hydrogen Atoms	Refined isotropic U
Weighting Scheme	$w^{-1} = \sigma^2(F)$
Number of Parameters Refined	474
Final R Indices (obs. data)	R = 3.14 %, wR = 3.46 %
(R Indices (all data))	R = 3.66 %, wR = 3.49 %
Goodness-of-Fit	3.24
Largest and Mean Δ/σ	0.002, 0.000
Data-to-Parameter Ratio	9.7:1
Largest Difference Peak	0.37 eÅ ⁻³
Largest Difference Hole	-0.29 eÅ ⁻³

Table 1. Atomic coordinates ($\times 10^4$) and equivalent isotropic displacement coefficients ($\text{\AA}^2 \times 10^4$)

	x	y	z	U(eq)
Molecule 1				
C(1)	6434(1)	1318(1)	1329.4(9)	219(5)
C(2)	5606(1)	661(1)	1044(1)	302(6)
C(3)	5620(2)	-103(1)	1559(1)	415(7)
C(4)	6440(2)	-203(1)	2382(1)	392(7)
C(5)	7263(1)	448(1)	2681(1)	325(6)
C(6)	7274(1)	1198(1)	2156(1)	270(5)
P(7)	6323.8(3)	2276.4(3)	577.6(2)	231(1)
O(8)	5226.1(8)	2258.5(8)	-158.1(7)	329(4)
C(9)	7468(1)	2127(1)	107(1)	265(5)
C(10)	8590(1)	1880(1)	803(1)	328(6)
C(11)	7572(2)	2976(1)	-425(1)	383(7)
C(12)	7097(2)	1335(1)	-558(1)	359(7)
C(13)	6447(1)	3329(1)	1255(1)	313(6)
C(14)	5709(2)	3188(2)	1841(1)	423(7)
C(15)	7627(2)	3575(1)	1856(1)	392(7)
C(16)	5963(2)	4118(1)	606(2)	443(8)
Molecule 2				
C(1')	8103(1)	6709(1)	1999(1)	255(5)
C(2')	8641(1)	6180(1)	2747(1)	301(6)
C(3')	8061(2)	5812(1)	3267(1)	384(7)
C(4')	6938(2)	5971(1)	3047(1)	443(8)
C(5')	6388(2)	6494(1)	2310(1)	439(7)
C(6')	6961(1)	6864(1)	1781(1)	350(6)
P(7')	8962.8(3)	7124.2(3)	1361.3(3)	229(1)
O(8')	10161.7(8)	6937.4(7)	1852.8(7)	305(4)
C(9')	8754(1)	8374(1)	1235(1)	300(6)
C(10')	8963(2)	8730(1)	2192(1)	436(8)
C(11')	9663(2)	8769(1)	901(1)	409(8)
C(12')	7622(2)	8695(2)	619(2)	456(8)
C(13')	8499(1)	6466(1)	304(1)	302(6)
C(14')	9084(2)	6806(2)	-338(1)	480(9)
C(15')	7242(2)	6449(2)	-171(2)	587(9)
C(16')	8900(2)	5492(1)	582(2)	496(9)

* Equivalent isotropic U defined as one third of the trace of the orthogonalized U_{ij} tensor

Table 2. Bond lengths (Å)

Molecule 1			
C(1)-C(2)	1.390(2)	C(1)-C(6)	1.398(2)
C(1)-P(7)	1.817(2)	C(2)-C(3)	1.383(3)
C(3)-C(4)	1.380(2)	C(4)-C(5)	1.382(2)
C(5)-C(6)	1.382(2)	P(7)-O(8)	1.492(1)
P(7)-C(9)	1.857(2)	P(7)-C(13)	1.858(2)
C(9)-C(10)	1.530(2)	C(9)-C(11)	1.534(3)
C(9)-C(12)	1.535(2)	C(13)-C(14)	1.538(3)
C(13)-C(15)	1.531(2)	C(13)-C(16)	1.534(2)
Molecule 2			
C(1')-C(2')	1.389(2)	C(1')-C(6')	1.399(2)
C(1')-P(7')	1.824(2)	C(2')-C(3')	1.386(3)
C(3')-C(4')	1.375(3)	C(4')-C(5')	1.376(3)
C(5')-C(6')	1.390(3)	P(7')-O(8')	1.491(1)
P(7')-C(9')	1.856(2)	P(7')-C(13')	1.851(2)
C(9')-C(10')	1.539(3)	C(9')-C(11')	1.539(3)
C(9')-C(12')	1.522(2)	C(13')-C(14')	1.529(3)
C(13')-C(15')	1.526(2)	C(13')-C(16')	1.534(3)

Table 3. Bond angles ($^{\circ}$)

Molecule 1

C(2)-C(1)-C(6)	118.5(1)
C(6)-C(1)-P(7)	125.3(1)
C(2)-C(3)-C(4)	120.0(2)
C(4)-C(5)-C(6)	120.3(1)
C(1)-P(7)-O(8)	110.2(1)
O(8)-P(7)-C(9)	110.0(1)
O(8)-P(7)-C(13)	110.0(1)
P(7)-C(9)-C(10)	114.2(1)
C(10)-C(9)-C(11)	110.9(1)
C(10)-C(9)-C(12)	108.3(1)
P(7)-C(13)-C(14)	106.5(1)
C(14)-C(13)-C(15)	109.2(1)
C(14)-C(13)-C(16)	108.3(2)

Molecule 2

C(2')-C(1')-C(6')	118.5(2)
C(6')-C(1')-P(7')	125.2(1)
C(2')-C(3')-C(4')	119.9(2)
C(4')-C(5')-C(6')	120.4(2)
C(1')-P(7')-O(8')	110.5(1)
O(8')-P(7')-C(9')	108.9(1)
O(8')-P(7')-C(13')	109.8(1)
P(7')-C(9')-C(10')	105.0(1)
C(10')-C(9')-C(11')	107.9(1)
C(10')-C(9')-C(12')	110.0(2)
P(7')-C(13')-C(14')	110.5(1)
C(14')-C(13')-C(15')	110.0(2)
C(14')-C(13')-C(16')	107.8(2)

C(2)-C(1)-P(7)	116.1(1)
C(1)-C(2)-C(3)	120.8(1)
C(3)-C(4)-C(5)	119.9(2)
C(1)-C(6)-C(5)	120.3(1)
C(1)-P(7)-C(9)	105.7(1)
C(1)-P(7)-C(13)	107.1(1)
C(9)-P(7)-C(13)	113.7(1)
P(7)-C(9)-C(11)	110.3(1)
P(7)-C(9)-C(12)	105.1(1)
C(11)-C(9)-C(12)	107.6(1)
P(7)-C(13)-C(15)	115.5(1)
P(7)-C(13)-C(16)	107.8(1)
C(15)-C(13)-C(16)	109.3(1)

C(2')-C(1')-P(7')	116.2(1)
C(1')-C(2')-C(3')	121.0(2)
C(3')-C(4')-C(5')	120.2(2)
C(1')-C(6')-C(5')	120.0(2)
C(1')-P(7')-C(9')	107.4(1)
C(1')-P(7')-C(13')	104.8(1)
C(9')-P(7')-C(13')	115.4(1)
P(7')-C(9')-C(11')	108.2(1)
P(7')-C(9')-C(12')	116.5(1)
C(11')-C(9')-C(12')	109.0(2)
P(7')-C(13')-C(15')	114.8(1)
P(7')-C(13')-C(16')	104.6(1)
C(15')-C(13')-C(16')	108.7(2)

Table 4. Anisotropic displacement coefficients ($\text{\AA}^2 \times 10^4$)

	U_{11}	U_{22}	U_{33}	U_{12}	U_{13}	U_{23}
Molecule 1						
C(1)	209(7)	236(8)	225(7)	1(6)	89(6)	2(6)
C(2)	230(8)	350(9)	319(9)	-44(7)	84(7)	11(7)
C(3)	310(10)	412(11)	515(11)	-127(8)	124(9)	84(9)
C(4)	403(10)	388(10)	428(10)	-11(8)	197(9)	153(8)
C(5)	345(9)	387(10)	237(8)	49(8)	90(7)	38(7)
C(6)	254(8)	283(9)	251(8)	-3(7)	56(7)	-13(7)
P(7)	187(2)	247(2)	226(2)	-16(2)	22(2)	21(2)
O(8)	225(6)	396(7)	295(6)	-22(5)	-5(5)	54(5)
C(9)	250(8)	308(9)	237(8)	-34(7)	79(6)	18(6)
C(10)	240(9)	427(11)	326(9)	4(8)	107(7)	24(8)
C(11)	400(11)	391(11)	361(10)	-80(9)	131(9)	88(8)
C(12)	407(11)	391(10)	310(9)	-74(8)	160(8)	-44(8)
C(13)	299(9)	252(8)	357(9)	34(7)	67(7)	-16(7)
C(14)	401(11)	452(12)	428(11)	112(9)	152(9)	-58(9)
C(15)	382(10)	284(9)	427(11)	-25(8)	24(9)	-83(8)
C(16)	427(12)	292(10)	547(13)	90(8)	76(10)	46(9)
Molecule 2						
C(1')	239(8)	309(8)	225(8)	-15(6)	86(6)	-18(7)
C(2')	305(9)	326(9)	258(8)	-33(7)	73(7)	-15(7)
C(3')	514(12)	378(10)	265(9)	-87(9)	135(8)	4(8)
C(4')	554(13)	486(11)	387(11)	-162(10)	289(10)	-70(9)
C(5')	328(10)	564(12)	500(12)	-32(9)	240(9)	-68(10)
C(6')	261(9)	461(11)	346(9)	38(8)	127(7)	26(8)
P(7')	170(2)	290(2)	219(2)	12(2)	55(2)	8(2)
O(8')	185(6)	358(6)	341(6)	23(5)	49(5)	16(5)
C(9')	287(9)	297(9)	321(9)	36(7)	108(7)	39(7)
C(10')	542(13)	352(11)	430(11)	33(9)	184(10)	-80(9)
C(11')	415(12)	334(10)	508(12)	-45(8)	192(10)	44(9)
C(12')	391(11)	445(12)	529(13)	119(9)	151(10)	180(10)
C(13')	273(8)	381(9)	269(8)	-64(7)	114(7)	-67(7)
C(14')	619(14)	536(13)	387(11)	-137(11)	303(11)	-89(10)
C(15')	358(12)	928(20)	402(12)	-123(12)	30(10)	-280(13)
C(16')	718(16)	359(11)	489(12)	-103(10)	303(12)	-115(9)

The anisotropic displacement factor exponent takes the form:

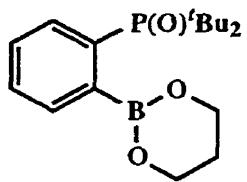
$$-2\pi^2 (h^2 a^2 U_{11} + \dots + 2klb^*c^*U_{23})$$

Table 5. H-Atom coordinates ($\times 10^4$) and isotropic displacement coefficients ($\text{\AA}^2 \times 10^3$)

	x	y	z	U
Molecule 1				
H(2)	4997(12)	746(10)	480(10)	29(4)
H(3)	5067(15)	-580(13)	1340(12)	53(6)
H(4)	6434(15)	-719(13)	2719(12)	49(5)
H(5)	7847(14)	387(12)	3242(11)	39(5)
H(6)	7867(13)	1634(11)	2374(10)	34(5)
H(10x)	9117(15)	1783(12)	477(11)	45(5)
H(10y)	8549(14)	1281(12)	1078(11)	40(5)
H(10z)	8857(15)	2353(13)	1254(12)	50(6)
H(11x)	7898(15)	3493(13)	-42(12)	51(6)
H(11y)	6857(15)	3172(12)	-839(12)	45(5)
H(11z)	8056(15)	2837(12)	-773(12)	48(5)
H(12x)	6982(14)	761(12)	-270(11)	41(5)
H(12y)	7675(16)	1178(13)	-799(12)	57(6)
H(12z)	6440(15)	1496(12)	-1055(12)	40(5)
H(14x)	6029(14)	2755(12)	2349(12)	41(5)
H(14y)	4976(16)	2970(12)	1497(12)	48(6)
H(14z)	5616(16)	3769(14)	2130(13)	60(6)
H(15x)	8109(15)	3756(13)	1506(12)	55(6)
H(15y)	8006(15)	3089(13)	2310(12)	43(5)
H(15z)	7576(14)	4128(12)	2211(11)	42(5)
H(16x)	5244(16)	3980(13)	216(12)	51(6)
H(16y)	6411(16)	4271(14)	206(13)	64(7)
H(16z)	5964(15)	4656(13)	960(12)	54(6)
Molecule 2				
H(2')	9419(14)	6067(12)	2887(11)	42(5)
H(3')	8474(14)	5423(12)	3786(11)	42(5)
H(4')	6537(16)	5706(14)	3390(13)	63(6)
H(5')	5605(16)	6620(13)	2119(12)	56(6)
H(6')	6555(13)	7225(11)	1279(11)	31(4)
H(10x')	8316(15)	8567(12)	2420(11)	48(5)
H(10y')	8949(16)	9396(14)	2172(12)	57(6)
H(10z')	9657(16)	8520(13)	2597(13)	53(6)
H(11x')	9545(15)	8626(13)	269(12)	50(6)
H(11y')	10405(16)	8545(13)	1248(12)	48(5)
H(11z')	9639(15)	9423(14)	913(12)	55(6)
H(12x')	7594(15)	9370(14)	651(12)	50(6)
H(12y')	7023(16)	8450(13)	789(12)	52(6)
H(12z')	7468(15)	8521(12)	-17(12)	45(5)
H(14x')	9001(15)	6376(14)	-827(13)	57(6)
H(14y')	9878(17)	6861(13)	-13(13)	51(6)
H(14z')	8764(17)	7421(15)	-616(13)	67(7)
H(15x')	7112(17)	6073(15)	-703(14)	68(7)
H(15y')	6995(20)	7089(17)	-417(16)	85(9)
H(15z')	6881(18)	6175(16)	240(15)	81(8)
H(16x')	8701(16)	5095(14)	43(13)	57(6)
H(16y')	8517(17)	5249(14)	957(13)	63(6)
H(16z')	9758(19)	5469(16)	894(15)	84(8)

5.5 Appendix 5 - X-ray analysis of 1.171n

The following 8 pages contain a structure determination summary as well as bond length and bond angle tables for single crystal X-ray diffraction analysis of 1.171n.



STRUCTURE DETERMINATION SUMMARY

Crystal Data

Empirical Formula	$C_{20}H_{35}BO_3P$
Color; Habit	Colourless pseudo-hexagonal prism
Crystal Size (mm)	0.25{001}x0.17{100}x0.21{110}
	Distances from common centre
Crystal System	Monoclinic
Space Group	C2/c
Unit Cell Dimensions	$\underline{a} = 20.663(2) \text{ \AA}$ $\underline{b} = 13.337(1) \text{ \AA}$ $\underline{c} = 15.604(2) \text{ \AA}$ $\beta = 101.745(7)^\circ$
Volume	4210.0(10) \AA^3
Z	8
Formula Weight	365.3
Density(calc.)	1.153 g/cm ³
Absorption Coefficient	1.46 cm ⁻¹
F(000)	1592

Data Collection

Diffractometer Used	Siemens P4
Radiation	MoK α ($\lambda = 0.71073 \text{ \AA}$)
Temperature (K)	180
Monochromator	Highly oriented graphite crystal
2θ Range	4.0 to 50.0 $^{\circ}$
Scan Type	ω
Scan Speed	Variable; 3.00 to 30.00 $^{\circ}$ /min. in ω
Scan Range (ω)	1.20 $^{\circ}$
Background Measurement	Stationary crystal and stationary counter at beginning and end of scan, each for 25.0% of total scan time
Standard Reflections	3 measured every 100 reflections
Index Ranges	$-24 \leq h \leq 23$, $0 \leq k \leq 15$ $0 \leq l \leq 18$
Reflections Collected	3689
Independent Reflections	3689 ($R_{\text{int}} = 0.00\%$)
Observed Reflections	2731 ($F > 6.0\sigma(F)$)
Absorption Correction	Face-indexed numerical
Min./Max. Transmission	0.9414 / 0.9558

Solution and Refinement

System Used	Siemens SHELXTL IRIS
Solution	Direct Methods
Refinement Method	Full-Matrix Least-Squares
Quantity Minimized	$\sum w(F_o - F_c)^2$
Extinction Correction	$\chi = 0.00023(3)$, where $F^* = F [1 + 0.002\chi F^2 / \sin(2\theta)]^{-1/4}$
Hydrogen Atoms	Riding model, refined isotropic U
Weighting Scheme	$w^{-1} = \sigma^2(F)$
Number of Parameters Refined	270
Final R Indices (obs. data)	R = 4.17 %, wR = 5.32 %
(R Indices (all data))	R = 5.42 %, wR = 5.37 %
Goodness-of-Fit	3.56
Largest and Mean Δ/σ	2.676, 0.224
Data-to-Parameter Ratio	10.1:1
Largest Difference Peak	0.29 eÅ ⁻³
Largest Difference Hole	-0.25 eÅ ⁻³

Table 1. Atomic coordinates ($\times 10^4$) and equivalent isotropic displacement coefficients ($\text{\AA}^2 \times 10^3$)

	x	y	z	U(eq)
C(1)	2361(1)	4592(2)	2773(2)	31(1)
C(2)	2290(1)	3937(2)	3447(2)	30(1)
C(3)	2814(1)	3872(2)	4162(2)	36(1)
C(4)	3373(2)	4461(2)	4202(2)	43(1)
C(5)	3419(2)	5124(3)	3532(2)	47(1)
C(6)	2917(2)	5195(2)	2809(2)	40(1)
P(7)	1628(1)	4515(1)	1939(1)	29(1)
O(8)	1210(1)	3779(1)	2351(1)	31(1)
C(9)	1207(1)	5735(2)	1805(2)	33(1)
C(10)	1220(2)	6104(2)	2739(2)	46(1)
C(11)	1551(2)	6502(2)	1319(2)	44(1)
C(12)	486(2)	5593(2)	1344(2)	48(1)
C(13)	1818(2)	3941(2)	948(2)	40(1)
C(14)	2096(2)	2903(3)	1231(3)	69(2)
C(15)	2332(2)	4526(3)	584(3)	79(2)
C(16)	1193(2)	3848(3)	236(2)	81(2)
B(17)	1590(2)	3375(3)	3335(2)	30(1)
O(18)	1202(1)	3754(1)	3927(1)	32(1)
C(19)	582(1)	3279(2)	3868(2)	39(1)
C(20)	661(2)	2158(2)	3914(2)	45(1)
C(21)	1019(2)	1803(2)	3219(2)	46(1)
O(22)	1626(1)	2308(1)	3271(1)	36(1)
C(23)	738(18)	8662(19)	3917(23)	191(17)
C(24)	166(13)	8761(33)	3960(33)	186(25)
C(25)	-198(21)	8626(13)	2713(47)	237(25)
C(26)	379(12)	8723(19)	4516(11)	109(8)
C(27)	492(17)	8963(20)	3688(16)	119(10)
C(28)	63(10)	9140(12)	2844(9)	116(7)

* Equivalent isotropic U defined as one third of the trace of the orthogonalized U_{ij} tensor

Table 2. Bond lengths (Å)

C(1)-C(2)	1.399(4)	C(1)-C(6)	1.393(4)
C(1)-P(7)	1.786(3)	C(2)-C(3)	1.390(4)
C(2)-B(17)	1.606(4)	C(3)-C(4)	1.389(4)
C(4)-C(5)	1.386(5)	C(5)-C(6)	1.372(4)
P(7)-O(8)	1.533(2)	P(7)-C(9)	1.838(3)
P(7)-C(13)	1.838(3)	O(8)-B(17)	1.666(3)
C(9)-C(10)	1.534(4)	C(9)-C(11)	1.531(5)
C(9)-C(12)	1.529(4)	C(13)-C(14)	1.529(5)
C(13)-C(15)	1.518(6)	C(13)-C(16)	1.527(5)
B(17)-O(18)	1.434(4)	B(17)-O(22)	1.429(4)
O(18)-C(19)	1.414(4)	C(19)-C(20)	1.504(4)
C(20)-C(21)	1.509(5)	C(21)-O(22)	1.410(4)
C(23)-C(24)	1.205(47)	C(24)-C(25)	1.946(83)
C(25)-C(28A)	1.184(62)	C(26)-C(27)	1.396(33)
C(27)-C(28)	1.451(28)	C(28)-C(25A)	1.184(62)

Symmetry code: A = -x, y, 1/2-z

Atoms C23-C28 represent a disordered and poorly resolved hexane molecule.

Table 3. Bond angles ($^{\circ}$)

C(2)-C(1)-C(6)	122.8(2)	C(2)-C(1)-P(7)	108.0(2)
C(6)-C(1)-P(7)	129.2(2)	C(1)-C(2)-C(3)	117.3(3)
C(1)-C(2)-B(17)	116.0(2)	C(3)-C(2)-B(17)	126.6(3)
C(2)-C(3)-C(4)	120.4(3)	C(3)-C(4)-C(5)	120.7(3)
C(4)-C(5)-C(6)	120.5(3)	C(1)-C(6)-C(5)	118.2(3)
C(1)-P(7)-O(8)	101.4(1)	C(1)-P(7)-C(9)	110.1(1)
O(8)-P(7)-C(9)	108.7(1)	C(1)-P(7)-C(13)	110.1(1)
O(8)-P(7)-C(13)	108.7(1)	C(9)-P(7)-C(13)	116.8(1)
P(7)-O(8)-B(17)	113.1(2)	P(7)-C(9)-C(10)	105.1(2)
P(7)-C(9)-C(11)	113.0(2)	C(10)-C(9)-C(11)	109.6(2)
P(7)-C(9)-C(12)	109.7(2)	C(10)-C(9)-C(12)	108.2(3)
C(11)-C(9)-C(12)	110.9(2)	P(7)-C(13)-C(14)	105.4(2)
P(7)-C(13)-C(15)	112.7(2)	C(14)-C(13)-C(15)	108.9(3)
P(7)-C(13)-C(16)	110.6(3)	C(14)-C(13)-C(16)	110.5(3)
C(15)-C(13)-C(16)	108.8(3)	C(2)-B(17)-O(8)	101.3(2)
C(2)-B(17)-O(18)	112.0(2)	O(8)-B(17)-O(18)	105.0(2)
C(2)-B(17)-O(22)	114.5(3)	O(8)-B(17)-O(22)	106.2(2)
O(18)-B(17)-O(22)	116.0(3)	B(17)-O(18)-C(19)	114.7(2)
O(18)-C(19)-C(20)	110.7(2)	C(19)-C(20)-C(21)	110.0(3)
C(20)-C(21)-O(22)	111.6(3)	B(17)-O(22)-C(21)	114.9(2)
C(23)-C(24)-C(25)	96.8(37)	C(24)-C(25)-C(28A)	125.4(29)
C(26)-C(27)-C(28)	133.7(29)	C(27)-C(28)-C(25A)	112.3(30)

Symmetry code: A = $-x, y, 1/2-z$

Table 4. Anisotropic displacement coefficients ($\text{\AA}^2 \times 10^3$)

	U_{11}	U_{22}	U_{33}	U_{12}	U_{13}	U_{23}
C(1)	32(2)	28(2)	35(2)	3(1)	10(1)	1(1)
C(2)	37(2)	23(2)	32(2)	6(1)	10(1)	-1(1)
C(3)	41(2)	30(2)	37(2)	8(1)	7(1)	3(1)
C(4)	38(2)	40(2)	48(2)	10(2)	-2(2)	1(2)
C(5)	33(2)	41(2)	64(2)	-5(2)	4(2)	3(2)
C(6)	34(2)	39(2)	49(2)	-2(1)	9(2)	10(2)
P(7)	34.3(4)	27.2(4)	27.4(4)	-1.2(4)	10.6(3)	3.2(4)
O(8)	37(1)	30(1)	27(1)	-5.1(9)	9.1(9)	2.1(9)
C(9)	35(2)	28(2)	36(2)	0(1)	7(1)	3(1)
C(10)	57(2)	36(2)	46(2)	7(2)	17(2)	-3(2)
C(11)	49(2)	32(2)	52(2)	0(2)	12(2)	12(2)
C(12)	41(2)	41(2)	59(2)	3(2)	3(2)	5(2)
C(13)	52(2)	39(2)	33(2)	1(2)	20(2)	1(1)
C(14)	118(4)	45(2)	53(2)	23(2)	42(2)	-1(2)
C(15)	109(4)	66(3)	85(3)	-3(3)	75(3)	-1(2)
C(16)	90(3)	110(4)	42(2)	10(3)	9(2)	-28(2)
B(17)	37(2)	27(2)	27(2)	6(2)	9(1)	4(1)
O(18)	37(1)	34(1)	29(1)	2(1)	12.5(9)	1.4(9)
C(19)	37(2)	49(2)	32(2)	5(2)	12(1)	2(2)
C(20)	38(2)	43(2)	56(2)	-2(2)	15(2)	15(2)
C(21)	44(2)	28(2)	69(3)	-1(2)	18(2)	4(2)
O(22)	38(1)	24(1)	50(1)	2.3(9)	18(1)	4.6(9)
C(23)	243(36)	114(14)	212(26)	72(16)	35(23)	-36(16)
C(24)	71(18)	150(28)	363(63)	-12(17)	104(32)	-49(39)
C(25)	197(32)	83(12)	459(62)	-60(15)	137(26)	-39(24)
C(26)	125(19)	139(14)	72(8)	-40(13)	43(9)	-15(8)
C(27)	121(21)	118(16)	100(12)	-72(17)	-20(13)	27(11)
C(28)	125(13)	146(14)	66(8)	26(13)	-7(9)	-35(8)

The anisotropic displacement factor exponent takes the form:

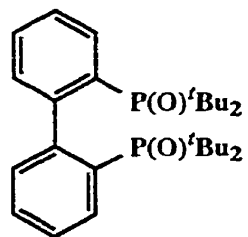
$$-2\pi^2 (h^2 a^2 U_{11} + \dots + 2klb^*c^*U_{23})$$

Table 5. H-Atom coordinates ($\times 10^4$) and isotropic displacement coefficients ($\text{\AA}^2 \times 10^3$)

	x	y	z	U
H(3)	2790	3414	4630	35(8)
H(4)	3727	4418	4705	51(10)
H(5)	3809	5528	3574	53(10)
H(6)	2946	5641	2336	46(9)
H(10x)	1661	6303	3012	58(6)
H(10y)	1071	5576	3069	58(6)
H(10z)	922	6660	2721	58(6)
H(11x)	2006	6582	1606	49(5)
H(11y)	1325	7133	1300	49(5)
H(11z)	1525	6279	728	49(5)
H(12x)	465	5394	748	63(6)
H(12y)	250	6211	1363	63(6)
H(12z)	284	5092	1645	63(6)
H(14x)	2206	2559	739	83(8)
H(14y)	1777	2517	1458	83(8)
H(14z)	2487	2970	1681	83(8)
H(15x)	2480	4155	133	98(9)
H(15y)	2698	4668	1055	98(9)
H(15z)	2144	5153	357	98(9)
H(16x)	1277	3406	-214	131(11)
H(16y)	1059	4488	-21	131(11)
H(16z)	840	3575	479	131(11)
H(19x)	297	3452	3321	37(8)
H(19y)	380	3511	4334	34(8)
H(20x)	238	1836	3849	43(9)
H(20y)	920	1982	4477	57(11)
H(21x)	744	1931	2656	36(9)
H(21y)	1096	1094	3272	63(11)

5.6 Appendix 6 - X-ray analysis of 1.176

The following 8 pages contain a structure determination summary as well as bond length and bond angle tables for single crystal X-ray diffraction analysis of 1.176.



STRUCTURE DETERMINATION SUMMARY

Crystal Data

Empirical Formula	$C_{28}H_{44}O_2P_2$
Color; Habit	Colourless plate fragment
Crystal Size (mm)	0.10{010}x0.32(011)x0.26(0 $\bar{1}$ 1) x0.32(111)x0.27(1 $\bar{1}$ 1)x0.21(1 $\bar{1}$ $\bar{1}$) x0.26(11 $\bar{1}$)x0.21($\bar{2}$ 01)x0.33($\bar{1}$ 0 $\bar{2}$)
	Distances from common centre
Crystal System	Monoclinic
Space Group	$P2_1/n$
Unit Cell Dimensions	$\underline{a} = 10.3648(13) \text{ \AA}$ $\underline{b} = 16.533(2) \text{ \AA}$ $\underline{c} = 16.272(2) \text{ \AA}$ $\beta = 95.115(9)^\circ$
Volume	$2777.4(7) \text{ \AA}^3$
Z	4
Formula Weight	474.6
Density(calc.)	1.135 g/cm^3
Absorption Coefficient	1.78 cm^{-1}
F(000)	1032

Data Collection

Diffractionmeter Used	Siemens P4
Radiation	MoK α ($\lambda = 0.71073 \text{ \AA}$)
Temperature (K)	295
Monochromator	Highly oriented graphite crystal
2θ Range	4.0 to 50.0 $^{\circ}$
Scan Type	ω
Scan Speed	Variable; 2.00 to 30.00 $^{\circ}$ /min. in ω
Scan Range (ω)	1.20 $^{\circ}$
Background Measurement	Stationary crystal and stationary counter at beginning and end of scan, each for 25.0% of total scan time
Standard Reflections	3 measured every 100 reflections
Index Ranges	$0 \leq h \leq 12, 0 \leq k \leq 19$ $-19 \leq l \leq 19$
Reflections Collected	5174
Independent Reflections	4887 ($R_{\text{int}} = 1.30\%$)
Observed Reflections	3345 ($F > 6.0\sigma(F)$)
Absorption Correction	Face-indexed numerical
Min./Max. Transmission	0.9382 / 0.9676

Solution and Refinement

System Used	Siemens SHELXTL IRIS
Solution	Direct Methods
Refinement Method	Full-Matrix Least-Squares
Quantity Minimized	$\sum w(F_o - F_c)^2$
Extinction Correction	$\chi = 0.00037(3)$, where $F^* = F [1 + 0.002\chi F^2 / \sin(2\theta)]^{-1/4}$
Hydrogen Atoms	Riding model, refined isotropic U
Weighting Scheme	$w^{-1} = \sigma^2(F)$
Number of Parameters Refined	334
Final R Indices (obs. data)	R = 3.51 %, wR = 3.55 %
(R Indices (all data))	R = 5.19 %, wR = 3.64 %
Goodness-of-Fit	2.25
Largest and Mean Δ/σ	0.003, 0.001
Data-to-Parameter Ratio	10.0:1
Largest Difference Peak	0.19 eÅ ⁻³
Largest Difference Hole	-0.21 eÅ ⁻³

Table 1. Atomic coordinates ($\times 10^4$) and equivalent isotropic displacement coefficients ($\text{\AA}^2 \times 10^3$)

	x	y	z	U(eq)
C(1)	4077(2)	2662(1)	1210(1)	33(1)
C(2)	3144(2)	2308(1)	1672(1)	37(1)
C(3)	1859(2)	2576(1)	1534(2)	49(1)
C(4)	1490(2)	3156(2)	961(2)	51(1)
C(5)	2387(2)	3486(2)	496(2)	51(1)
C(6)	3656(2)	3236(1)	621(1)	46(1)
P(7)	3514.1(6)	1526.1(4)	2455.2(4)	41(1)
O(8)	4924(1)	1373.6(9)	2600.4(9)	50(1)
C(9)	2681(2)	588(1)	2061(2)	53(1)
C(10)	1248(3)	661(2)	1741(2)	80(1)
C(11)	3419(3)	301(2)	1339(2)	79(1)
C(12)	2832(3)	-55(2)	2748(2)	75(1)
C(13)	2885(3)	1894(2)	3434(2)	59(1)
C(14)	3124(4)	2816(2)	3490(2)	86(2)
C(15)	1451(3)	1742(2)	3553(2)	88(2)
C(16)	3714(3)	1485(2)	4141(2)	89(2)
C(1')	5483(2)	2407(1)	1215(1)	34(1)
C(2')	6554(2)	2823(1)	1587(1)	35(1)
C(3')	7788(2)	2528(1)	1463(2)	48(1)
C(4')	7980(3)	1857(2)	991(2)	58(1)
C(5')	6932(3)	1461(2)	619(2)	54(1)
C(6')	5710(2)	1736(1)	728(1)	47(1)
P(7')	6427.5(6)	3713.7(4)	2242.6(4)	39(1)
O(8')	5066(1)	3877.0(9)	2401.1(9)	48(1)
C(9')	7065(2)	4587(1)	1680(2)	50(1)
C(10')	8404(3)	4490(2)	1361(2)	68(1)
C(11')	7086(3)	5336(2)	2242(2)	85(2)
C(12')	6089(3)	4730(2)	941(2)	81(1)
C(13')	7413(3)	3497(2)	3243(2)	58(1)
C(14')	7246(4)	2599(2)	3447(2)	92(2)
C(15')	6827(4)	4005(3)	3902(2)	101(2)
C(16')	8866(3)	3673(3)	3285(2)	95(2)

* Equivalent isotropic U defined as one third of the trace of the orthogonalized U_{ij} tensor

Table 2. Bond lengths (Å)

C(1)-C(2)	1.406(3)	C(1)-C(6)	1.391(3)
C(1)-C(1')	1.516(3)	C(2)-C(3)	1.403(3)
C(2)-P(7)	1.831(2)	C(3)-C(4)	1.367(3)
C(4)-C(5)	1.364(4)	C(5)-C(6)	1.375(3)
P(7)-O(8)	1.481(2)	P(7)-C(9)	1.861(2)
P(7)-C(13)	1.876(3)	C(9)-C(10)	1.534(4)
C(9)-C(11)	1.533(4)	C(9)-C(12)	1.541(4)
C(13)-C(14)	1.545(4)	C(13)-C(15)	1.536(4)
C(13)-C(16)	1.531(4)	C(1')-C(2')	1.398(3)
C(1')-C(6')	1.396(3)	C(2')-C(3')	1.400(3)
C(2')-P(7')	1.830(2)	C(3')-C(4')	1.374(4)
C(4')-C(5')	1.364(4)	C(5')-C(6')	1.372(4)
P(7')-O(8')	1.482(2)	P(7')-C(9')	1.862(2)
P(7')-C(13')	1.877(2)	C(9')-C(10')	1.533(4)
C(9')-C(11')	1.539(4)	C(9')-C(12')	1.520(4)
C(13')-C(14')	1.535(4)	C(13')-C(15')	1.530(5)
C(13')-C(16')	1.530(4)		

Table 3. Bond angles ($^{\circ}$)

C(2)-C(1)-C(6)	117.7(2)	C(2)-C(1)-C(1')	126.0(2)
C(6)-C(1)-C(1')	115.9(2)	C(1)-C(2)-C(3)	118.1(2)
C(1)-C(2)-P(7)	123.8(2)	C(3)-C(2)-P(7)	118.2(2)
C(2)-C(3)-C(4)	122.4(2)	C(3)-C(4)-C(5)	119.7(2)
C(4)-C(5)-C(6)	119.2(2)	C(1)-C(6)-C(5)	122.9(2)
C(2)-P(7)-O(8)	111.9(1)	C(2)-P(7)-C(9)	106.6(1)
O(8)-P(7)-C(9)	109.5(1)	C(2)-P(7)-C(13)	107.1(1)
O(8)-P(7)-C(13)	109.4(1)	C(9)-P(7)-C(13)	112.2(1)
P(7)-C(9)-C(10)	117.2(2)	P(7)-C(9)-C(11)	105.9(2)
C(10)-C(9)-C(11)	107.4(2)	P(7)-C(9)-C(12)	108.2(2)
C(10)-C(9)-C(12)	109.4(2)	C(11)-C(9)-C(12)	108.5(2)
P(7)-C(13)-C(14)	107.7(2)	P(7)-C(13)-C(15)	117.8(2)
C(14)-C(13)-C(15)	107.8(3)	P(7)-C(13)-C(16)	106.2(2)
C(14)-C(13)-C(16)	108.4(2)	C(15)-C(13)-C(16)	108.5(2)
C(1)-C(1')-C(2')	126.3(2)	C(1)-C(1')-C(6')	115.4(2)
C(2')-C(1')-C(6')	118.0(2)	C(1')-C(2')-C(3')	117.9(2)
C(1')-C(2')-P(7')	123.6(2)	C(3')-C(2')-P(7')	118.6(2)
C(2')-C(3')-C(4')	122.8(2)	C(3')-C(4')-C(5')	119.1(2)
C(4')-C(5')-C(6')	119.4(2)	C(1')-C(6')-C(5')	122.8(2)
C(2')-P(7')-O(8')	111.5(1)	C(2')-P(7')-C(9')	106.9(1)
O(8')-P(7')-C(9')	109.2(1)	C(2')-P(7')-C(13')	106.9(1)
O(8')-P(7')-C(13')	109.7(1)	C(9')-P(7')-C(13')	112.6(1)
P(7')-C(9')-C(10')	117.2(2)	P(7')-C(9')-C(11')	108.6(2)
C(10')-C(9')-C(11')	108.7(2)	P(7')-C(9')-C(12')	105.6(2)
C(10')-C(9')-C(12')	107.9(2)	C(11')-C(9')-C(12')	108.6(2)
P(7')-C(13')-C(14')	108.0(2)	P(7')-C(13')-C(15')	106.5(2)
C(14')-C(13')-C(15')	108.7(3)	P(7')-C(13')-C(16')	117.4(2)
C(14')-C(13')-C(16')	107.7(3)	C(15')-C(13')-C(16')	108.3(3)

Table 4. Anisotropic displacement coefficients ($\text{\AA}^2 \times 10^3$)

	U_{11}	U_{22}	U_{33}	U_{12}	U_{13}	U_{23}
C(1)	38(1)	30(1)	31(1)	-4(1)	-3(1)	-2(1)
C(2)	35(1)	35(1)	40(1)	1(1)	2(1)	1(1)
C(3)	39(1)	50(2)	60(2)	4(1)	9(1)	13(1)
C(4)	39(2)	50(2)	64(2)	10(1)	-3(1)	6(1)
C(5)	54(2)	48(2)	49(2)	4(1)	-9(1)	13(1)
C(6)	45(2)	48(2)	45(1)	-6(1)	1(1)	11(1)
P(7)	36.6(4)	39.2(4)	48.8(4)	0.0(3)	5.8(3)	11.7(3)
O(8)	36.5(9)	56(1)	57(1)	1.7(8)	-1.8(7)	14.1(9)
C(9)	45(2)	41(2)	72(2)	-4(1)	-1(1)	8(1)
C(10)	55(2)	60(2)	119(3)	-15(2)	-19(2)	15(2)
C(11)	87(3)	53(2)	95(3)	-5(2)	4(2)	-10(2)
C(12)	71(2)	44(2)	109(3)	-6(2)	-5(2)	23(2)
C(13)	65(2)	61(2)	53(2)	0(1)	20(1)	13(1)
C(14)	128(3)	69(2)	68(2)	-14(2)	43(2)	-9(2)
C(15)	83(2)	92(3)	98(3)	4(2)	52(2)	19(2)
C(16)	110(3)	107(3)	51(2)	-4(2)	11(2)	19(2)
C(1')	39(1)	32(1)	32(1)	0(1)	5(1)	4(1)
C(2')	34(1)	33(1)	38(1)	0(1)	2(1)	2(1)
C(3')	37(1)	44(2)	64(2)	1(1)	1(1)	1(1)
C(4')	48(2)	54(2)	74(2)	18(1)	18(1)	0(2)
C(5')	66(2)	44(2)	55(2)	7(1)	18(1)	-11(1)
C(6')	52(2)	45(2)	44(1)	-5(1)	7(1)	-7(1)
P(7')	34.7(4)	33.9(3)	47.1(4)	-2.7(3)	0.8(3)	-3.6(3)
O(8')	39.4(9)	46(1)	59(1)	-2.4(8)	10.0(8)	-9.4(8)
C(9')	40(1)	37(1)	75(2)	-4(1)	8(1)	4(1)
C(10')	54(2)	60(2)	91(2)	-8(1)	20(2)	11(2)
C(11')	80(2)	37(2)	141(3)	-9(2)	35(3)	-15(2)
C(12')	60(2)	72(2)	110(3)	-6(2)	-5(2)	46(2)
C(13')	59(2)	60(2)	50(2)	-8(1)	-12(1)	-6(1)
C(14')	114(3)	88(3)	65(2)	-25(2)	-33(2)	33(2)
C(15')	131(4)	112(4)	58(2)	-1(3)	-8(2)	-27(2)
C(16')	65(2)	117(3)	93(3)	-17(2)	-38(2)	5(3)

The anisotropic displacement factor exponent takes the form:

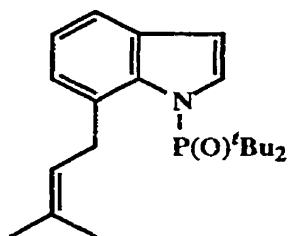
$$-2\pi^2 (h^2 a^2 U_{11} + \dots + 2klb^*c^*U_{23})$$

Table 5. H-Atom coordinates ($\times 10^4$) and isotropic displacement coefficients ($\text{\AA}^2 \times 10^3$)

	x	y	z	U
H(3)	1221	2337	1851	56(7)
H(4)	604	3331	889	44(6)
H(5)	2137	3889	88	48(7)
H(6)	4284	3468	291	54(7)
H(10x)	1166	1007	1266	81(10)
H(10y)	770	887	2165	121(15)
H(10z)	892	139	1595	93(10)
H(11x)	4320	256	1528	86(11)
H(11y)	3323	685	895	81(10)
H(11z)	3110	-215	1137	113(12)
H(12x)	3737	-137	2906	84(10)
H(12y)	2448	-560	2567	95(10)
H(12z)	2417	129	3218	143(17)
H(14x)	3984	2937	3351	116(13)
H(14y)	3010	3004	4037	99(11)
H(14z)	2497	3085	3115	122(15)
H(15x)	1264	1962	4075	125(14)
H(15y)	1266	1173	3553	124(14)
H(15z)	896	1999	3127	144(17)
H(16x)	3601	909	4106	93(12)
H(16y)	3479	1679	4662	100(11)
H(16z)	4605	1622	4097	114(14)
H(3')	8527	2813	1717	51(7)
H(4')	8840	1666	927	63(8)
H(5')	7047	994	283	52(7)
H(6')	4977	1458	458	44(6)
H(10'x)	8631	4977	1086	99(11)
H(10'y)	8398	4045	983	109(12)
H(10'z)	9040	4384	1814	88(11)
H(11'x)	6254	5413	2448	122(13)
H(11'y)	7318	5804	1939	104(11)
H(11'z)	7739	5259	2692	107(14)
H(12'x)	6315	5208	650	88(10)
H(12'y)	5236	4792	1119	84(10)
H(12'z)	6085	4272	578	100(13)
H(14'x)	7720	2464	3962	133(13)
H(14'y)	7537	2275	3010	246(28)
H(14'z)	6339	2495	3473	86(11)
H(15'x)	7066	3792	4442	138(15)
H(15'y)	5901	4002	3790	183(22)
H(15'z)	7117	4555	3867	133(16)
H(16'x)	9280	3556	3824	102(11)
H(16'y)	8989	4231	3149	117(14)
H(16'z)	9235	3349	2877	132(17)

5.7 Appendix 7 - X-ray analysis of 2.84c

The following 8 pages contain a structure determination summary as well as bond length and bond angle tables for single crystal X-ray diffraction analysis of 2.84c.



STRUCTURE DETERMINATION SUMMARY

Crystal Data

Empirical Formula	$C_{21}H_{32}NO$
Color; Habit	Colourless needle prism fragment
Crystal Size (mm)	0.92(100)x0.31(011)x0.27(0 $\bar{1}$ 1)
Crystal System	Monoclinic
Space Group	$P2_1/c$
Unit Cell Dimensions	$a = 12.4082(11) \text{ \AA}$ $b = 14.5597(9) \text{ \AA}$ $c = 11.4867(9) \text{ \AA}$ $\beta = 107.924(6)^\circ$
Volume	1974.5(3) \AA^3
Z	4
Formula Weight	345.4
Density(calc.)	1.162 g/cm^3
Absorption Coefficient	1.47 cm^{-1}
F(000)	752

Data Collection

Diffractometer Used	Siemens P4
Radiation	MoK α ($\lambda = 0.71073 \text{ \AA}$)
Temperature (K)	160
Monochromator	Highly oriented graphite crystal
2 θ Range	4.0 to 52.0 $^{\circ}$
Scan Type	ω
Scan Speed	Variable; 3.00 to 30.00 $^{\circ}$ /min. in ω
Scan Range (ω)	1.20 $^{\circ}$
Background Measurement	Stationary crystal and stationary counter at beginning and end of scan, each for 25.0% of total scan time
Standard Reflections	3 measured every 100 reflections
Index Ranges	$0 \leq h \leq 15$, $0 \leq k \leq 17$ $-14 \leq l \leq 13$
Reflections Collected	4050
Independent Reflections	3868 ($R_{\text{int}} = 1.25\%$)
Observed Reflections	3102 ($F > 6.0\sigma(F)$)
Absorption Correction	Face-indexed numerical
Min./Max. Transmission	0.9506 / 0.9658

Solution and Refinement

System Used	Siemens SHELXTL IRIS
Solution	Direct Methods
Refinement Method	Full-Matrix Least-Squares
Quantity Minimized	$\sum w(F_o - F_c)^2$
Extinction Correction	$\chi = 0.00241(13)$, where $F^* = F [1 + 0.002\chi F^2 / \sin(2\theta)]^{-1/4}$
Hydrogen Atoms	Refined isotropic U
Weighting Scheme	$w^{-1} = \sigma^2(F)$
Number of Parameters Refined	346
Final R Indices (obs. data)	R = 3.31 %, wR = 3.79 %
(R Indices (all data)	R = 4.07 %, wR = 3.82 %)
Goodness-of-Fit	2.99
Largest and Mean Δ/σ	0.005, 0.000
Data-to-Parameter Ratio	9.0:1
Largest Difference Peak	0.41 eÅ ⁻³
Largest Difference Hole	-0.26 eÅ ⁻³

Table 1. Atomic coordinates ($\times 10^4$) and equivalent isotropic displacement coefficients ($\text{\AA}^2 \times 10^4$)

	x	y	z	U(eq)
N(1)	7203(1)	154.5(9)	4784(1)	237(5)
C(2)	6806(2)	-211(1)	3597(2)	324(7)
C(3)	6937(2)	-1124(1)	3589(2)	311(7)
C(3A)	7453(1)	-1403(1)	4824(2)	245(6)
C(4)	7760(2)	-2278(1)	5318(2)	315(7)
C(5)	8243(2)	-2356(1)	6560(2)	367(8)
C(6)	8404(2)	-1578(1)	7292(2)	314(7)
C(7)	8106(1)	-693(1)	6857(2)	229(6)
C(7A)	7628(1)	-609(1)	5578(1)	205(6)
P(8)	7294.7(4)	1335.0(3)	4969.3(4)	197(1)
O(9)	7378(1)	1616.4(8)	6228(1)	274(4)
C(10)	8596(1)	1644(1)	4605(2)	269(6)
C(11)	8675(2)	1249(2)	3393(2)	411(8)
C(12)	9573(2)	1258(2)	5668(2)	382(8)
C(13)	8705(2)	2692(1)	4591(3)	415(9)
C(14)	5951(1)	1809(1)	3921(2)	237(6)
C(15)	4980(2)	1245(2)	4120(2)	383(8)
C(16)	5818(2)	1904(1)	2551(2)	319(7)
C(17)	5873(2)	2795(1)	4390(2)	337(7)
C(18)	8278(2)	54(1)	7822(2)	262(6)
C(19)	7342(2)	21(1)	8390(2)	273(6)
C(20)	7441(2)	-114(1)	9563(2)	279(6)
C(21)	8552(2)	-213(2)	10549(2)	389(8)
C(22)	6417(2)	-156(2)	9991(2)	469(10)

* Equivalent isotropic U defined as one third of the trace of the orthogonalized U_{ij} tensor

Table 2. Bond lengths (Å)

N(1)-C(2)	1.405(2)	N(1)-C(7A)	1.432(2)
N(1)-P(8)	1.731(1)	C(2)-C(3)	1.340(3)
C(3)-C(3A)	1.424(2)	C(3A)-C(4)	1.399(2)
C(3A)-C(7A)	1.420(2)	C(4)-C(5)	1.372(3)
C(5)-C(6)	1.388(3)	C(6)-C(7)	1.391(2)
C(7)-C(7A)	1.410(2)	C(7)-C(18)	1.520(2)
P(8)-O(9)	1.476(1)	P(8)-C(10)	1.844(2)
P(8)-C(14)	1.863(2)	C(10)-C(11)	1.537(3)
C(10)-C(12)	1.539(2)	C(10)-C(13)	1.532(3)
C(14)-C(15)	1.532(3)	C(14)-C(16)	1.537(3)
C(14)-C(17)	1.548(3)	C(18)-C(19)	1.498(3)
C(19)-C(20)	1.330(3)	C(20)-C(21)	1.498(3)
C(20)-C(22)	1.497(4)		

Table 3. Bond angles ($^{\circ}$)

C(2)-N(1)-C(7A)	106.0(1)	C(2)-N(1)-P(8)	119.0(1)
C(7A)-N(1)-P(8)	134.0(1)	N(1)-C(2)-C(3)	112.1(2)
C(2)-C(3)-C(3A)	107.1(2)	C(3)-C(3A)-C(4)	130.2(2)
C(3)-C(3A)-C(7A)	108.3(1)	C(4)-C(3A)-C(7A)	121.5(2)
C(3A)-C(4)-C(5)	118.3(2)	C(4)-C(5)-C(6)	119.8(2)
C(5)-C(6)-C(7)	124.4(2)	C(6)-C(7)-C(7A)	115.8(2)
C(6)-C(7)-C(18)	116.0(1)	C(7A)-C(7)-C(18)	128.2(1)
N(1)-C(7A)-C(3A)	106.6(1)	N(1)-C(7A)-C(7)	133.2(1)
C(3A)-C(7A)-C(7)	120.1(1)	N(1)-P(8)-O(9)	112.2(1)
N(1)-P(8)-C(10)	104.1(1)	O(9)-P(8)-C(10)	110.7(1)
N(1)-P(8)-C(14)	106.0(1)	O(9)-P(8)-C(14)	108.0(1)
C(10)-P(8)-C(14)	115.8(1)	P(8)-C(10)-C(11)	114.8(1)
P(8)-C(10)-C(12)	105.1(1)	C(11)-C(10)-C(12)	109.1(2)
P(8)-C(10)-C(13)	109.4(1)	C(11)-C(10)-C(13)	109.5(2)
C(12)-C(10)-C(13)	108.8(2)	P(8)-C(14)-C(15)	107.1(1)
P(8)-C(14)-C(16)	119.2(1)	C(15)-C(14)-C(16)	111.1(1)
P(8)-C(14)-C(17)	105.0(1)	C(15)-C(14)-C(17)	108.0(2)
C(16)-C(14)-C(17)	105.9(1)	C(7)-C(18)-C(19)	109.9(1)
C(18)-C(19)-C(20)	127.2(2)	C(19)-C(20)-C(21)	123.8(2)
C(19)-C(20)-C(22)	121.0(2)	C(21)-C(20)-C(22)	115.2(2)

Table 4. Anisotropic displacement coefficients ($\text{\AA}^2 \times 10^4$)

	U_{11}	U_{22}	U_{33}	U_{12}	U_{13}	U_{23}
N(1)	337(8)	191(7)	166(7)	-36(6)	54(6)	-21(6)
C(2)	466(12)	274(10)	189(9)	-23(9)	36(8)	-24(8)
C(3)	404(11)	261(10)	265(10)	-61(8)	101(9)	-87(8)
C(3A)	261(9)	230(9)	281(10)	-29(7)	138(8)	-17(7)
C(4)	396(11)	209(10)	398(12)	0(8)	206(9)	-34(8)
C(5)	480(12)	263(11)	408(12)	104(9)	210(10)	93(9)
C(6)	369(11)	322(11)	271(10)	70(8)	126(8)	68(8)
C(7)	218(8)	255(9)	230(9)	1(7)	94(7)	19(7)
C(7A)	199(8)	196(9)	246(9)	-14(7)	105(7)	9(7)
P(8)	234(2)	190(2)	173(2)	-11(2)	71(2)	-17(2)
O(9)	349(7)	276(7)	185(6)	30(5)	64(5)	-38(5)
C(10)	250(9)	250(9)	329(10)	-27(7)	121(8)	2(8)
C(11)	387(12)	520(14)	405(12)	8(11)	239(10)	-34(11)
C(12)	225(10)	427(13)	470(13)	-13(9)	75(9)	67(11)
C(13)	383(13)	293(12)	589(15)	-79(10)	182(12)	49(11)
C(14)	239(9)	283(10)	192(8)	13(7)	71(7)	10(7)
C(15)	270(11)	505(14)	378(12)	-17(10)	104(9)	72(11)
C(16)	375(12)	372(11)	191(9)	58(10)	59(8)	28(8)
C(17)	404(12)	333(11)	263(11)	143(9)	87(9)	5(8)
C(18)	286(10)	293(10)	180(9)	-24(8)	32(7)	10(8)
C(19)	255(9)	279(10)	259(9)	8(8)	40(8)	-62(8)
C(20)	396(11)	178(9)	300(9)	-45(8)	160(8)	-68(7)
C(21)	558(14)	358(13)	224(11)	-2(11)	80(10)	25(9)
C(22)	587(16)	415(15)	536(15)	-67(12)	366(14)	-112(12)

The anisotropic displacement factor exponent takes the form:

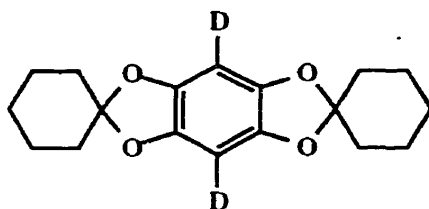
$$-2\pi^2 (h^2 a^2 U_{11} + \dots + 2klb^*c^*U_{23})$$

Table 5. H-Atom coordinates ($\times 10^4$) and isotropic displacement coefficients ($\text{\AA}^2 \times 10^3$)

	x	y	z	U
H(2)	6506(16)	201(13)	2926(17)	35(5)
H(3)	6754(16)	-1491(13)	2899(18)	42(6)
H(4)	7606(15)	-2779(13)	4798(16)	32(5)
H(5)	8472(16)	-2949(13)	6922(17)	37(5)
H(6)	8742(16)	-1671(13)	8156(18)	42(6)
H(11x)	9425(18)	1426(14)	3299(18)	50(6)
H(11y)	8089(19)	1483(14)	2672(19)	53(7)
H(11z)	8637(19)	562(16)	3426(20)	63(7)
H(12x)	10295(17)	1405(12)	5540(16)	35(5)
H(12y)	9510(18)	590(15)	5717(18)	51(7)
H(12z)	9569(19)	1539(14)	6508(21)	63(7)
H(13x)	8174(19)	2946(15)	3898(20)	47(6)
H(13y)	9459(18)	2839(14)	4566(18)	47(6)
H(13z)	8622(18)	2990(15)	5351(20)	55(7)
H(15x)	4233(18)	1553(13)	3693(18)	46(6)
H(15y)	5020(17)	1229(14)	4931(20)	44(6)
H(15z)	4958(17)	621(14)	3807(18)	44(6)
H(16x)	5068(17)	2188(13)	2154(17)	38(5)
H(16y)	5827(17)	1333(14)	2083(18)	43(6)
H(16z)	6413(16)	2296(13)	2404(16)	35(5)
H(17x)	6493(18)	3221(14)	4257(18)	49(6)
H(17y)	5926(16)	2797(13)	5240(19)	41(6)
H(17z)	5101(16)	3045(12)	3939(16)	34(5)
H(18x)	8308(15)	661(13)	7478(16)	34(5)
H(18y)	9004(16)	-68(12)	8440(16)	30(5)
H(19)	6566(17)	93(12)	7820(17)	37(5)
H(21x)	9140(25)	-528(19)	10335(25)	96(10)
H(21y)	8490(24)	-545(19)	11222(25)	93(10)
H(21z)	8862(23)	323(20)	10895(23)	81(9)
H(22x)	6462(17)	294(16)	10624(19)	50(6)
H(22y)	6392(20)	-756(16)	10346(21)	63(7)
H(22z)	5746(19)	-39(14)	9324(19)	46(6)

5.8 Appendix 8 - $^1\text{H-NMR}$ Spectra of 2.101a

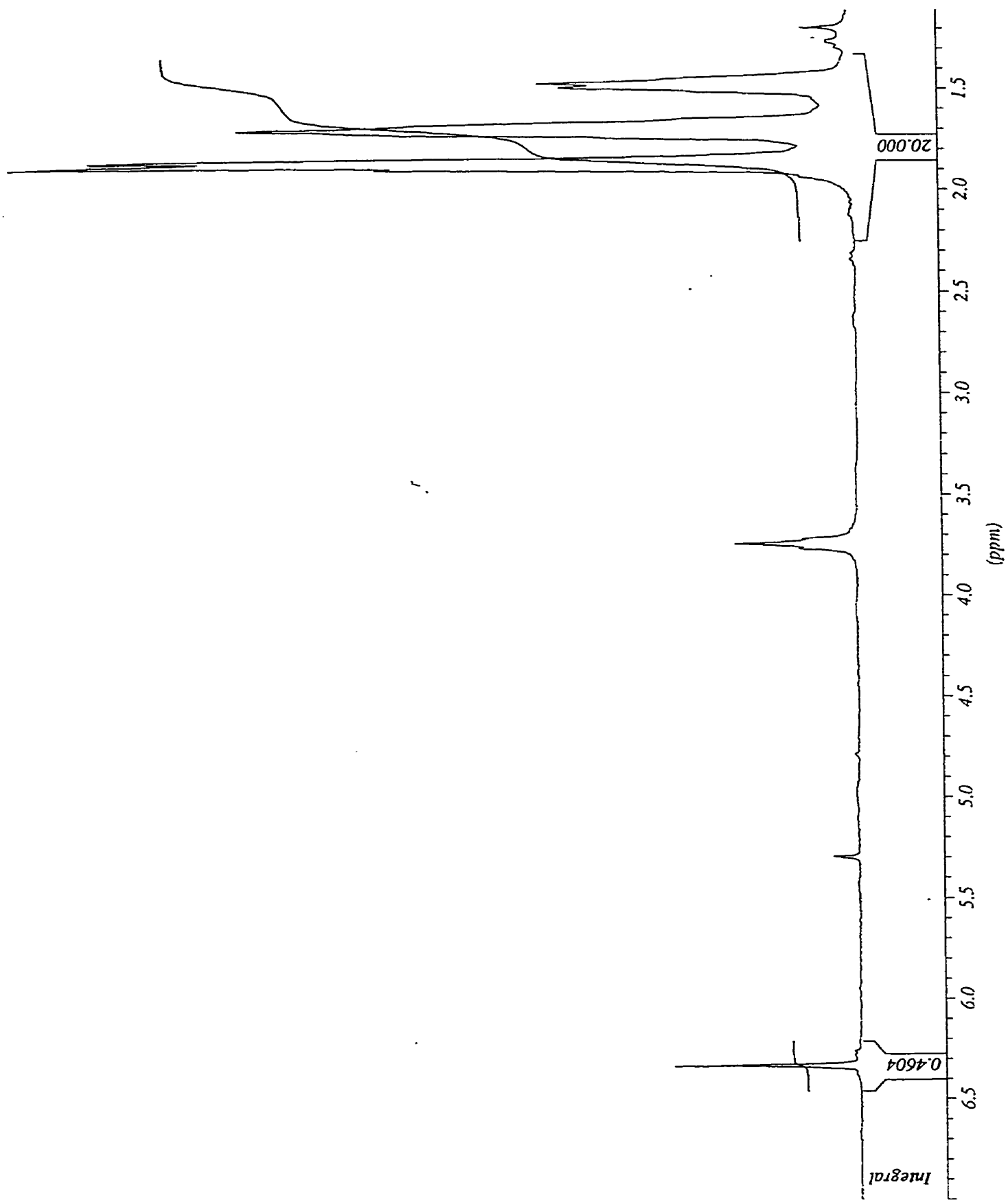
The following 3 pages contain $^1\text{H-NMR}$ spectra for 2.101a with varying degrees of deuterium incorporation as evidenced by the gradual disappearance of the signal at δ 6.33 ppm. Conditions for synthesis of each sample are summarized below (also, see Experimental Section).

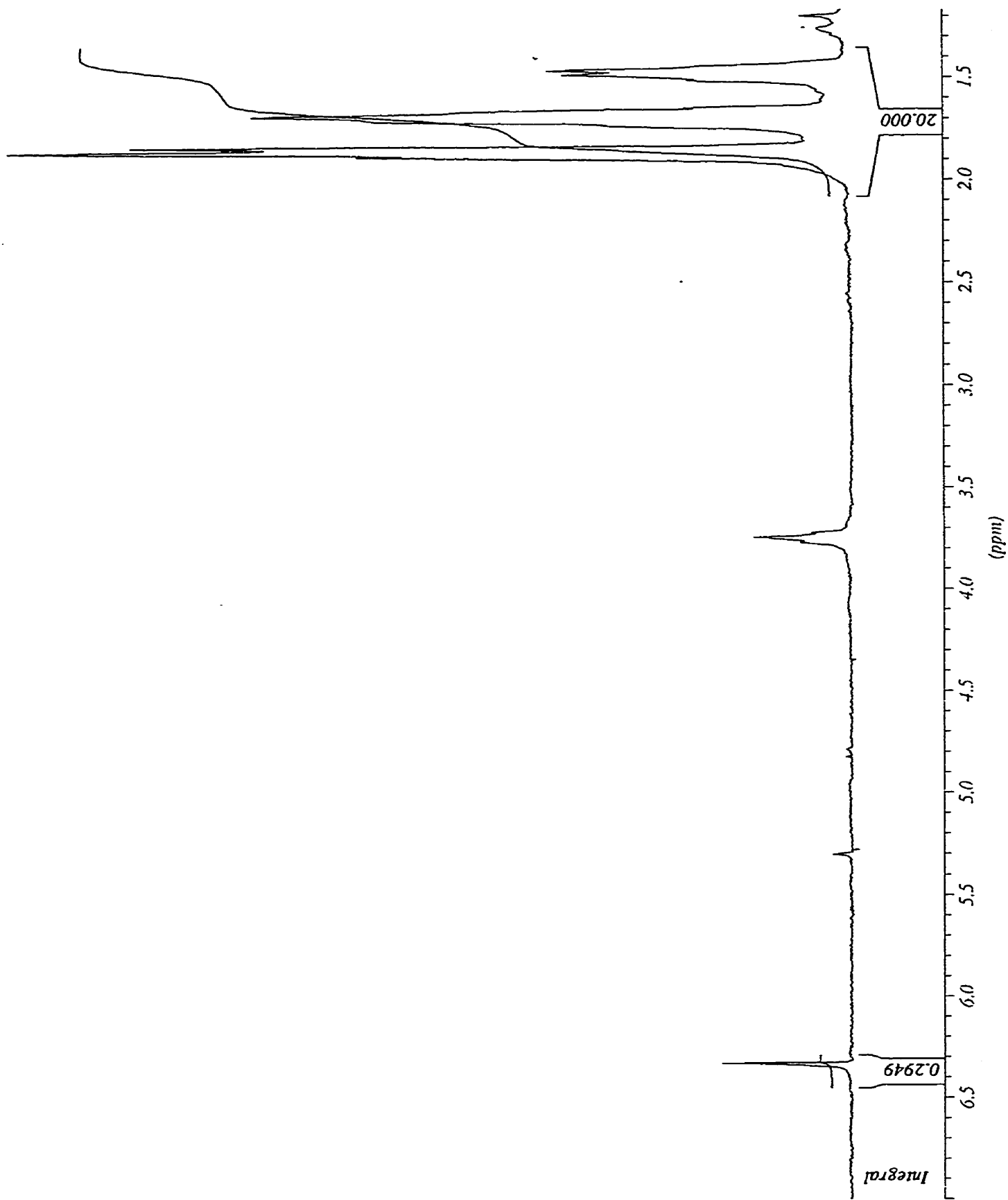


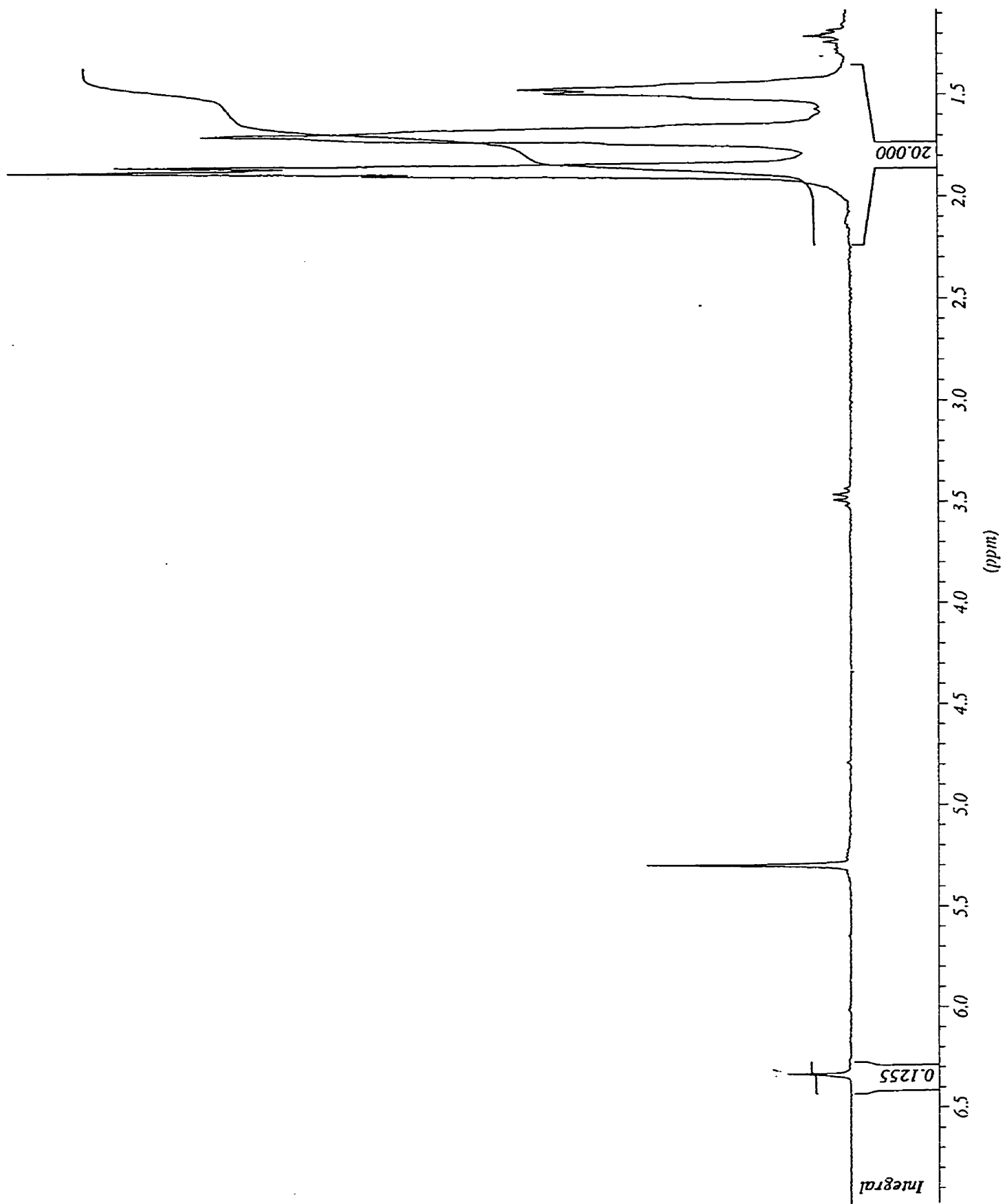
Spectrum 1: *t*-BuLi (3 equiv.) / THF / rt / 3.5 h

Spectrum 2: *t*-BuLi (5 equiv.) / THF / rt / 3.5 h

Spectrum 3: *t*-BuLi (3 equiv.) / Et₂O / rt / 18 h







6.0 References and Notes

1. Gilman, H.; Bebb, R. L. *J. Am. Chem. Soc.* **1939**, *61*, 109-112.
2. Wittig, G.; Fuhrman, G. *Chem. Ber.* **1940**, *73*, 1197-1218.
3. Gilman, H.; Morton Jr., J. W. *Org. React. (N.Y.)* **1954**, *8*, 258-304.
4. Gschwend, H. W.; Rodriguez, H. R. *Org. React. (N.Y.)* **1979**, *26*, 1-360.
5. Snieckus, V. *Heterocycles* **1980**, *14*, 1649-1676.
6. Beak, P.; Snieckus, V. *Acc. Chem. Res.* **1982**, *15*, 306-312.
7. Snieckus, V. *Chem. Rev.* **1990**, *90*, 879-933.
8. Beak, P.; Meyers, A. I. *Acc. Chem. Res.* **1986**, *19*, 356-363.
9. Klumpp, G. W. *Recl. Trav. Chim. Pays-Bas* **1986**, *105*, 1-21.
10. Larsen, R. D.; King, A. O.; Chen, C. Y.; Corley, E. G.; Foster, B. S.; Roberts, F. E.; Yang, C.; Lieberman, D. R.; Reamer, R. A.; Tschäen, D. M.; Verhoeven, T. R.; Reider, P. J.; Lo, Y. S.; Rossano, L. T.; Brookes, A. S.; Meloni, D.; Moore, J. R.; Arnett, J. F. *J. Org. Chem.* **1994**, *59*, 6391-6394.
11. Lo, Y. S.; Rossano, L. T.; Meloni, D. J.; Moore, J. R.; Lee, Y.-C.; Arnett, J. F. *J. Heterocycl. Chem.* **1995**, *32*, 355-357.
12. Hay, D. R.; Song, Z.; Smith, S. G.; Beak, P. *J. Am. Chem. Soc.* **1988**, *110*, 8145-8153.
13. Wakefield, B. J. *The Chemistry of Organolithium Compounds*; Pergamon: Oxford, 1974.
14. Collum, D. B. *Acc. Chem. Res.* **1992**, *25*, 448-454.
15. Tye, H.; Eldred, C.; Wills, M. *Synlett* **1995**, 770-772.
16. Meyers, A. I.; Mihelich, E. D. *Angew. Chem. Int. Ed. Engl.* **1976**, *15*, 270-281.
17. Reuman, M.; Meyers, A. I. *Tetrahedron* **1985**, *41*, 837-860.
18. Ubada, J. I.; Villacampa, M.; Avendano, C. *Synlett* **1997**, 285-286.
19. Fuhrer, W.; Gschwend, H. W. *J. Org. Chem.* **1979**, *44*, 1133-1136.
20. Batch, A.; Dodd, R. H. *J. Org. Chem.* **1998**, *63*, 872-877.

21. Ronald, R. C.; Winkle, M. R. *Tetrahedron* **1983**, *39*, 2031-2042.
22. Townsend, C. A.; Bloom, L. M. *Tetrahedron Lett.* **1981**, *22*, 3923-3924.
23. Winkle, M. R.; Ronald, R. C. *J. Org. Chem.* **1982**, *47*, 2101-2108.
24. Christensen, H. *Synth. Commun.* **1975**, *5*, 65-78.
25. Fitt, J. J.; Gschwend, H. W. *J. Org. Chem.* **1976**, *41*, 4029-4031.
26. Krizan, T. D.; Martin, J. C. *J. Am. Chem. Soc.* **1983**, *105*, 6155-6157.
27. Caron, S.; Hawkins, J. M. *J. Org. Chem.* **1998**, *63*, 2054-2055.
28. Beaulieu, F.; Snieckus, V. *Synthesis* **1992**, 112-118.
29. Mortier, J.; Moyroud, J. *J. Org. Chem.* **1994**, *59*, 4042-4044.
30. Watanabe, M.; Date, M.; Kawanishi, K.; Tsukazaki, M.; Furukawa, S. *Chem. Pharm. Bull.* **1989**, *37*, 2564-2566.
31. Dhawan, B.; Redmore, D. *J. Org. Chem.* **1986**, *51*, 179-183.
32. Takagishi, S.; Schlosser, M. *Synlett* **1991**, 119-121.
33. Schlosser, M.; Katsoulos, G.; Takagishi, S. *Synlett* **1990**, 747-748.
34. Figuly, G. D.; Loop, C. K.; Martin, J. C. *J. Am. Chem. Soc.* **1989**, *111*, 654-658.
35. Block, E.; Eswarakrishnan, V.; Gernon, M.; Ofori-Okai, G.; Saha, C.; Tang, K.; Zubieta, J. *J. Am. Chem. Soc.* **1989**, *111*, 658-665.
36. Smith, K.; Lindsay, C. M.; Pritchard, G. J. *J. Am. Chem. Soc.* **1989**, *111*, 665-669.
37. Quesnelle, C.; Iihama, T.; Aubert, T.; Perrier, H.; Snieckus, V. *Tetrahedron Lett.* **1992**, *33*, 2625-2628.
38. Baker, R. W.; Pocock, G. R.; Sargent, M. V.; Twiss, E. *Tetrahedron: Asymmetry* **1993**, *4*, 2423-2426.
39. Rebiere, F.; Riant, O.; Ricard, L.; Kagan, H. B. *Angew. Chem. Int. Ed. Engl.* **1993**, *32*, 568-570.
40. Truce, W. E.; Amos, M. F. *J. Am. Chem. Soc.* **1951**, *73*, 3013-3017.
41. Iwao, M.; Iihama, T.; Mahalanabis, K. K.; Perrier, H.; Snieckus, V. *J. Org. Chem.* **1989**, *54*, 24-28.

42. Cabiddu, M. G.; Cabiddu, S.; Fattuoni, C.; Floris, C.; Gelli, G.; Melis, S. *Phosphorus, Sulfur, and Silicon* **1992**, *70*, 139-143.
43. Beaulieu, F.; Snieckus, V. *J. Org. Chem.* **1994**, *59*, 6508-6509.
44. Clayden, J.; Cooney, J. J. A.; Julia, M. *J. Chem. Soc. Perkin. Trans. 1* **1995**, 7-14.
45. Quesnelle, C. A., Ph.D. Thesis, University of Waterloo (1996).
46. Comins, D. L.; Brown, J. D. *J. Org. Chem.* **1989**, *54*, 3730-3732.
47. Watanabe, H.; Gay, R. L.; Hauser, C. R. *J. Org. Chem.* **1968**, *33*, 900-903.
48. Alo, B. I.; Familoni, O. B.; Marsais, F.; Queguiner, G. *J. Heterocycl. Chem.* **1992**, *29*, 61-64.
49. Maillett, M.; Kalinin, A.; Snieckus, V., manuscript in preparation.
50. Flippin, L. A.; Muchowski, J. M.; Carter, D. S. *J. Org. Chem.* **1993**, *58*, 2463-2467.
51. Ziegler, F. E.; Fowler, K. W. *J. Org. Chem.* **1976**, *41*, 1564-1566.
52. Watanabe, H.; Schwarz, R. A.; Hauser, C. R.; Lewis, J.; Slocum, D. W. *Can. J. Chem.* **1969**, *47*, 1543-1546.
53. Harris, T. D.; Roth, G. P. *J. Org. Chem.* **1979**, *44*, 2004-2007.
54. Figuly, G. D.; Martin, J. C. *J. Org. Chem.* **1980**, *45*, 3728-3729.
55. Bonfiglio, J. N. *J. Org. Chem.* **1986**, *51*, 2833-2835.
56. Desponds, O.; Schlosser, M. *J. Organomet. Chem.* **1996**, *507*, 257-261.
57. Schaub, B.; Jenny, T.; Schlosser, M. *Tetrahedron Lett.* **1984**, *25*, 4097-4100.
58. Plaumann, H. P.; Keay, B. A.; Rodrigo, R. *Tetrahedron Lett.* **1979**, *20*, 4921-4924.
59. Stuckwisch, C. G. *J. Org. Chem.* **1976**, *41*, 1173-1176.
60. Dashan, L.; Trippett, S. *Tetrahedron Lett.* **1983**, *24*, 2039-2040.
61. Craig, D. C.; Roberts, N. K.; Tanswell, J. L. *Aust. J. Chem.* **1990**, *43*, 1487-1496.
62. Yoshifuji, M.; Ishizuka, T.; Choi, Y. J.; Inamoto, I. *Tetrahedron Lett.* **1984**, *25*, 553-556.
63. Nakanishi, T.; Masanobu, S.; Mashiba, A.; Ishikawa, K.; Yokotsuka, T. *J. Org. Chem.* **1998**, *63*, 4235-4239.

64. Ple, N.; Turck, A.; Heynderickx, A.; Queguiner, G. *Tetrahedron* **1998**, *54*, 4899-4912.
65. Gschwend, H. W.; Hamdan, A. *J. Org. Chem.* **1982**, *47*, 3652-3657.
66. Katsoulos, G.; Takagishi, S.; Schlosser, M. *Synlett* **1991**, 731-732.
67. Beak, P.; Brown, R. A. *J. Org. Chem.* **1977**, *42*, 1823-1824.
68. Cuevas, J.-C.; Patil, P.; Snieckus, V. *Tetrahedron Lett.* **1989**, *43*, 5841-5844.
69. Mohri, S.-i.; Stefinovic, M.; Snieckus, V. *J. Org. Chem.* **1997**, *62*, 7072-7073.
70. Brandão, M. A. F.; de Oliveira, A. B.; Snieckus, V. *Tetrahedron Lett.* **1993**, *34*, 2437-2440.
71. FAMILONI, O. B.; Ionica, I.; Bower, J. F.; Snieckus, V. *Synlett* **1997**, 1081-1083.
72. James, C. A.; Snieckus, V. *Tetrahedron Lett.* **1997**, *38*, 8149-8152.
73. Watanabe, M.; Snieckus, V. *J. Am. Chem. Soc.* **1980**, *102*, 1457-1460.
74. Sibi, M. P.; Snieckus, V. *J. Org. Chem.* **1983**, *48*, 1935-1937.
75. Miah, M. A. J., Ph.D. Thesis, University of Waterloo (1985).
76. Legrand, O.; Brunel, J. M.; Constantieux, T.; Buono, G. *Chem. Eur. J.* **1998**, *4*, 1061-1067.
77. Dankwardt, J. W. *J. Org. Chem.* **1998**, *63*, 3753-3755.
78. Comins, D. L.; Killpack, M. O. *J. Org. Chem.* **1987**, *52*, 104.
79. Bader, A.; Lindner, E. *Coord. Chem. Rev.* **1991**, *108*, 27-110.
80. Schmid, R.; Broger, E. A.; Cereghetti, M.; Cramer, Y.; Foricher, J.; Lalonde, M.; Muller, R. K.; Scalone, M.; Schoettel, G.; Zutter, U. *Pure & Appl. Chem.* **1996**, *68*, 131-138.
81. Togni, A. *Chimia* **1996**, *50*, 86-93.
82. Togni, A. *Angew. Chem. Int. Ed. Engl.* **1996**, *35*, 1475-1477.
83. Seyferth, D.; Welch, D. E.; Heeren, J. K. *J. Am. Chem. Soc.* **1963**, *85*, 642-643.
84. Seyferth, D.; Welch, D. E.; Heeren, J. K. *J. Am. Chem. Soc.* **1964**, *86*, 1100-1105.
85. Seyferth, D.; Welch, D. E. *J. Organomet. Chem.* **1964**, *2*, 1-7.

86. The authors make no mention of what method was used to determine relative amounts of carbanion intermediates.
87. Gilman, H.; Brown, G. E. *J. Am. Chem. Soc.* **1945**, *67*, 824-826.
88. Wittig, G.; Cristau, H.-J. *Bull. Soc. Chim. Fr.* **1969**, 1293-1298.
89. Price, D.; Simpkins, N. S. *Tetrahedron Lett.* **1995**, *36*, 6135-6136.
90. Ogawa, S.; Tajiri, Y.; Furukawa, N. *Bull. Chem. Soc. Jpn.* **1991**, *64*, 3182-3184.
91. Zbiral, E. *Tetrahedron Lett.* **1964**, 1649-1652.
92. Seyferth, D.; Hughes, W. B.; Heeren, J. K. *J. Am. Chem. Soc.* **1965**, *87*, 3467-3474.
93. Schaub, B.; Schlosser, M. *Tetrahedron Lett.* **1985**, *26*, 1623-1626.
94. Brown, J. M.; Woodward, S. *J. Org. Chem.* **1991**, *56*, 6803-6809.
95. Schmid, R.; Foricher, J.; Cereghetti, M.; Schönholzer, P. *Helv. Chim. Acta* **1991**, *74*, 370-389.
96. Jendralla, H.; Li, C. H.; Paulus, E. *Tetrahedron: Asymmetry* **1994**, *5*, 1297-1320.
97. Gray, M.; Chapell, B. J.; Taylor, N. J.; Snieckus, V. *Angew. Chem. Int. Ed. Engl.* **1996**, *35*, 1558-1560.
98. Kellner, K.; Tzschach, A. *Phosphorus Sulfur* **1987**, *30*, 692.
99. Alcock, N. W.; Brown, J. M.; Pearson, K. M.; Woodward, S. *Tetrahedron: Asymmetry* **1992**, *3*, 17-20.
100. Wardell, J. L. *Comprehensive Organometallic Chemistry*; Pergamon: New York, 1982; Vol. 1.
101. Bates, R. B.; Ogle, C. A. *Carbanion Chemistry*; Springer-Verlag: Berlin, 1983.
102. Fraenkel, G.; Winchester, W. R. *J. Am. Chem. Soc.* **1988**, *110*, 8720.
103. Schleyer, P. v. R. *Pure Appl. Chem.* **1984**, *56*, 151.
104. Setzer, W. M.; Schleyer, P. v. R. *Adv. Organomet. Chem.* **1985**, *24*, 353.
105. Schlosser, M. *Pure Appl. Chem.* **1988**, *60*, 1627-1634.
106. Mordini, A. In *Advances in Carbanion Chemistry*, Snieckus, V. Eds., JAI Press: Greenwich **1992**, *1*, 1-44.

107. Schlosser, M.; Maccaroni, P.; Marzi, E. *Tetrahedron* **1998**, *54*, 2763-2770.
108. Gros, P.; Fort, Y.; Caubère, P. *J. Chem. Soc., Perkin Trans. I* **1998**, 1685-1689.
109. Margerison, D.; Newport, J. P. *Trans. Faraday Soc.* **1963**, *59*, 2058-2063.
110. Lewis, H. L.; Brown, T. L. *J. Am. Chem. Soc.* **1970**, *92*, 4664-4670.
111. Fraenkel, G.; Henrichs, M.; Hewitt, M.; Su, B. M. *J. Am. Chem. Soc.* **1984**, *106*, 225.
112. West, P. *Inorg. Chem.* **1962**, *1*, 654.
113. West, P.; Waack, R. *J. Am. Chem. Soc.* **1967**, *89*, 4395-4399.
114. Quirck, R. P.; Kester, D. E. *J. Organomet. Chem.* **1974**, *72*, C23-C25.
115. McGarrity, J. F.; Ogle, C. A. *J. Am. Chem. Soc.* **1985**, *107*, 1805-1810.
116. McGarrity, J. F.; Ogle, C. A.; Brich, Z.; Loosli, H.-R. *J. Am. Chem. Soc.* **1985**, *107*, 1810-1815.
117. Settle, F. A.; Haggerty, M.; Eastham, J. F. *J. Am. Chem. Soc.* **1964**, *86*, 1076-1077.
118. Slocum, D. W.; Book, G.; Jennings, C. A. *Tetrahedron Lett.* **1970**, 3443-3445.
119. Chadwick, S. T.; Rennels, R. A.; Rutherford, J. L.; Collum, D. B. *J. Am. Chem. Soc.* **2000**, *122*, 8640-8647.
120. Langer, A. W., Jr. *Polyamine-Chelated Alkali Metal Compounds*; American Chemical Society: Washington, 1974; Vol. 130.
121. Schubert, U.; Neugebauer, W.; von Rague Schleyer, P. *J. Chem. Soc., Chem. Commun.* **1982**, 1184-1185.
122. Bauer, W.; Muller, G.; Pi, R.; Schleyer, P. v. R. *Angew. Chem. Int. Ed. Engl.* **1986**, *25*, 1103-1104.
123. Lucht, B. L.; Bernstein, M. P.; Remenar, J. F.; Collum, D. B. *J. Am. Chem. Soc.* **1996**, *118*, 10707.
124. Hoffmann, D.; Collum, D. B. *J. Am. Chem. Soc.* **1998**, *120*, 5810-5811.
125. Bauer, W.; Klusener, P. A. A.; Harder, S.; Kanters, J. A.; Duisenberg, A. J. M.; Brandsma, L.; Schleyer, P. v. R. *Organometallics* **1988**, *7*, 552-555.

126. Teclé, B.; Ilsley, W. H.; Oliver, J. P. *Organometallics* **1982**, *1*, 875-877.
127. Saá, J. M.; Deyá, P. M.; Suñer, G. A.; Frontera, A. *J. Am. Chem. Soc.* **1992**, *114*, 9093-9100.
128. Stratakis, M. *J. Org. Chem.* **1997**, *62*, 3024-3025.
129. Rennels, R. A.; Maliakal, A. J.; Collum, D. B. *J. Am. Chem. Soc.* **1998**, *120*, 421-422.
130. Kimachi, T. *Chem. Pharm. Bull.* **1998**, *46*, 139-141.
131. Bernstein, M. P.; Romesberg, F. E.; Fuller, D. J.; Harrison, A. T.; Collum, D. B.; Liu, Q.-Y.; Williard, P. G. *J. Am. Chem. Soc.* **1992**, *114*, 5100-5110.
132. Bernstein, M. P.; Collum, D. B. *J. Am. Chem. Soc.* **1993**, *115*, 789-790.
133. Bernstein, M. P.; Collum, D. B. *J. Am. Chem. Soc.* **1993**, *115*, 8008-8018.
134. Thurner, A.; Faigl, F.; Agai, B.; Toke, L. *Synth. Commun.* **1998**, *28*, 443-449.
135. Arai, S.; Tamarov, Y.; Lowe, D. W. *J. Cell. Plast.* **1988**, *24*, 284-298.
136. Roberts, J. D.; Curtin, D. Y. *J. Am. Chem. Soc.* **1946**, *68*, 1658-1660.
137. Horne, S.; Rodrigo, R. *J. Org. Chem.* **1990**, *55*, 4520-4522.
138. Anderson, D. R.; Faibish, N. C.; Beak, P. *J. Am. Chem. Soc.* **1999**, *121*, 7553-7558.
139. Resek, J. E.; Beak, P. *J. Am. Chem. Soc.* **1994**, *116*, 405-406.
140. Lutz, G. P.; Wallin, A. P.; Kerrick, S. T.; Beak, P. *J. Org. Chem.* **1991**, *56*, 4938-4943.
141. Beak, P.; Hunter, J. E.; Jun, Y. M.; Wallin, A. P. *J. Am. Chem. Soc.* **1987**, *109*, 5403-5412.
142. Beak, P.; Kerrick, S. T.; Gallagher, D. J. *J. Am. Chem. Soc.* **1993**, *115*, 10628-10636.
143. Sammakia, T.; Latham, H. A. *J. Org. Chem.* **1995**, *60*, 6002-6003.
144. Sammakia, T.; Latham, H. A.; Schaad, D. R. *J. Org. Chem.* **1995**, *60*, 10-11.
145. Kremer, T.; Junge, M.; Schleyer, P. v. R. *Organometallics* **1996**, *15*, 3345-3359.
146. van Eikema Hommes, N. J. R.; Schleyer, P. v. R. *Tetrahedron* **1994**, *50*, 5903-5916.

147. van Eikema Hommes, N. J. R.; Schleyer, P. v. R. *Angew. Chem. Int. Ed. Engl.* **1992**, *31*, 755-758.
148. Bauer, W.; Schleyer, P. v. R. *J. Am. Chem. Soc.* **1989**, *111*, 7191-7198.
149. Slocum, D. W.; Moon, R.; Thompson, J.; Coffey, D. S.; Li, J. D.; Slocum, M. G.; Siegel, A.; Gayton-Garcia, R. *Tetrahedron Lett.* **1994**, *35*, 385-388.
150. Slocum, D. W.; Coffey, D. S.; Siegel, A.; Grimes, P. *Tetrahedron Lett.* **1994**, *35*, 389-392.
151. Slocum, D. W.; Thompson, J.; Friesen, C. *Tetrahedron Lett.* **1995**, *36*, 8171-8174.
152. Slocum, D. W.; Hayes, G.; Kline, N. *Tetrahedron Lett.* **1995**, *36*, 8175-8178.
153. Slocum, D. W.; Jennings, C. A. *J. Org. Chem.* **1976**, *41*, 3653-3664.
154. Baumann, W.; Oprunenko, Y.; Günther, H. *Z. Naturforsch.* **1995**, *50*, 429.
155. Waldmüller, D.; Kotsatos, B. J.; Nichols, M. A.; Williard, P. G. *J. Am. Chem. Soc.* **1997**, *119*, 5479.
156. Saá, J. M.; Morey, J.; Frontera, A.; Deyá, P. M. *J. Am. Chem. Soc.* **1995**, *117*, 1105-1116.
157. Saá, J. M.; Martorell, G.; Frontera, A. *J. Org. Chem.* **1996**, *61*, 5194-5195.
158. Suñer, A.; Deyá, P. M.; Saá, J. M. *J. Am. Chem. Soc.* **1990**, *112*, 1467-1471.
159. Maggi, R.; Schlosser, M. *Tetrahedron Lett.* **1999**, *40*, 8797-8800.
160. Schlosser, M. *Angew. Chem., Int. Ed. Engl.* **1998**, *37*, 1497.
161. Snieckus, V. *Pure Appl. Chem.* **1994**, *66*, 2155-2158.
162. Beak, P.; Hunter, J. E.; Jun, Y. M. *J. Am. Chem. Soc.* **1983**, *105*, 6350-6351.
163. Gay, R. L.; Hauser, C. R. *J. Am. Chem. Soc.* **1967**, *89*, 2297-2303.
164. Eaborn, C.; Golborn, P.; Taylor, R. *J. Organomet. Chem.* **1967**, *10*, 171-174.
165. Narasimhan, N. S.; Ranade, A. C. *Ind. J. Chem.* **1969**, *7*, 538-539.
166. Shirley, D. A.; Cheng, C. F. *J. Organomet. Chem.* **1969**, *20*, 251-252.
167. Narasimhan, N. S.; Alurkar, R. H. *Ind. J. Chem.* **1969**, *7*, 1280.

168. Narasimhan, N. S.; Chandrachood, P. S.; Shete, N. R. *Tetrahedron* **1981**, *37*, 825-827.
169. Fu, J.-m.; Zhao, B.-p.; Sharp, M. J.; Snieckus, V. *J. Org. Chem.* **1991**, *56*, 1683-1685.
170. Fu, J.-m.; Zhao, B.-p.; Sharp, M. J.; Snieckus, V. *Can. J. Chem.* **1994**, *72*, 227-236.
171. Zhao, B.; Snieckus, V. *Tetrahedron Lett.* **1991**, *32*, 5277-5278.
172. Fu, J.-m.; Sharp, M. J.; Snieckus, V. *Tetrahedron Lett.* **1988**, *29*, 5459-5462.
173. Wang, X.; Snieckus, V. *Tetrahedron Lett.* **1991**, *32*, 4883-4884.
174. Chowdhury, S.; Zhao, B.; Snieckus, V. *Polycyclic Aromatic Compounds* **1994**, *5*, 27-34.
175. Benesch, L.; Bury, P.; Guillaneux, D.; Houldsworth, S.; Wang, X.; Snieckus, V. *Tetrahedron Lett.* **1998**, *39*, 961-964.
176. Wang, W.; Snieckus, V. *J. Org. Chem.* **1992**, *57*, 424-426.
177. MacNeil, S. L.; Gray, M.; Briggs, L. E.; Li, J. J.; Snieckus, V. *Synlett* **1998**, 419-421.
178. Jones, W. D., Jr.; Ciske, F. L. *J. Org. Chem.* **1996**, *59*, 3920-3922.
179. Kealy, T. J.; Pauson, P. J. *Nature (London)* **1951**, *168*, 1039.
180. Miller, S. A.; Tebboth, J. A.; Tremaine, J. F. *J. Chem. Soc.* **1952**, 632-635.
181. Wilkinson, G.; Rosenblum, M.; Whiting, M. C.; Woodward, R. B. *J. Am. Chem. Soc.* **1952**, *74*, 2125-2126.
182. Wilkinson, G. *J. Am. Chem. Soc.* **1952**, *74*, 6148-6149.
183. Fischer, E. O.; Pfab, W. *Z. Naturforsch.* **1952**, *7B*, 377.
184. Togni, A.; Hayashi, T.; Eds. *Ferrocenes*; VCH: New York, 1995.
185. Kuehne, M. E.; Bandarage, U. K. *J. Org. Chem.* **1996**, *61*, 1175-1179.
186. Kagan, H.; Diter, P.; Gref, A.; Guillaneux, D.; Masson-Szymczak, A.; Rebiere, F.; Riant, O.; Samuel, O.; Taudien, S. *Pure Appl. Chem.* **1996**, *68*, 29-36.
187. Hradsky, A.; Bildstein, B.; Schuler, N.; Schottenberger, H.; Jaitner, P.; Ongania, K.-H.; Wurst, K.; Launay, J.-P. *Organometallics* **1997**, *16*, 392-402.

188. Lion-Dagan, M.; Marx-Tibbon, S.; Katz, E.; Willner, I. *Angew. Chem. Int. Ed. Engl.* **1995**, *34*, 1604-1606.
189. Gruselle, M.; Malezieux, B.; Sokolov, V. I.; Troitskaya, L. L. *Inorg. Chim. Acta* **1994**, *222*, 51-61.
190. Sollott, G. P.; Mertwoy, H. E.; Portnoy, S.; Snead, J. L. *J. Org. Chem.* **1963**, *28*, 1090-1092.
191. Benkeser, R. A.; Goggin, O.; Schroll, G. *J. Am. Chem. Soc.* **1954**, *76*, 4025-4026.
192. Nesmeyanov, N. A.; Perevalova, E. G.; Golovnya, R. V.; Nesmeyanova, O. A. *Dokl. Akad. Nauk SSSR* **1954**, *97*, 459 [Chem. Abstr. **195449**:9633f].
193. Guillaneux, D.; Kagan, H. B. *J. Org. Chem.* **1995**, *60*, 2502-2505.
194. Seyferth, D.; Hoffman, H. P.; Burton, R.; Helling, J. F. *Inorg. Chem.* **1962**, *1*, 227-231.
195. Hedberg, F. L.; Rosenberg, H. *Tetrahedron Lett.* **1969**, 4011-4012.
196. Rausch, M. D.; Ciappenelli, D. J. *J. Organomet. Chem.* **1967**, *10*, 127-136.
197. Glidewell, C.; Royles, B. J. L.; Smith, D. M. *J. Organomet. Chem.* **1997**, *527*, 259-261.
198. Benkeser, R. A.; Fitzgerald, W. P.; Melzer, M. S. *J. Org. Chem.* **1961**, *26*, 2569-2571.
199. Slocum, D. W.; Rockett, B. W.; Hauser, C. R. *J. Am. Chem. Soc.* **1965**, *87*, 1241-1246.
200. Jones, F. N.; Zinn, M. F.; Hauser, C. R. *J. Org. Chem.* **1963**, *28*, 663-665.
201. Jones, F. N.; Vault, R. L.; Hauser, C. R. *J. Org. Chem.* **1963**, *28*, 3461-3465.
202. Slocum, D. W.; Koonsvitsky, B. P.; Ernst, C. R. *J. Organomet. Chem.* **1972**, *38*, 125-132.
203. Nesmeyanov, A. M.; Baukova, T.; Grandberg, K. *Izv. Akad. Nauk SSSR, Ser. Khim.* **1967**, 1867.
204. Huffman, J.; Keith, L.; Ausbury, R. *J. Org. Chem.* **1965**, *30*, 1600-1604.

205. Slocum, D. W.; Stonemark, F. E. *J. Org. Chem.* **1973**, *38*, 1677-1681.
206. Eberhard, L.; Lampin, J. P.; Mathey, F. *J. Organomet. Chem.* **1974**, *80*, 109-118.
207. Sawamura, M.; Yamauchi, A.; Takegawa, T.; Ito, Y. *J. Chem. Soc., Chem. Commun.* **1991**, 874-875.
208. Epton, R.; Marr, G.; Rogers, G. K. *J. Organomet. Chem.* **1978**, *150*, 93-100.
209. Schmitt, G.; Klein, P.; Ebertz, W. *J. Organomet. Chem.* **1982**, *234*, 63-72.
210. Iftime, G.; Moreau-Bossuet, C.; Manoury, E.; Balavoine, G. G. A. *Chem. Commun.* **1996**, 527-528.
211. Iftime, G.; Daran, J.-C.; Manoury, E.; Balavoine, G. G. A. *Organometallics* **1996**, *15*, 4808-4815.
212. Iftime, G.; Daran, J.-C.; Manoury, E.; Balavoine, G. G. A. *Angew. Chem. Int. Ed. Engl.* **1998**, *37*, 1698-1701.
213. Schlögl, K. *Top. Stereochem.* **1967**, *1*, 39.
214. Cahn, R. S.; Ingold, C.; Prelog, V. *Angew. Chem. Int. Ed. Engl.* **1966**, *5*, 385-415.
215. Nicolosi, G.; Patti, A.; Morrone, F.; Piattelli, M. *Tetrahedron: Asymmetry* **1994**, *5*, 1639-1642.
216. Cahn, R. S.; Ingold, C.; Prelog, V. *Experientia* **1956**, *12*, 81.
217. Cahn, R. S. *J. Chem. Ed.* **1964**, *41*, 116.
218. Richards, C. J.; Locke, A. J. *Tetrahedron: Asymmetry* **1998**, *9*, 2377-2407.
219. Hayashi, T.; Mise, T.; Fukushima, M.; Kagotani, M.; Nagashima, N.; Hamada, Y.; Matsumoto, A.; Kawakami, S.; Konishi, M.; Yamamoto, K.; Kumada, M. *Bull. Chem. Soc. Jpn.* **1980**, *53*, 1138-1151.
220. Sokolov, V. I.; Troitskaya, L. L.; Reutov, O. A. *J. Organomet. Chem.* **1980**, *202*, C58-C60.
221. Marquarding, D.; Klusacek, H.; Gokel, G.; Hoffmann, P.; Ugi, I. *J. Am. Chem. Soc.* **1970**, *92*, 5389-5393.

222. Nicolosi, G.; Patti, A.; Morrone, R.; Piattelli, M. *Tetrahedron: Asymmetry* **1994**, *5*, 1275-1280.
223. Nicolosi, F.; Morrone, R.; Patti, A.; Piattelli, M. *Tetrahedron: Asymmetry* **1992**, *3*, 753-758.
224. Riant, O.; Samuel, O.; Kagan, H. B. *J. Am. Chem. Soc.* **1993**, *115*, 5835-5836.
225. Nishibayashi, Y.; Uemura, S. *Synlett* **1995**, 79-81.
226. Park, J.; Lee, S.; Ahn, K. H.; Cho, C.-W. *Tetrahedron Lett.* **1995**, *36*, 7263-7266.
227. Park, J.; Lee, S.; Ahn, K. H.; Cho, C.-W. *Tetrahedron Lett.* **1996**, *37*, 6137-6140.
228. Richards, C. J.; Damalidis, T.; Hibbs, D. E.; Hursthouse, M. B. *Synlett* **1995**, 74-76.
229. Richards, C. J.; Mulvaney, A. W. *Tetrahedron: Asymmetry* **1996**, *7*, 1419-1430.
230. Uemura, M.; Hayashi, Y.; Hayashi, Y. *Tetrahedron: Asymm.* **1994**, *5*, 1427-1430.
231. Price, D. A.; Simpkins, N. S. *J. Org. Chem.* **1994**, *59*, 1961-1962.
232. Price, D. A.; Simpkins, N. S.; MacLeod, A. M.; Watt, A. P. *Tetrahedron Lett.* **1994**, *35*, 6159-6162.
233. Kündig, E. P.; Quattropiani, A. *Tetrahedron Lett.* **1994**, *35*, 3497-3500.
234. Nishibayashi, Y.; Arikawa, Y.; Ohe, K.; Uemura, S. *J. Org. Chem.* **1996**, *61*, 1172-1174.
235. van Leeuwen, P. W. N. M.; Kamer, P. C. J.; Reek, J. N. H.; Dierkes, P. *Chem. Rev.* **2000**, *100*, 2741-2770.
236. McGarrity, J.; Spindler, R.; Fuchs, R.; Eyer, M. (LONZA AG). EP-A 624 587 A2, **1995** [*Chem. Abstr.* **1995**, *122*, P81369q].
237. Togni, A.; Breutel, C.; Schnyder, A.; Spindler, F.; Landert, H.; Tijani, A. *J. Am. Chem. Soc.* **1994**, *116*, 4062-4066.
238. Hamann, B. C.; Hartwig, J. F. *J. Am. Chem. Soc.* **1998**, *120*, 7369-7370.
239. Tomori, H.; Fox, J. M.; Buchwald, S. L. *J. Org. Chem.* **2000**, *65*, 5334-5341.
240. Wolfe, J. P.; Buchwald, S. L. *Angew. Chem., Int. Ed. Engl.* **1999**, *38*, 2413.

241. Wolfe, J. P.; Singer, R. A.; Yang, B. H.; Buchwald, S. L. *J. Am. Chem. Soc.* **1999**, *121*, 9550.
242. Wolfe, J. P.; Tomori, H.; Sadighi, J. P.; Yin, J.; Buchwald, S. L. *J. Org. Chem.* **2000**, *65*, 1158.
243. Timmer, K.; Thewissen, D. H. M. W.; Marsman, J. W. *Recl. Trav. Chim. Pays-Bas* **1988**, *107*, 248-255.
244. Moulton, C. J.; Shaw, B. L. *J. Chem. Soc. Dalton Trans.* **1980**, 299-301.
245. Empsall, H. D.; Shaw, B. L.; Turtle, B. L. *J. Chem. Soc., Dalton Trans.* **1976**, 1500-1506.
246. Empsall, H. D.; Heys, P. N.; Shaw, B. L. *J. Chem. Soc. Dalton Trans.* **1978**, 257-262.
247. Tsukazaki, M., Ph.D. Thesis, University of Waterloo (1995).
248. Hoppe, D.; Hintze, F.; Tebben, P.; Paetow, M.; Ahrens, H.; Schwerdtfeger, J.; Sommerfeld, P.; Haller, J.; Guarnieri, W.; Kolczewski, S.; Hense, T.; Hoppe, I. *Pure Appl. Chem.* **1994**, *66*, 1479-1486.
249. Gallagher, D. J.; Beak, P. *J. Org. Chem.* **1995**, *60*, 7092-7093.
250. Thayumanavan, S.; Lee, S.; Liu, C.; Beak, P. *J. Am. Chem. Soc.* **1994**, *116*, 9755-9756.
251. Hoppe, D.; Hense, T. *Angew. Chem. Int. Ed. Engl.* **1997**, *36*, 2282-2316.
252. Tsukazaki, M.; Tinkl, M.; Roglans, A.; Chapell, B. J.; Taylor, N. J.; Snieckus, V. *J. Am. Chem. Soc.* **1996**, *118*, 685-686.
253. Molecular modeling performed by Dr. M.G. Campbell on Silicon Graphics Elan workstation using the Sybyl 6.1 program.
254. Experiment performed by Dr. M. Tinkl and Dr. A. Roglans.
255. Bessler, C.; Metallinos, C.; Snieckus, V. , unpublished results.
256. Metallinos, C.; Greene, L.; Snieckus, V. , unpublished results.
257. Guillaneaux, D., personal communication.

258. Sulfur electrophile graciously supplied by Dr. C.A. Quesnelle.
259. Mann, B. E.; Shaw, B. L.; Slade, R. M. *J. Chem. Soc. (A)* **1971**, 2976-2980.
260. Conditions for this synthesis were developed by Jakob Felding. It was found that the use of toluene in this synthesis is crucial since performing the reaction in either THF or Et₂O resulted in no product being isolated.
261. Chlorodi-*tert*-butylphosphine is commercially available only in 5 g quantities while dichlorophenylphosphine is available in quantities of 100 g or more. Attempts to synthesize ClP^{*t*}Bu₂ according to literature methods were unsuccessful (Fild, M.; Stelzer, O.; Schmutzler, R. *Inorg. Synth.* **1973**, *14*, 4; Naiini, A.A.; Han, Y.; Akinc, M.; Verkade, J.G. *Inorg. Chem.* **1993**, *32*, 5394-5395).
262. Haque, M.-u.; Ahmed, J.; Horne, W. *Acta Cryst.* **1983**, *C39*, 383-385.
263. Campbell, J. A.; Caughlan, C. N.; Fitzgerald, A.; Campana, C.; Cremer, S. E. *Acta Cryst.* **1984**, *C40*, 1918-1920.
264. Matsubara, H.; Tanaka, T.; Takai, Y.; Sawada, M.; Seto, K.; Imazaki, H.; Takahashi, S. *Bull. Chem. Soc. Jpn.* **1991**, *64*, 2103-2108.
265. Kliegel, W.; Preu, L.; Rettig, S. J.; Trotter, J. *Can. J. Chem.* **1986**, *64*, 1855-1858.
266. Ahlenstiel, E.; Kliegel, W.; Rettig, S. J.; Trotter, J. *Can. J. Chem.* **1993**, *71*, 263-271.
267. This sequence was performed by Dr. Jakob Felding.
268. Malakhova, I. G.; Tsvetkov, E. N.; Kabachnik, M. I. *Bull. Acad. Sci. USSR Div. Chem. Sci. (Engl. Transl.)* **1975**, *24*, 164-167.
269. Experiment performed by Dr. Matthew Gray. For details, see "Matthew Gray, Snieckus Group Final Report", University of Waterloo, 1996.
270. Sutter, M. A.; Seebach, D. *Ann.* **1983**, 939.
271. Gray, M.; Snieckus, V. , unpublished results.
272. Tinkl, M.; Roglans, A.; Campbell, M. G.; Miao, G.; Snieckus, V. , unpublished results.
273. Milburn, R., M.Sc. Thesis, University of Waterloo (1999).
274. Quinn, R.; Snieckus, V. , unpublished results.

275. Felding, J.; Snieckus, V. , unpublished results.
276. Somei, M.; Yokoyama, Y.; Murakami, Y.; Minomiya, I.; Kiguchi, T.; Naito, T. *The Alkaloids* **2000**, *54*, 193-259.
277. Lounasmaa, M.; Hanhihen, P. *The Alkaloids* **2001**, *55*, 1-89.
278. Husson, H. P. *The Alkaloids* **1985**, *26*, 1-50.
279. Sundberg, R. J. *Indoles*; Academic: Toronto, 1996.
280. Sugasawa, T.; Adachi, M.; Sasakura, K.; Kitagawa, A. *J. Org. Chem.* **1979**, *44*, 578.
281. Ito, Y.; Kobayashi, K.; Seko, N.; Saegusa, T. *Bull. Chem. Soc. Jpn.* **1984**, *57*, 73.
282. Batcho, A. D.; Leimgruber, W. *Org. Syn.* **1985**, *63*, 214-224.
283. Bartoli, G.; Palmieri, G.; Bosco, M.; Dalpozzo, R. *Tetrahedron Lett.* **1989**, *30*, 2129.
284. Kondo, Y.; Kojima, S.; Sakamoto, T. *Heterocycles* **1996**, *43*, 2741.
285. Greenhill, J. V. In *Comprehensive Heterocyclic Chemistry*, Katritzky, A. R. and Rees, C. W. Eds., Pergamon Press: Oxford **1984**, *4*, 497.
286. Shirley, D. A.; Roussel, P. A. *J. Am. Chem. Soc.* **1953**, *75*, 375-378.
287. Sundberg, R. J.; Russell, H. F. *J. Org. Chem.* **1973**, *38*, 3324-3330.
288. Hasan, I.; Marinelli, E. R.; Lin, L.-C. C.; Fowler, F. W.; Levy, A. B. *J. Org. Chem.* **1981**, *46*, 157-164.
289. Ishikura, M.; Matsuzaki, Y.; Agata, I. *Heterocycles* **1997**, *45*, 2309-2312.
290. Sakamoto, T.; Yoshinori, K.; Takazawa, N.; Yamanaka, H. *Heterocycles* **1993**, *36*, 941-942.
291. Edwards, M. P.; Ley, S. V.; Lister, S. G.; Palmer, B. D. *J. Chem. Soc., Chem. Commun.* **1983**, 630-633.
292. Muchowski, J. M.; Solas, D. R. *J. Org. Chem.* **1984**, *49*, 203-205.
293. Edwards, M. P.; Doherty, A. M.; Ley, S. V.; Organ, H. M. *Tetrahedron* **1986**, *42*, 3723-3729.
294. Katritzky, A. R.; Akutagawa, K. *Tetrahedron Lett.* **1985**, *26*, 5935-5938.
295. Bergman, J.; Venemalm, L. *Tetrahedron Lett.* **1987**, *28*, 3741-3744.

296. Bergman, J.; Venemalm, L. *Tetrahedron Lett.* **1988**, *29*, 2993-2994.
297. Hlasta, D. J.; Bell, M. R. *Heterocycles* **1989**, *29*, 849-852.
298. Katritzky, A. R.; Lue, P.; Chen, Y.-X. *J. Org. Chem.* **1990**, *55*, 3688-3691.
299. Gharpure, M.; Stoller, A.; Bellamy, F.; Firnau, G.; Snieckus, V. *Synthesis* **1991**, 1079-1082.
300. Kano, S.; Sugino, E.; Hibino, S. *J. Chem. Soc., Chem. Commun.* **1980**, 1241-1242.
301. Amat, M.; Hadida, S.; Sathyanarayana, S.; Bosch, J. *J. Org. Chem.* **1994**, *59*, 10-11.
302. Griffen, E. J.; Roe, D. G.; Snieckus, V. *J. Org. Chem.* **1995**, *60*, 1484-1485.
303. Saulnier, M. G.; Gribble, G. W. *J. Org. Chem.* **1982**, *47*, 757-761.
304. Saulnier, M. G.; Gribble, G. W. *J. Org. Chem.* **1983**, *48*, 2690-2695.
305. Gribble, G. W.; Barden, T. C. *J. Org. Chem.* **1985**, *50*, 5900-5902.
306. Wenkert, E.; Angell, E. C.; Ferreira, V. F.; Michelotti, E. L.; Piettre, S. R.; Sheu, J.-H.; Swindell, C. S. *J. Org. Chem.* **1986**, *51*, 2343-2351.
307. Conway, S. C.; Gribble, G. W. *Heterocycles* **1990**, *30*, 627-633.
308. Sakamoto, T.; Kondo, Y.; Takazawa, N.; Yamanaka, H. *Tetrahedron Lett.* **1993**, *34*, 5955-5956.
309. Gribble, G. W.; Saulnier, M. G. *J. Org. Chem.* **1983**, *48*, 607-609.
310. Johnson, D. A.; Gribble, G. W. *Heterocycles* **1986**, *24*, 2127-2132.
311. Rubiralta, M.; Casamitjana, N.; Grierson, D. S.; Husson, H.-P. *Tetrahedron* **1988**, *44*, 443-450.
312. Iwao, M. *Heterocycles* **1993**, *36*, 29-32.
313. Miller, J. D. *Ann. Rep. Med. Chem.* **1992**, *27*, 11-19.
314. Romero, A. G.; McCall, R. B. *Ann. Rep. Med. Chem.* **1992**, *27*, 21-30.
315. Roe, D. , personal communication.
316. Sengupta, S.; Snieckus, V. *J. Org. Chem.* **1990**, *55*, 5680.
317. Nechvatal, G.; Widdowson, D. A. *J. Chem. Soc., Chem. Commun.* **1982**, 467-468.

318. Beswick, P. J.; Greenwood, C. S.; Mowlem, T. J.; Nechvatal, G.; Widdowson, D. A. *Tetrahedron* **1988**, *44*, 7325-7334.
319. Nechvatal, G.; Widdowson, D. A.; Williams, D. J. *J. Chem. Soc., Chem. Commun.* **1981**, 1260-1262.
320. Masters, N. F.; Mathews, N.; Nechvatal, G.; Widdowson, D. A. *Tetrahedron* **1989**, *45*, 5955-5970.
321. Iwao, M.; Kuraishi, T. *Heterocycles* **1992**, *34*, 1031-1038.
322. Preobrazhenskaya, M. N. *Russian Chem. Rev.* **1967**, *36*, 753.
323. Ketcha, D. M.; Lieurance, B. A.; Homan, D. F. *J. Org. Chem.* **1989**, *54*, 4350-4356.
324. Ketcha, D. M. *Tetrahedron Lett.* **1988**, *29*, 2151-2154.
325. Cannon, J. G.; Roufos, I. *J. Heterocycl. Chem.* **1990**, *27*, 2093-2095.
326. Meyers, A. I.; Hellring, S. *Tetrahedron Lett.* **1981**, *22*, 5119-5122.
327. Beak, P.; Lee, W.-K. *Tetrahedron Lett.* **1989**, *30*, 1197-1200.
328. Meyers, A. I.; Milot, G. *J. Org. Chem.* **1993**, *58*, 6538-6540.
329. Bertini-Gross, K. M.; Jun, Y. M.; Beak, P. *J. Org. Chem.* **1997**, *62*, 7679-7689.
330. Fukuda, T.; Ryoichi, M.; Iwao, M. *Tetrahedron* **1999**, *55*, 9151-9162.
331. Begtrup, M.; Claramount, R. M.; Elguero, J. *J. Chem. Soc., Perkin Trans. 2* **1978**, 99.
332. Achenbach, H.; Renner, C. *Heterocycles* **1985**, *23*, 2075-2081.
333. Yamamoto, Y.; Arai, K. *The Alkaloids* **1986**, *29*, 185-263.
334. Brewer, D.; Jerram, W. A.; Taylor, A. *Can. J. Microb.* **1968**, *14*, 861-866.
335. Meiler, D.; Taylor, A. *Can. J. Microb.* **1971**, *17*, 83-86.
336. Brewer, D.; Jerram, W. A.; Meiler, D.; Taylor, A. *Can. J. Microbiol.* **1970**, *16*, 433-440.
337. Jerram, W. A.; McInnes, A. G.; Maass, W. S. G.; Smith, D. G.; Taylor, A.; Walter, J. A. *Can. J. Chem.* **1975**, *53*, 727-737.

338. Jerram, W. A.; McInnes, A. G.; Maass, S. G.; Smith, D. G.; Taylor, A.; Walter, J. A. *Can. J. Chem.* **1975**, *53*, 2031.
339. Arai, K.; Masuda, K.; Kiriyaama, N.; Nitta, K.; Yamamoto, Y.; Shimizu, S. *Chem. Pharm. Bull.* **1981**, *29*, 961-969.
340. Kaji, A.; Iwata, T.; Kiriyaama, N.; Wakusawa, S.; Miyamoto, K.-i. *Chem. Pharm. Bull.* **1994**, *42*, 1682-1684.
341. Mocek, U.; Schultz, L.; Buchan, T.; Baek, C.; Fretto, L.; Nzerem, J.; Sehl, L.; Sinha, U. *J. Antibiotics* **1996**, *49*, 854-859.
342. O'Leary, M. A.; Hanson, J. R. *Tetrahedron Lett.* **1982**, *23*, 1855-1856.
343. O'Leary, M. A.; Hanson, J. R.; Yeoh, B. L. *J. Chem. Soc., Perkin Trans. I* **1984**, 567-569.
344. Yamamoto, Y.; Nishimura, K.-i.; Kiriyaama, N. *Chem. Pharm. Bull.* **1976**, *24*, 1853-1859.
345. Hörcher, U.; Schwenner, E.; Franck, B. *Liebigs Ann. Chem.* **1986**, 1765-1771.
346. Arai, K.; Shimizu, S.; Taguchi, Y.; Yamamoto, Y. *Chem. Pharm. Bull.* **1981**, *29*, 991-999.
347. Kaji, A.; Kimura, K.; Iwata, T.; Kiriyaama, N. *Chem. Pharm. Bull.* **1995**, *43*, 1818-1819.
348. Arai, K.; Shimizu, S.; Yamamoto, Y. *Chem. Pharm. Bull.* **1981**, *29*, 1005-1012.
349. Kaji, A.; Saito, R.; Shinbo, Y.; Kiriyaama, N. *Chem. Pharm. Bull.* **1996**, *44*, 2340-2341.
350. Kaji, A.; Saito, R.; Hata, Y.; Kiriyaama, N. *Chem. Pharm. Bull.* **1999**, *47*, 77-82.
351. Arai, K.; Yamamoto, Y. *Chem. Pharm. Bull.* **1990**, *38*, 2929-2932.
352. Yamamoto, Y.; Kiriyaama, N.; Shimizu, S.; Koshimura, S. *Gann* **1976**, *67*, 623-624.
353. Shimizu, S.; Yamamoto, Y.; Koshimura, S. *Chem. Pharm. Bull.* **1982**, *30*, 1896-1899.
354. Kaji, A.; Kimura, K.; Teranishi, M.; Kiriyaama, N.; Nomura, M.; Miyamoto, K.-i. *Chem. Pharm. Bull.* **1998**, *46*, 1325-1329.

355. Ramage, R.; Hopton, D.; Parrott, M. J.; Kenner, G. W.; Moore, G. A. *J. Chem. Soc., Perkin Trans. I* **1984**, 1357-1370.
356. Gray, M.; Chapell, B. J.; Felding, J.; Taylor, N. J.; Snieckus, V. *Synlett* **1998**, 422-424.
357. Koizumi, T.; Haake, P. *J. Am. Chem. Soc.* **1973**, *95*, 8073-8079.
358. Tyssee, D. A.; Bauser, L. P.; Haake, P. *J. Am. Chem. Soc.* **1973**, *95*, 8066-8072.
359. Soai, K.; Hatanaka, T.; Miyazawa, T. *J. Chem. Soc., Chem. Commun.* **1992**, 1097-1098.
360. Keegstra, E. M. D.; Huisman, B.-H.; Paardekooper, E. M.; Hoogesteger, F. J.; Zwikker, J. W.; Jenneskens, L. W.; Kooijman, H.; Schouten, A.; Veldman, N.; Spek, A. L. *J. Chem. Soc., Perkin Trans. 2* **1996**, 229-240.
361. Weider, P. R.; Hegedus, L. S.; Asada, H.; D'Andreq, S. V. *J. Org. Chem.* **1985**, *50*, 4276-4281.
362. Jones, R. G.; Shonle, H. A. *J. Am. Chem. Soc.* **1945**, *67*, 1034.
363. Naumann, K.; Zon, G.; Mislou, K. *J. Am. Chem. Soc.* **1969**, *91*, 7012-7023.
364. Griffin, S.; Heath, L.; Wyatt, P. *Tetrahedron Lett.* **1998**, *39*, 4405-4406.
365. Coumbe, T.; Lawrence, N. J.; Muhammad, F. *Tetrahedron Lett.* **1994**, *35*, 625-628.
366. Monache, F. D.; Monache, G. D.; Souza, M. A. D. e.; Cavalcanti, M. D. S.; Chiappeta, A. *Gazz. Chim. Ital.* **1989**, *119*, 435-440.
367. Green, L.; Chauder, B.; Snieckus, V. *J. Heterocycl. Chem.* **1999**, *36*, 1453-1468.
368. Sharp, M. J.; Snieckus, V. *Tetrahedron Lett.* **1985**, *26*, 5997-6000.
369. Cheng, W.; Snieckus, V. *Tetrahedron Lett.* **1987**, *28*, 5097-5098.
370. Fu, J.-m., Ph.D. Thesis, University of Waterloo (1990).
371. Wang, X., Ph.D. Thesis, University of Waterloo (1992).
372. Fu, J.-m.; Snieckus, V. *Can. J. Chem.* **2000**, *78*, 905-919.
373. Corriu, R. J. P.; Masse, J. P. *J. Chem. Soc., Chem. Commun.* **1972**, 144.
374. Tamao, K.; Sumitani, K.; Kumada, M. *J. Am. Chem. Soc.* **1972**, *94*, 4374.

375. Tamao, K.; Minato, A.; Miyake, N.; Matsuda, T.; Kiso, Y.; Kumada, M. *Chem. Lett.* **1975**, 133.
376. Kendall, C., M.Sc. Thesis, Queen's University (2000).
377. Dieterich, F.; Stang, P. J. *Metal-Catalyzed Cross-Coupling Reactions*; Wiley-VCH: New York, 1998.
378. Stanforth, S. P. *Tetrahedron* **1998**, *54*, 263-303.
379. Miyaura, N.; Suzuki, A. *Chem. Rev.* **1995**, *95*, 2457-2483.
380. Fu, J.-m.; Snieckus, V. *Tetrahedron Lett.* **1990**, *31*, 1665-1668.
381. Oh-e, T.; Miyaura, N.; Suzuki, A. *J. Org. Chem.* **1993**, *58*, 2201-2208.
382. Sengupta, S.; Leite, M.; Raslan, D. S.; Quesnelle, C.; Snieckus, V. *J. Org. Chem.* **1992**, *57*, 4066.
383. Quesnelle, C. A.; FAMILONI, O. B.; Snieckus, V. *Synlett* **1994**, 349-350.
384. Stille, B. J. *Angew. Chem., Int. Ed. Engl.* **1986**, *25*, 508.
385. Negishi, E.-i.; King, A. O.; Okukado, N. *J. Org. Chem.* **1977**, *42*, 1821-1823.
386. Miyaura, N.; Yanagi, T.; Suzuki, A. *Synth. Commun.* **1981**, *11*, 513-519.
387. Davidson, J. M.; Triggs, C. *J. Chem. Soc. (A)* **1968**, 1324-1330.
388. Miyaura, N.; Yamada, K.; Suzuki, A. *Tetrahedron Lett.* **1979**, 3437-3440.
389. Miyaura, N.; Suzuki, A. *J. Chem. Soc., Chem. Commun.* **1979**, 866-867.
390. Miyaura, N.; Yano, T.; Suzuki, A. *Tetrahedron Lett.* **1980**, *21*, 2865-2868.
391. Subsequent work in our laboratories contradicted these results. Campbell, M.G., Ph.D. Thesis, University of Waterloo (1996)
392. Oh-e, Y.; Miyaura, N.; Suzuki, A. *Synlett* **1990**, 221.
393. Gronowitz, S.; Bobosik, V.; Lawitz, K. *Chem. Scripta.* **1984**, *23*, 120.
394. Gronowitz, S.; Honfeldt, A.-B.; Yang, Y. *Chem. Scripta* **1988**, *28*, 281.
395. Sharp, M. J.; Cheng, W.; Snieckus, v. *Tetrahedron Lett.* **1987**, *28*, 5093-5096.
396. Siddiqui, M. A.; Snieckus, V. *Tetrahedron Lett.* **1988**, *29*, 5463-5466.
397. Thompson, W. J.; Gaudino, J. *J. Org. Chem.* **1984**, *49*, 5237-5243.

398. Hoshino, Y.; Miyaura, N.; Suzuki, A. *Bull. Chem. Soc. Jpn.* **1988**, *61*, 3008-3010.
399. Watanabe, T.; Miyaura, N.; Suzuki, A. *Synlett* **1992**, 207-210.
400. Abraham, M. H.; Grellier, P. L. *The Chemistry of the Metal-Carbon Bond*; Hartley, F. R. and Patai, S. Eds.; Wiley: New York, 1985.
401. Old, D. W.; Wolfe, J. P.; Buchwald, S. L. *J. Am. Chem. Soc.* **1998**, *120*, 9722.
402. Bei, X.; Turner, H. W.; Weinberg, H.; Guram, A. S.; Peterson, J. L. *J. Org. Chem.* **1999**, *64*, 6797.
403. Weskamp, T.; Böhm, V. P. W.; Herrmann, W. A. *J. Organomet. Chem.* **1999**, 585, 348.
404. Litke, A. F.; Dai, C.; Fu, G. C. *J. Am. Chem. Soc.* **2000**, *122*, 4020.
405. Zhang, C.; Trudell, M. L. *Tetrahedron Lett.* **2000**, *41*, 595.
406. Krivoshchekova, O. E.; Stepanenko, L. S.; Mishchenko, N. P.; Denisenko, V. A.; Maksimov, O. B. *Khim. Prir. Soedin.* **1983**, 283-289.
407. Thomson, R. H. *Naturally Occurring Quinones III: Recent Advances*; 3 ed.; Chapman and Hall: New York, 1987.
408. Arnone, A.; Camarda, L.; Nasini, G.; Assante, G. *J. Chem. Soc., Perkin Trans. I* **1986**, 255.
409. Arnone, A.; Assante, G.; Nasini, G.; Camarda, L. *Gazz. Chim. Ital.* **1989**, *119*, 35.
410. Arnone, A.; Nasini, G.; De Pava, O. V. *Phytochemistry* **1991**, *30*, 2729-2731.
411. Cresp, T. M.; Giles, R. G. F.; Sargent, M. V. *J. Chem. Soc., Perkin Trans. I* **1974**, 2435-2447.
412. Sato, Y.; Kohnert, R.; Gould, S. J. *Tetrahedron Lett.* **1986**, *27*, 143-146.
413. Chi, J. J.; Hsu, S. T.; Hu, M.; Wang, S. *J. Chinese. Chem. Soc.* **1947**, *15*, 21.
414. Sargent, M. V.; Smith, D. O. *J. Chem. Soc. (C)* **1970**, 329-331.
415. Sachihiko, I. *J. Sci. Hiroshima Univ., Ser. A-2* **1971**, *35*, 161-170.
416. Ewersmeyer-Wenk, B.; Zahner, H.; Krone, B.; Zeeck, A. *J. Antibiotics* **1981**, *34*, 1531-1537.

417. Krone, B.; Hinrichs, A.; Zeeck, A. *J. Antibiotics* **1981**, *34*, 1538-1543.
418. Polonsky, J.; Johnson, B. C.; Cohen, P.; Lederer, E. *Bull. Soc. Chim. France* **1963**, 1909.
419. Gaudemar, A.; Polonsky, J.; Alais, L. *Bull. Soc. Chim. France* **1963**, 1918.
420. Lounasmaa, M.; Zylber, J. *Bull. Soc. Chim. France* **1969**, 3100-3103.
421. Giles, R. G. F.; Mitchell, P. R. K.; Sargent, M. V. *J. Chem. Soc., Perkin Trans. I* **1983**, 2147-2152.
422. Alo, B. I.; Kandil, A.; Patil, P. A.; Sharp, M. J.; Siddiqui, M. A.; Josephy, P. D.; Snieckus, V. *J. Org. Chem.* **1991**, *56*, 3763-3768.
423. Zhao, B.-p., Ph.D. Thesis, University of Waterloo (1994).
424. Majumder, P. L.; Bandyopadhyay, D.; Joardar, S. *J. Chem. Soc., Perkin Trans. I* **1982**, 1131.
425. Majumder, P. L.; Datta, N. *Indian J. Chem.* **1982**, *21B*, 534.
426. Majumder, P. L.; Sarker, A. K.; Chakraborti, J. *Phytochemistry* **1982**, *21*, 2713.
427. Majumder, P. L.; Datta, N. *Phytochemistry* **1984**, *23*, 671-673.
428. Patai, S. *The Chemistry of The Quinonoid Compounds*; Interscience: New York, 1974.
429. Ogilvie, A.; Kersten, W. *Quinone Antibiotics.*; Hahn, F. E.; Springer-Verlag: New York, **1978**, *V-I*, 243-263.
430. Parker, K. A.; Coburn, C. A. *J. Org. Chem.* **1991**, *56*, 1666-1668.
431. Sargent, M. V.; Timmons, C. J. *J. Chem. Soc.* **1964**, 5544-5552.
432. Wood, C. S.; Mallory, F. B. *J. Org. Chem.* **1964**, *29*, 3373-3377.
433. Pearson, D. E.; Wysong, R. D.; Breder, C. V. *J. Org. Chem.* **1967**, *32*, 2358.
434. Giles, R. G. F.; Sargent, M. V. *J. Chem. Soc., Perkin Trans. I* **1974**, 2447.
435. Kharlampovich, G. D.; Morotskii, O. A. *Koks Khim.* **1967**, 39-43 [CA 53918v **1967**, 67].
436. Wenxiang, C. , CA 153943z **1989**, 110.

437. Ninomiya, I.; Yamamoto, O.; Naito, T. *J. Chem. Soc., Perkin Trans. I* **1983**, 2165-2170.
438. Ninomiya, I.; Yamamoto, O.; Naito, T. *J. Chem. Soc., Perkin Trans. I* **1983**, 2171-2174.
439. Firouzabadi, H.; Sardarian, A. R.; Naderi, M.; Vessal, B. *Tetrahedron* **1984**, *40*, 5001-5004.
440. Kamikawa, T.; Isao, K. *Synthesis* **1986**, 431.
441. Firouzabadi, H.; Seddighi, M.; Mottaghinejad, E.; Bolourchian, M. *Tetrahedron* **1990**, *46*, 6869-6878.
442. Stuhr-Hansen, N.; Henrikson, L. *Synth. Commun.* **1997**, *27*, 89-94.
443. Tamarkin, D.; Benny, D.; Rabinovitz, M. *Angew. Chem. Int. Ed. Engl.* **1984**, *23*, 642-643.
444. Tamarkin, D.; Rabinovitz, M. *J. Org. Chem.* **1987**, *52*, 3472-3474.
445. Mohr, B.; Enkelmann, V.; Wegner, G. *J. Org. Chem.* **1994**, *59*, 635-638.
446. Neugebauer, W.; Kos, A. J.; Schleyer, P.v.R. *J. Organomet. Chem.* **1982**, *228*, 107-118.
447. Mueller-Westerhoff, U. T.; Zhou, M. *J. Org. Chem.* **1994**, *59*, 4988-4992.
448. Chapell, B. J.; Snieckus, V. , unpublished results.
449. Tüzün, C.; Ogliaruso, M.; Becker, E. I. *Org. Synth.* **1961**, *41*, 1-4.
450. Sartori, G.; Bigi, F.; Canali, G.; Maggi, R.; Casnati, G.; Tao, X. *J. Org. Chem.* **1993**, *58*, 840-843.
451. Trost, B. M. *J. Am. Chem. Soc.* **1969**, *91*, 918-923.
452. Plummer, V. F.; Al-Saigh, Z. Y.; Arfan, M. *J. Org. Chem.* **1984**, *49*, 2069.
453. Becker, H. D.; Hansen, L.; Anderson, K. *J. Org. Chem.* **1985**, *50*, 277.
454. Sangaiah, R.; Gold, A. *J. Org. Chem.* **1987**, *52*, 3205-3211.
455. Mills, R. J.; Taylor, N. J.; Snieckus, V. *J. Org. Chem.* **1989**, *54*, 4372-4385.
456. Mills, R. J.; Snieckus, V. *J. Org. Chem.* **1989**, *54*, 4386-4390.

457. Wang, X.; de Silva, S. O.; Reed, J. N.; Billedeau, R.; Griffen, E. J.; Chan, A.; Snieckus, V. *Org. Syn.* **1994**, *72*, 163.
458. Syper, L. *Synthesis* **1989**, 167-172.
459. Syper, L.; Mlochowski, J. *Tetrahedron* **1988**, *44*, 6119-6130.
460. Syper, L.; Kloc, K.; Mlochowski, J. *J. Prakt. Chem.* **1985**, *327*, 808-822.
461. Matsumoto, M.; Kobayashi, H.; Hotta, Y. *J. Org. Chem.* **1984**, *49*, 4740-4741.
462. Mitchell, R. H.; Lai, Y.-h.; Williams, R. V. *J. Org. Chem.* **1979**, *44*, 4733-4735.
463. Inoue, T.; Shigemitsu, Y.; Odaira, Y. *J. Chem. Soc., Chem. Commun.* **1972**, 668.
464. Watson, S. C.; Eastham, J. F. *J. Organomet. Chem.* **1967**, *9*, 165.
465. Sharpless, K. B.; Young, M. V. *J. Org. Chem.* **1975**, *40*, 947.
466. Ishii, H.; Chen, I.-S.; Ueki, S.; Masuda, T.; Morita, K.; Ishikawa, T. *J. Chem. Soc., Perkin Trans. 1* **1987**, 2415-2420.
467. Dickinson, R.; Heilbron, I. M.; Irving, F. *J. Chem. Soc.* **1927**, 1888-1897.
468. Ishii, H.; Ishikawa, T.; Wada, H.; Miyazaki, H.; Kaneko, Y.; Harayama, T. *Chem. Pharm. Bull.* **1992**, *40*, 2614-2619.